HyNEAT

HYDROGEN SUPPLY NETWORKS' EVOLUTION FOR AIR TRANSPORT – FINAL PROJECT REPORT

December 2025

Imprint

Project Spokesperson
Prof. Dr.-Ing. Hanke-Rauschenbach
Leibniz University Hannover, Institute of Electric Power Systems – Department of Electric Energy Storage Systems
Appelstr. 9A, 30167 Hannover

Project website: https://www.hyneat.de/en/

Project consortium
Leibniz Universität Hannover
Institut für Festkörperphysik (FKP)
Institut für Elektrische Energiesysteme (IfES)
Institut für Umweltökonomik und Welthandel (IUW)
Technische Universität Braunschweig
Institut für Automobilwirtschaft und Industrielle Produktion (AIP)
Institut für Mathematische Optimierung (IMO)
Junior Research Group "Overall System Evaluation" (JRG-A)
Technische Universität Clausthal
Institut für Aufbereitung, Recycling und Kreislaufwirtschafts-systeme (IFAD-CES)
Technische Universität München
Lehrstuhl für Anlagen- und Prozesstechnik (APT)
Technische Universität Hamburg
Arbeitsgruppe Resilient and Sustainable Operations and Supply Chain Management (W-EXK1)
Institut für Luft- und Kältetechnik gemeinnützige Gesellschaft mbH
Hauptbereich 1: Kryotechnik und Tieftemperaturphysik

Recommended citation
HyNEAT Project, Hydrogen Supply Networks' Evolution for Air Transport – Final Project Report, (2025).
https://doi.org/10.15488/20037

Hints

Funding
The project HyNEAT – Hydrogen Supply Networks' Evolution for Air Transport is funded by the German Federal Ministry of Research, Technology and Space (BMFTR) in the field of energy research programme. The project is supervised by Project Management Jülich (PtJ).

List of Contributors
Finn Schenke – Leibniz Universität Hannover
Dr.-Ing. Julian Hoelzen – Leibniz Universität Hannover
Prof. Dr.-Ing. Richard Hanke-Rauschenbach – Leibniz Universität Hannover
Leon Schomburg – Leibniz Universität Hannover
Marlon Schlemminger – Leibniz Universität Hannover
Alexander Mahner – Leibniz Universität Hannover
Dr. Dennis Bredemeier – Leibniz Universität Hannover
Dr. Raphael Niepelt – Leibniz Universität Hannover
Prof. Dr.-Ing. Rolf Brendel – Leibniz Universität Hannover
Tobias Müller – Leibniz Universität Hannover
Dr. Steven Gronau – Leibniz Universität Hannover
Dr. Etti Winter – Leibniz Universität Hannover
Prof. Dr. Ulrike Grote – Leibniz Universität Hannover

Karen Fiedler – Technische Universität Braunschweig
Dr. Alexander Barke – Technische Universität Braunschweig
Lisa-Marie Manke – Technische Universität Braunschweig
Dr. Imke Joormann – Technische Universität Braunschweig
Prof. Dr. Thomas S. Spengler – Technische Universität Braunschweig
Rebecca Marx – Technische Universität Braunschweig
Prof. Dr. Sebastian Stiller – Technische Universität Braunschweig

Akin Ögrük – Technische Universität Hamburg
Prof. Dr. Christian Thies – Technische Universität Hamburg

Annika Hoppe – Technische Universität Clausthal
Prof. Dr.-Ing. Christine Minke – Technische Universität Clausthal

Laura Stops – Technische Universität München
Dr.-Ing. Sebastian Rehfeldt – Technische Universität München
Prof. Dr.-Ing. Harald Klein – Technische Universität München

Dr. Andreas Kade – ILK Dresden
Dr. Matthias Schneider – ILK Dresden

Design
www.peppermint.de

With funding from the:
Federal Ministry of Research, Technology and Space

Executive summary

This report provides a comprehensive assessment of the potential for a liquid hydrogen (LH_2) supply infrastructure for hydrogen (H_2)-powered aviation in Europe. H_2 is a key defossilization tool and will be critical for emission reduction in aviation, either through direct use as a fuel or as a feedstock for sustainable aviation fuels. Rather than advocating for H_2-powered aviation as the main solution, this report explores how such an LH_2 supply infrastructure could be realized, what implications it would entail, and how it might interact with the broader European energy system.

To capture the inherent uncertainties in technology development and policy commitment, we developed a series of scenarios for the uptake of H_2-powered aircraft: the Baseline, Ambitious Policy, and Moonshot scenario. Using a system dynamics model, we determined the future LH_2 demands for a European airport network for these scenarios. In order to meet these demands as cost-effectively as possible, we developed a H_2 supply network model which determines the cost optimal supply network for a target picture in the year 2050 as well as the transition path to reach that target picture. The supply network can consist of multiple H_2 supply routes available for the airports (on-site LH_2 production, GH_2 pipelines, LH_2 trucks and LH_2 vessels). The potential H_2 supply volumes and costs are determined using an energy system transition model which is used to evaluate the integration of H_2 production into the general energy system transformation on three perspectives: International H_2 import options, H_2 production within the European energy system as well as the impact of LH_2 supply for aviation on the local energy system. As LH_2 availability and supply costs vary greatly between airports, we use a flight network model to evaluate how these costs influence the future flight networks.

The study also includes the ecological evaluation using a life cycle assessment to determine the ecological impact of H_2 production and compare the different supply routes. In addition, we examine potential business models, stakeholder perspectives, and policy instruments to support this transition, with the goal of informing decision-making in industry, policy, and science. Finally, the macroeconomic impact of implementing such a supply infrastructure is analysed using a Social Accounting Matrix (SAM)-based multiplier model.

What we have found

- The airport's location and H_2 demand volumes are key cost drivers for LH_2 supply costs. The largest cost shares are related to the renewable energy sources, liquefaction, and electrolysis. The supply costs can be reduced for locations with high potential for renewable energy sources, as well as through economies of scale for high-demand airports.

- While H_2 supply costs may become economically viable by 2050, the costs during the initial development phase will be significantly higher. Establishing an H_2 supply network for European airports can reduce the supply costs by optimising the H_2 production location and maximizing the utilisation of production and transport components.

- For airports without access to low-cost on-site H_2 supply, importing H_2 can significantly reduce costs. For larger LH_2 demands, the access to the European Hydrogen Backbone (EHB) is critical. The most important cost factors are the proximity to the EHB as well as to the nearest port for LH_2 imports. Also, the transport distance through the EHB drives cost while the vessel supply distance increases supply costs less severe.

- Although Europe has the technical potential to meet its H_2 demands through domestic production, importing H_2 from regions with lower production costs leads to lower overall network costs. Next to the techno-economic potential, the exporting countries' weighted average cost of capital is a key factor of H_2 import cost.

- Significant LH_2 demand in aviation arises only under ambitious and coordinated policy frameworks. With limited support, H_2-powered aircraft remain marginal, leading to a comparably low demand (<0.2 MtH_2/a by 2050). In contrast, strong incentives, higher CO_2 prices, and targeted H_2 subsidies in the Ambitious and Moonshot scenarios enable H_2 to become a relevant aviation energy carrier. Early market entry and stable long-term policy support are therefore essential to achieve scale effects and lower future LH_2 supply costs.

- The flight network analysis shows, that carefully designed and well-calibrated subsidy strategies can substantially increase the adoption of H_2 in aviation with limited additional financial effort, highlighting the cost-effectiveness of regionally targeted support mechanisms.

- The main environmental impact of green H_2 supply is accountable to renewable energy sources due to the high energy demand of H_2 production and liquefaction. H_2 transport also significantly increases the greenhouse gas emissions depending on the transport distances. Additionally, H_2 leakage is a major environmental concern, with H_2 leakage along the supply chain posing the potential to double the total specific GHG emissions.

- The development of LH_2 infrastructure has significant implications for national economies. The macroeconomic analysis emphasizes that a country's potential to benefit from the network is influenced by its industrial structures, import dependencies for critical components, and the origin of investments. These factors should encourage the formation of strategic partnerships that unlock investment capital and ensure a stable supply and fair distribution of value added along the supply chain.

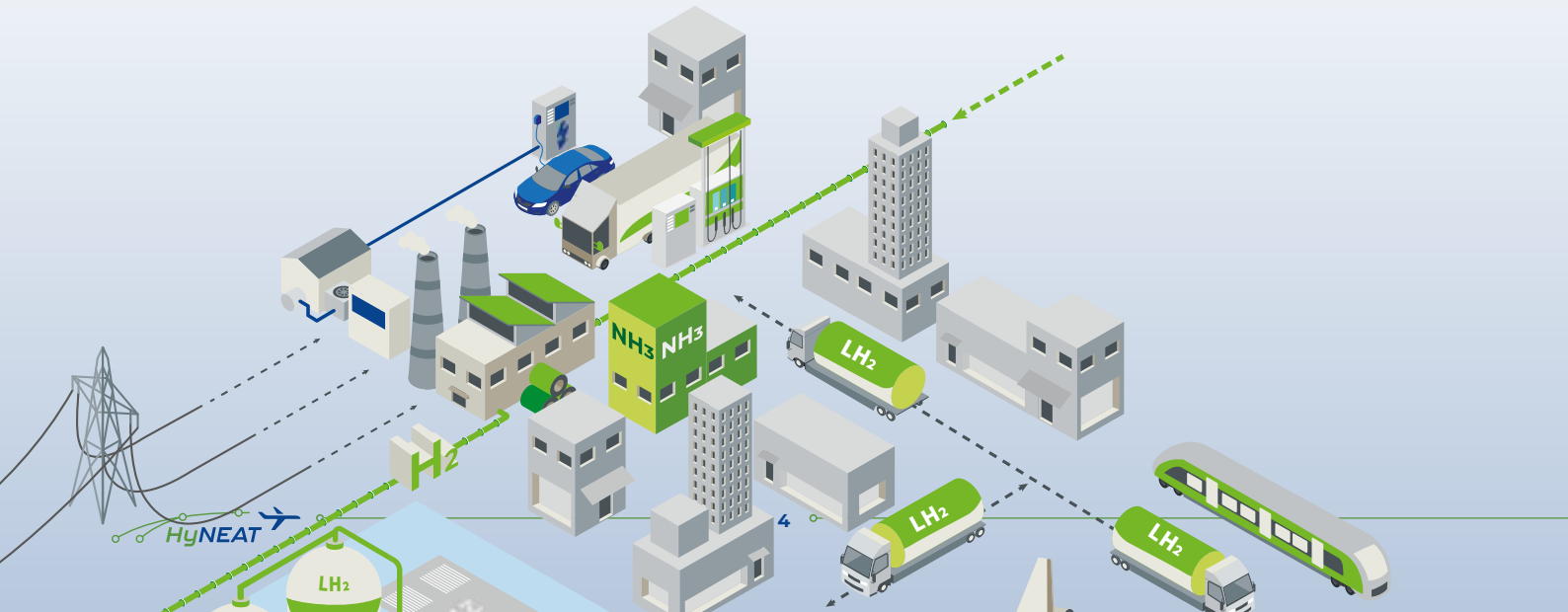

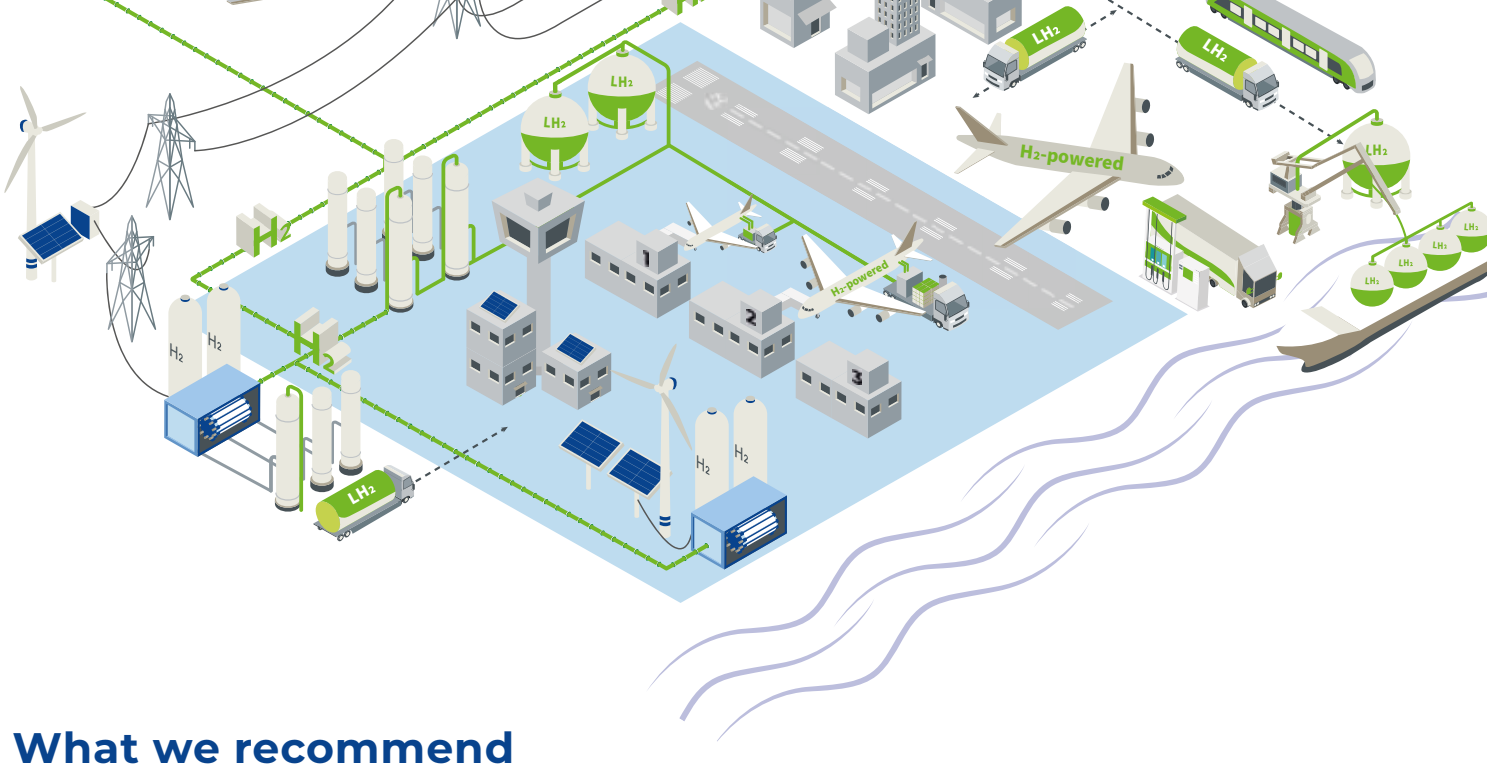

What we recommend

- Support a substantial uptake of H_2 in European aviation through stable, long-term policy frameworks that combine effective CO_2 pricing with targeted support for H_2 production, airport infrastructure, and aircraft deployment.
- Address the early-stage “chicken-and-egg” problem by promoting off-take agreements between airlines, fuel suppliers, and airports to reduce investment risk and mobilize capital.
- Develop clear policy roadmaps to provide stakeholders with a definitive timeline when and where H_2 infrastructure will be required. Introduce suitable policy support instruments to reduce initial supply costs, attract investors, and ensure long-term market stability.
- Plan LH_2 supply as a coordinated network across European airports to exploit economies of scale, reduce unit costs, and stimulate demand. Close cooperation among stakeholders is required to share knowledge, risks, and infrastructure.
- Establish international partnerships with politically and economically stable regions to import low-cost green H_2. Mutual benefits exist from multi-dimensional trade relationships by exporting key equipment to H_2-producing nations and importing low-cost green H_2 back to Europe.
- Adopt a hybrid supply strategy that combines domestic H_2 production with imports to diversify supply sources, mitigate geopolitical and price risks, and lower overall system costs.
- Design the H_2 supply network with full life-cycle emissions in mind, minimizing H_2 leakage and improving boil-off management along the supply chain to reduce climate impacts and avoid efficiency losses.

In addition to the results and recommendations presented, several challenges remain that will shape the feasibility and pace of introducing H_2-powered aviation. Industry-wide standards and certification frameworks must be established, including robust safety, handling, and operational procedures for LH_2 at airports. A successful scale-up also depends on the availability of qualified personnel. The expansion of LH_2 supply infrastructure, and airport operations requires specialized technical skills that are not yet widely established. Addressing labour shortages and skill gaps will therefore be necessary to ensure reliable and safe implementation. Also, the interaction between LH_2 supply for direct use and H_2-based synthetic aviation fuels requires further research, as both competition for renewable energy resources and synergies in shared infrastructure may arise.

Looking ahead, the transition to H_2-powered aviation will depend not only on technological and economic progress but also on coordinated decision-making across aviation, energy, and industrial policy. Ensuring alignment between aircraft development timelines, infrastructure deployment, and energy system transformation will be critical. This makes early strategic planning and cross-sector cooperation central to realizing the potential role of H_2 in the future aviation system.

Advisory board

Afrika-Verein der deutschen Wirtschaft

AIRBUS

DEUTSCHE AIRCRAFT

DLR Deutsches Zentrum für Luft- und Raumfahrt German Aerospace Center

EWE

FMO FLUGHAFEN MÜNSTER OSNABRÜCK

Hamburg Airport

hannover airport

Linde

LUFTHANSA GROUP

McKinsey & Company

MTU Aero Engines

MUNICH AIRPORT

SIEMENS energy

The representations in this document do not necessarily reflect the opinions of the companies on the Advisory Board.

Table of contents

INTRODUCTION

1

1 Introduction

Aviation serves as a vital driver of global mobility and economic exchange, yet it is increasingly contributing to climate change. The sector currently accounts for approximately 2-3% of global CO_2 emissions, with the International Civil Aviation Organization (ICAO) projecting that international aviation emissions could triple by 2050 compared to 2015 levels without mitigation efforts [1]. This growth, combined with faster defossilization in other industries, could elevate aviation's share of global CO_2 emissions to as much as 25% by 2050 [2]. In addition to CO_2, aviation generates significant non-CO_2 climate impacts, including contrails and cirrus clouds formed by water vapour and soot particles, as well as nitrogen oxides (NOx). These effects are thought to amplify the sector's overall climate footprint by roughly the same magnitude as CO_2 alone, though considerable uncertainty persists in these estimates [3,4]. While governments and the aviation industry have committed to reaching net-zero emissions by 2050, progress remains limited due to slow ramp-up of sustainable aviation fuel (SAF) projects and setbacks in developing next-generation aircraft technologies [3,5].

To make net-zero aviation a reality, several technology options are being investigated from SAFs to battery-electric or hydrogen (H_2)-powered aircraft. Rather than competing directly, these options could play complementary roles across different market segments (see below for more details).

H_2 has emerged as a promising energy carrier for future aviation. Due to the relatively low volumetric energy density of gaseous H_2, cryogenic liquid hydrogen (LH_2) is required in commercial aircraft. In principle, its use could eliminate direct CO_2 emissions and substantially reduce certain non-CO_2 effects [6]. However, the magnitude of its contribution to aviation defossilization remains uncertain [7]. Recent assessments have revised down the expected long-term market share of H_2-powered aircraft, reflecting both technical challenges and competing defossilization pathways [6]. Nevertheless, there is a strong commitment from aircraft OEMs, airlines and policy to introduce H_2-powered aircraft, which will be particularly relevant in the regional and short-range segments, with technical feasibility extending into medium-range flight segments.

The introduction of H_2 into aviation is associated with fundamental technological and infrastructural challenges. On the aircraft side, entirely new designs are required, incorporating dedicated powertrains, LH_2 storage systems, and on-board distribution system. While H_2 combustion in modified turbines is technically possible, current development efforts primarily focus on fuel-cell-electric propulsion concepts [8,9]. At the same time, deployment depends critically on the availability of a suitable LH_2 supply infrastructure at airports. This infrastructure comprises multiple complex components, including green H_2 production, liquefaction, storage, and distribution systems. Establishing such systems poses a significant challenge for the aviation sector, but also offers an opportunity for European airports and industry to assume a pioneering role in a key technology of the energy transition.

This report aims to provide a holistic assessment of the development and impact of H_2 supply infrastructure for aviation in Europe. The intention is not to advocate for H_2-powered aviation as the sole solution to defossilize the sector, but rather to explore how such an infrastructure could be realized, what implications it would entail, and how it might interact with the broader European energy system.

The analysis is based on scenarios for the uptake of H_2-powered aircraft and investigates how LH_2 supply networks could be structured across Europe. This includes both a target picture for 2050 and the transition pathways leading to it. A central focus lies on the resulting LH_2 supply costs at European airports, as well as their regional variability. To derive these cost trajectories, the study integrates H_2 production within the European energy system, considers potential H_2 imports, and evaluates the impact of LH_2 demand from aviation on local energy system.

Beyond techno-economic aspects, the report expands its scope in several directions:

- **Aviation network implications:** Given the heterogeneity of LH_2 supply costs across Europe, the potential impact on the structure and competitiveness of future air transport networks is analysed.
- **Environmental assessment:** The ecological impact of different supply routes is quantified, including lifecycle greenhouse gas emissions.
- **Stakeholder and policy perspectives:** The report explores possible business models for LH_2 supply, identifies relevant stakeholder constellations, and

assesses policy instruments that could enable or accelerate implementation.

» **Macroeconomic dimension:** Finally, the broader economic effects of establishing an LH_2 infrastructure for aviation in Europe are examined, including potential industrial opportunities and regional value creation.

By combining these perspectives, the report provides a comprehensive picture of the opportunities and challenges associated with LH_2 infrastructure for aviation, and thus seeks to inform decision-making by industry, policy makers, and the scientific community alike.

The remainder of this report is structured as follows. Chapter 2 outlines the overall study design and provides a summary of the sub-model methodologies; full technical details are given in Appendix C. Chapter 3 defines the scenarios and derives the resulting LH_2 demand, which serves as the basis for all subsequent analyses. Chapter 4 presents the main results for LH_2 supply chains, beginning with dedicated infrastructures for archetypical airports and extending to an integrated European airport network. This chapter also examines the resulting flight networks and illustrates the transition path of the supply chains through a case study of nine German airports. The energy system perspective is addressed in Chapter 5, which considers both H_2 production within the European energy system and potential import options, as well as their impacts at European and regional levels. Chapter 6 assesses the ecological effects of alternative supply chains, complemented by a parameter study on transport distances. Chapter 7 analyses stakeholder roles, business models, financing options, and relevant policy instruments. Recognizing the multinational character of LH_2 supply chains, Chapter 8 evaluates their macroeconomic implications for selected countries. Finally, Chapter 9 provides a summary of the findings and an outlook. Supplementary deep-dives on H_2 liquefaction and LH_2 refueling strategies are included in Appendix A and B.

Options to defossilize aviation

Among the major contributors to aviation emissions are the direct CO_2 emissions from the combustion of conventional jet fuel, which are associated with a high degree of certainty [4]. In addition to CO_2 emissions, aircraft in flight are responsible for a range of non-CO_2 effects – such as nitrogen oxides (NOx), water vapor, and contrails—that significantly contribute to aviation's overall climate impact. Current studies suggest that these effects may amplify aviation's total climate impact by a factor of two to four, with contrails and cirrus cloud formation playing a dominant role [10]. Persistent contrails formed in ice-supersaturated regions can evolve into these cirrus clouds, which both reflect incoming solar radiation during the day and trap outgoing longwave radiation. Overall, they exert a net warming effect on the climate, though the magnitude varies with time of day, season, and location and uncertainties are high [11]. Defossilization technologies therefore need to be assessed not only for their CO_2 reduction potential but also for their influence on non-CO_2 effects.

The available options for emission reduction differ mainly by their underlying energy carriers. Importantly, they are not mutually exclusive: each can address specific market segments and, in combination, contribute to a portfolio of solutions. All options, however, require very large amounts of renewable energy and H_2, creating both potential competition and synergies across the energy system.

Battery-electric aircraft:
Battery-electric propulsion offers the highest potential for reducing both CO_2 and non-CO_2 effects, with additional benefits such as altitude-independent operation and high overall efficiency. However, the low energy density and high weight of batteries currently limit this option to short distances and small aircraft [12]. Realizing battery-electric aviation requires entirely new aircraft designs as well as the deployment of dedicated charging infrastructure at airports. Furthermore, the production of batteries presents a considerable environmental challenge, as the replacement of batteries during an aircraft's operational life may lead to substantial life-cycle emissions [13].

Major advantage | Challenge | Major challenge

Disruptive fuels or technologies	Impact on aircraft design	Fuel & airport infrastructure	Climate impact inflight[2]	Fuel energy efficiency
SAF	**No significant change** Drop-in for existing fleet and all segments[1]	**New fuel production** Infrastructure required	**30-60 % reduction[3]** No change in CO_2 emissions – but potentially net-zero CO_2	**20-40 % efficiency** of renewable energy for PtL, biomass-SAF with limited supply
H_2 turbine	**New aircraft design** Limited applicability for wide-body aircraft	**New fuel production and supply/distribution** Infrastructure required – also implications on aircraft refueling and airport design	**50-75 % reduction** Zero CO_2 emissions	**45-60 % efficiency** of renewable energy for green H_2 production
H_2 fuel cell	**New aircraft design** Limited applicability for single-aisle & wide-body aircraft		**75-100 % reduction** Zero CO_2 emissions	
Battery-electric	**New aircraft design** Limited applicability for regional/larger aircraft	**New charging infrastructure** Eventually grid constraints	**100 % reduction** Zero emissions	**No energy conversion** Charging efficiency up to 95 %

[1] Not certified yet and potentially minor changes for engine and/or fuel system required; [2] Including CO_2, NOx, water vapor and contrail formation; [3] For PtL with fully decarbonized supply chain and using CO_2 from direct air carbon capture; [4]Assuming 100% renewable electricity

Figure 1: Overview of fuel or propulsion technologies for defossilizing aviation concerning their impact on aircraft design, fuel and airport infrastructure, climate impact and fuel energy efficiency based on [10]

H_2-powered aircraft:

H_2 can either be combusted in modified turbines or used in fuel cells to power electric motors. In both cases, direct CO_2 emissions are eliminated, with potential reductions in NOx emissions and contrail formation, although high uncertainty in the potential reduction of contrail formation [10]. To achieve the required energy density for commercial operations, H_2 must be stored in liquid form, which makes it particularly suitable for short- and medium-haul flights. This comes with several challenges especially storage and distribution of LH_2 along the fuselage [13]. Therefore, H_2-powered aviation requires new aircraft designs to efficiently utilise the advantages of LH_2 as well the establishment of a dedicated LH_2 supply and refueling infrastructure at airports.

Sustainable Aviation Fuels:

Several technological pathways exist for the production of sustainable aviation fuels (SAF), all of which are compatible with current aircraft and infrastructure and in principle could enable a 100% substitution of fossil kerosene with only minor adjustments. At present, the dominant pathway is Hydrotreated Esters and Fatty Acids (HEFA), which uses feedstock such as animal fats, vegetable oils, and used cooking oil. HEFA is a mature technology, but its scalability is constrained by the limited availability of suitable feedstock [14]. Other conversion routes, including alcohol-to-jet and biomass gasification, can process a broader range of biomass feedstock. These pathways benefit from relatively low feedstock costs, but their sustainable potential remains limited due to high land requirements and competition with food production [3]. In the long term, the greatest potential is associated with Power-to-Liquid (PtL) fuels, which are produced from green H_2 and CO_2. The CO_2 can be sourced either from concentrated point sources or directly from the atmosphere via direct air capture. While PtL offers the largest scalability potential, it requires very large amounts of renewable energy and costs remain uncertain [14].

Further solutions for defossilization:

In addition to alternative propulsion and fuel options, several further approaches exist to reduce the climate impact of aviation. One example is contrail avoidance, where flight routes are adjusted to limit the formation of contrails and related cirrus clouds. However, accurately predicting ice-supersaturated regions and reliably assessing the climate impact of individual contrails remain major challenges [11]. Efficiency improvements in aircraft technology, operational practices, and air traffic management can further increase fuel efficiency and reduce emissions [3]. Finally, remaining fossil fuel use can be addressed through CO_2 removal technologies, such as direct air capture combined with geological storage. While these approaches could compensate for residual emissions, their scalability and costs remain uncertain [15]. Offsetting emissions also requires transparent auditing to ensure credibility and prevent double counting [3].

METHODOLOGY

2 Methodology

To provide context for the study results, this chapter first outlines the future H_2 aviation ecosystem. It also introduces the overall study design and model framework. Given the wide range of models and methodologies applied in this interdisciplinary project, the specific methodology of each model is briefly discussed in this chapter to support a clearer understanding of the results. A detailed description of the complete methodology, including model equations and assumptions, is provided in Appendix C.

2.1 Hydrogen in the aviation ecosystem

The following section provides a brief overview of the H_2 aviation ecosystem, highlighting the relevant stakeholders and their potential roles. It also outlines the components of the green LH_2 supply infrastructure and the supply routes considered in this study.

2.1.1 Potential stakeholder

Several stakeholders could be directly involved in owning and/or operating LH_2 supply infrastructure for aviation. Their potential roles can be understood by examining their current involvement in the aviation sector, possible roles within an H_2 aviation ecosystem, and existing business models.

Airport operators are naturally positioned to own and operate parts of the H_2 supply and refueling infrastructure or to lease areas at the airport for such purposes. Ownership structures vary, with airports being privately owned or partly to fully state-owned [16]. While LH_2 infrastructure will likely fall under the airport's purview, it is unlikely that airports will directly fund or operate such infrastructure due to the significant capital requirements and the operational expertise needed. Additionally, airports typically operate under low-profit margins, making investments in infrastructure less attractive [17].

Into-plane service providers (ITP) currently manage conventional aircraft refueling operations and often have ownership structures involving major fuel suppliers, airlines, consortiums, ground handling companies, or joint ventures between these actors [18]. These providers already possess operational experience and access to airports and generally operate with high-profit margins [17,19]. This positions them well to potentially take over LH_2 airport infrastructure including refueling operations, but they currently lack specific experience with LH_2 technologies.

H_2 actors, specifically established industrial gas companies, bring the technical expertise required for H_2 production, liquefaction, storage, and logistics. Although they are not currently active within the aviation sector, they possess relevant infrastructure, logistics capabilities, and regulatory experience while operating with high-profit margins [20–22].

Renewable energy system (RES) actors possess know-how in renewable energy and the H_2 sector but are not traditionally involved in aviation. These actors are the most likely to take over the generation of renewable energy and could also play a role in gaseous green H_2 production. Their profit margins have recently declined due to excess capacity, intense competition, and falling prices in the renewables market [23].

Oil and gas actors are involved in the aviation sector through the supply of jet fuel, with approximately 9% of global crude oil consumption attributed to air transport [24]. These actors can handle large investments and are increasingly diversifying into the H_2 and renewable energy sectors, bringing substantial experience in infrastructure, logistics, and regulatory environments. Due to their high asset bases and financial robustness, they are equipped to manage and absorb substantial commercial and technical risks, particularly those associated with large-scale infrastructure projects. Furthermore, their business models often require and can generate significant capital returns to justify the long-term, high-capital expenditure nature of their assets [17].

Joint ventures are already a common model within the aviation industry [25] and have already emerged for LH_2 supply infrastructure in aviation [26]. Joint ventures can include all stakeholder groups, enabling the pooling of resources and expertise, and are a likely model for risk-sharing and integrated infrastructure development in H_2 aviation.

In addition to the directly involved actors, several stakeholders play indirect yet critical roles in enabling and supporting LH_2 infrastructure for aviation. Airlines drive the demand for H_2 as they pursue defossilization goals, with interests in securing long-term fuel contracts and investing in infrastructure to ensure price stability and supply security [27]. Governments shape the strategic direction through roadmaps and policy frameworks while providing political support and, in

some cases, acting as facilitators or co-investors to advance H_2 infrastructure development. Regulatory bodies are essential for defining and enforcing safety, environmental, and infrastructure standards, ensuring certification and standardization of LH_2 systems at airports. Financial institutions provide the large-scale project financing needed for infrastructure deployment, often requiring clear return perspectives and risk mitigation strategies, while specialized public banks such as the European Investment Bank (EIB) offer targeted financing instruments for sustainable infrastructure projects [28]. Private investors are increasingly seeking long-term, ESG-aligned investment opportunities in the H_2 supply sector. Although aircraft OEMs are not direct infrastructure developers, they have a vested interest in a reliable LH_2 supply to support the operation of H_2-powered aircraft, and their influence extends to shaping technology standards and supply chain requirements within the aviation H_2 ecosystem.

2.1.2 Green liquid hydrogen supply routes and components

In this section, the LH_2 supply routes evaluated in this study are introduced including the required components for these supply routes. This section should only provide a broad overview of the supply routes and associated components, for a more detailed description of the components please refer to Hoelzen [29]. Figure 2 shows the components of the supply chain considered in this study.

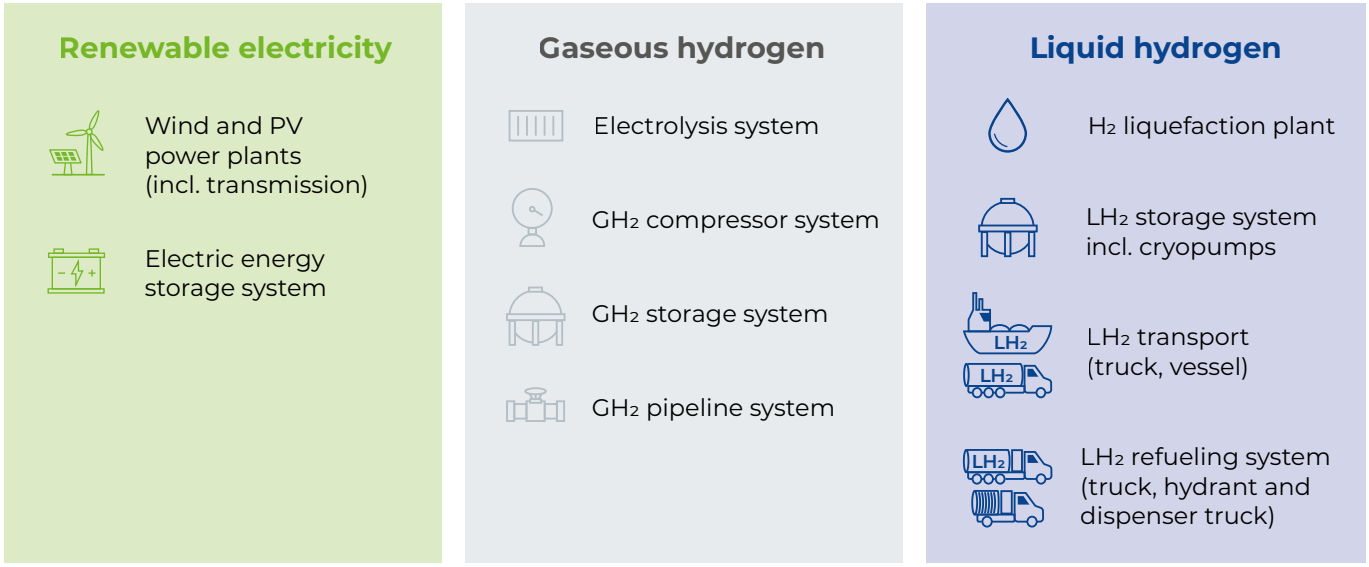

Figure 2: Overview of LH_2 supply chain components considered in this report [29]

Renewable electricity components

As green H_2 production requires newly build renewable electricity capacities according to the European regulation [30], in this study only H_2 production with wind power and photovoltaic (PV) power is assumed. For the H_2 production from the European energy system more details are provided in Section 5. As the availability of renewable energy sources (RES) is highly volatile due to wind speeds and sun radiation, grid scale electric energy storages can be installed to buffer the energy. In this study, lithium-ion storages are selected to smoothen RES fluctuations throughout the day.

Gaseous hydrogen components

There are several water electrolysis technologies available with the most prominent discussed being: alkaline electrolysis (AEL), proton exchange membrane electrolysis (PEMEL), and solid oxide electrolysis (SOEL). In this study the PEMEL is assumed as a main technology for H_2 production due to its ability to operate with flexible loads as low as 5% nominal power as well as a high efficiency [31]. As H_2 has very low volumetric density, for storage and transportation higher densities are required for better volumetric efficiency and therefore better economics. Several compressor technologies are available with piston engine and centrifugal compressors being mostly used. In order to further buffer fluctuating RES availability

and LH_2 demand storage in GH_2 above ground storages and GH_2 cavern storages are available. In GH_2 above ground storages, H_2 is stored in containerized storage tanks, which are often build in cylindrical form with 200 bar pressure being most economical for storages without space constraints [32]. Storage in geological formations such as salt or rock caverns have significantly lower costs due to very large volumes available. These caverns are mostly operated at maximum pressures of 180-200 bar [33]. Due to the comparably low volumetric density of H_2 even if compressed, truck transport with GH_2 containers is not favourable [34]. Therefore, in this study only the transport with GH_2 pipeline systems is considered, which consist mainly of pipes and compressors along the route to ensure more constant flow speeds. In this study, either new pipelines are built for the H_2 supply or existing decommissioned natural gas pipelines could be retrofitted to be able to transport GH_2. As Europe plans an international pipeline system, the European Hydrogen Backbone [35], this network is considered as an available transportation mode in this report.

Liquid hydrogen components

As for larger commercial H_2-powered aircraft H_2 will be required in liquid state, a H_2 liquefaction plant (LFP) is required. In this study, the Claude Cycle process is considered; in Appendix A a deep-dive into the current state of H_2 liquefaction is conducted. As LH_2 demand at the airports will also be fluctuating due to the short turnaround times at airports, LH_2 storages are available to buffer these fluctuations. In addition, storage of three days the airports demand are assumed to ensure supply security [10]. In this study, spherical double wall vacuum insulated storage tanks are considered to reduce heat input from the outside. Nevertheless, so-called boil-off losses due to the ortho-to-para-conversion of H_2 cannot fully be prevented which needs to be vented off the storage. In order to reach fast loading and un-loading times, cryopumps are used. Appendix B will deep-dive into the airport LH_2 infrastructure including LH_2 storages and cryopumps. In this study, LH_2 transport via trucks for short distances and via vessel for long import distances is considered. The trucks capacity is around 4-5 tons of LH_2, which is only economic for short distances under 500 km. The import of H_2 via large vessels also requires the corresponding import and export terminal infrastructure mainly consisting of LH_2 storages and cryopumps. Finally refueling at the airport can either be done with LH_2 refueling trucks which directly refuel the airport with on-board tanks and cryopumps or using a pipeline and dispenser truck system comparably to the current jet fuel refuelling [36]. A deep-dive into the refuelling systems is provided in Appendix B.

Supply routes

Figure 3 shows the considered supply routes in this study. The first route A is the on-site LH_2 supply route, where every component is located directly at or near the airport. If there is no low-cost electricity, water or space available at the airport, gaseous hydrogen (GH_2) can be imported through either a new or a repurposed pipeline in supply route B. In this case, H_2 liquefaction still takes place at or near the airport. The supply route C represents the LH_2 import case using a LH_2 vessel and a LH_2 truck from the nearest port to the airport. In this case, H_2 production and liquefaction takes place at the export location and only a LH_2 storage and the refueling system is located at the airport. In a supply network, such as the one examined in this study, the supply routes could vary throughout the years and multiple supply locations as well as supply routes could be utilised at the same time.

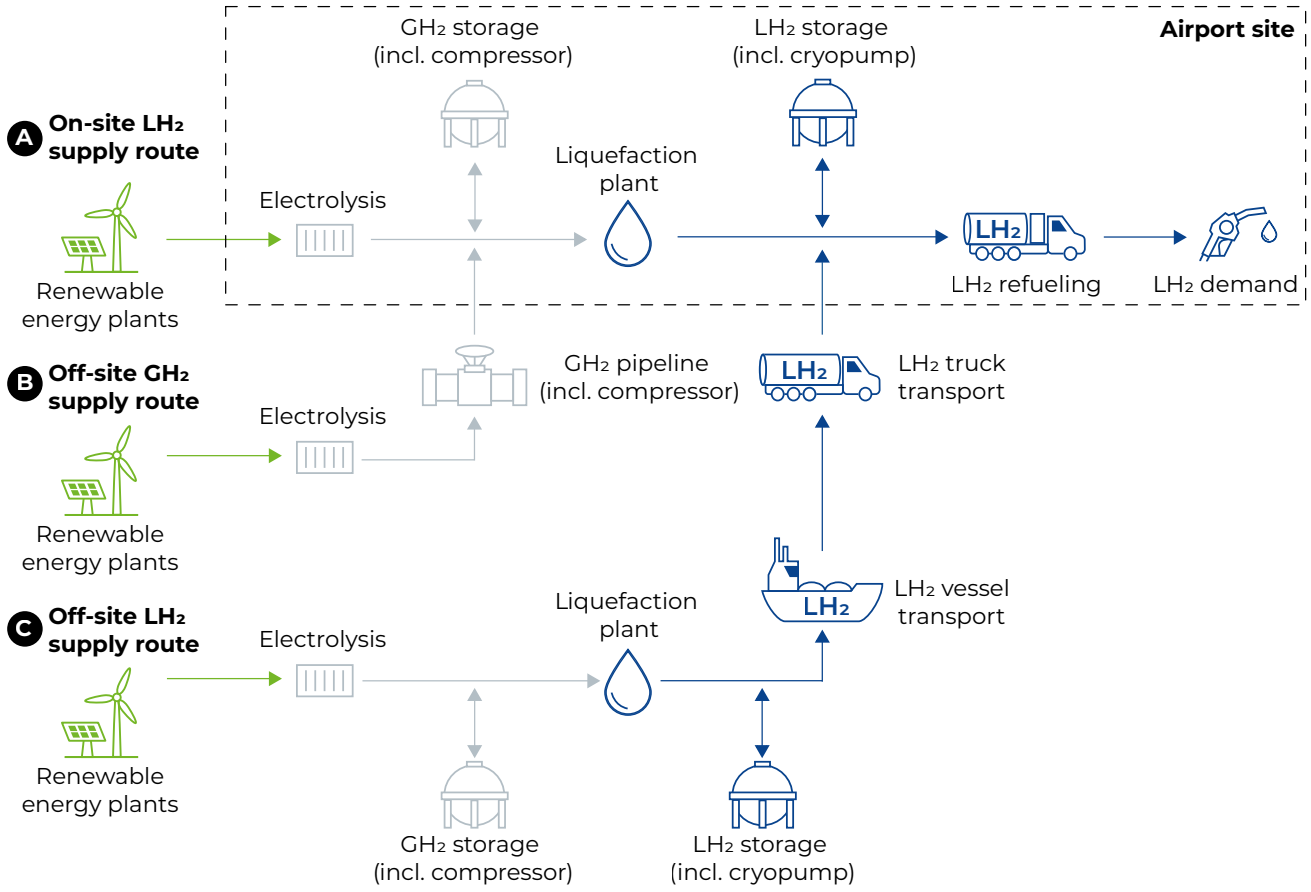

Figure 3: LH_2 supply routes in considered in this study: A: On-site LH_2 supply, B: Off-site GH_2 supply, C: Off-site LH_2 supply

2.2 Study design and model framework

In this section, the study design for the LH_2 supply network evaluation is introduced. All evaluations of this report are based on overarching scenarios, which are discussed in detail in Section 3. For the main evaluation of LH_2 supply in Section 4, first, a generic airport is evaluated to show the influence of the location and in particular the impact of the conditions for renewable energy on the LH_2 supply infrastructure and costs. The different locations are shown in the Appendix C. In addition, the impact of LH_2 demand at the airport, as well as the transport distance for the different supply routes is shown.

To show how the supply network for multiple European airports could take shape, an airport network is assumed based on Hoelzen et al. [37]. Figure 4 shows the airport selection, which is based on a hub-and-spoke air traffic network with the hub in Frankfurt.

Figure 5 shows the model framework for this study. For each airport from the airport network, the future LH_2 demand is determined based on scenarios using a system dynamics model as further discussed in Section 3. Using an energy system transformation model to model the future European energy system, the potential H_2 production capacities and costs from the energy system as well as import capacities and costs are determined. With both of these inputs, using the H_2 supply chain network model the resulting LH_2 supply infrastructure and costs for the airport network can be evaluated.

As the resulting LH_2 supply costs at the airports are highly variable, also the flight networks will vary in the future. This impact will be evaluated using a model to captures essential decisions about routing, aircraft type allocation, fuel logistics, and infrastructure limitations. To show the impact of H_2 production for aviation on the energy system, the energy system transformation model is evaluated from a global and regional perspective. In addition, a lifecycle analysis is conducted using the supply routes of the supply network to show the ecological impact of LH_2 supply. Finally, a macroeconomic model based on the results of the supply network analysis is used to evaluate the macroeconomic impact of H_2 production on selected countries.

Figure 4: Airport network under consideration

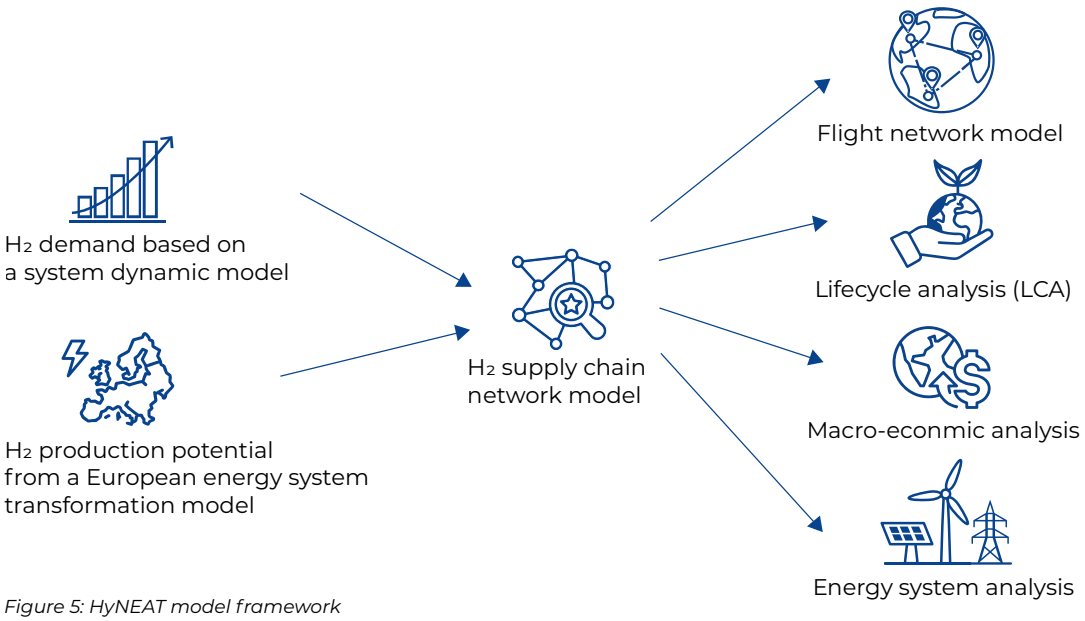

Figure 5: HyNEAT model framework

2.3 Methodology for the individual studies

In the following, the applied models in this study are briefly introduced. All costs in this report are stated in USD2023, with literature values corrected to USD using a conversion factor of 1.09 EUR/USD. The inflation effects are considered using the Chemical Engineering Plant Cost Index (CEPCI) to convert the assumptions to USD2023 [38]. The techno-economic assumptions in this study are shown in Appendix C. It is important to note that, the cost assumptions used in this study represent only one possible development path. A more robust assessment of future costs would require a comprehensive sensitivity analysis. However, due to the high computational effort and long runtimes of the applied models, such an analysis is not feasible within this study. As the main source of emissions, only commercial aviation is included in this study.

2.3.1 System dynamics model for the hydrogen demand scenarios

To estimate the future LH_2 demand in European aviation, a system dynamics model was developed within the project. System dynamics enables the modelling, simulation, and analysis of complex socio-technical systems and is particularly suited to exploring interdependencies, feedback loops, and time delays between stakeholders. By capturing both short- and long-term behavioural dynamics, the method allows for a better understanding of systemic developments and transformation processes.

The aviation sector involves several interacting stakeholders whose decisions mutually influence one another. In the model, the focus lies on three main actors: aircraft manufacturers, airlines, and airports. Their interactions determine the pace and scale of H_2 adoption within the aviation sector. To explore these interdependencies, a dynamic hypothesis was formulated. Aircraft manufacturers produce H_2-powered aircraft that airlines can order. Airlines will only order such aircraft if LH_2 infrastructure is available at their operating airports. Conversely, airports will only invest in LH_2 infrastructure if there is sufficient airline demand. This creates a “chicken-and-egg” problem.

The model considers a single airline sector operating a fleet across different route segments: regional, short-, medium-, and long-range. Passenger numbers are allocated to these route segments over time based on airport-specific flight volume data and country-specific demand forecasts. The resulting passenger demand must be covered by the airline fleet. This fleet comprises both operational and maintenance-phase aircraft. When passenger demand exceeds available capacity, the airline orders new aircraft in the affected segment. At the time of ordering, the decision between kerosene-based and H_2-powered aircraft, if available on the market, is made based on the total cost of ownership (TCO). In addition, parameters such as aircraft size, seat load factor, maintenance costs and duration, and aircraft lifetime are considered for each segment. This allows for a reflection of realistic fleet renewal cycles and investment behaviour.

Aircraft manufacturers responding to airline demand. They produce aircraft in accordance with incoming orders, taking into account production backlog. Production capacity is modelled as a dynamic variable that can increase over time, influencing the lead time between order and delivery. This feedback mechanism ensures that the model captures how manufacturing constraints and gradual capacity expansions affect the availability of H_2-powered aircraft.

Airports act as infrastructure providers within the system. To circumvent the infrastructure dependency challenge described earlier (the “chicken-and-egg” problem), it is assumed that the necessary LH_2 infrastructure becomes available at every airport as soon as it is required by the airline sector. This simplifying assumption is justified by modelling the initial H_2 supply as truck-based delivery, which requires only limited infrastructure investment. Further details on infrastructure, investment needs, and cost implications are provided in Section 4.2.

Based on the interactions among the three stakeholders, the system dynamics model enables the estimation of European LH_2 demand for future aviation operations. Passenger demand at airports is allocated to the route segments and combined with the market penetration of H_2-powered aircraft. From this, the LH_2 demand per airport and over time can be derived. By aggregating across all airports, the model provides an estimate of the total LH_2 demand for the European aviation sector.

2.3.2 Energy system transformation model (ESTRAM)

To assess the potential H_2 production volumes and costs, an energy system transformation model is developed. As part of the defossilization of the energy system, many sectors currently supplied with fossil fuels will be electrified. However, certain sectors remain particularly challenging to electrify. These so-called hard-to-abate sectors include not only specific processes in the industry but also transportation, with aviation standing out as a critical example.

The key challenge, therefore, lies in the transition of today's energy system in a way that ensures that future energy demands across all sectors can be met while adhering to the remaining carbon emission budget. To address this, the energy system transformation model (ESTRAM) is developed, which optimises transition pathways from the present energy system to a highly renewable one under macroeconomic considerations. The objective of ESTRAM is to identify and evaluate possible pathways for the energy transition, thereby providing insights into feasible strategies for achieving climate targets. The optimisation framework ESTRAM is based on a spatial and temporal discretisation of the European energy system. For the spatial representation, the NUTS (European Union Nomenclature of territorial units for statistics) classification down to the NUTS-1 level is used, corresponding to distinct European regions. Temporally, the model operates with a five hourly resolution, capturing the evolution of the energy system from the present up to 2050.

As a first step, data on the current energy system are collected, including existing power plants and the installed capacities of RES such as photovoltaics and wind power. Each spatial node, representing a NUTS-1 region, is modelled to exchange energy with neighbouring nodes. This is enabled through the integration of existing European transmission grids, as well as the inclusion of planned future grid expansions. In addition to supply-side data, sector specific energy demand profiles are compiled. These demands are projected into the future by accounting for factors such as demographic developments and renovation rates of the building stock. Coupling of sectors is performed via the introduction of sector coupling technologies such as battery-electric vehicles or heat pumps.

The collected data form the basis for the optimisation problem, which is formulated as a linear programming (LP) model. Subsequently, ESTRAM determines the cost-optimal dimensioning of energy sources, converters, storages and consumers. A variety of constraints are incorporated into the LP to ensure realistic and policy-consistent outcomes. These include the energy balance at each individual node and at all times, annual limits on the expansion rate of renewable energy technologies, and the remaining lifetimes of existing power plants. Furthermore, the optimisation is constrained by an annual carbon emission limit, with explicit consideration of national climate strategies and regulatory frameworks where such information is available.

The LP model is solved with the objective of minimising the total energy system costs. For this, techno-economic assumptions have been made for all relevant system components, including RES, storage technologies, consumer, and converters such as electrolysers. These assumptions (shown in Appendix C) include values for the capital expenditures (CAPEX), operational expenditures (OPEX), component lifetimes and technical parameters such as conversion efficiencies for each step of the transition path. This approach enables ESTRAM to identify least-cost transition pathways while remaining consistent with both system limitations and political targets. The result contains both dimensioning and dispatch of all components for all nodes and timesteps of the model. On a global scale, ESTRAM is used to calculate import costs of green H_2 from production sites around the world. To this end, global island energy systems are modelled consisting of electrolysers coupled with photovoltaics and wind power and determine the marginal costs of the produced H_2.

2.3.3 Hydrogen supply network model

To determine cost-optimal H_2 supply chain networks (HSCNs) for aviation, a mixed-integer linear programming (MILP) model is developed that captures strategic infrastructure decisions and operational H_2 flow planning across a spatially and temporally resolved network. The model minimizes the total model cost of the H_2 network, including capital expenditures, operational costs, and maintenance for all facilities and transport infrastructure.

Strategic decisions in the model include where and when to invest in H_2 production, import terminals,

liquefaction plants, storage facilities, and transportation modes, along with their respective capacity levels. At the operational level, the model determines the amount of H_2 to be produced, transported, stored, and delivered. It accounts for spatial and temporal variation in H_2 supply and demand, the resulting variations in H_2 production costs, and specific H_2 handling characteristics such as losses during transport and storage.

The models include constraints to ensure that airport LH_2 demand is met, supply limits are respected, and all H_2 flows are balanced throughout the network. It enforces capacity limits for facilities and transport assets, ensures stock consistency over time at storage locations, and incorporates handling losses. All decisions are subject to logical and technical feasibility requirements, including investment timing and minimum deployment thresholds. The model was implemented in Python and solved using the Gurobi Optimizer. The model is tested in case studies and results provide valuable insights into the optimal structure and cost of H_2 supply for aviation. The results of the H_2 supply network model describe which airports are supplied by specific production hubs, the transport modes employed under the varying conditions, the roles of storage and liquefaction, and the resulting LH_2 supply costs at each airport. They also comprise a detailed cost breakdown across all supply chain components, supporting data-driven infrastructure planning and policy decisions. Details of the H_2 supply network optimization model are provided in Appendix C.

2.3.4 Flight network model

The Hydrogen Aviation Network Problem (HANP) addresses the strategic challenge of integrating H_2-powered aircraft into an existing aviation network, with the goal of minimizing overall operating costs while accounting for technical, logistical, and economic constraints. It is framed as a MILP that captures essential decisions about routing, aircraft type allocation, fuel logistics, and infrastructure limitations.

At the heart of the model lies a network representation of the aviation system, where airports are modelled as nodes and flight legs as arcs. Each flight can be operated by either kerosene- or H_2-powered aircraft. The model assumes kerosene supply is unconstrained and costs are distance-based, while H_2 is treated as a limited, location-dependent resource with varying costs, adapted from the costs at the different airports computed with the Hydrogen Supply Network Model in Section 4.2, and restricted availability, coming from the LH_2 demand of different airports computed in the system dynamics model presented in Section 3.3.

Passenger demand between origin–destination pairs is served via two parallel flow systems – one for each propulsion type. These flows are governed by conservation constraints to ensure demand is met and that passengers are neither lost nor artificially created in the network.

To capture the operational feasibility of H_2-powered aviation, the model includes:

- range constraints on H_2 aircraft,
- airport-level H_2 availability caps, and
- a market penetration parameter to reflect future fleet limitations, adapted from the results in Section 3.3.

A core component of the model is its treatment of H_2 transport within the network. Since H_2 may be more economically sourced at specific nodes, the model allows for fuel to be carried across multiple flight legs, subject to per-passenger transport capacity limits. This is operationalized through the concept of H_2 excess paths, which track how H_2, purchased at one airport, can be used downstream at another.

Finally, the objective function seeks to minimize total costs, including maintenance and fuel, for both aircraft types, while complying with all technical and logistical constraints. The resulting MILP provides an integrated decision-support framework that combines route planning and fuel logistics into a single optimization model.

Due to the high dimensionality and combinatorial nature of the problem, solving the model directly is computationally intensive. Therefore, a dynamic programming labeling algorithm is developed called Hydrogen Aviation Network Labeling Algorithm (HANLA) to reduce the problem size by intelligently filtering the feasible solution space, making the approach tractable for larger networks.

2.3.5 Life cycle assessment

This study applies a cradle-to-grave Life Cycle Assessment (LCA) in accordance with ISO 14040/14044 to quantify the climate impacts of H_2 supply chains for aviation. The functional unit is 1 kg of LH_2 available at the aircraft refueling point. The system boundary spans H_2 production via electrolysis, liquefaction, gaseous and liquid storage, pipeline transmission, maritime and road transport as well as airport refueling infrastructure.

Foreground processes are parameterized for 2050 under SSP2 (Shared Socioeconomic Pathway 2 “Middle of the Road”). Energy inputs for electrolysis, liquefaction and compression are provided by project partners. Background data are sourced from Ecoinvent 3.9.1 via the Activity Browser, with European-average SSP2 projections from Premise to ensure consistent future energy mixes and technology assumptions. Impacts are calculated with ReCiPe 2016 (H) midpoint v1.03, focusing exclusively on Global Warming Potential (GWP100 in $kgCO_2$-eq).

2.3.6 Cash-flow model

For the evaluation of business models and policy instruments, a multi-period energy system optimization is applied. In order to incorporate the timing of investment decisions, the cash-flow method was employed. The infrastructure and associated costs are determined using a bi-level optimization model based on Schenke et al. [39]. On the top level, the design of the LH_2 supply components is optimized. For each design, a linear dispatch optimization is conducted on the bottom level for the individual years analysed. This ensures that the transition path of the design is viable and allows for the calculation of OPEX. Given the assumption of a three-year step size in this study, the model accounts for five distinct investment periods. The model‘s output is the cost-optimal infrastructure design for these five investment years, which are then analysed as individual project components to determine the resulting LH_2 price. This analysis assumes staggered investments with individual payback periods that vary depending on the stakeholders involved. As discussed in prior research, off-take agreements could be a valuable mechanism to mitigate high initial costs and guarantee supply security. Consequently, a constant price is assumed for each investment period in this study. To accurately reflect the pricing of already amortized components, the opportunity cost of capital is utilized. This reflects the forgone return from using an already depreciated asset for the LH_2 supply instead of allocating it to an alternative investment. Multiple stakeholder constellations are evaluated with the main difference being their financial criteria, specifically their Weighted Average Cost of Capital (WACC) and Return of Invested Capital (ROIC) after a specific payback period.

2.3.7 Macroeconomic analysis

The macroeconomic potential of future LH_2 infrastructure is analysed in selected countries. A particular focus lies on socioeconomic indicators, including employment and household income. While input-output (IO) modelling is the conventional approach for such analyses [40–42], it is deficient in terms of socioeconomic detail [43,44]. Therefore, this study employs a Social Accounting Matrix (SAM)-based multiplier model [45–47].

A SAM is a data framework that captures transactions within an economy for a particular period [48]. Next to production, trade, consumption, and investment, the SAM integrates income distribution across institutional sectors [49], which is essential for capturing the broader socioeconomic implications of LH_2 supply chains [50]. The SAM construction is based on supply and use tables and national accounts data from governmental institutions, mostly national statistical offices. A detailed overview of the construction and data sources used is provided in Appendix C.

The challenge inherent in this study pertains to the forward-looking nature of LH_2 infrastructure that does not yet exist and thus is not represented in official macroeconomic data. Typically, SAMs encompass between 50 and 100 economic activities and a comparable range of commodities, contingent upon the characteristics of the country under consideration. The activities and commodities cover aggregated categories of relevant industrial sectors, such as agriculture or manufacturing of vehicles. To integrate

a novel LH_2 industry into the framework, a multi-stage procedure is employed, consisting of supply chain analysis and synthetic industry construction [51].

First, LH_2 supply costs are disaggregated into 15 technologies, using the techno-economic inputs from other working packages. For each technology, CAPEX and OPEX are separated. These are subsequently translated into three phases of economic activity: (1) key component manufacturing, (2) installation & balance of plant (BoP) supply, and (3) operation. Next, a detailed supply chain analysis is conducted for all phases of each technology [52]. Based on techno-economic literature, the phases are broken down to receive a detailed composition of the cost components. Finally, the cost components are assigned to industries outlined in the SAM (LH_2 enabler activities), using the internationally standardized classification of economic activities (ISIC) [53]. As a result, synthetic LH_2 industries are constructed for the three phases [45,51].

Prior to the macroeconomic analysis of LH_2, a linkage analysis is performed to show the relevance of the air transport system in Europe's economy [42,45,54]. Subsequently, the structural potential for countries to gain from LH_2 infrastructure is examined. In addition, a multiplier analysis reveals broader impacts from the scale-up of LH_2 infrastructure on key economic indicators, namely production levels, gross domestic product (GDP), household income, and employment. The multipliers in the selected countries are quantified for an exemplary LH_2 network in 2050 under different economic scenario conditions. The scenarios vary in terms of domestic production shares, import dependency, and capital sources, reflecting different potential cases of a transboundary LH_2 network. Finally, total effects within a transition phase are quantified for Europe, based on the techno-economic analysis of the project.

SCENARIO DEFINITION AND LIQUID HYDROGEN DEMANDS

3 Scenario definition and liquid hydrogen demands

In this chapter, the scenario framework and the resulting LH_2 demand for European aviation are presented. Section 3.1 provides an overview of the scenario approach and the resulting LH_2 demand trajectories. Following on this, Section 3.2 describes the model structure and data setup used for the simulations. Section 3.3 defines the three policy and market scenarios (Baseline, Ambitious policy, and Moonshot) while Section 3.4 presents the model results, including fleet development, total European LH_2 demand, and airport-specific demand profiles.

3.1 Scenario overview and resulting liquid hydrogen demands

To investigate the potential transition of the aviation sector towards the use of H_2 as an energy carrier, future LH_2 demand must be estimated over time. These demand trajectories form the basis for designing and dimensioning the required H_2 infrastructure. The estimation of LH_2 demand is carried out using the system dynamics model described in Section 2.3.1, which captures the interactions between aircraft manufacturers, airlines, and airports.

Within this study, a set of scenarios was developed to estimate the future LH_2 demand based on different policy goals regarding the support of H_2-based aviation, the market introduction dates of H_2-powered aircraft, and their availability. Each scenario represents a distinct policy and market pathway, reflecting varying levels of political support for H_2-based aviation, differences in entry-into-service (EIS) dates, and the rate at which H_2-powered aircraft become available. These scenarios serve as input for the system dynamics model, which simulates the resulting development of aircraft fleets and estimates the resulting future LH_2 demand over time.

The combination of passenger demand at airports, aircraft availability, and fleet composition allows for the estimation of LH_2 demand per airport and, by aggregation, for the entire European aviation sector. The scenario analysis highlights a strong coupling between policy measures and technological progress. Ambitious political support and early market entry accelerate the diffusion of H_2-powered aircraft and lead to significantly higher LH_2 demand, whereas delayed market introduction results in slower uptake and lower cumulative demand.

Baseline

EIS of H_2-powered aircraft:

- Regional-range 2045
- Short-range 2050
- Medium-range 2055

Policies:

- Standard EU ETS
- No subsidies

» LH_2 demand in 2050: **0.19 $MtLH_2/a$**

» Cumulated LH_2 demand until 2050: **0.46 $MtLH_2$**

Ambitious policy

EIS of H_2-powered aircraft:

- Regional-range 2040
- Short-range 2045
- Medium-range 2050

Policies:

- High EU ETS
- High subsidies

» LH_2 demand in 2050: **1.8 $MtLH_2/a$**

» Cumulated LH_2 demand until 2050: **5.88 $MtLH_2$**

Moonshot

EIS of H_2-powered aircraft:

- Regional-range 2035
- Short-range 2040
- Medium-range 2045

Policies:

- Ambitious EU ETS
- High subsidies

» LH_2 demand in 2050: **13 $MtLH_2/a$**

» Cumulated LH_2 demand until 2050: **47.84 $MtLH_2$**

Figure 6: Overview of the three scenarios and the resulting LH_2 demands in 2050

Figure 6 provides an overview of the three main scenarios and their resulting LH_2 demand trajectories. In the Baseline scenario with a late market introduction, total LH_2 demand reaches approximately 0.19 million tonnes ($MtLH_2$) per year by 2050 in Europe. In the Ambitious policy scenario, which assumes stronger political incentives and faster technology deployment, demand increases to around 1.8 $MtLH_2$ per year by 2050 in Europe. In the Moonshot scenario, characterised by early aircraft availability and comprehensive policy support, LH_2 demand could reach up to 13 $MtLH_2$ per year by 2050 in Europe. When considering the cumulative LH_2 demand up to 2050, the scenarios reveal a similar pattern. Approximately 0.46 $MtLH_2$ are required in the Baseline scenario, 5.88 $MtLH_2$ in the Ambitious policy scenario, and 47.84 $MtLH_2$ in the Moonshot scenario.

3.2 Modelling and scenario setup

The estimation of H_2 demand within this report relies on a comprehensive set of input data describing the current and future structure of the European aviation sector. The underlying system dynamics model uses this data to simulate interactions among airlines, aircraft manufacturers, and airports over time and to estimate the resulting LH_2 demand under different policy and market conditions. A schematic overview of the model, including the most relevant actors and their inter-relations, is presented in Figure 7.

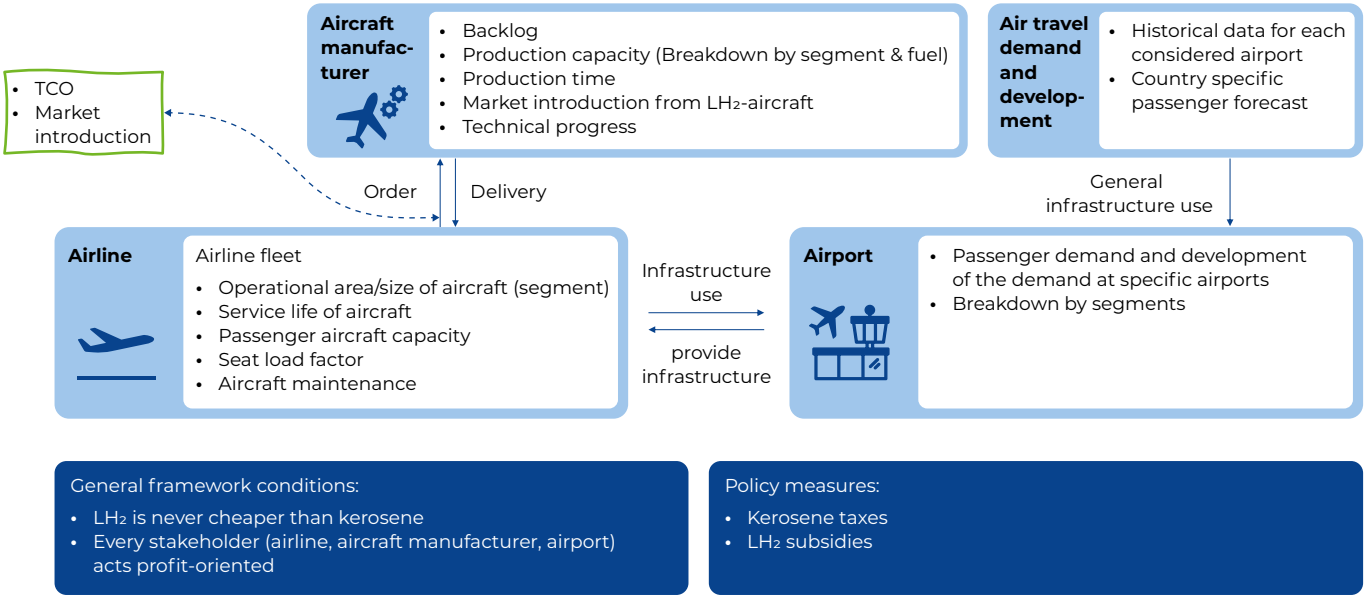

Figure 7: Subsystem diagram of the sys tem dynamics model

For the European aviation sector, several overarching assumptions were made regarding the segments in which the airline sector operates and the characteristics of H_2-powered aircraft. Passenger demand is divided into four distance-based segments: regional-range up to 500 km, short-range between 500 and 1,500 km, medium-range between 1,500 and 3,500 km, and long-range above 3,500 km. However, long-range operations are not considered in the model, as it remains technically uncertain whether H_2-powered aircraft can operate efficiently on distances greater than 4,000 km [55]. Passenger demand is estimated from Eurostat historical data and projected using country-specific growth rates provided by Eurocontrol [56]. Baseline passenger numbers reflect air traffic data from late 2024 and early 2025 [57]. These figures, combined with the respective growth rates, allow the calculation of future passenger demand at each airport included in this study.

To cover the passenger demand in each of the three operational segments, representative aircraft types were defined that operate in the segment. These include turboprop aircraft for regional-range, single-aisle aircraft for short-range, and medium widebody aircraft for medium-range. The initial fleet composition

is based on the current European commercial fleet. H_2-powered aircraft differ from conventional aircraft in several key characteristics. Due to the integration of cryogenic H_2 tanks, which require more fuselage space than kerosene tanks, their passenger capacity is assumed to be 20% lower than that of comparable conventional aircraft [36]. In addition, H_2-powered aircraft are associated with higher purchase prices and increased maintenance effort. Maintenance costs are assumed to be 14% higher, and purchase costs 10% higher, particularly in the early market phase, due to the new technological systems and handling requirements [37]. Maintenance intervals are longer than for kerosene-based aircraft, reflecting the additional inspection and safety requirements of H_2 systems. Over time, these differences are expected to diminish through technological learning and economies of scale. Similarly, the TCO used in the model for the airline's decision-making includes acquisition, maintenance, and energy carrier costs, as well as scenario-specific policy instruments such as LH_2 subsidies, CO_2 emission fees, and kerosene taxes.

Aircraft production data are based on Airbus order books and delivery statistics [58]. The model assumes an initial production backlog reflecting current market conditions. When H_2-powered aircraft are introduced to the market, production capacity for conventional aircraft is reduced by 10% to allow for the ramp-up of H_2-powered aircraft manufacturing. If delivery times exceed five years, production capacity is increased by 20% to meet demand more efficiently. These assumptions ensure that industrial adaptation dynamics are captured in the model.

3.3 Scenario definition

To analyse the potential development of H_2-based aviation in Europe, three policy and market scenarios were developed within the HyNEAT project. These scenarios describe alternative pathways for the introduction and diffusion of H_2-powered aircraft and provide the basis for estimating corresponding LH_2 demand trajectories at the airport and European level.

Each scenario reflects a distinct level of political ambition regarding H_2-based aviation and its interaction with competing technologies. They differ primarily in terms of policy instruments (including LH_2 subsidies, CO_2 emission pricing, and kerosene taxation) and the resulting timelines for the market introduction of H_2-powered aircraft. By comparing these scenarios, the model allows an assessment of how policy priorities and industrial responses jointly influence the pace of LH_2 adoption and the scale of LH_2 demand by 2050.

3.3.1 Baseline scenario

The Baseline scenario represents a conservative policy pathway in which policymakers continue to prioritise the development and deployment of SAFs as the main strategy for reducing aviation emissions. LH_2 plays only a limited role, and no dedicated subsidies or financial incentives are introduced to support its use.

Under this policy environment, the EU ETS carbon price grows moderately at 3% per year, reaching approximately 159.6 €/tCO_2 by 2050. Aircraft manufacturers adjust their innovation strategies accordingly, introducing H_2-powered aircraft only gradually and at a later stage. In this scenario, regional-range aircraft enter the market in 2045, short-range aircraft in 2050, and medium-range aircraft in 2055.

The combination of low policy support and delayed technological maturity results in a slow market uptake of H_2-powered aircraft. Consequently, LH_2 demand remains low throughout the period considered, reflecting a gradual and incremental transition rather than a transformative shift.

3.3.2 Ambitious policy scenario

The Ambitious policy scenario envisions a balanced technological approach, in which both SAFs and H_2 are actively supported to accelerate aviation decarbonisation. Policymakers strengthen regulatory frameworks and introduce targeted incentives for LH_2 production, distribution, and aircraft adoption.

In this scenario, the EU ETS carbon price increases by 5% annually, reaching approximately 323.7 €/tCO_2 by 2050. The combination of stronger policy incentives and improved cost competitiveness leads aircraft manufacturers to bring H_2-powered aircraft to market earlier than in the baseline case. Regional-range aircraft are introduced in 2040, short-range aircraft in 2045, and medium-range aircraft in 2050.

As a result, H_2-powered aircraft begin to replace conventional models earlier, particularly in the regional- and short-range segments. LH_2 demand continues to grow but remains moderate overall, reflecting a gradual yet significant step towards decarbonisation.

3.3.3 Moonshot scenario

The Moonshot scenario represents a high-ambition policy pathway focused on the large-scale transformation of aviation towards H_2 as the primary energy carrier. Policymakers introduce comprehensive support mechanisms, including substantial H_2 subsidies, additional kerosene taxes, and an accelerated increase in EU ETS prices.

The EU ETS carbon price grows by 6% per year, reaching around 477.9 €/tCO_2 by 2050. These strong policy signals and market incentives prompt an accelerated technological transition. Aircraft manufacturers introduce regional-range H_2-powered aircraft as early as 2035, short-range aircraft in 2040, and medium-range aircraft in 2045.

This early and coordinated rollout leads to rapid adoption across the European fleet and significantly increases LH_2 demand. The scenario demonstrates the scale of transformation achievable when political commitment, industrial capacity, and technological readiness are aligned towards a H_2-based aviation system.

3.4 Liquid hydrogen demands

In this section, the results regarding the development of the European airline fleet and the resulting LH_2 demand are presented. First, the evolution of the airline fleet under the three policy scenarios and the corresponding market penetration of H_2-powered aircraft is described. Following on this, the aggregated LH_2 demand for the European aviation sector are summarised and key differences between the scenarios are highlighted. Finally, airport-specific LH_2 demands are analysed and insight into regional variations as well as the influence of passenger volumes and route structures are provided.

3.4.1 Development of the airline fleet

The system dynamics model simulates the development of the European airline fleet over time, accounting for airport-specific passenger demand, aircraft lifetimes, production delays, and ordering behaviour. As passenger numbers increase, airlines expand their fleets to maintain capacity. When a new aircraft is required, a time delay occurs between the order and delivery due to production lead times and existing manufacturer backlogs. Once H_2-powered aircraft become available, airlines will decide at each order whether to purchase conventional or H_2-powered aircraft. This decision is based on the TCO, which depends on fuel prices, maintenance costs, and scenario-specific policy instruments such as H_2 subsidies and CO_2 emission fees within the EU ETS. Since these parameters differ between the three scenarios, so do the market introduction dates and adoption rates of H_2-powered aircraft.

Market penetration is calculated by comparing the number of H_2-powered aircraft to the total fleet size within each route segment. Figure 8 illustrates the fleet development for all scenarios. In the Baseline scenario, H_2-powered aircraft achieve a market penetration of around 10% in the regional-range segment by 2050, while no H_2-powered aircraft are yet in operation in the short- or medium-range segments. In the Ambitious policy scenario, market penetration reaches approximately 43% in the regional-range segment and 7% in the short-range segment by 2050. In the Moonshot scenario, H_2-powered aircraft reach 77% in the regional-range segment, 29% in the short-range segment, and 11% in the medium-range segment by 2050.

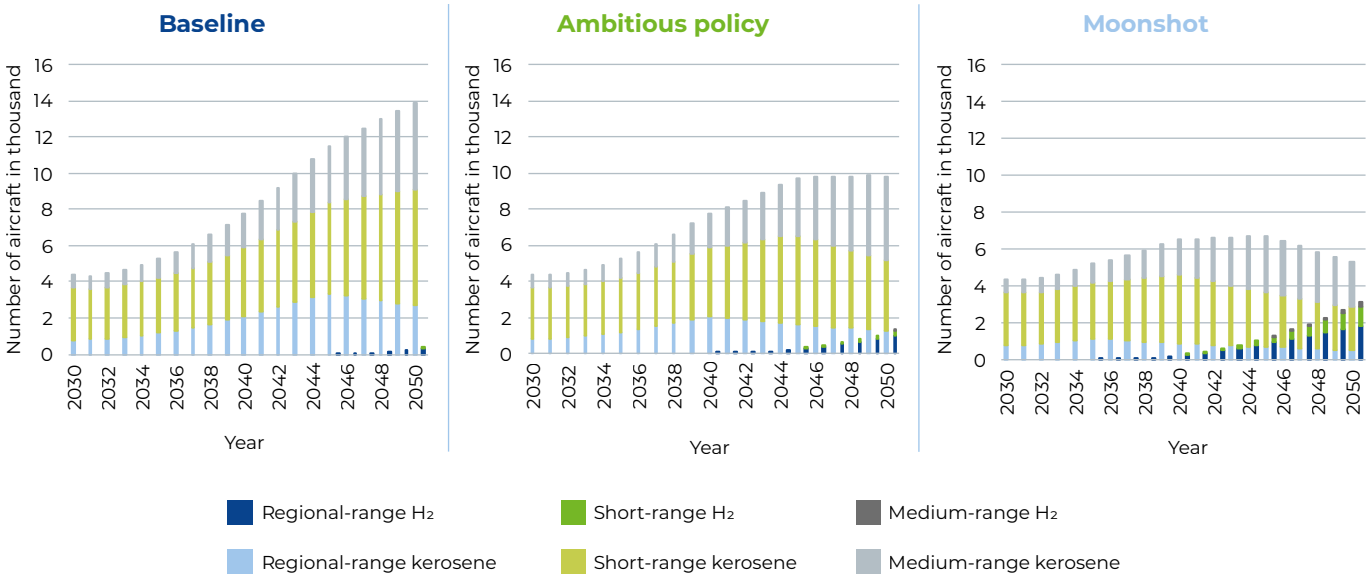

Figure 8: Development of the airline fleet in the three scenarios over time

The results indicate a substitution effect between H_2-powered and kerosene-based aircraft. As H_2-powered aircraft enter service, the number of conventional aircraft declines. Interestingly, the total number of new aircraft introduced in the Moonshot scenario is lower than in the Baseline scenario. This is primarily due to the lower production capacity for H_2-powered aircraft compared to conventional models, combined with airlines' exclusive preference for H_2-powered aircraft once their TCO becomes favourable.

3.4.2 European liquid hydrogen demand

The simulated fleet compositions result in distinct LH_2 demand trajectories across Europe. The total LH_2 demand in 2050 and the cumulated LH_2 demand until 2050 vary significantly between the scenarios:

Baseline scenario:

- Total LH_2 demand in 2050: 0.19 $MtLH_2/a$
- Cumulated LH_2 demand until 2050: 0.46 $MtLH_2$

Ambitious policy scenario:

- Total LH_2 demand in 2050: 1.8 $MtLH_2/a$
- Cumulated LH_2 demand until 2050: 5.88 $MtLH_2$

Moonshot scenario:

- Total LH_2 demand in 2050: 13 $MtLH_2/a$
- Cumulated LH_2 demand until 2050: 47.84 $MtLH_2$

These variations reflect both the different market introduction timelines of H_2-powered aircraft and the varying levels of policy support. Earlier technology availability and stronger political incentives lead to faster adoption rates and, consequently, higher LH_2 demand (see Figure 9). Across all scenarios, H_2-powered aircraft in the regional-range segment enter the market first. Due to smaller aircraft sizes and lower passenger volumes, LH_2 demand in this segment remains comparatively low. In the Baseline scenario, H_2 use is therefore limited to the regional-range segment, as short- and medium-range aircraft have not yet entered service by 2050. In the Ambitious policy scenario, short-range H_2-powered aircraft are introduced in 2045, resulting in a noticeable acceleration of LH_2 demand from that point onward. Short-range operations consume more LH_2 than regional-range flights because of larger aircraft and higher passenger volumes. In addition, higher production capacities for short-range aircraft compared to regional-range aircraft contribute to the faster growth in LH_2 demand. In the Moonshot scenario, the market introduction of medium-range H_2-powered aircraft in 2045 significantly increases overall demand. Medium-range flights show the highest LH_2 consumption per aircraft and per passenger segment due to larger aircraft sizes and higher passenger numbers. As a result, the overall LH_2 demand grows most rapidly in this scenario, reflecting the combined effect of early technology deployment, higher production rates, and comprehensive policy support.

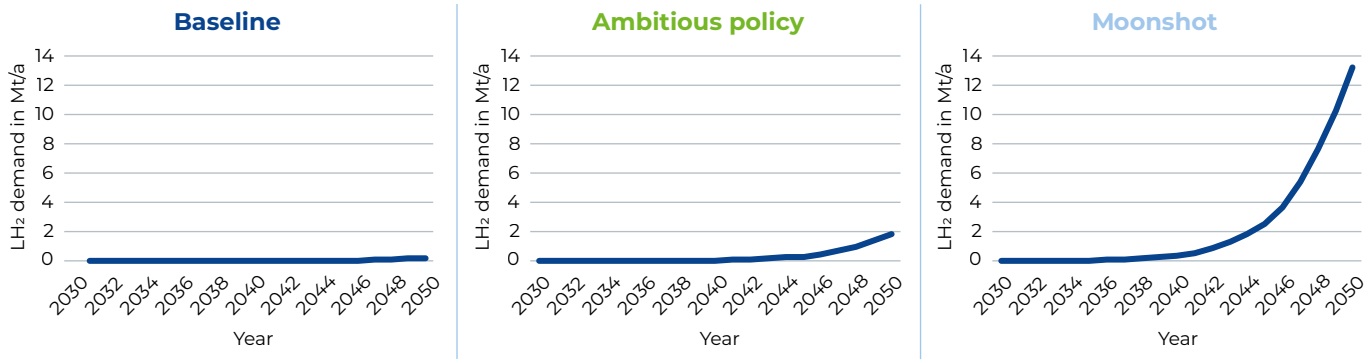

Figure 9: LH_2 demand of the European aviation sector over time

3.4.3 Airport-specific liquid hydrogen demand

To analyse the spatial distribution of H_2 demand across Europe, airport-specific LH_2 consumption was evaluated within the Ambitious policy scenario. The analysis provides insights into how differences in passenger volumes, route structures, and market introduction timelines affect H_2 demand at individual airports. Figure 10 illustrates the projected LH_2 demand for several major European airports.

The results show a strong correlation between total passenger traffic and LH_2 demand. Large hubs such as Amsterdam, Zurich, Barcelona, and Warsaw exhibit the highest LH_2 requirements due to their extensive flight networks and high passenger throughput. Between 2045 and 2050, LH_2 demand increases significantly at most airports, coinciding with the market introduction of short-range H_2-powered aircraft in 2045. Airports with a large share of short-range operations experience particularly steep growth during this period.

In contrast, airports such as Dublin and Stockholm show more moderate growth in LH_2 demand, reflecting their smaller passenger base within the short-range segment. The analysis further indicates that the average flight distance and segment composition have a substantial influence on H_2 consumption. Airports with a higher proportion of short-range flights and strong passenger activity, such as Amsterdam or Barcelona, exhibit markedly higher growth rates in LH_2 demand following the technology's market introduction.

Overall, the results underline that airport-specific LH_2 demand is primarily driven by passenger numbers, route mix, and the timing of H_2-powered aircraft deployment.

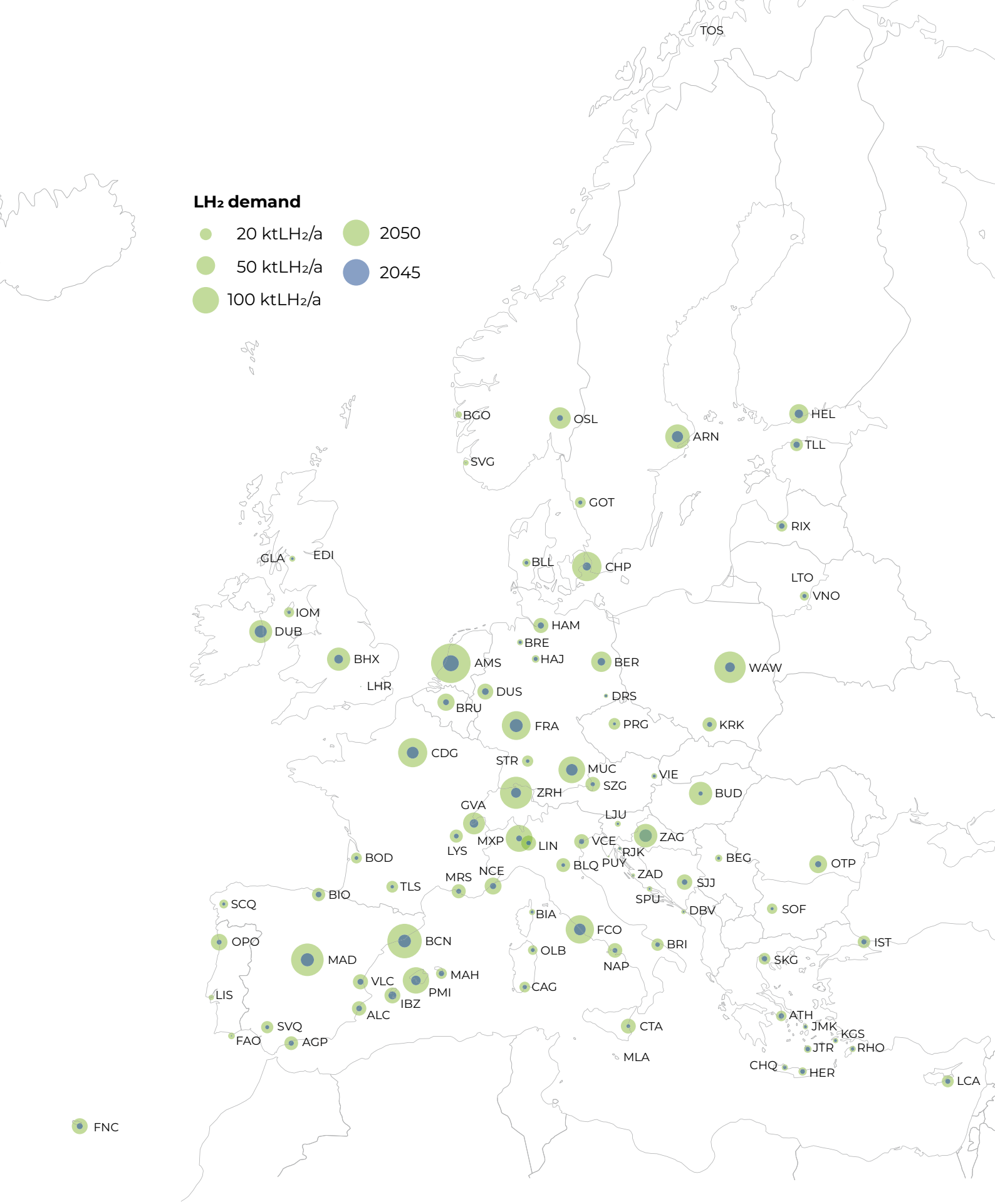

Figure 10: Overview of the airport-specific LH₂ demands in Europe within the Ambitious policy scenario

To further investigate the spatial distribution of LH_2 demand, selected airports were analysed in greater detail. The airports of Stuttgart, Hamburg, and Amsterdam were chosen due to their active involvement in research and innovation projects and their strong interest in future-oriented aviation technologies, such as H_2. The resulting LH_2 demands for the three selected airports in the three scenarios are depicted in Figure 11. The specific LH_2 demands for all airports considered in this report can be found in Appendix C.

In the Baseline scenario, LH_2 demand in 2050 remains limited to the regional-range segment, since short- and medium-range H_2-powered aircraft have not yet entered service. In this scenario, Hamburg airport requires approximately 2 $ktLH_2$ per year, Stuttgart 0.6 $ktLH_2$, and Amsterdam 12 $ktLH_2$.

In the Ambitious policy scenario, earlier market introduction and stronger policy support lead to higher adoption levels. LH_2 demand increases to about 9.5 $ktLH_2$ per year in Stuttgart, 17 $ktLH_2$ in Hamburg, and 118 $ktLH_2$ in Amsterdam. The high value for Amsterdam results from both higher passenger volumes and a strong concentration of flights in the short-range segment.

In the Moonshot scenario, LH_2 demand grows substantially due to the accelerated diffusion of H_2-powered aircraft across all segments. Stuttgart Airport reaches approximately 83 $ktLH_2$ per year in 2050, Hamburg 118 $ktLH_2$, and Amsterdam 674 $ktLH_2$. The higher values at Hamburg and Amsterdam reflect their large passenger bases and their significant share of short- and medium-range flights. Across all airports, LH_2 demand is dominated by the medium-range segment, as larger aircraft with higher seat capacities consume more LH_2 per flight. Nevertheless, total LH_2 demand is also strongly influenced by passenger numbers and route structure. While Hamburg and Stuttgart have high passenger volumes in the medium-range category, Amsterdam's demand is concentrated in the short-range segment due to its extensive network of intra-European connections.

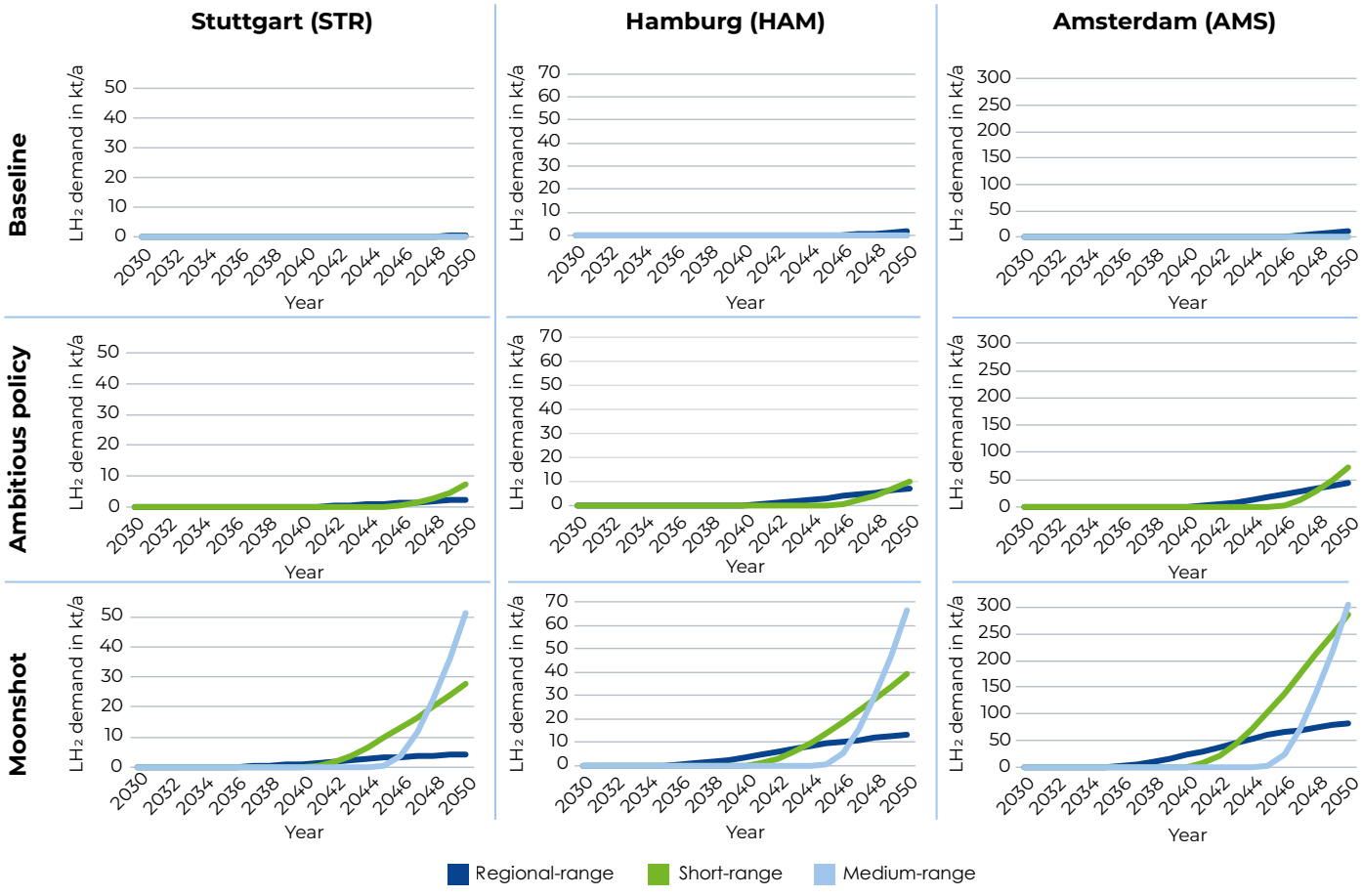

Figure 11: LH_2 demands for the three demand scenarios at selected airports

LIQUID HYDROGEN SUPPLY FOR H_2-POWERED AVIATION

4 Liquid hydrogen supply for H_2-powered aviation

In this chapter, the LH_2 supply infrastructure will be discussed first for archetypical airports to show general effects of the energy system analysis and discuss design rules for LH_2 energy systems. Following, in Section 4.2, the LH_2 supply network for a European airport network will be discussed for a target picture in the year 2050. As the resulting LH_2 supply costs at the airports vary significantly, in Section 4.3, future flight networks are analysed for the airport network. Finally, the transition phase for a LH_2 supply network is discussed based on a case study for nine German airports in Section 4.4.

4.1 Liquid hydrogen supply for archetypical airports

In this section, the LH_2 supply for archetypical airports is evaluated with an island energy system approach, meaning there is no connection to either the electrical grid or an H_2 market. The required H_2 therefore has to be produced with the electricity from the dedicated built wind and PV power systems. For this section the target picture for the year 2050 is analysed. First, the on-site LH_2 supply costs will be evaluated for different locations and LH_2 demands and subsequently the off-site LH_2 supply costs will be analysed based on the transport distance.

4.1.1 On-site liquid hydrogen supply

Figure 12 shows the resulting LH_2 supply costs for a generic airport at four different locations: PV – a location with high solar radiation, WIND – a location with good conditions for wind turbines, GREAT HYBRID – a location with good conditions for both PV and wind power, WEAK HYBRID – a location with low solar radiation and wind speeds. For the generic airport a LH_2 demand of 50 ktH_2 based on Schenke et al. [39] is assumed, which corresponds to a larger airport in the Ambitious policy scenario as shown in the previous section. The highest cost share in most location is allocated to the RES, electrolysis and liquefaction. The storage costs are account for only a small proportion of the supply costs as well as refueling costs. The GREAT HYBRID location leads to the lowest costs as components can reach high utilization. The highest supply costs occur at the WEAK HYBRID location where a low utilization of RES lead to a large design of wind and PV power. For a more detailed evaluation of the LH_2 energy system and resulting design rules refer to Hoelzen et al. [33]. It has to be noted that This example reflects an ideal scenario with optimal conditions in terms of both the availability of renewable energies and the space available at and around the airport, and is therefore only suitable for providing general insights into the energy system analysis.

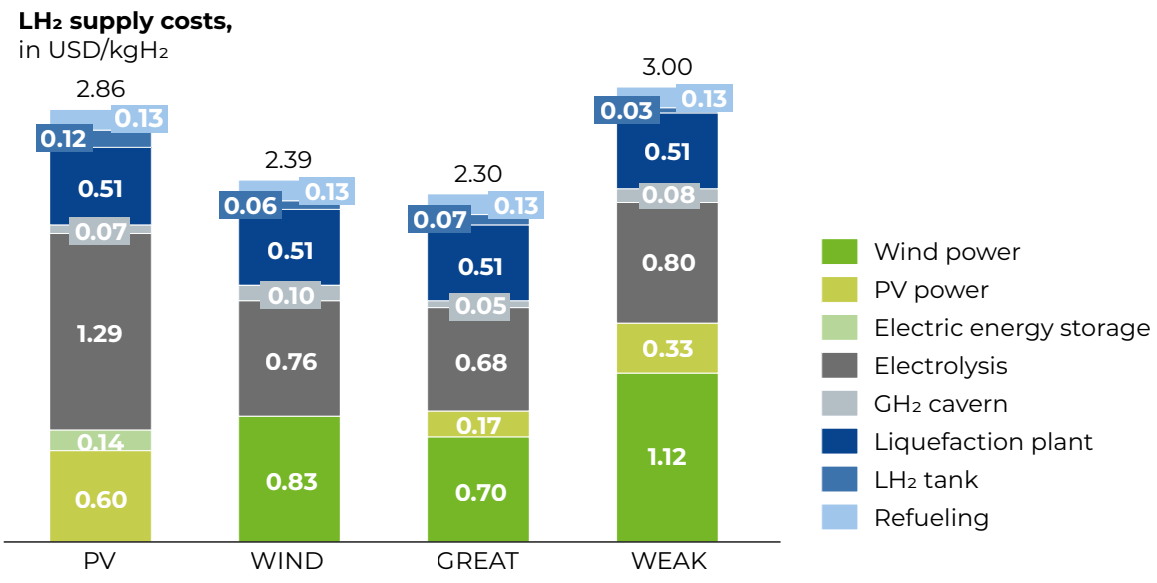

Figure 12: LH_2 supply costs for a generic airport selected locations in the year 2050

Figure 13 shows the impact of LH_2 demand at the airport on the LH_2 supply costs. For all locations, LH_2 costs are reduced with increasing LH_2 demand. This is due to two factors: First, the economies of scale of LH_2 components lead to specific CAPEX with increasing design size. Second, with higher LH_2 demand the utilization of components increases leading to lower specific supply costs.

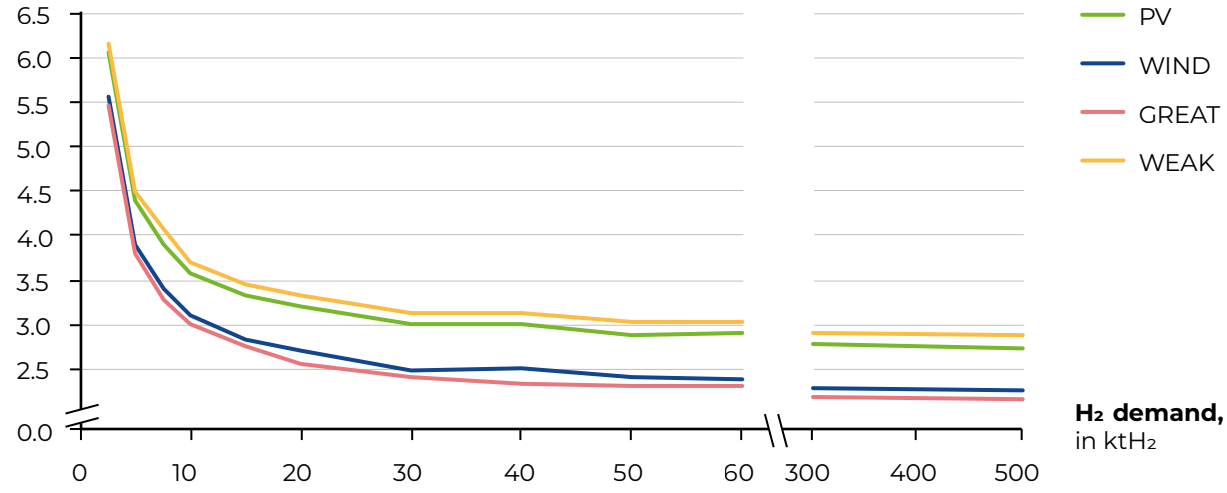

Figure 13: LH_2 supply costs at selected locations

The evaluation of the on-site LH_2 production at the archetypical airports highlights two major insights: The on-site LH_2 supply costs is highly dependent on the location and the potential for RES with a possible supply cost reduction of up to 25% at a location with very good natural conditions for RES. Second, the LH_2 demand at the airport is one of the most important influencing factors, with more than double the costs for low LH_2 demand compared to very high LH_2 demands over 100 ktH_2.

4.1.2 Off-site liquid hydrogen supply

Figure 14 shows the LH_2 supply costs for the three supply routes depending on the transport distance of the European Hydrogen Backbone (EHB), LH_2 vessel and truck. The supply costs increase linear with the transport distance for the EHB and vessel distance for the generic airport. At low transport distances under 2000 km, import via the EHB leads to lower cost compared to on-site LH_2 production. The vessel transport leads to lower supply costs if the import port is located in under 300 km of the airport. With higher truck transport distances, the transport costs exceed cost savings from better potential for RES.

As shown in this analysis, the transport distance is essential for the resulting LH_2 costs for H_2 import routes. Therefore, all H_2 supply routes has to be evaluated individually. For an in depth analysis of the LH_2 supply cost of a European airport network, refer to Hoelzen et al. [37]. The analysis also shows that the utilization of CAPEX intensive components like the liquefaction plant and transport components such as vessels and trucks are essential for low cost LH_2 supply.

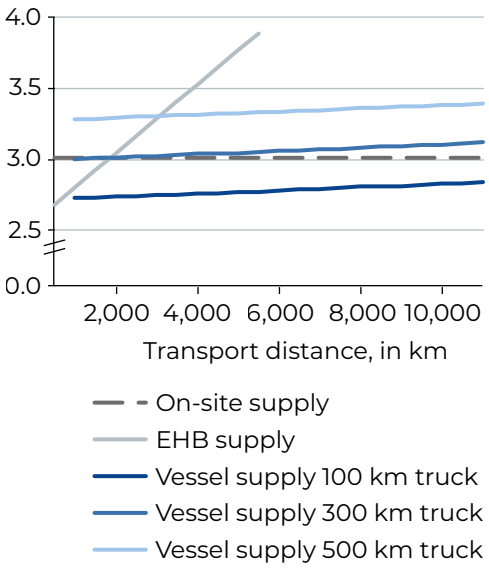

Figure 14: LH_2 supply costs for different transport distances for the supply route B: GH_2 supply and supply route C: LH_2 vessel transport Therefore, the overall LH_2 supply costs could be reduced by introducing a LH_2 supply network for European airports where the supply infrastructure is not optimized for a single airport but rather for the whole airport network. This is evaluated in detail in the next section.

4.2 Liquid hydrogen supply network for European airports

To design a cost-optimal H_2 supply network for the target year 2050, the optimization model is applied to a comprehensive case study involving 68 European airports, 18 European NUTS-1 level production hubs, and two intercontinental low-cost production hubs Chile and Morocco (see Appendix C for details). The H_2 supply for the airports not connected to the EHB are determined with island energy systems as discussed in Section 5. The network is evaluated under the three demand scenarios described in Section 3.2, namely Baseline, Ambitious policy, and Moonshot. Under the Moonshot scenario, the average network cost of LH_2, including production, storage, liquefaction, and transportation, are 4.46 USD/kgH_2, compared to 4.33 USD/kgH_2 in the Ambitious policy scenario and 4.08 USD/kgH_2 in the Baseline scenario. Although high demand yields cost reductions through economies of scale, competition for access to low-cost H_2 offsets this advantage, resulting in slightly lower overall costs in the Baseline scenario. The breakdown of the average network cost is shown in Figure 15 where large portion of the cost (around 80-85%) is incurred by H_2 production and liquefaction, depending on the demand scenario.

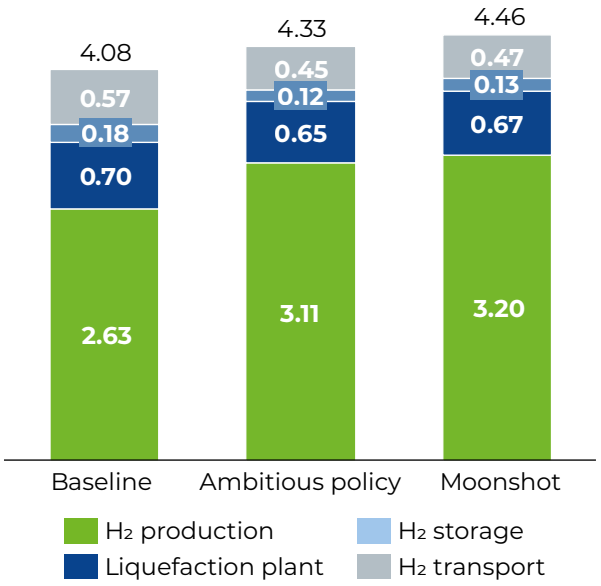

Figure 15: Average network costs for different demand scenarios with cost component breakdown

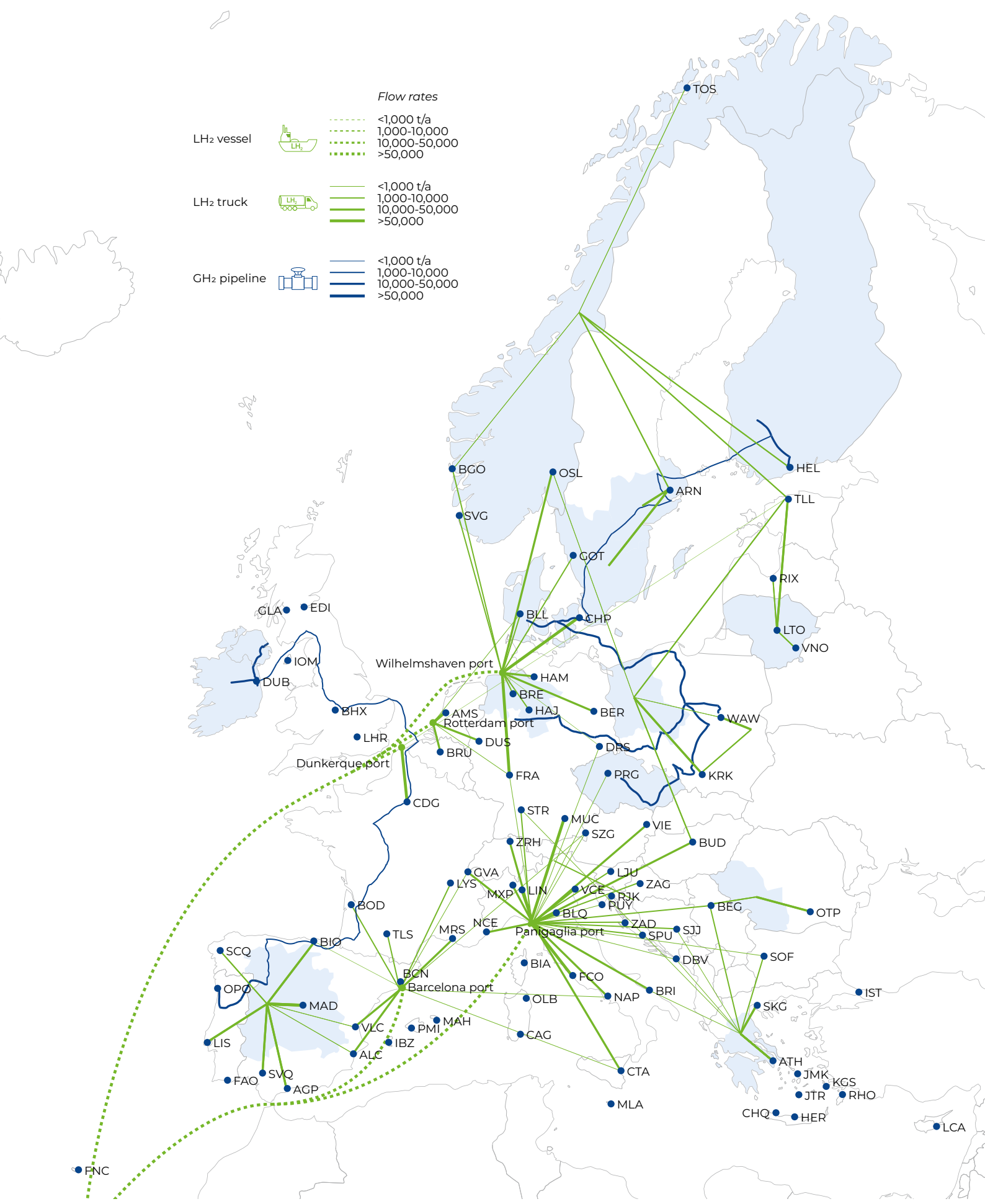

Figure 16: Optimal network map for target year 2050 for the Ambitious policy scenario

Figure 16 shows the optimal network configuration connecting the H_2 production potentials discussed in Section 5 with the LH_2 demands discussed in Section 3 for the Ambitious policy scenario. The corresponding figures for the other LH_2 demand scenarios are provided in the Appendix C. This map illustrates the supply relationships within the network, indicating which production regions supply which airports. It also highlights the major production regions under cost-optimal conditions, assuming that regional H_2 production capacity constraints are not exceeded. The primary supply originates from Chile, driven by the limited availability of low-cost production capacity within Europe. The imported H_2 is distributed to airports via major European seaports. In contrast, H_2 produced locally within the EU generally shows a pattern in which airports are supplied by geographically proximate regions.

Figure 17 presents the share of H_2 transported by different modes. The results indicate that for smaller demand levels, LH_2 vessel and truck intermodal transport and trucking are the most frequently used modes. As demand increases, the EHB and newly built pipelines also begin to account for a significant share of transportation. This is because investments in EHB connections or new pipelines become economically viable only at larger demand scales. These findings highlight the crucial role of the EHB infrastructure in shaping the future large-scale H_2 economy.

In addition, the model provides airport-specific LH_2 supply costs from production to the airport, while refuelling costs from the airport to the aircraft are calculated separately for each airport based on its individual demand. For the Ambitious policy scenario, these results are illustrated in Table 1. Airports with relatively small LH_2 demand, such as Pula (PUY) and Sarajevo (SJJ), experience high LH_2 supply and refuelling costs due to the low utilization of infrastructure components, including delivery trucks, refuelling trucks, liquefaction plants, and pipelines. In contrast, major airports such as Amsterdam (AMS) and Barcelona (BCN) benefit from economies of scale and high infrastructure utilization, resulting in comparatively lower supply and refuelling costs. Furthermore, proximity to low-cost production hubs and the EHB pipeline network significantly reduces costs. For instance, Dublin Airport (DUB), located near two cost-effective production hubs in Ireland and Northern Ireland, exhibits the lowest overall LH_2 supply cost. Overall, these findings highlight that airport-specific LH_2 supply costs are influenced by several factors, including airport size, infrastructure utilization rates, and proximity to production hubs and the H_2 pipeline network.

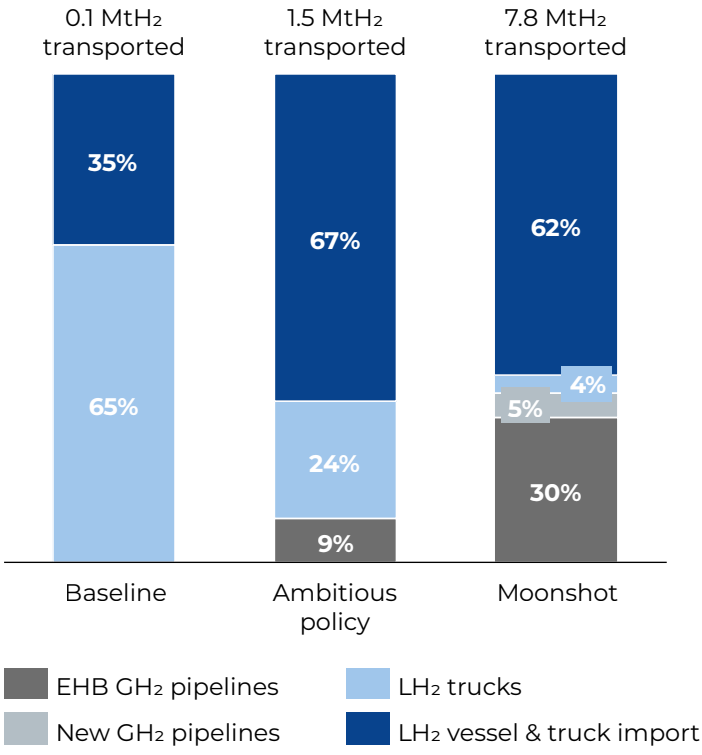

Figure 17: Share and total amount of H_2 transported by different transportation modes for the demand scenarios.

Table 1: LH_2 supply and refuelling costs at the airport network for the target year 2050 and the Ambitious policy scenario.

Airport (IATA)	H_2 supply cost, in USD/ kgH_2	Refueling cost, in USD/ kgH_2	Total supply cost, in USD/ kgH_2	Airport (IATA)	H_2 supply cost, in USD/ kgH_2	Refueling cost, in USD/ kgH_2	Total supply cost, in USD/ kgH_2
ALC	4.45	0.14	4.59	MAD	4.10	0.13	4.24
AMS	4.17	0.13	4.30	AGP	4.33	0.15	4.48
ARN	4.02	0.14	4.16	MXP	4.27	0.14	4.41
ATH	4.60	0.13	4.73	MRS	4.42	0.14	4.56
BCN	4.11	0.13	4.24	MUC	4.50	0.14	4.64
BEG	4.84	0.17	5.01	NAP	4.58	0.13	4.71
BGO	4.56	0.30	4.87	NCE	4.33	0.15	4.48
BER	4.58	0.14	4.72	OSL	4.72	0.15	4.87
BIO	4.28	0.16	4.44	BRI	4.75	0.18	4.93
BLL	4.34	0.20	4.54	CDG	4.28	0.13	4.42
BLQ	4.25	0.15	4.39	LIS	4.27	0.15	4.42
BOD	4.50	0.22	4.73	PUY	4.88	3.09	7.96
BRE	4.23	0.35	4.58	RIX	4.64	0.22	4.85
BRU	4.21	0.14	4.35	SZG	4.66	0.83	5.50
OTP	4.39	0.17	4.57	SCQ	4.27	0.18	4.44
BUD	4.91	0.13	5.04	SJJ	4.86	0.45	5.31
CTA	4.82	0.13	4.95	SVQ	4.27	0.18	4.45
CPH	4.53	0.13	4.66	SOF	4.73	0.13	4.86
DRS	4.73	0.69	5.42	SPU	4.69	0.44	5.13
DUB	3.66	0.13	3.79	SVG	4.61	0.41	5.03
DBV	4.84	0.61	5.45	STR	4.52	0.21	4.73
DUS	4.34	0.16	4.51	TLL	4.20	0.17	4.37
FCO	4.39	0.13	4.51	SKG	4.55	0.20	4.75
OPO	4.83	0.16	4.99	TLS	4.32	0.20	4.52
FRA	4.42	0.14	4.56	TOS	4.22	3.92	8.15
GVA	4.48	0.13	4.61	VLC	4.38	0.13	4.50
HAM	4.28	0.13	4.41	VCE	4.36	0.13	4.49
HAJ	4.31	0.23	4.54	VNO	4.56	0.16	4.72
HEL	4.30	0.15	4.45	WAW	3.84	0.13	3.97
KRK	4.19	0.14	4.32	VIE	4.77	0.13	4.90
GOT	4.61	0.22	4.83	ZAD	4.67	0.83	5.50
LIN	4.23	0.13	4.36	ZAG	4.68	0.25	4.93
LJU	4.58	0.37	4.95	ZRH	4.41	0.15	4.56
LYS	4.54	0.16	4.70				

4.3 European hydrogen flight networks

This section examines how the European flight network could evolve under the introduction of H_2 as an aviation fuel. The analysis draws on the H_2 network problem (HANP) presented in Appendix C, the airport-level H_2 availability and market penetration estimates from Section 3.4, and the cost assumptions for H_2 production and distribution discussed in the previous section. Within the model, H_2-powered flights are compared to conventional kerosene-powered flights and take into account that H_2-powered aircraft are only available in limited numbers by 2050.

The simulated LH_2 demand per airport from Section 3.4 serves as an upper bound for the volume of H_2 that can be utilized for outgoing flights and for H_2 transported onward as aviation fuel. Additionally, H_2-powered aircraft are assumed to remain limited in availability by 2050, reflecting gradual fleet replacement and limited production capacities. Therefore, the market penetration rate is imposed – i.e., the proportion of H_2-powered aircraft within the total operational fleet – as a further upper bound on each individual flight leg. Section 4.2 provides the corresponding H_2 cost assumptions, which vary between airports and influence the overall cost-effectiveness of H_2-powered operations.

The results indicate that, under current cost projections, flying with H_2 remains more expensive than kerosene – by approximately 0.90 USD/kgH_2 for the H_2 supply costs, even under optimistic assumptions concerning renewable energy supply, production and transport scaling. Without any additional subsidies beyond those discussed in Section 3.3, there would be no H_2-powered aviation within Europe. Only when considering an additional subsidy of 0.6 USD/kgH_2 the H_2-powered network arising from the solution to the HANP consists primarily of a limited set of routes operating from Dublin. In this scenario, approximately 2.97 million passengers are transported using H_2-powered aircraft, when investing a total of 4.27 million USD. Ireland is particularly well-suited for early H_2 deployment due to its high wind energy potential, which can facilitate cost-efficient H_2 production, and its short-haul connectivity to the United Kingdom, which falls within the expected operational range of H_2 aircraft. On these routes, round-trip H_2 operations are already feasible. In Figure 18, lighter green connections indicate flight legs where the market penetration limit is achieved, whereas darker green connections do not. The darker connection between Birmingham and Paris arises from the limited surplus H_2 refuelled in Dublin for use on subsequent flight segments. Because empty positioning flights are not permitted, the passenger volume on the Dublin routes directly constrains the available surplus H_2 on subsequent legs. As these Irish routes carry fewer passengers overall, the number of passengers that can make use of the Birmingham–Paris link is consequently limited by this smaller number.

Figure 18: H_2-powered flight network with additional subsidy of 0.6 USD/kgH_2

- *H_2-powered at market penetration level*
- *H_2-powered under market penetration level*

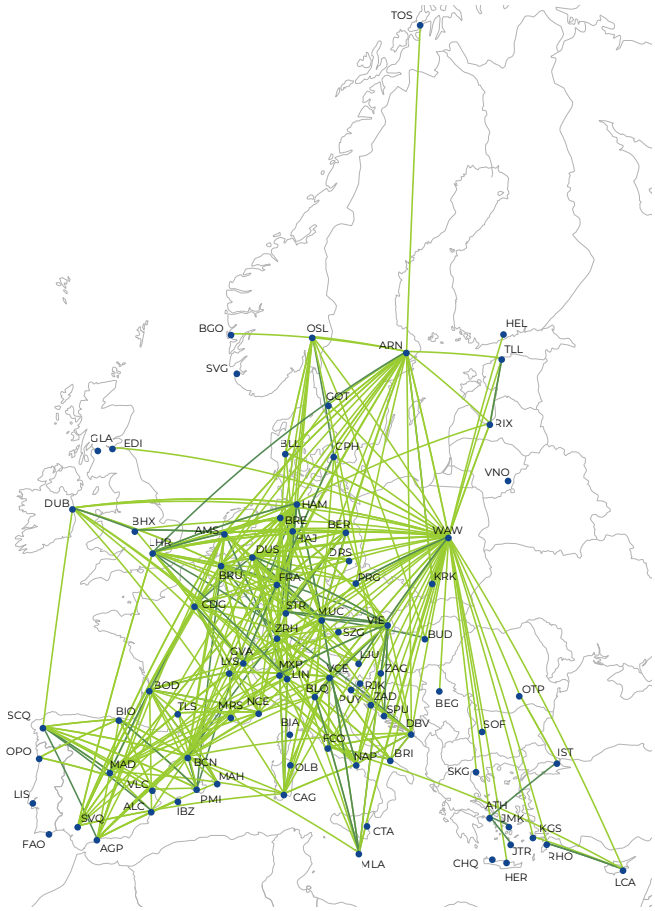

Figure 19: H_2-powered flight network with additional subsidy of 1.3 USD/kgH_2

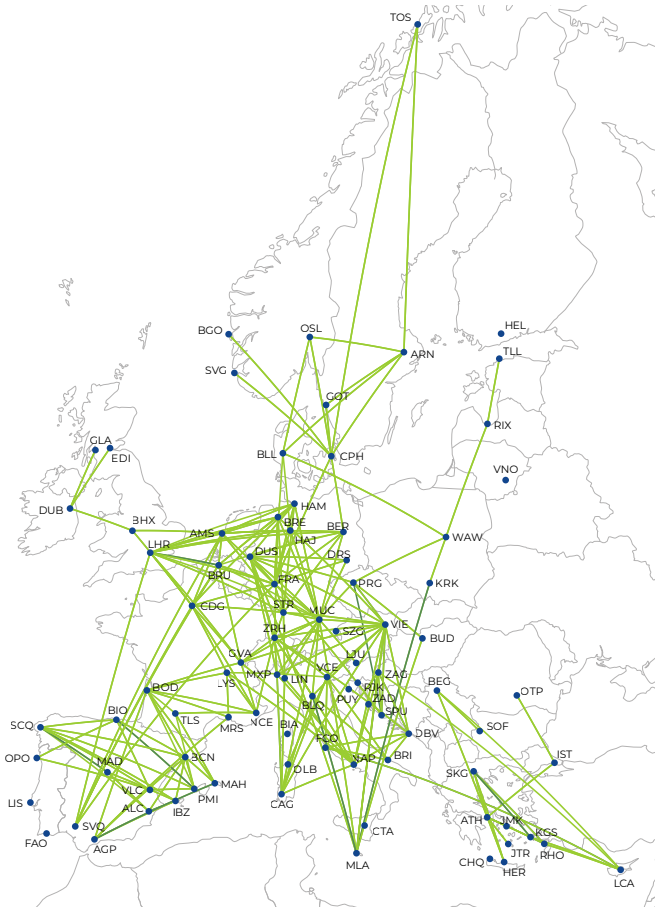

Figure 20: H_2-powered flight network with additional subsidy of 1.8 USD/kgH_2 with a threshold of 3.2 USD/kgH_2

Introducing a moderate subsidy of 1.3 USD/kgH_2 results in a total system investment of approximately 657 million USD, enabling 15.8% (around 99.1 million) of all passengers to be served by H_2-powered aviation. The resulting network is shown in Figure 20. The highest concentration of H_2 operations emerges in Germany, France, Belgium, the Netherlands, and Switzerland, where airports are geographically close and strongly interconnected. In these areas, H_2-powered aviation either reaches the market penetration limit or the full airport-level H_2 supply is utilised. Notably, a hub forms around Warsaw, where H_2 is fully used either on outgoing flights or redistributed to other destinations. This reflects the fact that airports with comparatively lower H_2 costs benefit more strongly under this subsidy regime.

When the subsidy is raised to 1.8 USD/kgH_2 and combined with a price threshold of 3.2 USD/kgH_2, i.e., no subsidy is granted once H_2 prices fall below this level, the total expenditure remains close to 473 million USD. However, this support scheme enables a larger uptake of H_2 aviation, with approximately 112.9 million passengers, or 18% of all passengers, flying on H_2-powered routes. As illustrated in Figure 19, the network continues to be concentrated in Central Europe, yet H_2 use is more evenly spread across airports, and the previously observed hub at Warsaw does not emerge. Remarkably, this broader distribution is achieved while lowering the subsidy cost by about 184 million USD resulting in a notable improvement in passenger coverage for nearly the same financial commitment.

Overall, the comparison demonstrates that carefully designed and well-calibrated subsidy strategies can substantially increase the scale of H_2 aviation with minimal additional financial effort, highlighting the cost-effectiveness of regionally targeted support mechanisms. The results further suggest that regional characteristics – such as renewable energy potential and existing network connectivity – play a decisive role in identifying airports that can act as early H_2 aviation hubs. In particular, Ireland stands out as a promising location for establishing initial H_2 aviation corridors, owing to its combination of favourable production conditions, dense short-haul network, and established international flight operations.

The end of this section provides an overview of all evaluated subsidy configurations, comparing different combinations of H_2 subsidy levels and corresponding threshold values. Figure 21 summarizes these effects: Figure 21a illustrates how the share of passengers transported by H_2-powered aircraft increases with rising H_2 subsidies, while Figure 21b shows the associated development of total subsidy costs. The comparison demonstrates that higher subsidies reliably increase H_2 adoption, but they also result in substantially higher total costs. This trade-off indicates that the effectiveness of a subsidy policy depends critically on regional production conditions and the structure of the flight network, as these factors determine how quickly H_2 becomes competitive and where additional support yields the largest impact.

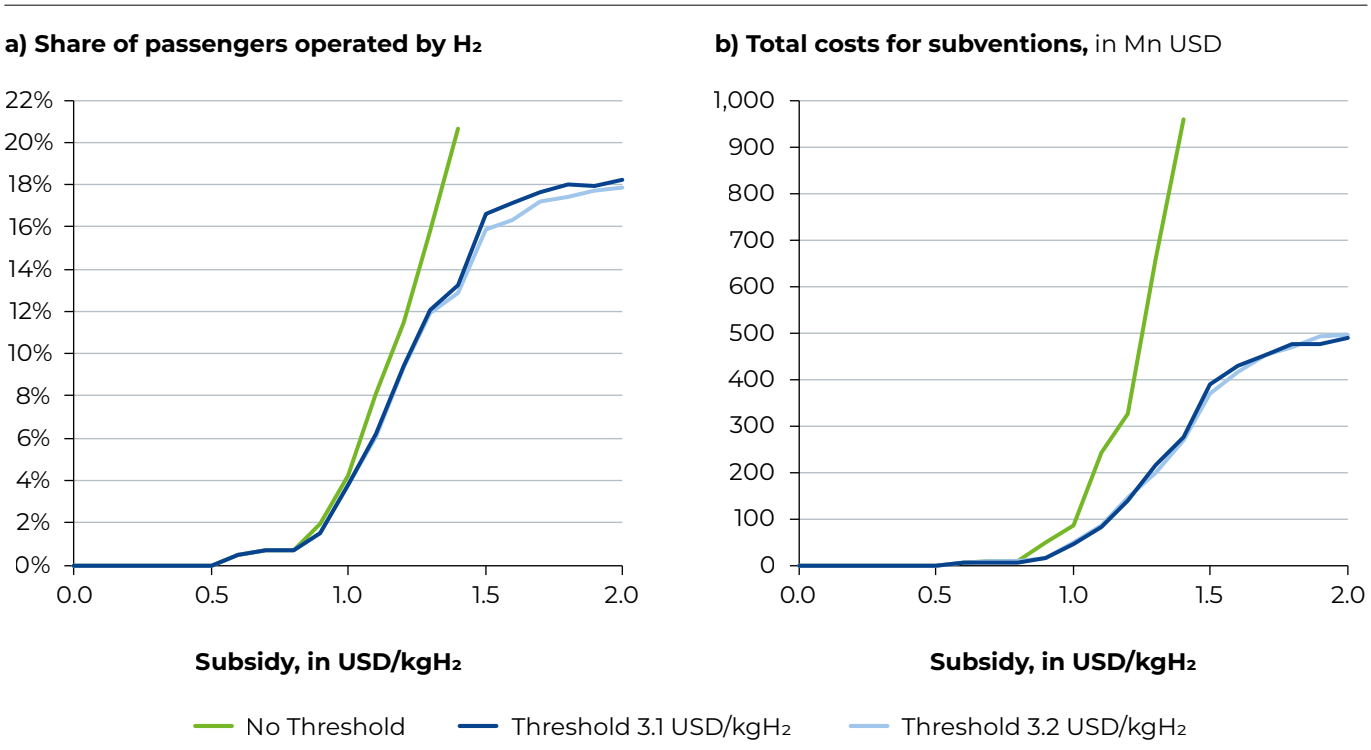

Figure 21: a) Share of passengers and b) total cost for subventions for varying subsidies

4.4 Transition phase of a hydrogen supply network

To design a cost-optimal H_2 supply network for the transition period between 2036 (when initial demand begins to emerge) and 2050 (when demand reaches maturity), the optimization model is applied to analyse the transition pathway for a case study involving nine German airports, 13 EU NUTS-1 level and two intercontinental low-cost production hubs Chile and Morocco, as well as nine underground H_2 storage structures (see Appendix C for details of the case study setting). The selected airports cover a range of sizes (small, medium, and large) and are geographically well-distributed across Germany, ensuring a representative analysis. Due to model limitations, a smaller set of airports was considered compared to the analysis for the target year 2050. Consequently, the analysis focuses exclusively on German aviation. The 13 EU NUTS-1 level and two intercontinental production hubs are chosen based on their cost competitiveness.

The period between 2036 and 2050 is analysed using a monthly temporal resolution to capture the evolution of H_2 utilization in aviation, from its initial deployment to broader market maturity. Operational decisions (e.g., H_2 flows and storage volumes) are modelled on a monthly basis, while strategic decisions (e.g., investments in production facilities and transportation infrastructure) are assumed to occur at five-year intervals. This distinction reflects the long-term nature of strategic planning, which is typically constrained by binding contracts and infrastructure commitments that limit flexibility over shorter horizons. Accordingly, the model divides the timeline into five-year strategic planning periods. The case study is evaluated under the Moonshot and Ambitious policy scenarios, yielding valuable insights into the cost dynamics of a H_2 supply network over time.

The Baseline scenario is not analysed due to the late ramp-up of demand. According to the optimal network design results (see Figure 22), the average LH_2 supply cost across the entire network in the Ambitious policy scenario is higher in 2041–2045 (5.63 USD/kgH_2) due to low demand, but declines to 4.79 USD/kgH_2 for the period 2046–2050. As demand in the Ambitious policy scenario only begins to emerge in 2041, data for the initial five-year period (2036–2041) are unavailable. In the Moonshot scenario, the corresponding costs are estimated as 5.81 USD/kgH_2, 5.14 USD/kgH_2, and 4.73 USD/kgH_2 for the periods 2036–2040, 2041–2045, and 2046–2050, respectively. Although these figures are not directly comparable with those for the target year 2050 due to differences in the network configuration and temporal setting, the average network costs for both scenarios toward 2050 exhibit a parallel trend and converge within a similar range.

These results indicate a cost reduction of more than 19% over ten years (from 2036–2040 to 2046–2050) in the Moonshot, and approximately 15% over five years (from 2041–2045 to 2046–2050) in the Ambitious policy scenario. The primary driver of this cost decline is the projected decrease in green electricity costs, which directly lowers the cost of both H_2 production and liquefaction. Additionally, the scaling up of LH_2 demand enables the system to exploit economies of scale and achieve greater efficiency across liquefaction, storage, and transportation. A significant portion of the total LH_2 supply cost – ranging between 76% and 87%, depending on the period and scenario – is attributed to the combined costs of H_2 production and liquefaction. Transportation also contributes substantially in the earlier years, accounting for for 18% of the total cost. However, with rising demand and the transition from truck-based to pipeline-based transport (see Figure 22), this share declines to approximately 12% in the later periods. Under the assumptions of the case study, including a three-day LH_2 storage buffer at airports, LH_2 storage costs account for only 1–6% of the total cost. By contrast, an additional GH_2 underground storage does not play a role in the modelled system during the analysed period (GH_2 storages are already considered for GH2 production in the transition of the European energy system see Chapter 5).

Figure 23–Figure 25 show the optimal network layouts for the respective time periods for the Moonshot scenario. The Ambitious policy scenario results are shown in Appendix C. Over time, as demand increases, new production hubs become active. In other words, the number of operational production hubs grows, and each airport increasingly receives

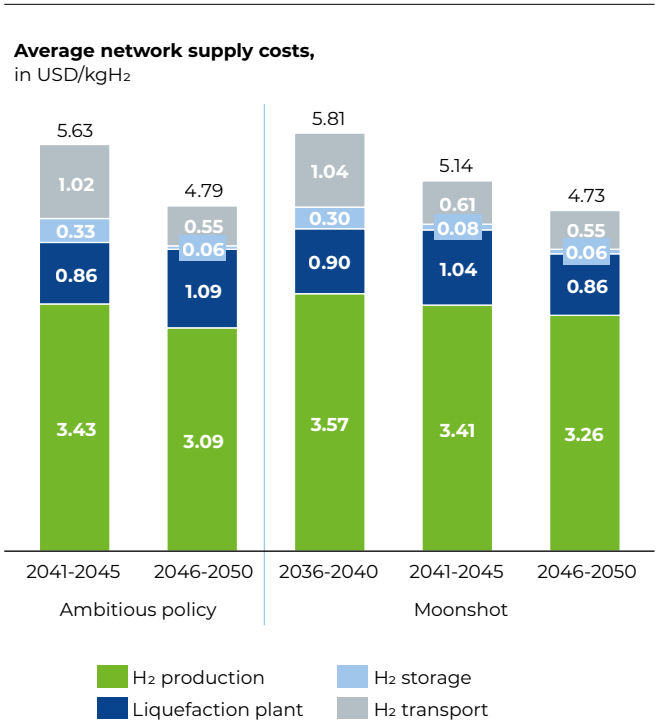

Figure 22: Average total network cost with cost component over the modelling periods and demand scenarios

supply from multiple production hubs. One reason for this is that, due to monthly production capacity limits, new suppliers must be activated to meet the increasing demand. Another contributing factor is that, while LH_2 truck transportation is preferred at low demand levels, it becomes economically less favourable as demand rises. Consequently, pipeline transport gradually replaces trucks, making it feasible to supply airports even from distant, low-cost European production hubs. For example, during the 2046–2050 strategic period, supply connections via pipelines are also emerging from locations such as Sweden and Ireland. As expected, these dynamics lead to increased network complexity over time, driven by the rising demand. Differing climate conditions across regions influences the production costs of green electricity, and consequently, the cost of H_2. As a result, airports are supplied by multiple production hubs (besides capacity and transportation mode factors mentioned above) to ensure access to the cheapest available H_2 and due to the changing monthly capacities of the production hubs. This result implies that additional underground storage is not economically favorable in this case. Producing excess H_2 during low-cost periods and storing it leads to higher costs than maintaining a diversified supply portfolio. Consequently, the model does not select an additional underground storage under the conditions of this case study. An important aspect, not accounted for in this case, is the increased

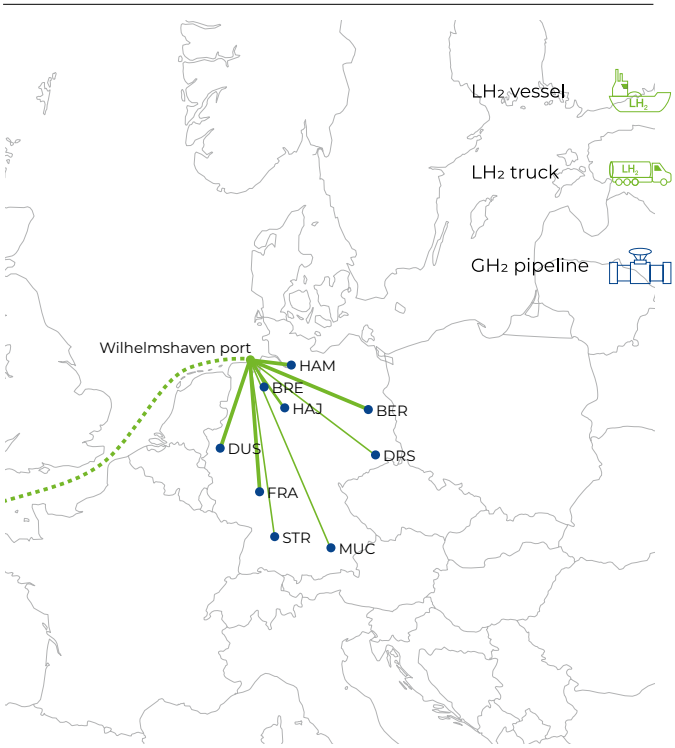

Figure 23: Optimal network map for the period 2036-2040 for the Moonshot scenario

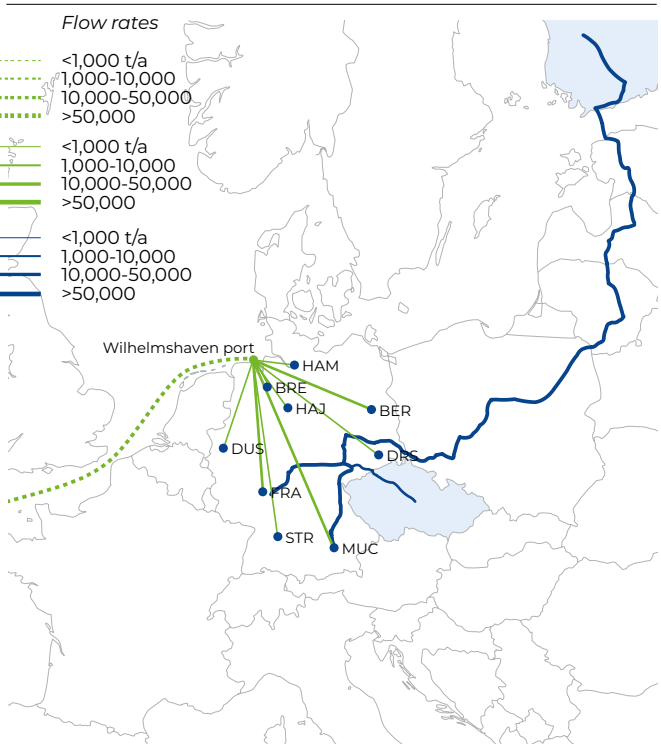

Figure 24: Optimal network map for the period 2041-2045 for the Moonshot scenario

operational complexity associated with multiple H_2 supply routes. Further constraints, such as space availability at the airport or limitations on the number of trucks that can be handled daily, may also restrict the feasibility of certain supply routes.

As shown in Figure 24, during period 2036–2040 – when H_2 demand is still low – the entire LH_2 is imported from Chile. The model avoids early investment in European small-size pipelines and liquefaction infrastructure and instead pays the additional transport costs associated with LH_2 import. Although production costs in Chile are not necessarily lower than in Europe, the infrastructure investments required in Europe are disproportionately high at such low demand levels. This illustrates that dedicated LH_2 infrastructure only becomes economically viable once demand reaches a sufficiently large scale.

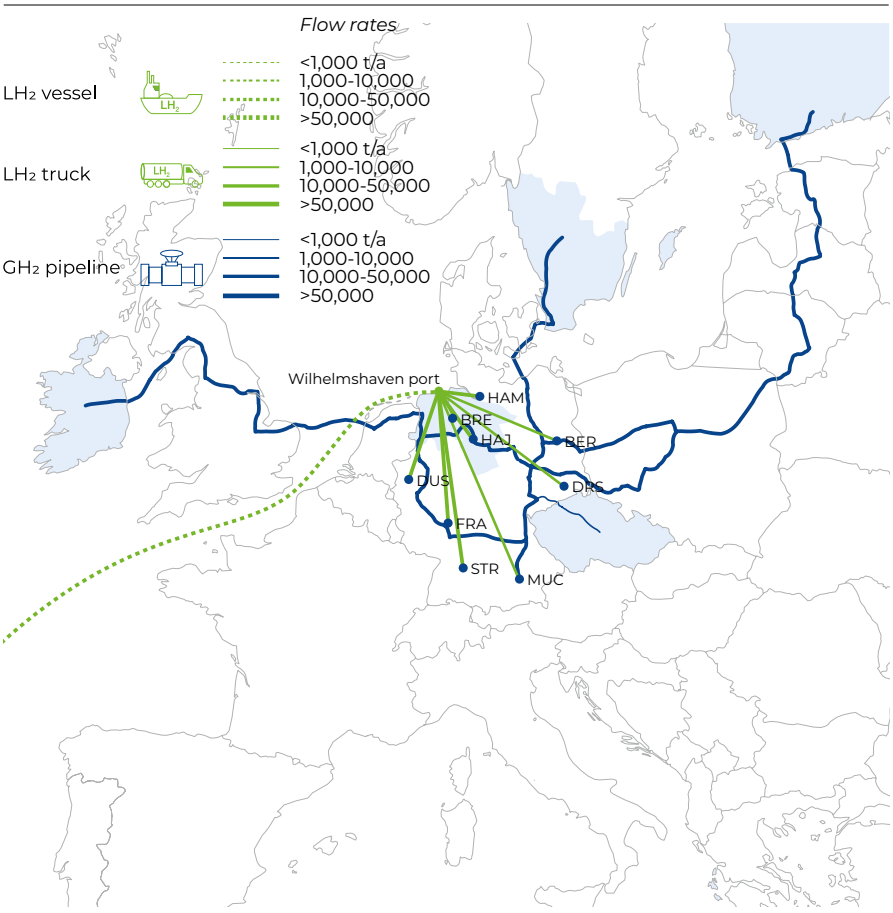

Figure 25: Optimal network map for the period 2046-2050 for the Moonshot scenario

As mentioned previously in this section, the use of trucks decreases over time as demand increases, while the share of existing pipelines (i.e. projected EHB pipelines) rises. The reason pipelines are not utilized extensively in the first strategic period is that there are still upfront investments required to connect existing pipelines to both the airports and the production hubs. These investments become economically favourable only when the scale of operations justifies them. After the first period, the share of H_2 transported via the existing pipelines increases. Details are shown in Figure 26. No new pipeline installations are observed that are independent of the EHB, indicating that even under the Moonshot scenario, the scale of LH_2 demand is insufficient to justify such high investment costs, and that production hubs located near existing pipelines are preferentially selected. The utilization of EHB pipelines can also be attributed to the well-developed backbone in Germany. Thanks to this advanced infrastructure, trucks are also less used for transportation in the latter periods.

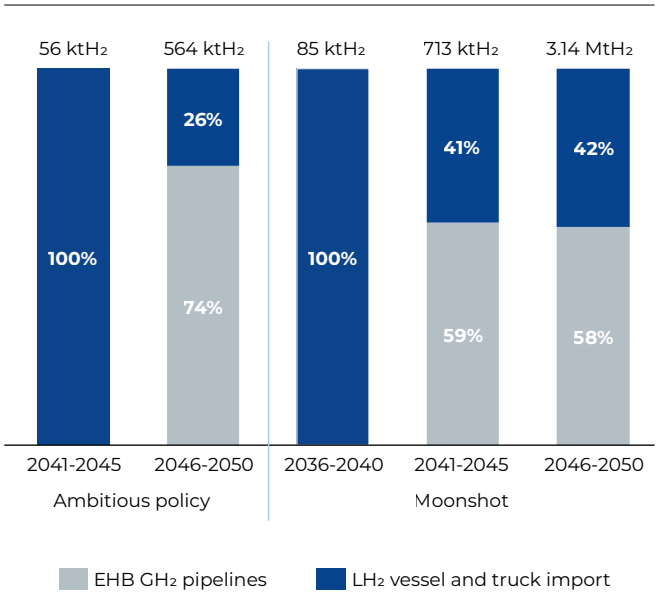

Figure 26: Transportation mode share and amount of H_2 transported for different periods and scenarios

An examination of costs at individual airports reveals a significant reduction in supply costs over the analysed time periods. Notably, the supply cost continues to decline in the final period, 19% less comparing to the first period, driven by decreasing production costs in Chile and more efficient use of transportation trucks between seaports and airports. During the 2046–2050 period, when demand is higher, airports are less affected by the inefficiencies associated with LH_2 truck transport. This results in a cost advantage for airports located closer to seaports. For instance, although Bremen (BRE) is not a high-demand airport, it exhibits the lowest supply cost due to its proximity to the selected seaport. In the initial periods, low demand leads to the low utilization of refuelling trucks, resulting in high refuelling costs. However, by the final period, refuelling costs decrease substantially, accounting for only about 7–23% of the supply cost. A strong inverse correlation is observed between refuelling cost and the level of demand at each airport. Major airports with the highest demand, Frankfurt (FRA), Munich (MUC), and Berlin (BER), experience lower refuelling costs compared to smaller airports such as Dresden (DRS). Figure 27 illustrates both the LH_2 supply and refuelling costs at each airport under the Moonshot scenario. Although the analysis covers the period 2036–2050, results for 2036–2040 are omitted from the figure due to the exceptionally high refuelling costs during that period.

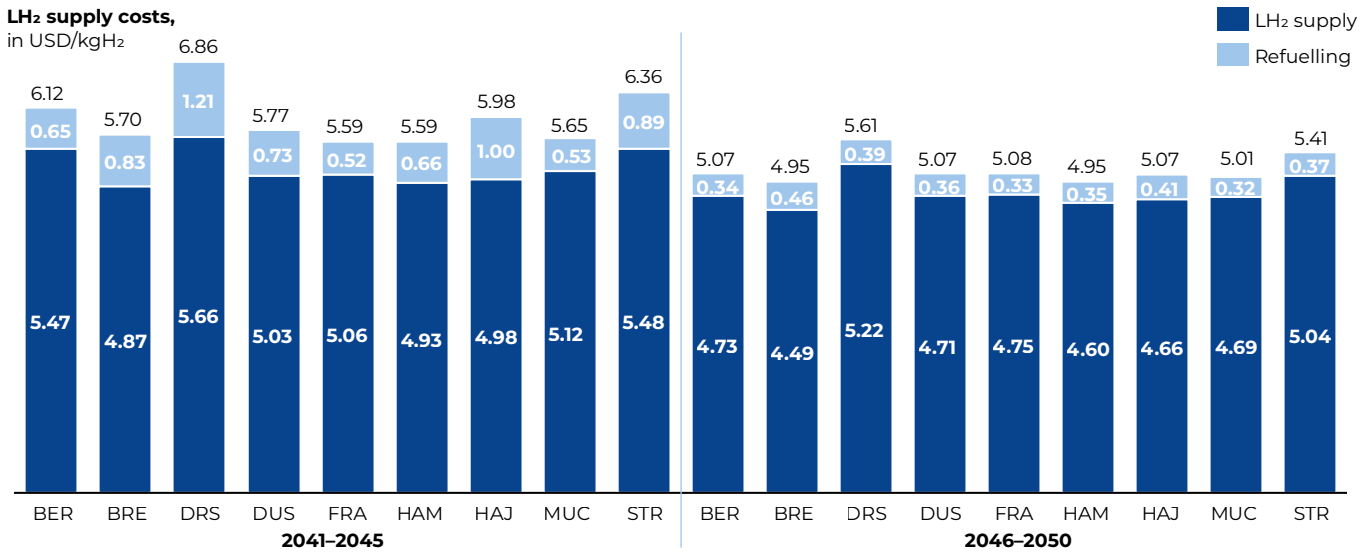

Figure 27: LH_2 supply and refuelling costs at each airport for different periods for the moonshot scenario

ENERGY SYSTEM PERSPECTIVE

5 Energy system perspective

In this chapter, the results of the energy system analysis for Europe are introduced. The results are presented as a transition pathway until the year 2050, where each year builds upon the state of the preceding one. Consequently, the target picture for 2050 equals the last year of this transition path.

A central focus of the analysis is the potential for domestic production of green H_2 within the European energy system. In Section 5.1, spatially resolved cost-quantity data for the production of green H_2 is provided for each year of the transition path. In Section 5.2, the alternative of importing green H_2 from abroad is considered. To this end, the cost-quantity data for green H_2 is determined globally and transportation costs from the respective production site to Europe are added. For production sites outside of Europe, also local investment risks are taken into account. Local investment risks are reflected in capital costs specific to the respective location. Location specific capital costs are derived using the method described by Terrapon-Pfaff et al. [59] and Horst et al. [60] with input data from Damodaran [61].

These domestic and global supply options are subsequently integrated into the Hydrogen Supply Network Model discussed in Section 2.3.3. This model evaluates the economic feasibility of different supply pathways and identifies the cost optimal option in the context of the future aviation network as shown in Section 4.3. Finally, the selected H_2 supply routes are integrated into the ESTRAM energy system model. This allows us to investigate the impact of the additional demand for H_2-powered aviation on the energy system, which is presented in Section 5.3.

5.1 Hydrogen supply from the European energy system

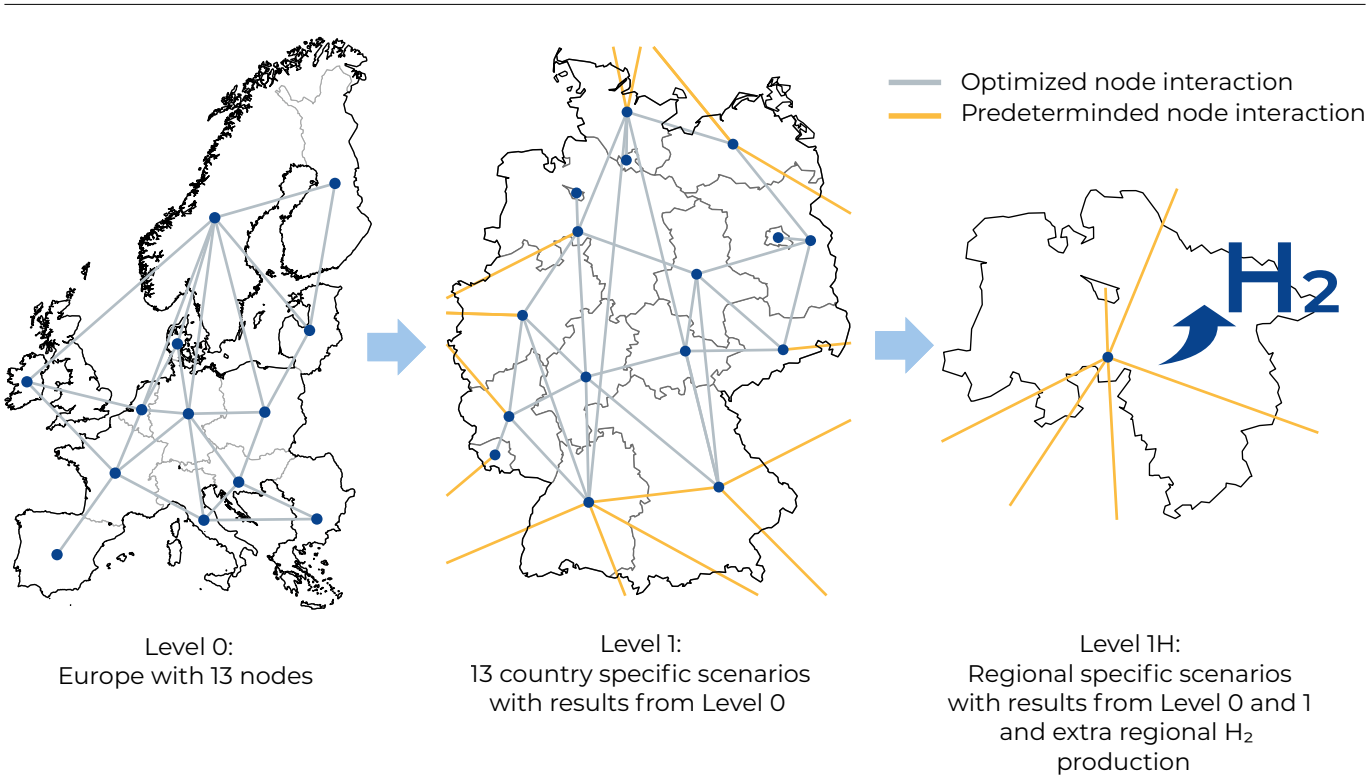

Figure 28: Application of the hierarchical approach on the example of Lower Saxony embedded in the German national energy system which itself is embedded in the European energy system. Blue dots are nodes and solid lines are interconnections between nodes. With each next step, the result of the previous calculation is used as predetermined node interaction in the next step.

The calculation of cost-quantity data for the production of green H_2 within the European energy system is based on the transition path analysis at the NUTS-1 level. Due to the high spatial and temporal resolution of this approach, a direct optimization across the entire system is computationally expensive. To overcome this limitation, a hierarchical approach is developed that decomposes the optimization problem into multiple subproblems with increasing spatial granularity. Consistency between the subproblems is ensured using the solution of each preceding optimization as a boundary condition for the subsequent, more detailed problem. This three-step approach is visualized in Figure 28. The optimization is first carried out on the level of the European energy system using 13 clustered NUTS-0 nodes including all EU-27 member states and the United Kingdom, Switzerland and Norway (level 0). Based on this result, the next step (level 1) involves recalculating each NUTS-0 node with increased spatial resolution (NUTS-1). Each NUTS-1 sub-problem is constrained by the outcome of its parent NUTS-0 node. The constraints include the energy exchange between the respective nodes, energy imports and the installed capacities of all energy consumers.

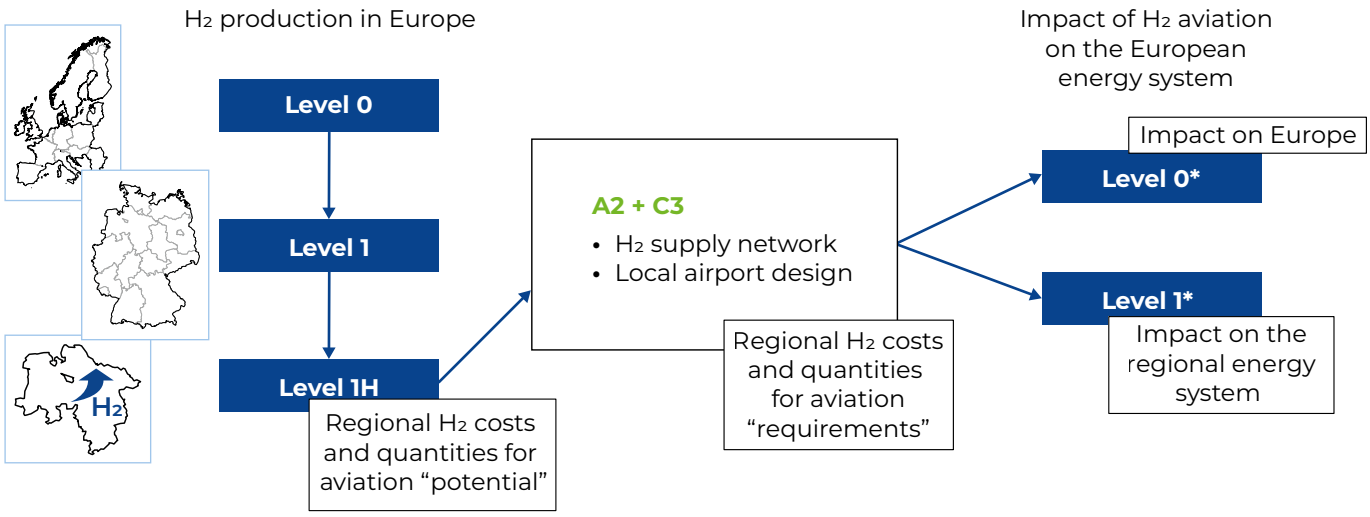

Figure 29: Schematic of the three-step approach to calculate cost-quantity data for the domestic green H_2 production. The result of the level 1H calculation is the regional potential for the green H_2 production given the constraints of the energy system. This data is supplied to the H_2 supply network model which then decides on the actually utilised potentials discussed in Chapter 4. Finally, these required amounts of green H_2 are integrated into the energy system model and the impact of the European and local energy system is analysed.

The regional production costs of H_2 are determined in a subsequent step where the node interactions are fixed to the values from level 1 and increase the regional H_2 demand (level 1H). This approach ensures that H_2 produced at certain costs in a given region is in fact produced within that region rather than imported via existing grid capacities from cheaper regions. This approach is in line with the current regulations on green hydrogen production in Europe. Therefore, the calculations at levels 0 and 1 are performed without the H_2 demand for aviation, as this demand is added in the later level 1H calculation on a regional basis. This calculation is repeated for different amounts of additional annual H_2 demand (20 kt, 200 kt, 1000 kt and 2000 kt) as well as for each timestep of the energy transition and marginal H_2 costs are extracted in each run. This three-step procedure, as illustrated in Figure 29, ensures that spatially and temporally resolved quantity-cost data for the production of green H_2 is provided while respecting the limitations of the local energy system.

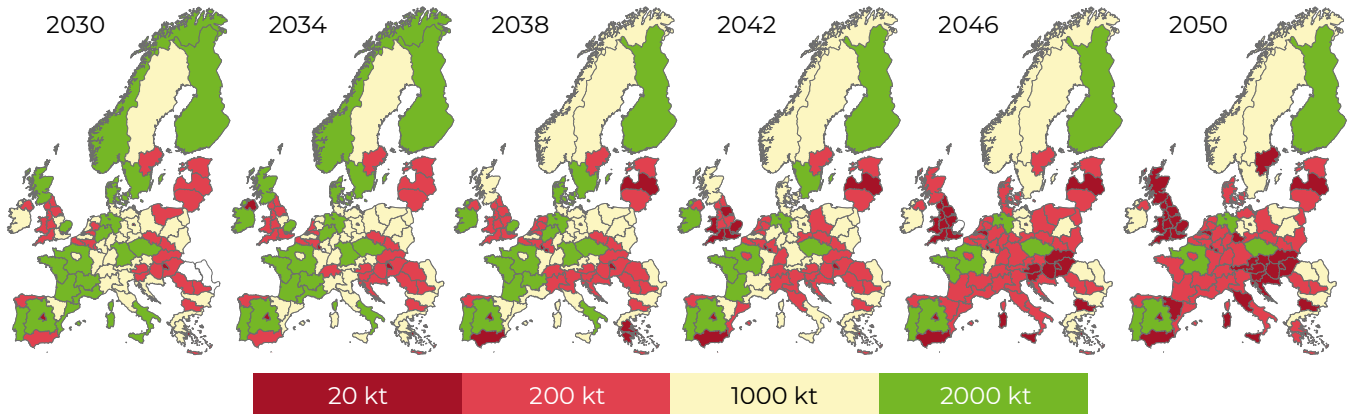

Figure 30: Maximum amount of H_2 produced additionally for the aviation sector per NUTS-1 region during the transition to 2050.

The maximum amount of H_2 that can be produced in a specific NUTS-1 region is limited by the local potential for RES as well as competing H_2 demands by other sectors within the energy system. Figure 30 shows the maximum amount of H_2 that can be produced in each NUTS-1 region for all steps of the transition path to 2050. Most NUTS-1 regions are capable of producing at least 200 ktH_2 per year for all years of the transition. The amount of 200 ktH_2 roughly corresponds to the forecasted demand for the Amsterdam Schiphol Airport (160 ktH_2) for 2050 in the Ambitious policy scenario which has the largest LH_2 demand in the Ambitious policy scenario and is therefore a good benchmark.

From Figure 30 it becomes apparent, that the maximum amount of additional H_2 that can be produced in a specific NUTS-1 region declines over the transition path. The reason for this is that the potentials for RES required for the H_2 production are increasingly being used to meet increasing demands in other sectors.

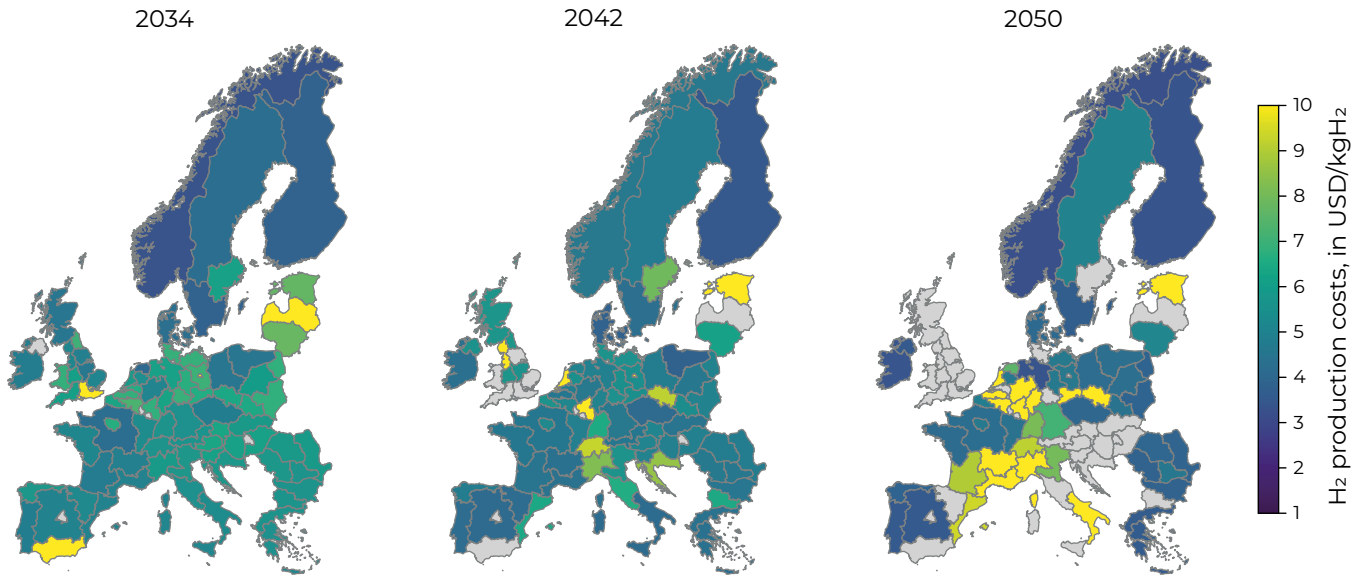

Figure 31: Marginal cost for the production of H_2 at a fixed amount of 200 ktH_2 produced within each NUTS-1 region. Grey-colored NUTS-1 regions are not capable of producing 200 ktH_2 at that specific time step.

In contrast to the maximum amount of H_2 that can be produced, Figure 31 shows the production costs of H_2 at a fixed amount of 200 kt per NUTS-1 region. Production costs at this amount range from 3.2–10.0 USD/kgH_2 with a trend for increasing H_2 costs towards the end of the transition path. Interestingly, this result is highly dependent on the amount of produced H_2. At a later stage in the transition path, the available potentials have already been largely utilized, meaning that less additional H_2 can be produced. However, up to this production potential per NUTS-1 region, H_2 can be produced at lower costs due to lower component costs and efficiency gains towards the end of the transition path. In addition to that most regions that show high costs early on in the transition path are later unable to supply the specified amount of H_2 later on in the transition. This suggests that high H_2 costs are caused by a high utilization of the existing potentials for RES. However, even in 2050, there are plenty of NUTS-1 regions that are capable of supplying H_2 at costs as low as 3.5 USD/kgH_2.

Figure 32 shows the aggregated additional H_2 amounts over all NUTS-1 regions versus the associated production costs at multiple timesteps of the transition. The shape of the curve is very similar for all timesteps. Small amounts of H_2 (up to ≈500 ktH_2) can be produced at low costs, because the necessary components like electrolysers and RES are already installed for the remaining energy system and not yet fully utilized. After that, the H_2 cost curve rises slowly with increasing H_2 production volume. The reason for this is that new components have to be built in order to produce these quantities. Since the additional costs of these components are spread over a correspondingly larger amount of produced H_2, no significant increase in production costs is expected. The observed increase, however, comes from the fact that favourable locations for the deployment of RES are a limited resource. Locations with high number of full-load hours for photovoltaics and wind power are utilized first. Once the potential there has been exhausted, only locations with fewer full-load hours remain causing the increase in production costs. However, at a specific amount of H_2 the available potentials for RES are fully utilized and thus the production costs for even larger amounts of H_2 show a steep increase. Depending on the timestep during the transition path, this point is reached at different amount of produced H_2. In 2038, relatively early on in the transition path, there are larger potentials for RES still available, meaning that production costs will start to rise sharply at around 55,000 ktH_2. In contrast, this point is already reached at around 25,000 ktH_2 in 2050.

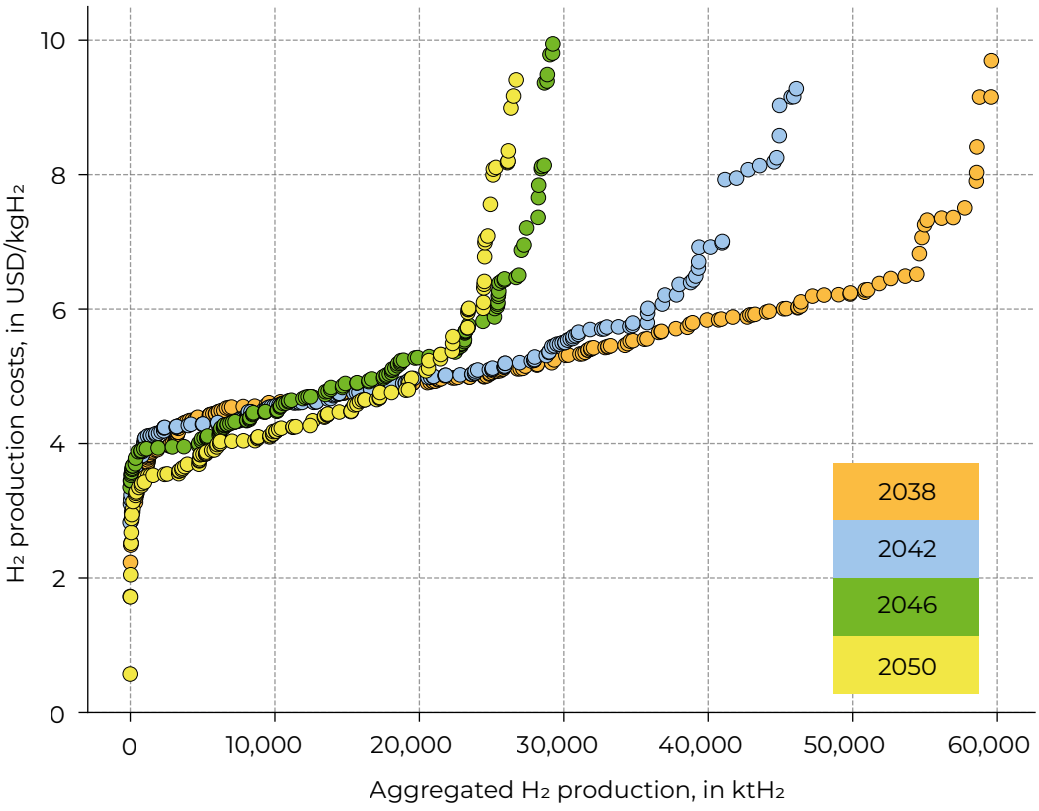

Figure 32: H_2 costs plotted versus the aggregated production of additional H_2 over all NUTS-1 regions in Europe.

5.2 Global potential for hydrogen export to Europe

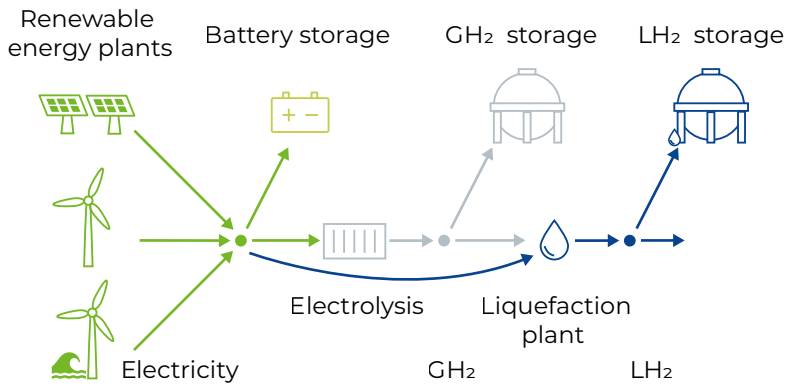

Figure 33: Schematic of the island energy systems that are used for the calculation of import costs of green H_2 from global production sites.

In addition to domestic production, green H_2 can also be produced at other locations worldwide and subsequently imported into Europe. Many global regions benefit from more favourable weather conditions for renewable energy generation, such as higher insolation or stronger and more consistent wind resources. However, the costs associated with transporting H_2 over long distances must be taken into account when evaluating these options.

For this purpose, global weather datasets [62] are used and energy system islands are considered for H_2 production. As displayed in Figure 33, these systems rely on PV and wind power as RES, with both onshore and offshore wind power included. Electrical energy can be stored in batteries, while electrolysis produces GH_2 that can either be exported directly via pipeline or liquefied on-site and exported by LH_2 vessel. GH_2 as well as LH_2 can be stored using corresponding storages ensuring to meet the export demand at all times.

For each potential production site, the ESTRAM model is applied to optimise both the dimensioning of the RES as well as the dispatch of all components. This calculation is performed for each year of the transition path as a greenfield optimisation, i.e. the results for one year do not depend on the results from the year before. The evolution of the production costs for green H_2 is derived using the marginal H_2 costs from each calculation. Cost reductions during the transition path result from time-dependent techno-economic assumptions. Since these island energy systems are not connected to the respective national energy system, the resulting production costs for green H_2 are independent of the production volume as long as sufficient potentials for RES are available. Country-specific potentials for RES are derived from a spatial potential analysis that integrates multiple geospatial layers, such as arable land, protected areas, terrain slope, water depth for offshore wind, and land-use classifications [63]. Based on land-use intensity assumptions (MW/km^2) for each RES (photovoltaics, onshore wind, offshore wind), combined with site-specific weather data, the H_2 production potential is determined for each country. This purely technical assessment, explicitly excluding any social, environmental, or macroeconomic constraints in the exporting countries, defines the so-called technical potential, which serves as an upper boundary for feasible H_2 export volumes.

Figure 34 shows the production costs of green H_2 for countries outside of Europe by 2050. The production costs depend on the annualized investment as well as operation and maintenance costs of all components. In order to compare global investments, local investment risks must be taken into account. To reflect these uncertainties, region-specific weighted average capital costs (WACC) are considered as shown in Appendix C. Many countries will be able to produce green H_2 for around 5 USD/kgH_2, but there are significant outliers with productions costs of more than 10 USD/kgH_2. Interestingly, the impact of the assumed WACC is substantial and often more pronounced than the impact of favourable conditions for solar PV and wind power. This favours the production of green H_2 in politically and economically stable countries which is associated with low investment risks.

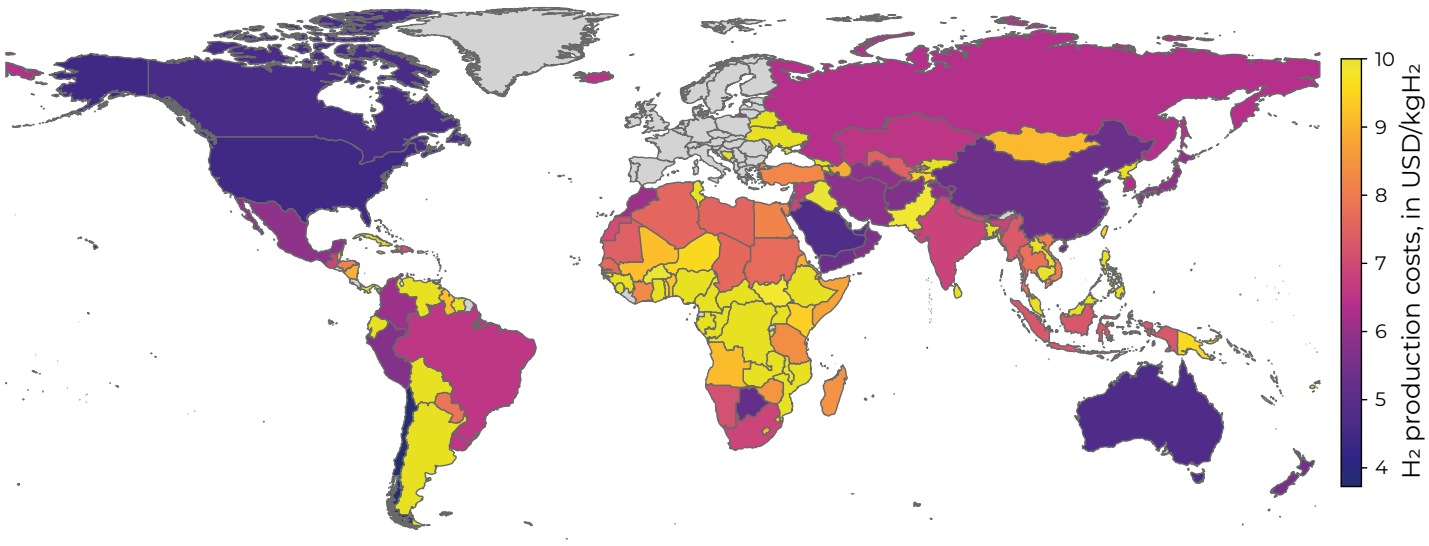

Figure 34: Production costs of green H_2 for countries outside of Europe by 2050. Large differences between neighbouring countries are caused by the assumption of region-specific WACC. Depending on the optimal transport option to Europe, production costs may also include liquefaction costs to routes served by vessel transport.

Finally, transport costs are incorporated by modelling LH_2 shipping and GH_2 pipeline routes with European ports as final destinations, respectively. Transport costs are derived from the transport distance and specific costs for transport distance and amount of H_2. It is assumed that transport via GH_2-pipelines is possible only for countries that are already today connected to Europe via pipeline. This mainly applies to the MENA region being connected to Southern Europe and Russia being connected to Eastern and Central Europe. In this way, it is possible to determine export country-, port- and year-specific H_2 import costs to Europe.

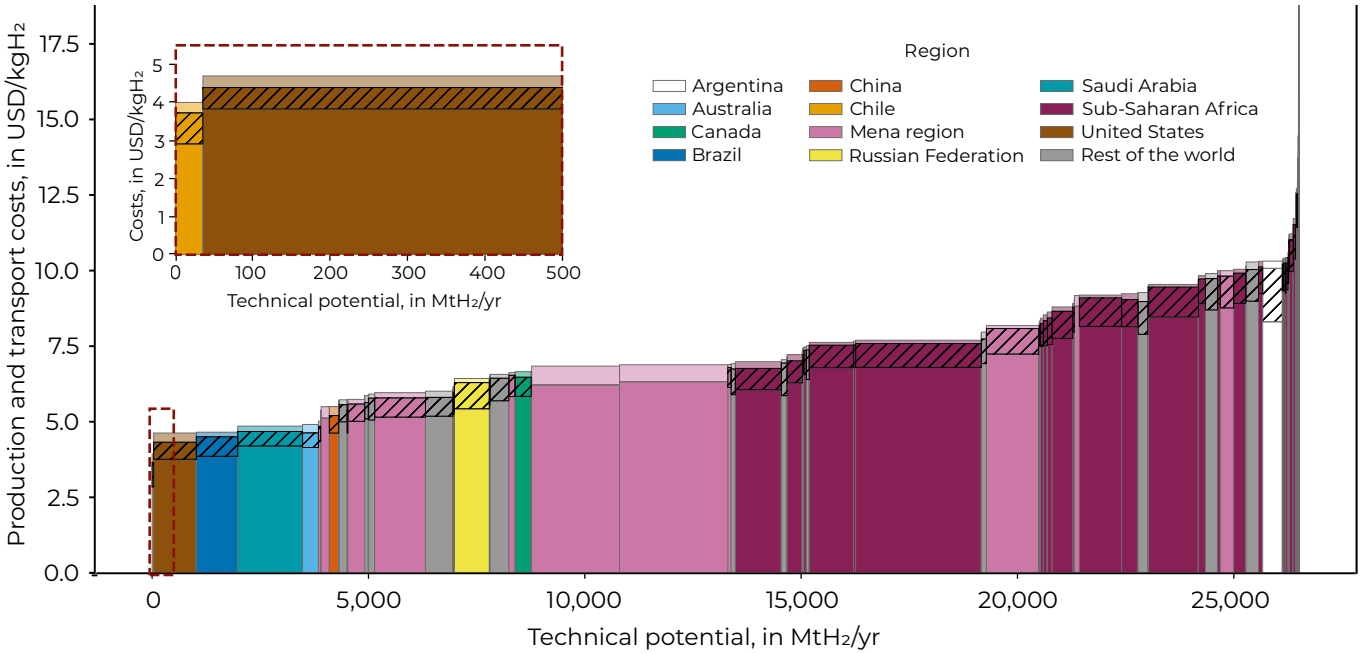

Figure 35: Cost-quantity data for the import of green H_2 into Europe from global production sites for 2050. Each bar represents the cost composition of a production site, consisting of production costs (darker colour) and transport costs (lighter colour). Additional costs for liquefaction, if transport is carried out over longer distances by LH_2 vessels, are marked separately as a hatched area. Countries are coloured and grouped into 12 regions. The inset in the figure zooms in on the cost-quantity data between 0 and 500 MtH_2/yr to highlight Chile's technical potential.

Figure 35 displays the H_2 import costs along with the aggregated technical production potential for 2050. For each export country the most favourable transport route is shown. This is either transport by LH_2 vessel (including liquefaction costs) or GH_2 transport by pipeline. As shown in Figure 35, there is an annual global potential of around 4 GtH_2 at costs below 5 USD/kgH_2, with Chile being the cheapest exporter but lagging far behind in terms of technical production potential compared to the following countries (United States, Canada, Saudi Arabia and Australia). Importantly, the according to the Ambitious policy scenario assumed H_2 demand for European aviation in 2050, can already be covered by using 4.5% of Chile's technical potential.

5.3 Impact of H_2-powered aviation on the energy system

The cost-quantity data for both domestic production and global imports of green H_2 serve as the decision basis for the Hydrogen Supply Network Model discussed in Section 2.3.3. This model determines, on the basis of cost optimisation, which supply options are utilised to ensure that the green LH_2 demand at each airport site is met. In this section, the interaction and feedback effects of these supply decisions on the energy system are analysed at both the local and the European level.

To this end, the H_2 quantities allocated by the Hydrogen Supply Network Model are integrated into the European energy system model. Figure 36 shows the resulting local demands for green H_2 as well as the electricity demand for the operation of local liquefaction plants for the Ambitious policy scenario by 2050. In this scenario, the total green LH_2 demand for aviation using domestic production sites is 509 ktH_2 (16.8 TWh) by 2050. The additional electricity required for liquefaction amounts to 3.14 TWh. In the following, we use units referring to energy rather than mass to ensure consistency across all energy carriers. To cover these domestic demands, additional capacities for RES and storages for electricity and H_2 must be built at production sites. Alternatively, if this is more cost-effective, existing resources will be reallocated or utilised more efficiently.

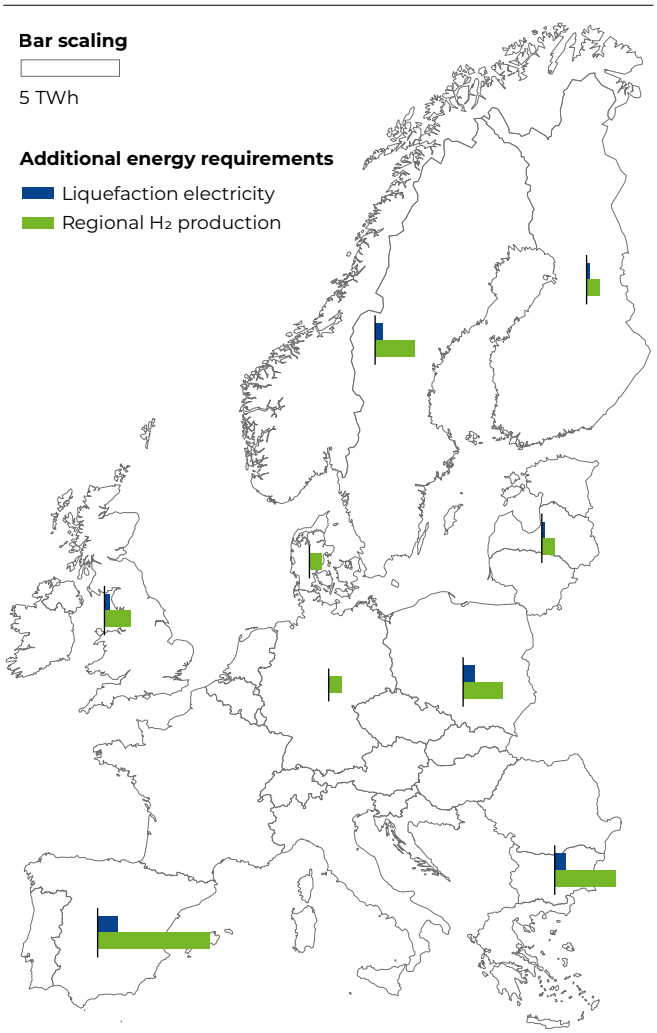

Figure 36: Aggregated amount of local green H_2 production for the Ambitious policy scenario by 2050. Green H_2 is produced at favourable locations and co-located with liquefaction plants. Operation of the liquefaction plants results in additional electricity demands which must be supplied by the energy system.

To evaluate the impact of LH_2 demand in the Ambitious policy scenario on the European energy system, reference scenario without LH_2 demands for aviation is compared to the Ambitious policy scenario in terms of installed capacities of energy system components. Figure 37 shows the change of these capacities evaluated for the year 2050. On the Iberian Peninsula, the increase of installed solar PV and electrolyser capacity is most pronounced. However, this increase is 6 GW for solar PV and thus only 2.7% on the Iberian Peninsula in 2050. Looking at Europa as a whole, the increase in installed solar PV capacity is 18 GW (1%) compared to the reference scenario. Interestingly, for all production sites across Europe, the additional

energy demand is mainly covered by an increase in solar PV capacity. This is because the locations that are advantageous for wind power are already being used for the transition of the energy systems. Even if the total potential for wind power has not been exhausted, the yield achievable at the less favourable locations is nevertheless significantly lower. This underscores the role of solar PV for the future energy system, as it is the most least-effective source of electricity generation in many places and the available potentials for utility-scale PV and for decentralized PV, e.g., on buildings, are comparatively large.

The importance of analysing a fully-interconnected energy system across all sectors becomes apparent when looking at the H_2 production in the United Kingdom and Ireland (UK+IE) as well as in the node spanning Poland, Slovakia and the Czech Republic (PL+SK+CZ). In both areas, an interaction between the supply of H_2 for aviation and the heating sector can be observed. In this scenario, space heating in UK+IE is largely provided by heat pumps and electric heaters. While heat pumps primarily provide the base load, the electric heaters are used to cover peak loads. This saves costs as the heat pumps can be sized smaller and the electric heaters can respond flexibly to supply peaks, e.g. electricity from solar PV. However, due to the additional demand for H_2, these supply peaks are used for electrolysis. For this reason, the heat pumps in this case are larger, as they now also have to cover a larger part of the peak load. Another example is PL+SK+CZ, where in the reference scenario a small fraction of the space heating demand is covered using H_2. In the scenario with the additional LH_2 demand, this demand is covered using heat pumps and the H_2 is rerouted to the aviation sector instead.

As mentioned above, the additional energy demand for aviation is comparably low from the perspective of the overall energy system, but the impact at the local level may be significantly more pronounced. One example is the node NUTS-1 node ES4 (Centro) on the Iberian Peninsula, where the entire additional demand for H_2 and electricity for aviation is located. Compared to the reference scenario, there are 6 GW of solar PV added to this region which equals to a relative increase of 18%. In addition to solar PV, the electrolysis capacity increases from 7 GW in the reference scenario to 9 GW (+28.6%) in the scenario with the additional LH_2 demand (Ambitious policy scenario). Looking at the transition path in both the reference scenario and the base scenario, it becomes clear that the additional demands from the aviation sector result in a pronounced increase in expansion, particularly towards the end of the transition path. Since the transition of the Spanish energy system must be largely complete by 2046 in order to meet the carbon emission targets, the reference scenario does not show any further expansion of PV and only a minor expansion of electrolysis (0.15 GW) between 2046 and 2050. However, looking at the Ambitious policy scenario, this addition rises to 4.6 GW and 1.76 GW for solar PV and electrolysis, respectively. For comparison, according to the base scenario, there are 285 GW of electrolysis installed in Europe by 2050. This result highlights the significant impact of forecasts for future LH_2 demands in aviation on the temporal development of the energy transition until 2050 and beyond.

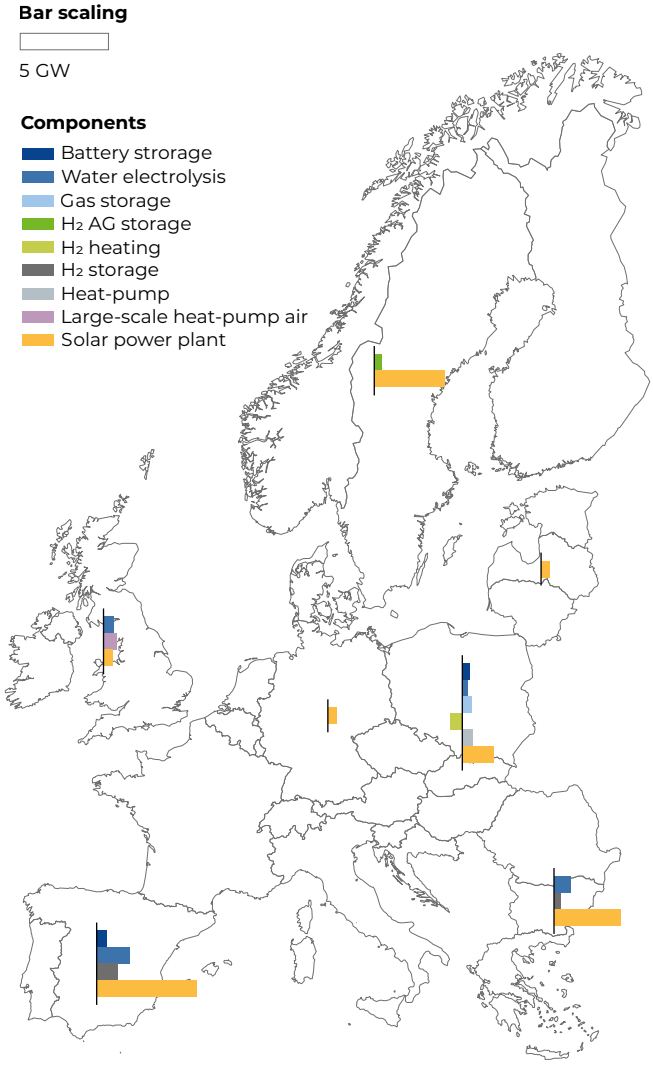

Figure 37: Change of installed capacities of energy system components between the reference scenario without additional H_2 demand and the Ambitious policy scenario. Bars to the right indicate an increase in installed capacity, while bars to the left indicate a decrease in capacity. Installed capacities are evaluated for the year 2050.

ECOLOGICAL IMPACT OF LIQUID HYDROGEN SUPPLY ROUTES

6 Ecological impact of liquid hydrogen supply routes

This Chapter presents a detailed assessment of the greenhouse gas emissions associated with different H_2 supply chain configurations, focusing on the infrastructure-related emissions during both the construction and operational phases. The analysis includes all components of the supply chain including water electrolysis, H_2 storage, liquefaction, transport and refueling. By comparing on-site and off-site production pathways under different energy scenarios – wind, photovoltaic, and a hybrid mix of – this study aims to highlight emission hotspots.

In this chapter, first, the specific emissions per kilogram of LH_2 are determined, identifying dominant emissions of the components of the supply chains such as electrolysis and leakages. Following on this, the absolute emissions for archetypical airports are analysed with varying LH_2 demands, illustrating the scalability challenges of H_2 infrastructure. Finally, the third part introduces a parameter study that varies transport distances for trucks, vessels, and pipelines to highlight the sensitivity of emissions to logistics, providing critical insights into the optimization of future H_2 supply networks.

6.1 Study design

In this study, Life Cycle Assessment (LCA) models have been developed for each component. These components include a 100 MW PEM electrolyser, a liquefaction unit with a capacity of 100 tons per day, GH_2 cavern storage including compression, LH_2 storage in a 50,000 m^3 tank, GH_2 pipelines with compressors every 125 km, and both repurposed and new pipelines. Additionally, LH_2 transportation utilizes a 280,000 m^3 vessel with a fuel cell, and a 4.6 tLH_2 truck equipped with a fuel cell. Refueling infrastructure involves LH_2 refueling trucks and cryo-pumps. More details and further assumptions are provided in Appendix C.

The study covers both construction and operation phases. Energy data for electrolysis, liquefaction, and compression storage were provided by project partners, while transport modes including the pipeline, vessel, and truck were developed based on literature. Components are assembled according to their respective supply chain configurations to comprehensively assess emissions and their environmental impacts. For the comparison of the total emissions for different archetypical airports, a small (10,000 tH_2/a), medium (40,000 tH_2/a), and large (70,000 tH_2/a) airport is analysed with the corresponding LH_2 demand.

6.2 Specific emissions of the infrastructure for the three supply chains

In this section, the specific emissions of LH_2 supply for H_2-powered aviation is analysed for three supply chains. The study examines key components of the supply chains with a focus on emissions during construction and operation. Electrolysis emissions arise from construction and operational phases. Storage includes GH_2 and LH_2 emissions from infrastructure and maintenance. Liquefaction involves emissions from facility construction and operations. Transport and distribution cover emissions linked to GH_2 pipelines, LH_2 trucks, LH_2 vessels, and refueling infrastructure. This comprehensive analysis aims to identify emission reduction opportunities across the supply chain.

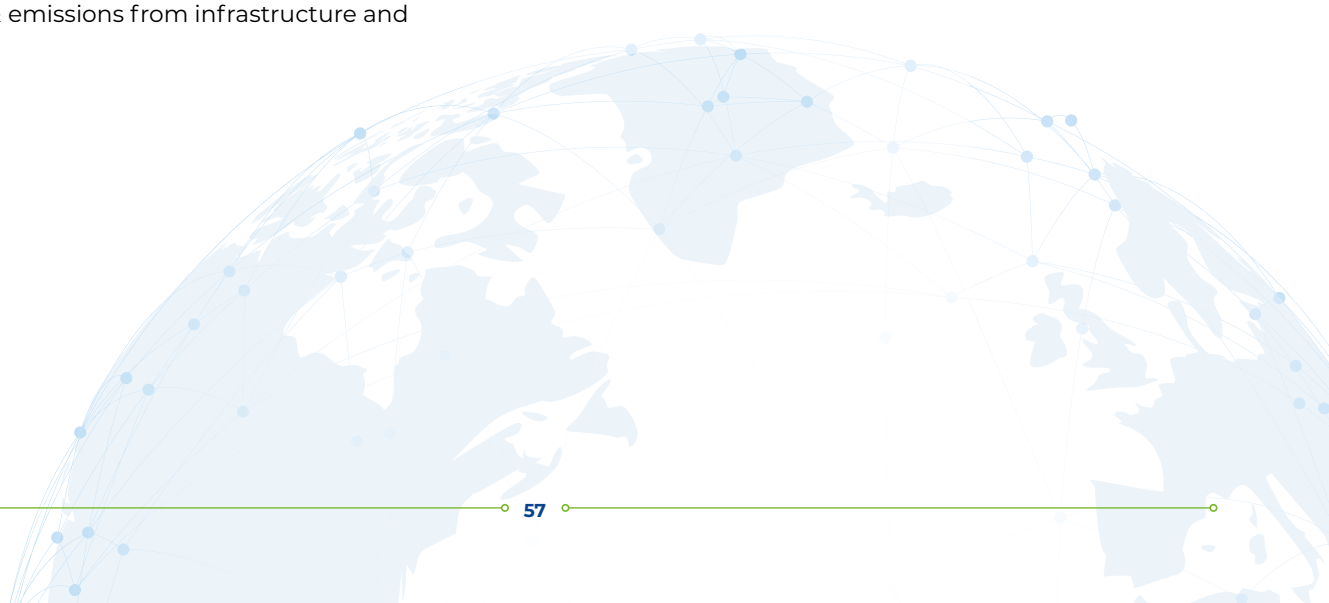

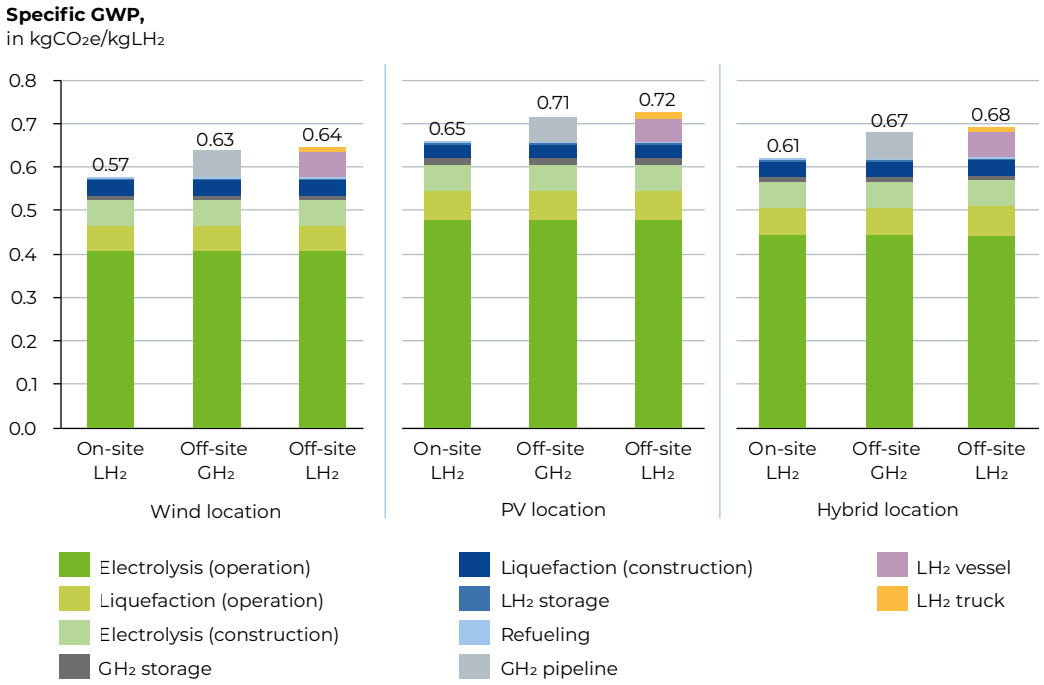

Figure 38: Specific GWP for H_2 supply chains under different energy scenarios

Figure 38 presents a comparison of the specific greenhouse gas emissions (in $kgCO_2e/kgLH_2$) associated with the infrastructure of three different H_2 supply chain configurations: On-Site production, off-site supply of GH_2 and off-site supply of LH_2. These are further evaluated under three energy scenarios: wind, PV and a hybrid energy mix of wind and PV. Each segment represents a distinct emission source within the H_2 supply infrastructure.

The analysis of specific emissions clearly shows that the operation of electrolysis is the dominant contributor, accounting for approximately 70–80% of total greenhouse gas emissions across all supply chain types and energy scenarios. Liquefaction processes – including both construction and operation – contribute around 13–15% to the total emissions. In cases of H_2 import, the pipeline transport pathway adds approximately 12%, while LH_2 vessel and truck transport contribute around 10%. In contrast, refuelling and storage infrastructure play only a minor role in the overall emissions profile.

On-site production of LH_2 consistently demonstrates the lowest total emissions, particularly in the wind scenario. This can be attributed to the minimal need for transportation. In contrast, off-site supply of LH_2 results in the highest emissions. This is primarily due to the additional transport infrastructure required, such as LH_2 vessels and trucks. The PV scenario results in higher emissions than the hybrid scenario and the wind scenario, which is due to the higher GWP value of solar compared to wind energy. The hybrid scenario is at a medium emission level. In contrast, off-site and LH_2-based supply paths lead to significantly higher emissions, mainly due to the additional energy demand and logistical requirements.

To provide a more comprehensive view of the emission profile of H_2 supply chains, Figure 39 presents the same supply chain configurations, but the emissions are displayed in relative terms, normalized to 100% for the baseline infrastructure emissions, excluding leakage. On top of these baseline values, the dark grey bar segments represent the additional GWP resulting from H_2 leakage occurring along the supply chain. These leakages typically take place during critical handling and transfer operations, such as refueling stations or throughout refilling. Given H_2 GWP over a 100-year time horizon (GWP100) of 11.6, even small leakage rates can have a significant effect on the overall emission profile. In this figure, scenario-specific leakage rates are considered, with 3.5% leakage for on-site production, 4.0 % for off-site gaseous H_2 supply, and 6.4% for off-site LH_2 supply. As a result, the additional emissions from H_2 leakage are clearly visible and pronounced, especially for the off-site LH_2 scenario.

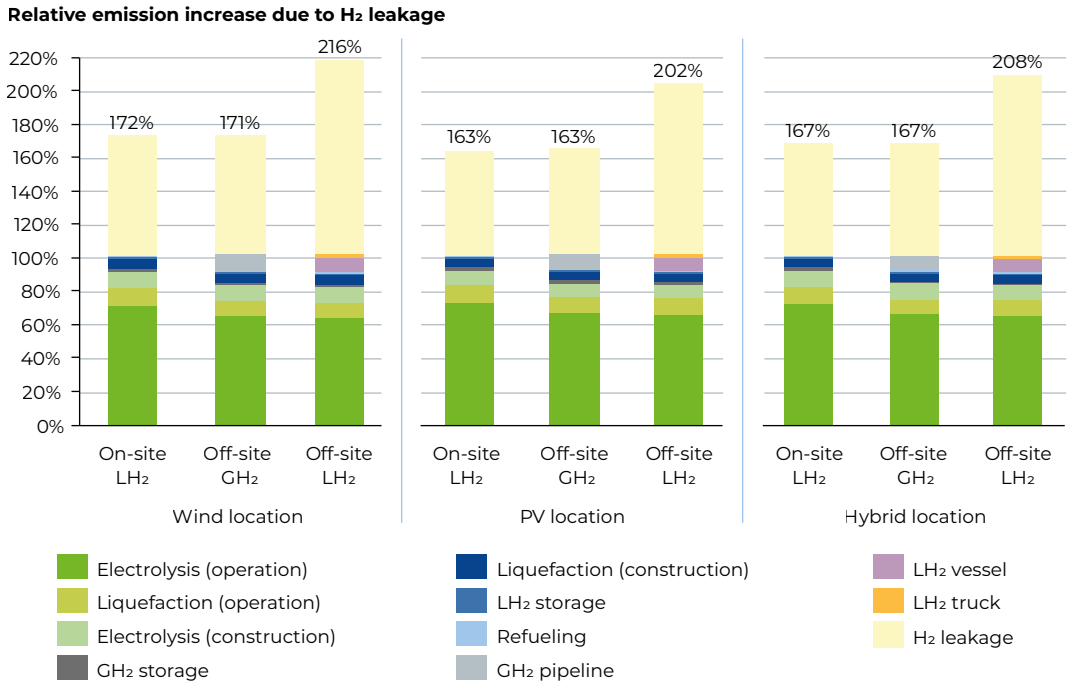

Figure 39: Relative emissions of H_2 supply chains including leakage impacts. H_2 losses significantly increase total emissions due to a high GWP100 value of 11.6

6.3 Absolute emissions for archetypical airports for the supply chains

In this section, the total emissions for three archetypical airports are analysed. In Figure 40, the bar chart illustrates the annual CO_2-equivalent emissions (in $kgCO_2e/a$) associated with different H_2 supply chain configurations – On-Site, Off-Site GH_2, and Off-Site LH_2 – for three airport demand categories: small (10,000 tH_2/a), medium (40,000 tH_2/a), and large (70,000 tH_2/a). The emissions scale proportionally with LH_2 demand, ranging from approximately 5,000–7,000 $kgCO_2e/a$ for small airports, 22,000–30,000 $kgCO_2e/a$ for medium airports, and peaking between 40,000 and over 50,000 $kgCO_2e/a$ for large airports. Among the energy supply options, wind consistently results in the lowest emissions across all airport sizes and supply chains, while PV leads to the highest values due to its higher specific GWP. Off-site supply pathways – especially those involving LH_2 – are generally associated with higher emissions compared to on-site production, primarily due to additional energy and transport infrastructure.

It is important to note that this representation does not include emissions from H_2 leakage, which can further increase total greenhouse gas impacts in real-world applications.

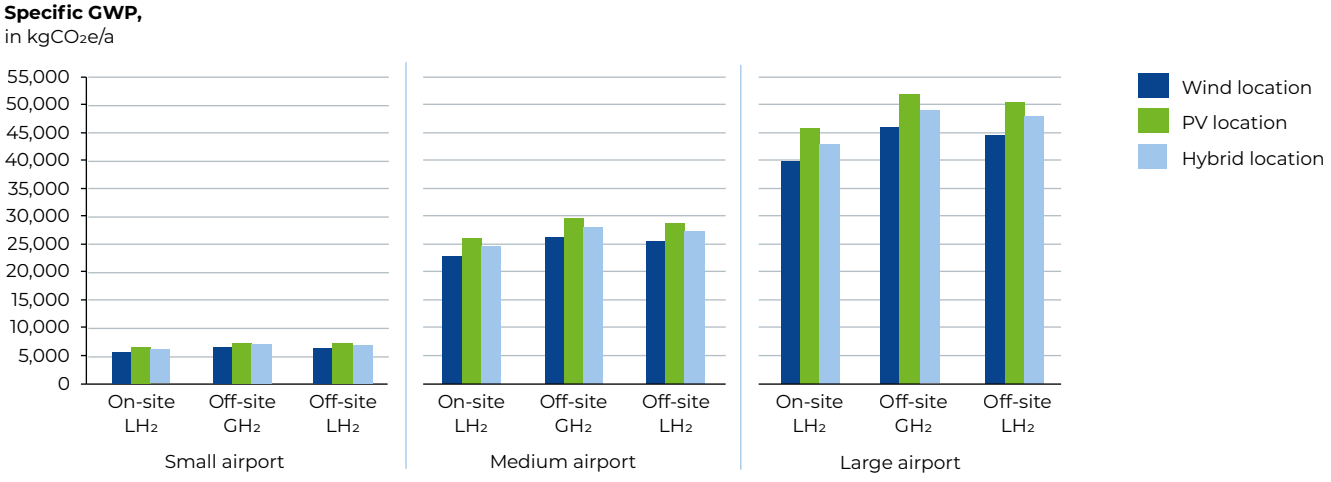

Figure 40: Annual CO_2-equivalent emissions for different H_2 supply chains and airport sizes (small, medium, large) under wind, PV, and hybrid energy scenarios

6.4 Variation of transport distances

As the emissions are highly dependent on the transport option and therefore also on the transport distance, in the following a parameter study for these distances is provided. The scenarios consider on-site production and various off-site transportation methods, highlighting emissions variations based on transport distances. The study examines transport distances through a parameter variation approach. Truck distances range from 50–300 km, vessel distances from 3000–9000 km, and the European Hydrogen Backbone (EHB) ranges from 500–3000 km.

For LH_2 trucks, emissions, measured in $kgCO_2$-equivalent, notably increase with distance. This trend is particularly evident in solar energy scenarios, which show higher emissions compared to wind and hybrid systems. Shorter distances prove to be more environmentally efficient, reducing the carbon footprint associated with H_2 logistics. Vessels, covering long distances, also show substantial emission increases, especially at 9000 km. The solar scenario consistently results in the highest emissions, underscoring the importance of optimizing energy choices for maritime transport. EHB pipelines display a similar pattern, with emissions rising incrementally with distance. Again, solar energy results in higher emissions compared to wind and hybrid alternatives.

Table 2: Impact of transport distances on specific emissions in $CO_2e/kgLH_2$

	Wind	Solar	Hybrid
On-Site	0.57	0.65	0.61
Off-Site Pipeline (500 km)	0.59	0.68	0.63
Off-Site Pipeline (2000 km)	0.66	0.74	0.70
Off-Site Pipeline (3000 km)	0.70	0.78	0.74
Off-Site Vessel (3000 km)	0.64	0.72	0.68
Off-Site Vessel (5000 km)	0.69	0.78	0.74
Off-Site Vessel (9000 km)	0.75	0.83	0.79
Off-Site Truck (50 km)	0.63	0.71	0.67
Off-Site Truck (150 km)	0.64	0.72	0.68
Off-Site Truck (300 km)	0.65	0.73	0.69

In contrast, on-site H_2 production consistently achieves the lowest emissions across all energy options. This approach eliminates the need for extensive transport, significantly reducing the overall carbon footprint and reinforcing the benefits of localized production.

6.5 Recommendations

Based on the study results, several recommendations can be made:

- Promote on-site LH_2 production: From an ecological point of view, on-site H_2 production, especially using wind energy, should be prioritized to minimize environmental impact.
- Optimize transport and logistics: Emissions increase with transport distance. Optimizing logistics, such as using closer production sites or more efficient transport methods, can significantly reduce emissions.
- Adopt hybrid energy systems: Combining wind and PV energy can help lower emissions and enhance the reliability of energy supply for H_2 production.
- Innovate in liquefaction and storage technologies: Investments in advanced liquefaction and storage technologies can increase energy efficiency and reduce associated emissions.
- Address leakage along the supply chain: H_2 leakage may account for 3–6% of losses along the supply chain, but it has the potential to more than double the overall emissions. Special attention should be paid to minimizing leakage during refilling and refueling processes to significantly reduce the total greenhouse gas impact of the supply chain and lower its overall GWP.
- Enhance infrastructure development: Expanding specific infrastructure, like optimized pipelines and storage capacities, can improve the efficiency of the entire H_2 transport and utilization system.
- Plan long-term and invest in sustainability: Considering the results for the target year 2050 highlights the need to invest early in sustainable technologies and infrastructure to meet future environmental standards.

BUSINESS MODELS, FINANCING STRATEGIES AND POLICY INSTRUMENTS

7 Business models, financing strategies and policy instruments

This chapter examines different stakeholder constellations and their business models, financing strategies, and policy support mechanisms for LH_2 supply infrastructure in H_2-powered aviation. As previous chapters have primarily focused the LH_2 supply cost, the viability of business models and price formation was neglected. This chapter is based on Schenke et al. [64] and addresses following research questions:

- Which stakeholder constellations and business models are most effective in fostering the ramp-up of the LH_2 supply infrastructure for H_2-powered aviation?
- What financing strategies are suitable for developing LH_2 supply infrastructure?
- Which policy instruments are most appropriate to support the identified business models?
- What LH_2 supply prices can be expected at the airport under these conditions?

To answer these research questions, this study builds on a range of analyses related to financing strategies and business models in the broader H_2 and sustainable aviation fuel (SAF) sectors [16,65–68]. Additionally, the study incorporates insights from policy support analyses conducted in the broader H_2 sector [69–72]. Both the financing strategies and policy support mechanisms are examined in detail in the present study to identify viable pathways for developing LH_2 supply infrastructure for H_2-powered aviation.

The section is structured as follows: Section 7.1 provides a preliminary analysis of stakeholders and their financing strategies within the aviation ecosystem. Section 7.2 outlines the study design, the complete methodology including model equations and the optimization problem is provided in Appendix C. The results are presented in two parts. First, stakeholder constellations are compared with respect to their impact on LH_2 supply infrastructure and resulting supply price. Second, an overview of relevant policy support mechanisms is presented and their influence on the identified business models is analysed. Finally, the chapter concludes by summarizing the key findings.

7.1 Stakeholders in the hydrogen aviation ecosystem

To evaluate stakeholder constellations and their business models for LH_2 supply infrastructure, this section conducts a preliminary analysis of relevant actors, their potential roles, and available financing instruments within the H_2 aviation ecosystem.

The potential stakeholders involved in the LH_2 supply infrastructure were already introduced in Section 2.1. The main actors and potential roles in the ecosystem can be summarised as follows:

- **Airport operators and Into-plane service providers (ITP):** Potentially own and operate parts of the airport LH_2 infrastructure like LH_2 storage and refueling
- **H_2 actors:** Potentially own and operate H_2 production, liquefaction and storage infrastructure
- **Renewable energy system actors:** Potentially own and operate the wind and power plants as well as H_2 production infrastructure
- **Oil and gas actors:** Potential to own and operate parts or the entire LH_2 supply infrastructure
- **Joint ventures:** Consisting of some or all of the actors, potential to own and operate the entire LH_2 supply infrastructure

There are several financing strategies which could be viable for these stakeholders available. In Appendix C an overview of the available financing options is giving. Based on the analysis of financing strategies, several conclusions can be drawn for investments in LH_2 supply infrastructure for aviation. Government loans and grants are particularly suitable for demonstrator projects, initial H_2 hubs, and locations with strong public support. Green bonds and loans present viable options for sustainability-oriented airports

and utilities, provided that clear CO_2 accounting and reporting structures are established. Private capital can effectively support investments in smaller infrastructure components, whereas larger projects are more appropriately financed through public-private partnerships and multilateral bank loans or grants, although these mechanisms typically involve higher administrative requirements. As technology matures, demand stabilizes, and associated risks decrease, commercial loans and conventional bonds become viable options for financing LH_2 supply infrastructure.

Table 3 presents a semi-quantitative evaluation of business model criteria for different stakeholders, derived from the stakeholder evaluation and their associated financing options. Additionally, the table outlines the range of financial criteria assumed in this study, based on financial reports from individual companies and meta-studies across the relevant sectors. The weighted average cost of capital (WACC) shown are company-specific in order to enable comparison between the stakeholders. The WACCs also differ significantly for projects of the individual stakeholders due to their risk and share of equity.

Table 3: Overview of stakeholders in a future LH_2 supply ecosystem regarding their financial criteria

	Airport operator [18,73]	Into plane service providers [18,19,74]	H_2 actors [21,22,75]	RES actors [76,77]	Oil and gas actors [76,78–81]	Joint venture
WACC[1]	6-8%	7-9%	6-8%	5-7%	7-11%	7-10%
ROIC after payback period	7-12%	12-16%	8-10%	5-7%	12-18%	8-12%
Payback period in years	15–20	3–7	10–15	8–15	10–20	15–20
Access to financing						
Access to equity						
ROIC						
Payback period						
Ability to take high risk						
Overhead costs						
Know-how of (L)H_2 sector						
Dependency on aviation sector						

[1] *stated WACC is nominal as commonly indicated in market reports [78]*

The return of invested capital (ROIC) is the share of investment that needs to be generated after the payback period. The variation in WACC across stakeholders reflects differences in capital structure, sector-specific risk, and access to financing. Airport operators and H_2 actors typically show lower WACC values due to stable, regulated revenue streams and long-term infrastructure investments, while oil and gas actors face higher WACC ranges owing to higher project risk and market volatility. ITP providers operate in a competitive environment with shorter investment cycles, leading to moderately higher WACC and ROIC expectations. RES actors benefit from low financing costs driven by policy support and predictable cash flows. Joint ventures exhibit intermediate values, as risk is distributed among partners but financing terms depend on the involved entities' profiles. The ROIC values mirror these trends, with higher targets in sectors exposed to greater risk or shorter payback expectations.

7.2 Study design

In the present study, the analysis focuses on the on-site LH_2 supply case, where renewable energy generation, H_2 production, storage and liquefaction are all located at or near the airport. This setup allows for results that are broadly transferable to various LH_2 supply scenarios in aviation. The same generic airport evaluated in Section 4.1 is assumed, with a projected demand of 50 ktH_2 in 2050. For RES the GREAT HYBRID location is chosen which lead to lowest supply costs. As previously discussed, a timescale starting from 2035 may no longer be viable due to Airbus postponing its entry into service (EIS) for H_2-powered aircraft, but the overall conclusions of the study remain valid. In this context, demand trajectories may shift and cost trends for several components are likely to continue declining.

The different potential stakeholder constellations along the LH_2 supply chain are shown in Appendix C. Stakeholders may both own and operate the entire supply chain or only specific segments of it. In this framework, the transport of H_2 – whether via pipeline, vessel, or truck – is considered a third-party service rather than being directly owned by the stakeholders analysed. Based on this structure, three archetypal stakeholder constellations are established, which comprehensively represent the relevant configurations and lead to comparable conclusions. The primary differentiation among these constellations lies in the number of stakeholders involved:

Constellation 1: Single source supply chain
In this scenario, a single stakeholder owns and operates the entire supply infrastructure. This stakeholder is most likely a joint venture composed of various actors as discussed in Section 2. Such a constellation is particularly relevant during the initial development phase, characterized by high investment requirements and significant risk, alongside a lack of experience among individual stakeholders.

Constellation 2: Dyadic supply chain
Here, one stakeholder – assumed to be an into-plane service provider (ITP) – owns and operates the airport LH_2 infrastructure, while a second stakeholder is responsible for the entire upstream and midstream infrastructure. This setup would involve a large oil and gas company with the financial resources and H_2 expertise necessary for managing the production and supply infrastructure. The configuration closely resembles the current jet fuel supply chain structure.

Constellation 3: Supply chain network
In this constellation, each major segment of the supply chain is owned and operated by a different stakeholder. The ITP operates the airport infrastructure, the H_2 actor manages production and liquefaction, and the RES actor owns and operates the renewable energy generation facilities. This model allows each stakeholder to remain within their core business while contributing to the overall LH_2 supply chain.

These constellations differ in their financial criteria, such as WACC, ROIC, and payback periods. An investment where the WACC and ROIC are equal only covers its cost of capital. When the ROIC after the payback period exceeds the WACC, economic profit is generated, whereas a ROIC below the WACC results in negative economic value creation. In this study, the ROIC is therefore assumed to be higher than the WACC for all stakeholders. The constellations also differ in overhead costs and access to subsidies. The specific financial criteria assumed for these archetypal stakeholder constellations are detailed in Appendix C.

The influence of policy support mechanisms on these constellations will be analysed within the modelling framework in Section 7.4, where the detailed methodology for policy categories will also be presented.

7.3 Comparison of stakeholder constellations

In this section, the effects of the stakeholder constellations on the cash-flow structures and the resulting LH_2 supply price at the airport are evaluated. The stakeholder constellations can also impact the design of the LH_2 supply infrastructure, which is discussed in detail in Appendix C. Due to the mechanics of the discounted cash flow method, a lower WACC increases the relative weight of future cash flows, making earlier investments more economically favourable. A lower WACC in combination with economies of scale can therefore change the design of the infrastructure and subsequently the timing and scale of investments.

As the different stakeholders have varying WACC and ROIC requirements following their respective payback periods, the cash flow structures and resulting LH_2 prices differ across the stakeholder constellations.

Figure 41 presents the resulting discounted cash flow for Constellation 1 (Single source supply chain) across all investment periods. The resulting cash flows for Constellations 2 and 3 are provided in Appendix C. The figure illustrates the investments across the five investment periods alongside the corresponding revenues, as well as fixed and variable OPEX. All values are shown in discounted terms, resulting in lower absolute values in later years. Dashed lines indicate the cumulative discounted cash flow for each investment period. Investments, including the required ROIC, are recovered following the defined payback period, which is 15 years after the initial investment in this constellation. The additional revenue generated after the payback period reflects the opportunity cost of capital for the residual value of the infrastructure. For some components, the operational lifetime is shorter than the overall project duration. Although the reinvestment for component replacement is illustrated in the figure, these replacement investments are not included in the cash flow calculation.

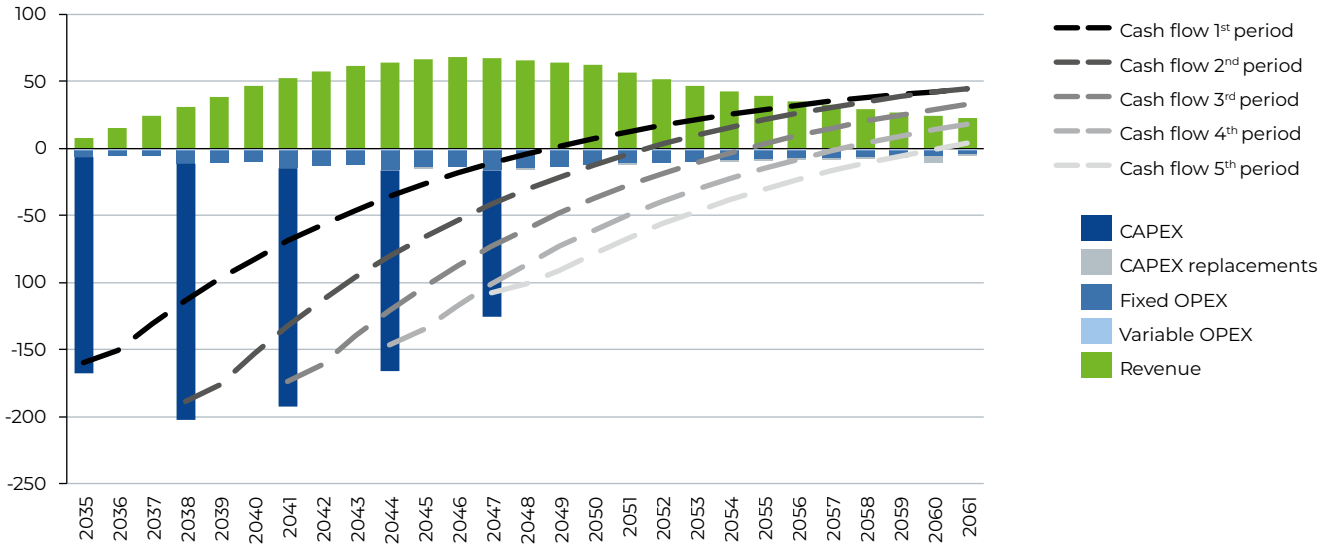

Figure 41: Total cash flow for the constellation 1: Single source supply chain at the generic airport

The cash flow structures directly determine the resulting LH_2 supply prices for each stakeholder constellation. Based on the recovered investments and the required ROIC, the resulting prices reflect the conditions under which the infrastructure can operate sustainably while covering capital and operational costs. Figure 42 presents the LH_2 prices for the considered stakeholder constellations. For each investment period, the price is kept constant under the assumption of off-take agreements, ensuring supply security and price stability throughout the payback period. The resulting price curves shown in the figure represent the weighted average price across the total LH_2 demand, as determined by the individual off-take prices in each period. In the early years, prices range between 9.56 and 10.55 USD/kgH_2 for the archetypical constellations, decreasing to values between 4.86 and 5.36 USD/kgH_2 in the long term.

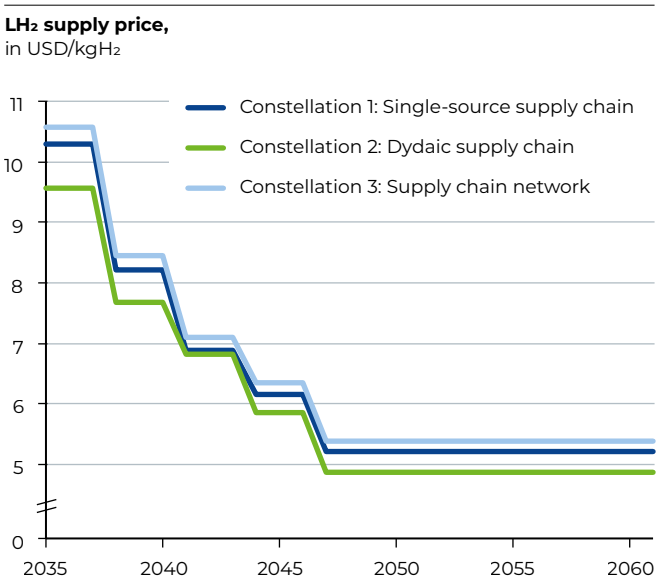

Figure 42: LH_2 supply price at the airport for the different stakeholder constellations

Among the constellations analysed, Constellation 2 results in the lowest LH_2 supply price, primarily due to the comparatively low WACC of the oil and gas actors involved in this configuration.

From this analysis, general insights regarding the influence of stakeholder constellations can be derived. Depending on the stakeholders involved and their financial criteria, the cost-optimal infrastructure design may vary across configurations. Stakeholder selection within the LH_2 supply chain has a significant impact on the resulting LH_2 price; for example, the long term LH_2 price in the supply chain network is over 10% higher than in the dyadic supply chain, despite similar total expenditures in both cases. The primary driver of these price differences is the stakeholders' WACC, with lower WACC values leading to lower LH_2 supply prices.

7.4 Policy support mechanisms

Without support from governments at the EU or national level, H_2-powered aviation will not become economically viable at the calculated LH_2 prices, particularly during the initial years of market development. As the defossilization of aviation serves the public interest, several policy support mechanisms can be considered to facilitate the development of LH_2 infrastructure for aviation. This section first provides an overview of different policy mechanisms based on insights from the broader H_2 sector. Subsequently, the section analyses the influence of selected support mechanisms on LH_2 prices using the single source supply chain scenario as a case study.

7.4.1 Overview

Based on insights from the broader H_2 sector, policy support mechanisms applicable to LH_2 supply infrastructure can be categorized into five clusters. These clusters are discussed with respect to their aims, operational mechanisms, and current application within the H_2 sector.

Direct financial support

Direct financial support aims to reduce the high upfront capital costs associated with H_2 infrastructure, making projects economically viable, particularly during the early stages of market deployment. This type of support compensates companies that act as early movers in the market [70]. One form of direct support involves grants and subsidies, which provide non-repayable funds for specific projects. For example, the IPCEI funding program has allocated up to €6.9 billion in subsidies for H_2 infrastructure, including electrolysis, storage, and transport [82]. Another form involves state aid schemes, which are government-backed mechanisms designed to lower infrastructure development costs. An example is Germany's Hydrogen Core Network, supported by a €3 billion state aid program to develop an H_2 pipeline network, covering part of the investment costs and ensuring long-term financial viability [83].

Loan-based support

Loan-based support aims to mitigate financial risks for investors by offering low-interest loans and government-backed guarantees to facilitate investment in H_2 infrastructure [84]. Low-interest loans are offered by institutions such as the European Investment Bank and the German Credit Institute for Reconstruction (KfW), which provide favourable financing conditions specifically for H_2 projects [85,86. Loan guarantees, in turn, reduce investment risks for private actors through government-backed assurances. For example, the Hydrogen Loan Guarantee Program by the US Department of Energy offers guarantees for loans taken by companies investing in H_2 infrastructure, lowering financial barriers to market entry [87].

Market-based instruments

Market-based instruments aim to leverage market mechanisms and economic incentives to achieve environmental objectives while bridging the cost gap between production and market prices for H_2 [84]. Contracts for Difference (CfD) provide price stability by having governments cover the difference between a predefined production strike price and the actual market price. If the market price falls below the strike price, the government compensates the producer for the difference, while payments flow back if the market price exceeds the strike price. An example includes the CfD structure proposed under the European Hydrogen Bank [88]. Double auction mechanisms, such as those implemented by H_2Global, function by purchasing H_2 from producers through competitive auctions to secure the lowest possible price, while selling the H_2 to consumers at a fixed, lower price through a second auction. The difference between the purchase and sales price is covered using public funds, ensuring price stability for buyers while maintaining competitive price

discovery on the supply side [89]Additionally, carbon-pricing incentives indirectly benefit H_2 by increasing the cost of fossil alternatives, thus improving the competitiveness of H_2 projects. Under systems like the EU Emissions Trading System (ETS), H_2 projects can also benefit from carbon credits or exemptions, which incentivise lower-emission alternatives by imposing carbon costs on emitters [90].

Tax incentives

Tax incentives aim to lower the fiscal burden on companies investing in H_2 technologies, thereby improving the financial attractiveness of H_2 infrastructure projects [84]. Tax credits and deductions reduce corporate tax liabilities for investments in H_2 infrastructure. For example, the US Inflation Reduction Act (IRA) offers production tax credits of up to 3 USD/kgH_2 for green H_2 production, providing a direct incentive for early market deployment [91]. Exemptions and depreciation benefits further support investment by allowing companies to accelerate the depreciation of H_2-related assets, thus reducing taxable income. An example is Germany's "Superabschreibung" for climate-friendly investments, which enables firms to apply accelerated depreciation for H_2 infrastructure, improving cash flow and reducing upfront financial barriers [92].

Regulatory & Policy Support

Regulatory and policy support provides long-term certainty and accelerates the deployment of H_2 infrastructure by introducing mandatory quotas, fast-track permitting, and streamlined administrative procedures. Mandatory quotas and standards require the use of renewable H_2 within specific sectors. An example is the EU Renewable Energy Directive (RED III), which establishes mandatory quotas for the use of renewable H_2 in industry and transport, thereby ensuring demand and providing market security for producers [93]. In aviation, the recently adopted ReFuelEU Aviation Regulation introduces blending mandates for sustainable aviation fuels, while also setting specific sub-targets for renewable H_2 and e-fuels [94]. These aviation-specific quotas provide a first step towards creating a guaranteed market for H_2-based fuels at airports, thereby directly addressing the demand-side risks identified in this study. Permitting and fast-track approvals simplify and accelerate administrative procedures for the construction and operation of H_2 infrastructure. For instance, France's Hydrogen Fast-Track Permitting Program has introduced a streamlined approval process for electrolysers and H_2 storage projects, supporting faster market deployment [95].

7.4.2 Impact on the liquid hydrogen supply price

In the following, the five policy support categories are evaluated with respect to their applicability and impact on LH_2 infrastructure for aviation.

Direct financial support

Direct financial support is analysed by assuming a 38% CAPEX funding ratio, consistent with the IPCEI HyTECH programme [96]. This funding ratio is incorporated into the cash-flow model to assess its effect on the resulting LH_2 price. The planned infrastructure and required investments remain unchanged, as the objective of this mechanism is to support the stakeholder's business models and not to change these so that the companies make higher profits.

Figure 43 illustrates the discounted cash flow for Constellation 1 when CAPEX funding is applied to the initial investment period. The funding significantly reduces the cumulative cash flow during this phase. Correspondingly, Figure 44 shows the impact on the total LH_2 price. Although CAPEX funding accounts for approximately 4% of the total undiscounted investments, it lowers the initial LH_2 supply price in 2035 by 30%, substantially increasing the project's attractiveness for investors. However, the drawbacks of this mechanism include its limited long-term effect and potential market distortions, as support is restricted to selected projects, in this case specific airports.

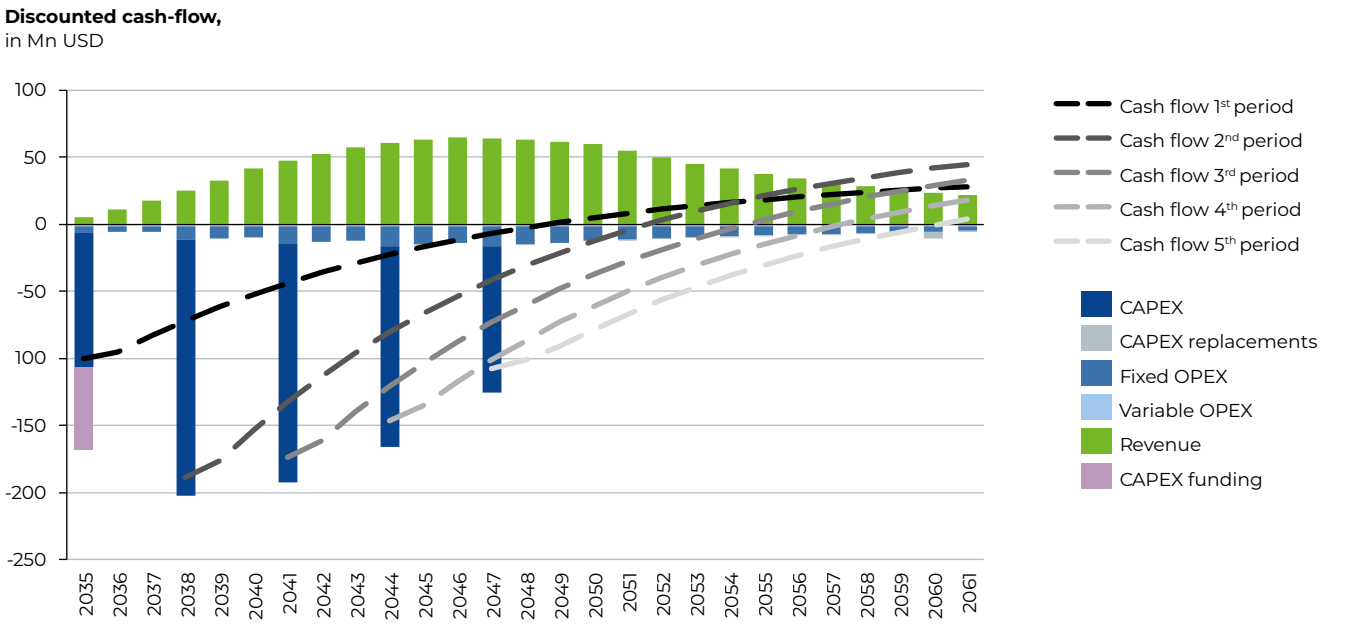

Figure 43: Cash flow of the Constellation 1: Single source supply chain with direct CAPEX funding in the first investment period

Loan-based support

Loan-based support is evaluated by modelling a reduction of 2% in the WACC for the stakeholder business models, reflecting the impact of low-interest loans and government-backed loan guarantees. This adjustment accounts for the higher risk profile typically associated with early-stage H_2 projects.

By lowering the WACC, loan-based support improves investor attractiveness and reduces long-term LH_2 supply price. As shown in Figure 44, a 2% reduction in WACC corresponds to a decrease in the long-term LH_2 price of approximately 9%. In addition to price benefits, this mechanism has the advantage of imposing no direct financial cost on public institutions. However, similar to other support measures, it may lead to potential market distortions.

Market based instruments

Market-based instruments are analysed through CfD, as considered by the European Hydrogen Bank to bridge the cost gap between green and grey H_2 produced from natural gas. Green H_2 production represents approximately 60% of the total LH_2 supply costs in this study. The average levelized cost of grey H_2 in Europe is estimated between 2.80 and 5.50 EUR/kgH_2 [97], with a constant value of 3.76 USD/kgH_2 assumed here. Figure 44 illustrates the resulting LH_2 supply price under a CfD scheme.

In this example, CfDs reduce the initial supply price by about 23% and after 2044, no further funding is required, as green H_2 becomes cost-competitive with grey H_2. Compared to CAPEX funding with a similar budget, CfDs achieve less reduction in both initial and long-term LH_2 prices for this reference price. The required budget and impact on the LH_2 price are highly sensitive to the grey H_2 reference price. Assuming the lower bound grey H_2 price, more than triple the budget is needed, with funding required until the project's end. In contrast, under the higher grey H_2 price, only about 1% of the budget is required, with green H_2 becoming competitive by 2038. A key advantage of CfDs is price predictability, which reduces investment risk. Furthermore, CfDs are not project-specific, mitigating market distortions and avoiding inefficient over-subsidization. However, implementing CfDs involves administrative complexity and relies heavily on sustained political commitment and substantial government financial backing.

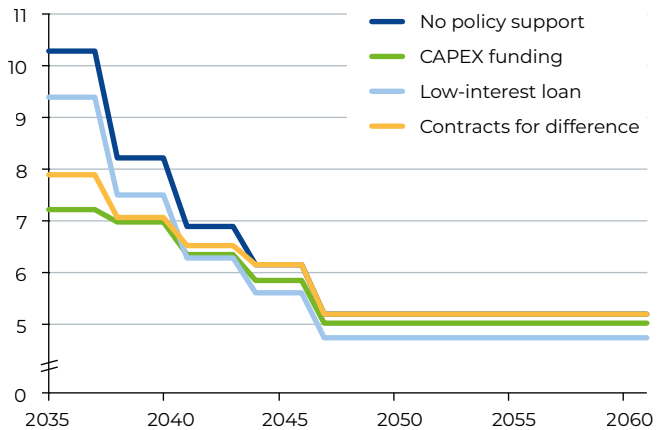

Figure 44: LH_2 supply price for the single source supply chain with the investigated policy support mechanisms

Tax incentives

Tax incentives are not explicitly modelled in this study, as their effects depend on individual investor tax capacities and national tax regulations, which cannot be generalised consistently within the cash flow framework. Tax incentives enhance investor attractiveness and can contribute to reducing long-term LH_2 supply prices. Compared to direct subsidies, tax incentives typically result in lower government expenditures and can be combined effectively with other support mechanisms. While administrative complexity is generally lower than for direct funding instruments, potential market distortions may still arise. The effectiveness of tax incentives depends on the tax capacity of the investors, which can limit participation among certain stakeholder groups.

Regulatory and policy support

Regulatory and policy support mechanisms are not explicitly modelled in this study, as their impacts are highly dependent on evolving political frameworks and regional regulatory conditions, which cannot be consistently quantified within the applied cash flow approach. Regulatory and policy support fosters long-term market stability and, when combined with infrastructure support, can effectively stimulate demand creation. However, these mechanisms face risks related to policy uncertainty and inconsistency, which may undermine investor confidence. Implementation is often slow and bureaucratically complex, potentially leading to market distortions. Moreover, without complementary market-based instruments, regulatory measures alone do not guarantee sufficient investment levels.

In the aviation context, mandates for renewable fuels could play a particularly important role. Similar to existing blending requirements for sustainable aviation fuels, a gradual obligation to integrate renewable H_2 into aviation fuel supply would secure offtake and reduce revenue risk for investors. Such mandates are especially relevant for capital-intensive constellations with long payback periods, as they enhance bankability and mitigate demand-side uncertainty during early deployment.

Parallel funding, meaning the combination of multiple support mechanisms for a single LH_2 infrastructure project, can increase investment attractiveness and reduce financing gaps, particularly in capital-intensive early deployment phases. This approach can combine, for example, direct subsidies with tax incentives or low-interest loans to achieve lower effective costs of capital, as evidenced in the U.S. under the Inflation Reduction Act, where stacked tax credits and production incentives significantly reduce green H_2 costs [98].

However, parallel funding also carries risks of overcompensation and market distortions, requiring clear governance and transparency to prevent inefficiencies [70]. Regulatory restrictions often limit combined support. For example, CfD schemes under the European Hydrogen Bank and Germany's H_2Global mechanism are designed to avoid simultaneous direct investment grants for the same H_2 volumes, thereby reducing the risk of double subsidization. Similarly, EU State Aid Guidelines (CEEAG) restrict the cumulation of operational aid with investment aid for the same eligible costs [99]. While tax incentives and low-interest loans can typically be combined with investment grants, mechanisms tied to output-based support (e.g., CfDs or production premiums) frequently exclude additional CAPEX funding for the same capacity. Therefore, the design of support packages for LH_2 infrastructure requires careful alignment with regulatory frameworks to maximize the benefits of parallel funding while avoiding legal conflicts and inefficiencies.

7.5 Conclusion

In this chapter, first the key stakeholders within the H_2 aviation ecosystem are introduced and discussed their respective financing options and constraints. Building on this, the impact of three archetypical stakeholder constellations on the design of the energy system and the resulting LH_2 supply prices at airports is examined. Following this analysis, five categories of policy support mechanisms are presented, drawing on insights from the broader H_2 sector. Finally, the application of these policy instruments for LH_2 supply infrastructure are discussed, focusing on their impact on LH_2 prices and the implications for enabling H_2-powered aviation.

The analysis presented in this study shows that the stakeholder constellation and their financial criteria have a decisive influence on the resulting LH_2 supply infrastructure design and price at airports, with the stakeholders' WACC emerging as the main driver. A lower WACC significantly reduces supply costs, underlining the importance of the financial framework for infrastructure development.

Early-stage infrastructure projects can benefit from public loans, grants, green bonds, and public-private partnerships, which help to manage risk and high upfront CAPEX requirements. As technology and demand mature, commercial loans and bonds become viable financing instruments, enabling projects to access capital with lower risk premiums. To reduce the high initial investments and risks for investors, direct financial support and market-based instruments can be effective mechanisms for advancing the H_2 aviation ecosystem, although these require substantial public funding. In contrast, loan-based support and tax incentives can lower LH_2 supply prices in the long term while requiring less government expenditure, although with the potential for market distortions. Overall, a combination of multiple support mechanisms with regulatory measures can facilitate the initial development phase of LH_2 supply infrastructure, create long-term market stability, and encourage demand for H_2-powered aviation.

The findings further suggest that different stakeholder constellations require tailored policy support. Joint ventures in the single-source constellation, facing the highest initial risk, benefit most from direct CAPEX grants and concessional loans to overcome high capital barriers. Dyadic constellations, where oil and gas actors assume upstream investment, are better positioned to access commercial loans or issue green bonds once infrastructure matures, reflecting their lower WACC and financing capacity. Supply chain networks, involving multiple specialized actors, are particularly sensitive to stable revenue streams; instruments such as contracts for difference or blending mandates can distribute risk across stakeholders and provide the long-term certainty needed for coordinated investments. Policymakers should therefore align support instruments with the financing structures of the underlying business models rather than adopting a one-size-fits-all approach.

This study provides a first consistent framework linking stakeholder constellations, financing strategies, and policy instruments to LH_2 supply prices for H_2-powered aviation, offering a foundation for targeted infrastructure planning. Future policy frameworks should align financial instruments with stakeholder-specific risk profiles to lower capital costs while maintaining incentives for efficient infrastructure deployment. Moreover, developing coordinated and regionally adapted investment and policy roadmaps will be crucial to scale LH_2 supply infrastructure in line with aircraft uptake and aviation sector defossilization targets.

MACROECONOMIC IMPACT OF FUTURE LIQUID HYDROGEN SUPPLY INFRASTRUCTURE

8 Macroeconomic impact of future liquid hydrogen supply infrastructure

This chapter presents the macroeconomic analysis of LH_2 infrastructure. This dimension is of crucial importance to policymakers and industry stakeholders, but also for promoting social acceptability and ensuring long-term economic sustainability [54]. The analysis focuses on countries that are likely to play a relevant role in a future LH_2 network. The selected countries are examined in terms of their structural potential to benefit from LH_2 value chains. Furthermore, the impacts of LH_2 networks on macroeconomic indicators are considered, based on different economic scenarios.

8.1 Study design

This section presents the countries considered in this study, describes the supply chain analysis and the economic scenarios. More details are provided in Appendix C.

8.1.1 Country selection

The analysis focuses on Europe and the Middle East and Northern Africa (MENA). In total, five countries plus the European Union (EU) are included, each representing different roles and capabilities in a future LH_2 network. An overview of the selected countries with relevant economic indicators is shown in Figure 45.

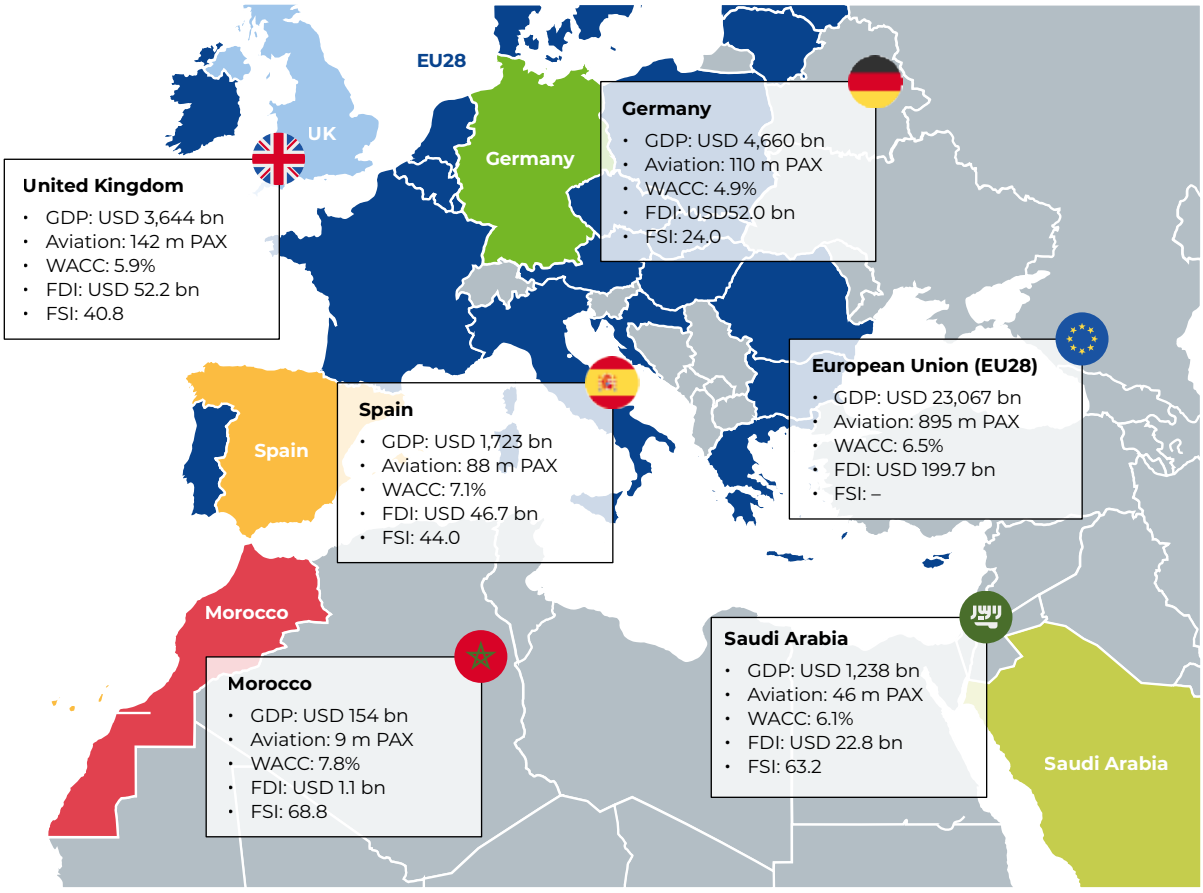

Figure 45: Overview of the selected countries/regions with economic indicators. GDP data is given for 2024 [100]. For aviation, passengers (PAX) include both domestic and international aircraft passengers of air carriers registered in the country [101]. WACC data are obtained from project-internal estimations for LH_2 infrastructure and shown without inflation adjustment. Foreign direct investment (FDI) reflects the inflows into the respective country in 2023 [102]. The Fragile States Index (FSI) is shown for 2024 [103]. Germany, the United Kingdom and Spain are shown separately, but they are also included within the EU28.

Morocco and Saudi Arabia are selected due to their large RES potential, making them prospective exporters of green H_2 [104–108]. Moreover, they are characterized by relative political and economic stability in the region, which has prompted European countries and the EU to initialize green H_2 collaborations with both countries [40,109–117].

Spain, Germany, and the United Kingdom (UK) are selected to represent the European perspective. They reflect relevant aviation markets with a potentially large future LH_2 demand. Yet, they vary in terms of green H_2 production potential and economic structure. Spain has high potential for RES [118–120] along with a large aviation sector driven by tourism [121,122]. Germany is one of the largest aviation markets in Europe but is expected to rely on H_2 imports due to limited RES capacity [123–125]. The UK is a major aviation hub with strong offshore wind resources and an ambitious H_2 strategy [126–128]. In addition to the five countries, the EU is considered as an economic and political region. The year 2019 is selected as the base year for all SAMs. This year provides the most recent and comprehensive data, unaffected by the distortions caused by the COVID-19 pandemic and the war in Ukraine, which had a major impact on European energy markets [129]. As the UK was still part of the EU in 2019, this analysis refers to the EU28.

8.1.2 Supply chain analysis

In this analysis, the LH_2 infrastructure consists of 15 technologies across five categories, which can be organized into various supply chain configurations based on techno-economic evaluations [130]. The categories comprise RES, conversion systems, storage systems, transport systems, and refuelling systems. In addition, eight key components are identified. They reflect components that are critical for the infrastructure and require a certain level of know-how and industrial capacity, e.g. wind turbines, PEM electrolyser stacks or H_2 compressors [131,132]. A detailed overview of all technologies and key components is provided in Appendix C. As outlined in Section 2.3.7, the techno-economic assumtions need to be converted into a macroeconomic framework [6]. This requires the disaggregation of CAPEX and OPEX into three phases of economic activity during the lifetime of each technology. These are (1) key component manufacturing, (2) installation & BoP supply, and (3) operation.

8.1.3 Design of economic scenarios

The economic scenarios reflect potential pathways, based on structural conditions and recent trends in the respective countries. The scenarios consider three dimensions:

Degree of self-supply for key components: Key components represent complex equipment that requires specific capabilities and knowledge, which is not available in every country [131,132]. These industries are often located in established clusters with few firms (e.g., wind turbines) or regions (e.g., electrolysers) dominating the world market [133,134]. It is unlikely that all countries can supply these components, which is reflected in the scenarios [135]

Domestic share in the installation and operation phase: The installation & BoP supply and operation phase contain less specialized activities and require fewer preconditions. In these phases, the share of domestic contribution is varied, reflecting so-called local content policies, which are particularly prevalent in emerging economies [136,137]. They aim to ensure that host countries receive a fair share of the value when sustainable energy is exported.

Origin of investments: This dimension reflects the financial resources, which are a major challenge for green H_2 networks [138,139]. Projects in emerging countries, where investment risks are relatively high due to unclear or unstable political and economic conditions, often depend on capital from industrialized countries [140,141]. In such cases, revenues from the project are likely to flow back to the capital providing countries, which reduces the income-induced effects in host regions.

The scenarios are country-specific, depending on structural conditions and current trends. For Europe, the focus is on key components, reflecting current ambitions [142–144]. With a relocation of PV and battery production from Europe to Asia in the past decade, geopolitical resilience and energy independence have become major topics for the EU [145]. To avoid further dependencies on crucial technologies, the

EU aims to protect its key industries, especially in the field of sustainable energy [146]. Thus, for the EU28, Germany, Spain and the UK, domestic capacities for key component manufacturing are varied in the scenarios, alongside with the foreign investment share. For the MENA countries, due to a lack of key component industries [131,132], the scenarios focus more on local content in supporting activities and the origin of project capital [147,148]. For each country, three economic scenarios are constructed:

Base: The base scenarios are a status-quo projection. The degree of self-supply for key components is based on the countries' trade balances, using the Comtrade database [149]. Domestic shares in installation & BoP supply are derived from the SAMs. Investment sources are based on foreign direct investment (FDI) stock data.

Domestic boost: The domestic boost scenarios represent pathways with enhanced local value chains and investment, driven by policy measures, such as local content requirements, investment support or incentivizing of domestic industries.

Foreign dependency: The foreign dependency scenarios, in contrast, project a relocation of key component industries, supporting sectors, and the dependence on foreign capital.

A detailed overview of the economic scenarios is provided in Appendix C.

8.2 Results

The first part compares the air transport system with other H_2-demanding industries from a macroeconomic perspective to reflect a potential prioritization in the case of H_2 shortage. The second part presents enabler activities for LH_2 networks. The third part analyses the structural potential of the selected countries to benefit from LH_2 value chains. Following this, the fourth part shows country-specific multipliers under various economic scenarios for an LH_2 supply network in 2050. The multipliers reflect the response of the economic system to an exogenous change, which is the scale-up of LH_2 supply chains in the context of this study. Finally, the fifth part examines the total economic impacts during the transition phase of an exemplary small LH_2 network.

8.2.1 Macroeconomic relevance of hydrogen-demanding industries

This section assesses the macroeconomic relevance of the air transport system. Green H_2 supply is currently scarce, and it remains questionable whether the infrastructure will be scaled up in time to meet the demand in all hard-to-abate industries [133,150,151]. A competition for H_2 is thus a realistic scenario, especially in the short-term. To evaluate the prioritization of the air transport system in case of H_2 shortage, its relevance for the economy is compared to other H_2-demanding industries. The EU28 is used for the analysis because of the cross-border nature of aviation and because a potential H_2 shortage would not necessarily be confined to one country [145,152]. Figure 46 presents a linkage map of the inter-industrial dependencies in the EU28. Aviation-related industries are highlighted, along with other potential green H_2 demanders.

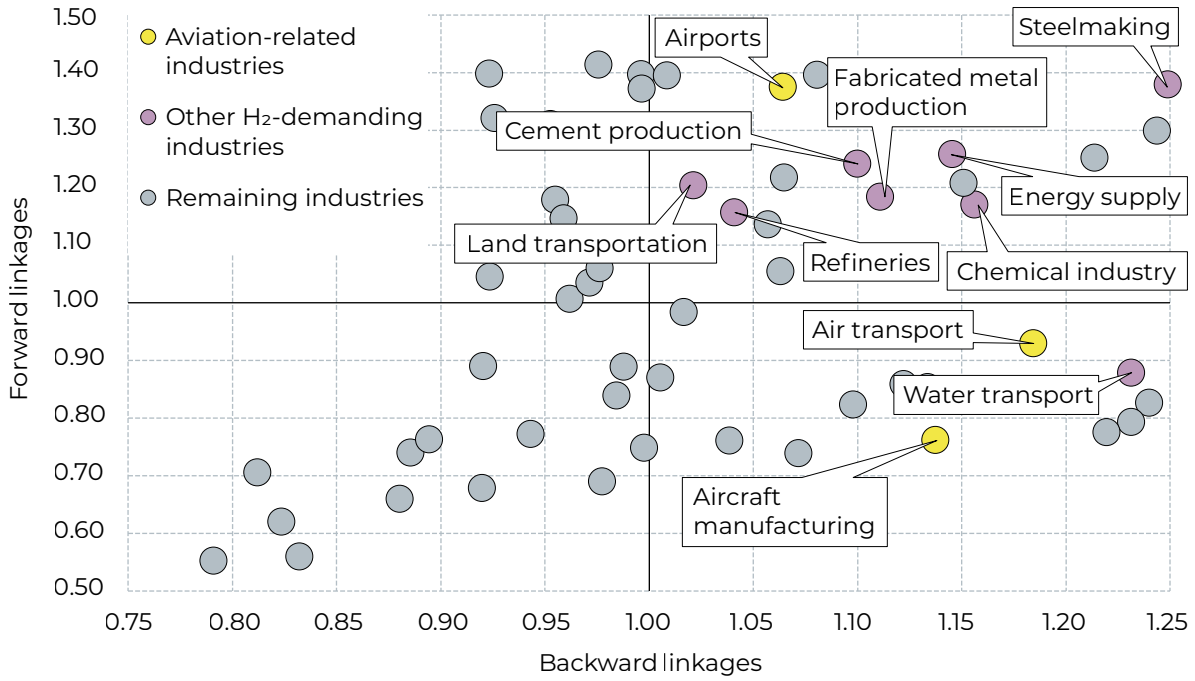

Figure 46: Normalized input-output-based linkage map of all industries in the EU28. Aviation-related industries and other potential H_2 demanders are highlighted. Some industries are not visible due to the scaling of the axes. Aircraft manufacturing is part of the aggregate "Manufacturing of other transport equipment". Airports are part of the aggregate "Warehousing and support activities for transportation".

A backward linkage (BL) shows how much a sector depends on domestic industries by demanding inputs from these. In contrast, a forward linkage (FL) shows how relevant a sector is for other industries by supplying output to these. BL (FL) larger than 1.0 imply a strong upstream (downstream) integration. Industries positioned in the upper right quadrant are thus important as demanders and suppliers for the economy [153].

The linkage analysis demonstrates that the air transport system has an important role in the inter-industrial network of the EU28. Aircraft manufacturing and air transport are positioned in the lower right quadrant, indicating that they are major customers of other industries' output. Aircraft manufacturing, for instance, relies on multiple upstream sectors, such as manufacturing of electronics, machinery, or metals [154,155]. Among all H_2-demanding industries, air transport ranks at the third position in terms of backward integration. That means that an increase in air transport output triggers a cascade of upstream activities, with many sectors involved, such as refineries, infrastructure providers, and several service providing industries. However, both sectors are less relevant as suppliers, particularly aircraft manufacturing. Water transport, that might use H_2 for the decarbonization of ships, is also positioned in the lower right quadrant and has lower FL, but higher BL than air transport.

Although airports have a lower BL than the other aviation-related industries, they are positioned in the upper right quadrant. This position underlines their essential role as demander and supplier within the EU28's economic system [156,157]. In terms of downstream integration, airports even rank second among all H_2-demanding sectors. The remaining H_2 consumers are also found in the upper right quadrant, emphasizing their importance to the EU28 economy. Steelmaking, a major GHG emitter, stands out with the highest BL and FL. Similarly, the chemical industry and manufacturing of fabricated metals show a high interconnectedness within European industries [158]. Land transportation and energy supply do not surpass the BL of airports, but they are crucial providers of infrastructure services and thus essential to the overall economy.

The linkage analysis suggests that, in a context of scarcity, aviation might not be the most important H_2 user from a macroeconomic perspective. While air transport has the third highest BL, its relevance in the downstream supply chain falls behind industries that provide intermediate products, such as the chemical industry and steelmaking. Similarly, although airports have the second highest FL, they are less essential on the upstream side. Yet, the analysis only considers inter-industrial linkages, neglecting final consumers and aviation's global connectivity function, which enables the cross-border exchange of technological, scientific, and cultural knowledge [159,160].

8.2.2 Enabler industries for the liquid hydrogen supply chain

LH_2 networks depend on a diverse set of economic activities to provide the necessary goods, infrastructure, and services. The supply chain analysis defines 44 new LH_2 activities, three phases of economic activity for all 15 technologies except for the power grid, which has no key component manufacturing. Based on ISIC classifications, the cost structure of these activities is assigned to existing industries (activities) to derive synthetic LH_2 industries with a SAM-consistent production input structure. A total of 27 enabler activities is identified. Figure 47 lists these activities and categorizes them into three groups: manufacturing industries, infrastructure sectors and services.

Manufacturing activities, such as basic metals, machinery, and chemical products, provide key components and additional equipment. Infrastructure activities are required for the setup and operation of essential facilities and processes, such as water supply, construction, and transportation. Services comprise various activities to support the deployment and operation of the LH_2 network, such as financial, legal, and engineering activities. The classification reflects the diverse and complex nature of LH_2 networks and highlights their interconnectedness with the wider economic system [130].

Manufacturing	Infrastructure	Services
Mining and quarrying	Energy supply	Financial services
Electronic and optical products	Warehousing and transport support	Other business support
Chemical products	Water supply	Insurance and related services
Electrical equipment		Public administration
Rubber and plastics	Construction work	Real estate services
Machinery and equipment		
Glass and ceramics	Maintenance and repair of vehicles	Legal, tax and other consultancy
Motor vehicle and vehicle parts		
Basic metal products	Land and pipeline transport	Engineering and technical services
Transport equipment		
Fabricated metal products	Water transport	Research and development
Repair and installation		

Figure 47: LH_2 enabler activities, grouped into three sectoral categories.

8.2.3 Country-specific structural potentials for liquid hydrogen value chains

This section examines the countries' structural potential to benefit from LH_2 industries. A series of synthetic industries are constructed to depict the 44 activities in a format consistent with the SAM. The assumption of this analysis is that all LH_2 activities are performed domestically, including the manufacturing of all components. The country-specific multipliers for the economic indicators are displayed in Figure 48 (IO-based) and in Figure 49 (SAM-based). The IO-based multipliers only reflect the total inter-industrial effects that LH_2 activities trigger in each country's economy.

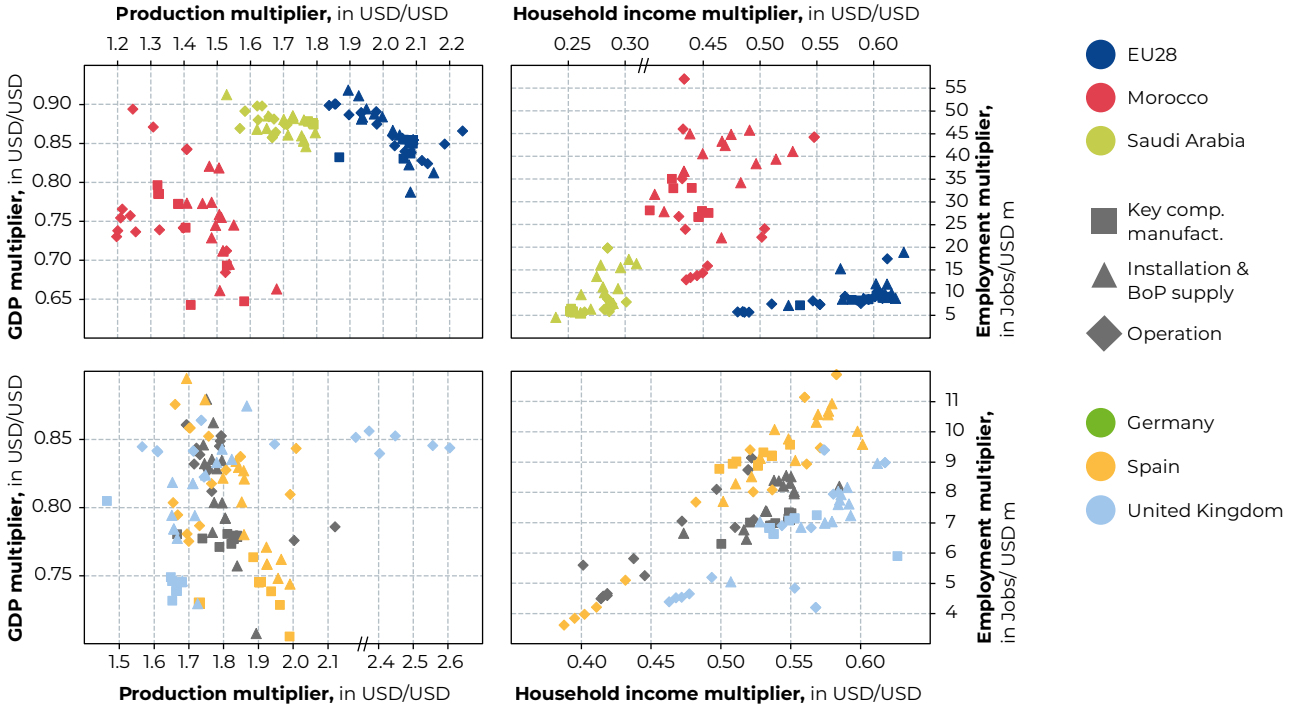

Figure 48: IO-based multipliers of the LH_2 industries for relevant macroeconomic indicators.

The EU28 shows higher production and GDP multipliers than the MENA countries, indicating stronger interlinkages with domestic industries. Yet, higher multipliers also result from the size of the EU28 as an economic region, which allows a higher degree of self-sufficiency [153,161,162]. Within MENA, Saudi Arabia has stronger effects from LH_2 infrastructure on production and GDP, while Morocco shows higher impacts on household income and employment. This implies that Morocco's population benefits more from LH_2 value creation. Employment multipliers in Morocco even exceed those in the EU28, largely because of lower wages and labour productivity [163,164].

Across European countries, the results are more homogenous, with the UK having the lowest multipliers. Key component manufacturing yields higher effects in European countries than in MENA, resulting from larger capacities in upstream industries, such as chemical industry, metallurgy or electrical equipment. Yet, installation and operation dominate for most indicators. Across all countries, employment is particularly driven by these phases, while key component manufacturing remains more capital-intensive.

While the IO-based multipliers cover inter-industrial dependencies, they neglect consumption-induced production effects that result from income generation. This dimension is captured by SAM-based multipliers, which are provided in Figure 49. Compared to the IO-based results, SAM-based multipliers are higher and reveal new patterns with stronger divergence between the countries. While Morocco previously showed the lowest production and GDP multipliers, it now aligns more closely with Saudi Arabia. Some of Morocco's key industries are driven by final consumption, such as food and textile production. Thus, Morocco benefits disproportionately from income generation in LH_2 activities, because it triggers production in sectors that are not directly part of the LH_2 value chain. The EU28, due to its large geographical and economic coverage,

has the largest multipliers, except for employment. For the European countries, the picture changes substantially. What appeared as a rather homogenous group under IO-based results, now breaks into separate clusters of countries. Germany shows the lowest multipliers, while Spain yields the highest effects for production, GDP and employment, and the UK for household income.

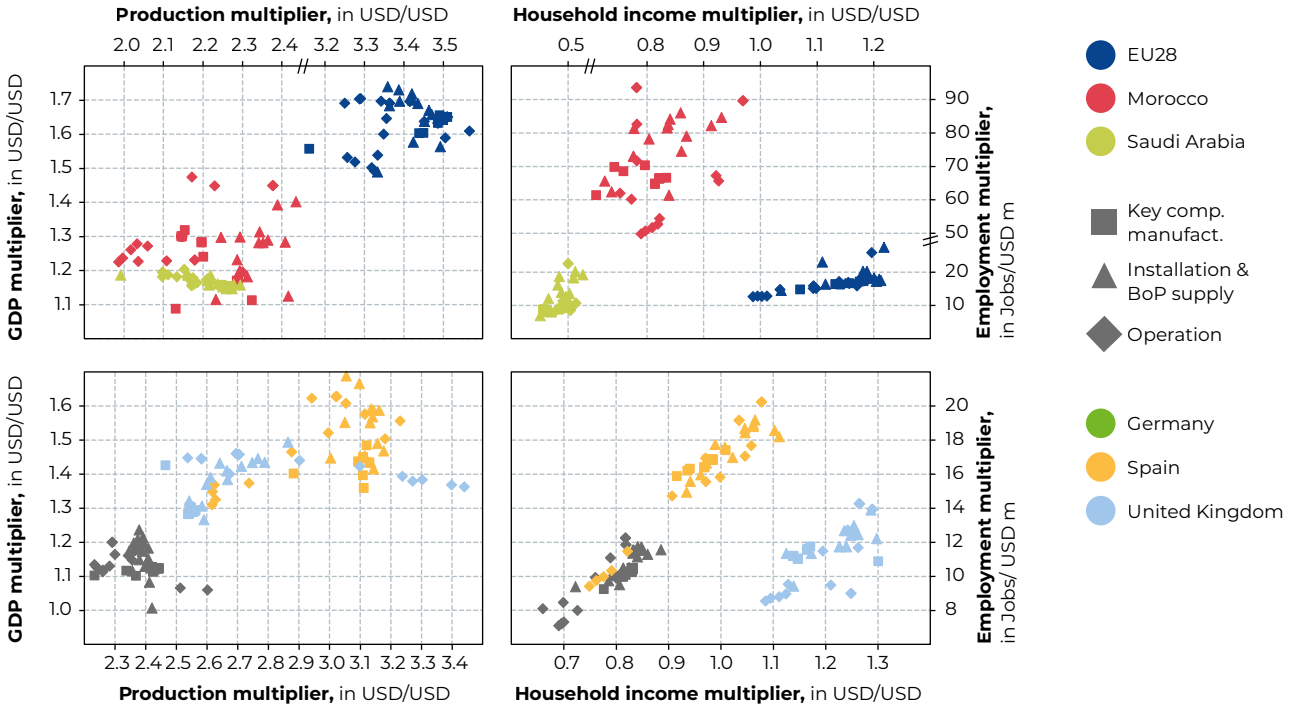

Figure 49: SAM-based multipliers of the LH₂ industries for relevant macroeconomic indicators.

Overall, the SAM-based results are dominated by country patterns. These patterns are mainly attributable to country-specific characteristics. For instance, Germany has much higher savings rates for households and tax rates for income, which means that a smaller share of income is effectively used for consumption [165,166]. These structural differences reduce the comparability of countries. To contextualize the SAM-based results in their country-specific environment, the normalized SAM-based multipliers are examined, which assess the LH₂ multipliers relatively in the context of the respective country and its economy.

Figure 50 shows the normalized SAM-based GDP multipliers. This representation allows for an assessment of how countries benefit from LH₂ activities, in relation to their remaining economy. The results differ significantly from Figure 49. Relatively to its economy, Morocco benefits substantially from LH₂ infrastructure, especially during the operation phases. Peaks are found for operating electrolysers, onshore wind parks, and PV power plants. For key component manufacturing, the EU28 still yields the highest multipliers, while Saudi Arabia is far behind in most activities. A shift is also found for the European countries. While Germany had the lowest multipliers before, it is now surpassing Spain and the UK in many phases. This accounts particularly for the key component manufacturing activities, where the UK shows the weakest results. This reflects the UK's structural change in the past decades, shifting from an industrialized economy to a more service-based society [167–169]. In the installation phases, the results are more diverse, with Germany still having the lead in most activities.

Overall, the normalization reveals how the relative economic impact of LH₂ activities differs between countries. It complements the SAM-based perspective, providing a clearer understanding of country-specific income distribution and use.

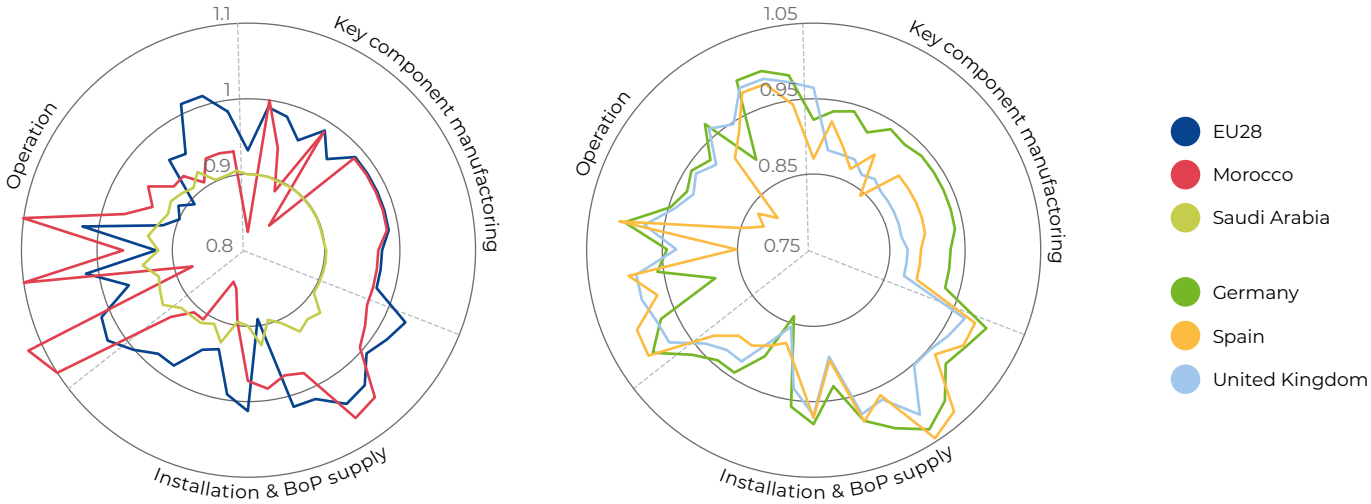

Figure 50: Normalized SAM-based GDP multipliers of LH_2 activities

8.2.4 Scenario-specific economic multipliers of liquid hydrogen networks

The macroeconomic effects in this section are based on the supply network for European airports presented in Section 4.2. In that network, MENA is not integrated as export region due to the higher supply cost. Thus, the analysis of Morocco and Saudi Arabia is based on the global potential analysis from Section 5.2. Within the network, the European countries have different roles and infrastructure profiles that must be considered when interpreting the results: Spain produces and demands LH_2; the UK exports LH_2 to mainland Europe; Germany produces a small amount and imports its main demand of LH_2. Thus, the resulting LH_2 activities vary between the countries.

Figure 51 illustrates the multipliers for the aggregated LH_2 infrastructure profile in each country. While the previous section assumed that all activities are performed domestically, this analysis incorporates import dependencies and capital outflow when foreign investors are involved. The multipliers reflect the impact from a demand increase of USD 1 (USD 1 million for employment) of LH_2. Two potential pathways are measured against the Baseline scenario.

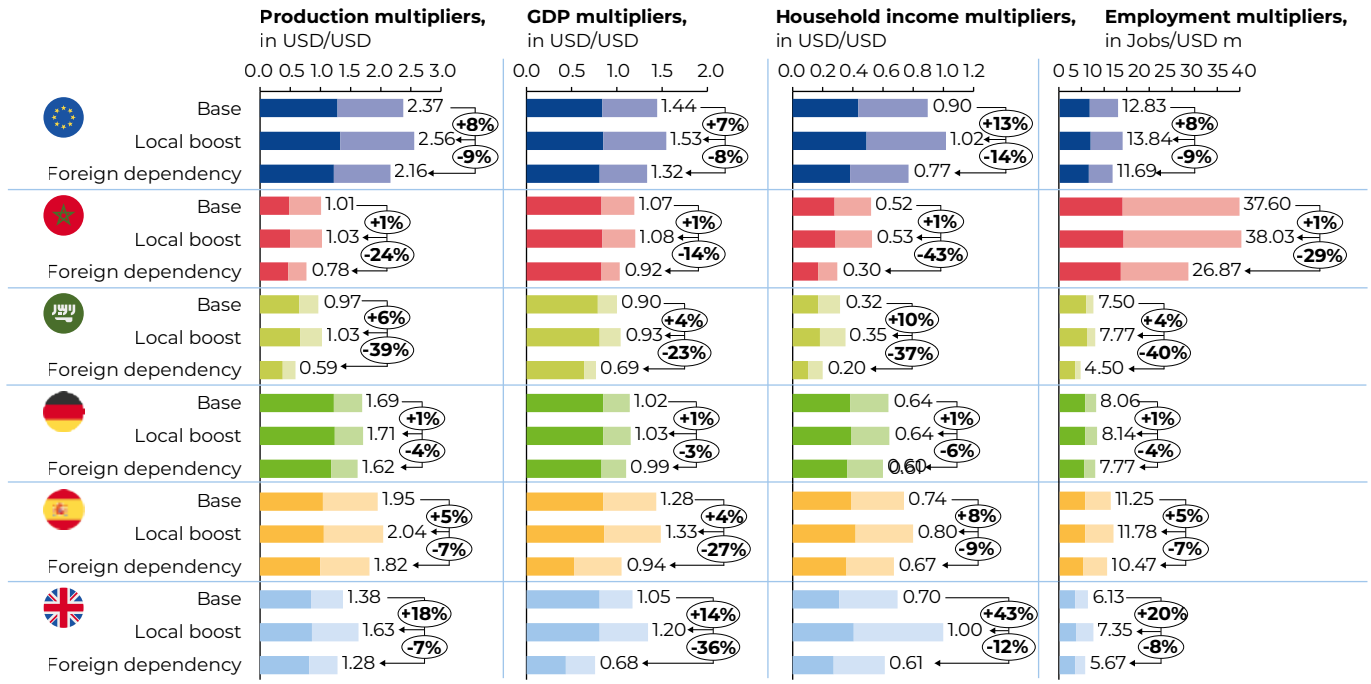

Figure 51: SAM-based multiplier effects across the selected countries under different economic scenarios in the exemplary network. The dark part of the bar charts indicates the input-output-based effect, while the bright part shows the consumption-induced impact. For production, the initial injection is excluded.

High production multipliers are evident in European countries across all scenarios, while Morocco and Saudi Arabia show much smaller influence on the domestic economy. In Germany, multipliers are lower than in Spain for most scenarios and indicators, which might be caused by the higher tax and savings rates, as explained in the previous section. Consumption-induced effects play the largest role in Morocco, followed by the UK and Spain. In Saudi-Arabia, consumption-induced feedback is marginal, which might result from the unequal distribution of income in the country and the high remittances from the large share of migrant workers [170–173].

All indicators demonstrate that the EU28 should adopt a strategy of moderate domestic boost and focus on its diverse economy and large internal market. When comparing the scenarios, Germany appears relatively stable. Domestic boost has nearly no impact as the country already has a strong position in the manufacturing of key components, such as wind turbines, compressors, and electrolysers [133,149,174]. In the foreign dependency scenario, the welfare loss is still modest. Yet, the largest share of activity in Germany in the exemplary network results from LH_2 truck transport. The variations might be more pronounced for a different infrastructure profile. These are shown for Spain and the UK, where foreign dependency shows a significant decline in most multipliers, which can be partially explained by the lower income-induced effects due to the capital outflow [45,46]. Yet, most of the decline might be caused by the fact that key component manufacturing is outsourced to a large extent.

For Morocco, domestic boost policies seem to be rarely effective. Although the domestic share in key component manufacturing doubles in this scenario, the effect is minimal, highlighting that Morocco's economic structure is not suitable to significantly benefit from these activities [175,176]. The country could benefit more from labour-intensive support activities in the subsequent phases. In contrast, dependence on foreign investments is particularly negative for Morocco as it restricts the income-induced feedback effects that are highly important for Morocco's key industries, such as agriculture, food production and textile manufacturing [175,177,178]. Due to high financing costs, which are reflected in the net operating surplus in this analysis, outflowing capital is an important determinant of total effects. Similarly, for Saudi Arabia, greater dependence on other countries could also have negative consequences, even though it is less dependent on foreign capital due to its large public investment fund [179,180]. Instead, the smaller multipliers arise from dependence on imported products and services throughout the supply chain, a consequence of an economy that remains focused on oil exports and lacks diversification [181,182].

8.2.5 Economic impacts in the transition phase of liquid hydrogen networks

This section presents the total economic impacts during the transition phase of the LH_2 infrastructure scale-up. As shown in Section 4.4, the transition phase reflects the gradual development of a small exemplary network, covering nine German airports. The economic impacts during the transition phase (2041-2050) are shown for the EU28 as a whole and are only applied to the base scenario. Figure 52 illustrates the effects on production resulting from the LH_2 supply network during the transition phase. The stacked bars show the effects resulting from investing in new infrastructure, distinguishing between the impacts of key component manufacturing and installation & BoP supply as well as IO-based and consumption-induced effects. The additional line captures the effects of operating the already existing infrastructure in each period.

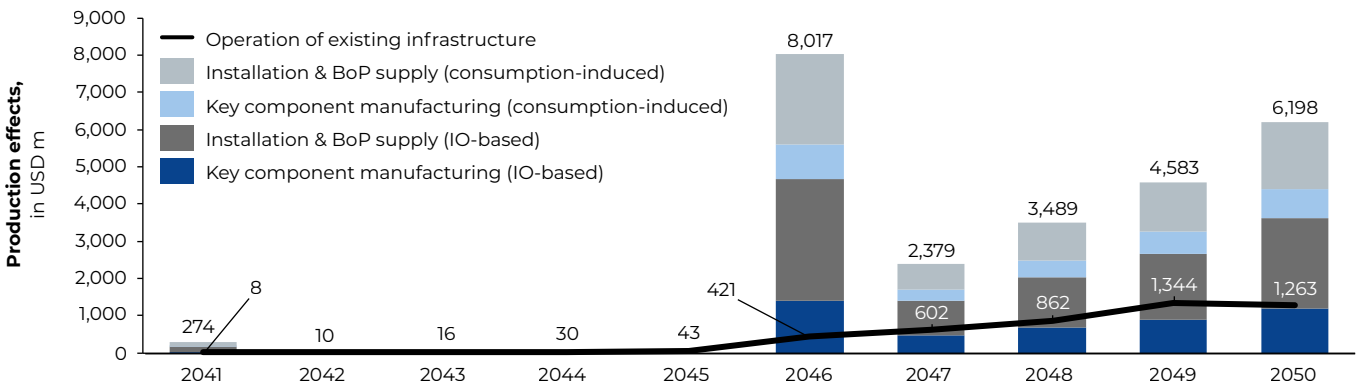

Figure 52: SAM-based production effects resulting from LH_2 infrastructure in the EU28 in the transition phase

During the first years, only minor effects occur, due to the low LH_2 demand. Furthermore, no LH_2 is produced in Europe at this stage and demand is met solely through imports. The initial investment in 2041 is made for the construction of LH_2 storage facilities and transport vehicles. The operation of the network causes marginal effects until 2045. A major expansion occurs in 2046, when a production infrastructure is established in Europe, including RES hubs, electrolysers, liquefaction plants and GH_2 pipelines. This large investment triggers the highest annual production effects (USD 8 billion). In relation to the total production in the EU 28 (USD 40,033 billion in 2019), these figures are rather modest. In subsequent years, the scale-up proceeds at a moderate pace. The results show that building new infrastructure generates considerably higher effects than operating the existing network, with installation activities contributing the largest share. While consumption-induced impacts are smaller than IO-based effects, they still represent a relevant share of the total economic activity.

Figure 53 presents the corresponding employment effects, shown in two separate diagrams for better visibility. The patterns are similar to the production effects, with a modest peak resulting from the initial investment in 2041. Yet, the total effect is relatively small, considering that the 1,373 jobs refer to the entire EU28 with a working population of more than 200 million people [183]. In 2042, the employment drops as the network operation requires less workforce. In addition, the income feedback is minor in this early period, causing limited consumption-induced effects in other sectors.

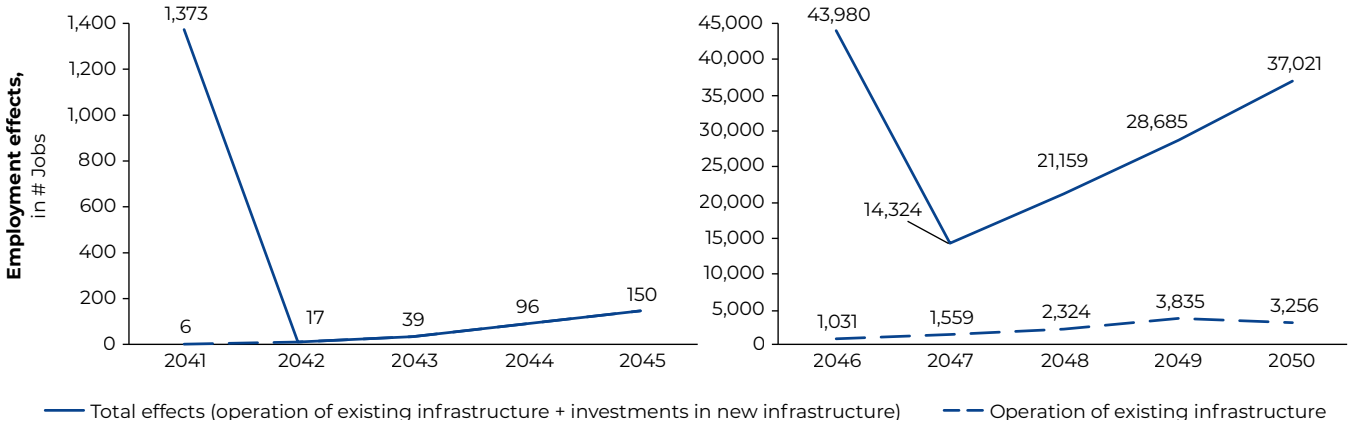

Figure 53: SAM-based employment effects resulting from LH_2 infrastructure in the EU28 in the transition phase. Total effects include the scale-up of new infrastructure and the operation of existing infrastructure

As seen in Figure 52, a significant increase occurs in 2046. The major effect is caused by new infrastructure, while the existing network causes moderate labour demand, with around 3,800 jobs by 2049. These results imply that job-related benefits mainly depend on LH_2 infrastructure expansion. These jobs are not permanent and indicate a large fluctuation, depending on the required investments in the respective year. When large amounts of new infrastructure are needed, this leads to significant peaks in labour demand. These fluctuations pose challenges regarding labour availability. It remains questionable if workforce is immediately available when needed, especially in times of demographic change and shortage of skilled labour in Europe [184–187]. To gain further insights into the economic consequences of LH_2 networks, Figure 54 examines the multiplier structure exemplarily for 2046. The left diagram shows the production effects in other industries, and the right one displays the sources of gross value creation by showing the GDP effect composition. For both diagrams, the operation of existing infrastructure is separated from the scale-up of new infrastructure. In addition, IO-based and SAM-based results are differentiated.

The results reveal significant production spillovers into other industries, particularly from new investments. While infrastructure scale-up primarily stimulates the construction and manufacturing industries in the upstream supply chain, network operation generates stronger impacts in energy and water supply and in transportation sectors. Industries that are dependent on final demand, such as retail trade, diverse services, and real estate, benefit disproportionately from consumption-induced effects.

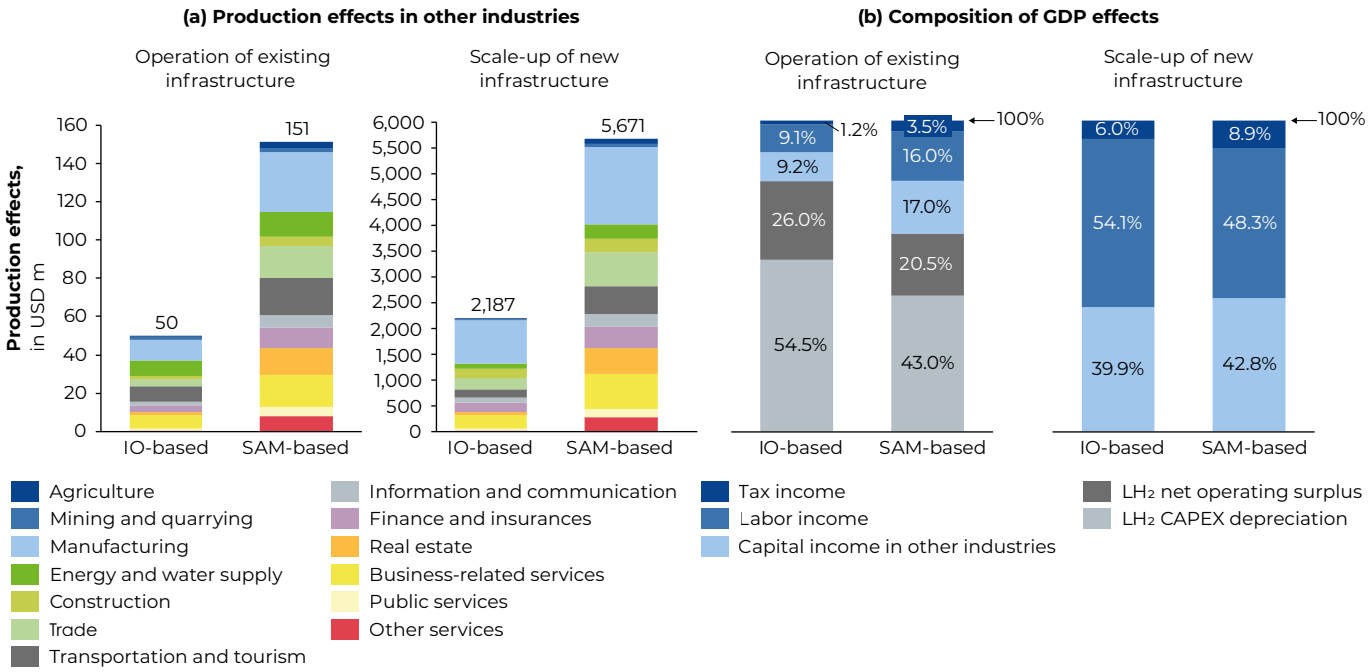

Figure 54: (a) Production effects in other industries and (b) composition of GDP effects resulting from LH_2 infrastructure, shown for the year 2046. Both diagrams are shown for the operation of existing and the scale-up of new infrastructure separately and differentiate IO-based and SAM-based effects.

The GDP composition provides additional insights: during the investment phase, value creation is mainly driven by labour income, which corresponds to the findings from Figure 53. In contrast, when operating the existing infrastructure, GDP contributions shift towards the depreciation of existing assets (LH_2 infrastructure facilities) and the net operating surplus of the LH_2 industry. This reflects the capital-intensive nature of the LH_2 infrastructure and the high financing costs involved [138]. Although the depreciation of LH_2 facilities contributes to GDP, it does not generate net value.

Overall, the transition phase demonstrates that infrastructure scale-up dominates the economic effects, while infrastructure operation gradually increases to a moderate impact by 2050. In relation to the EU28's overall economy, the effects within the small network are marginal. The results also emphasize the inconsistent stimulating effect of the scale-up with temporary peaks [45]. This is particularly crucial for labour markets, where a strong fluctuation causes challenges regarding skilled workforce availability. This issue could be mitigated by constantly expanding and renewing infrastructure.

8.3 Recommendations

Based on the macroeconomic analysis, six key recommendations are derived.

Specialization and cooperation along the LH_2 value chain foster strategic partnerships and generate complementary benefits. It is unlikely that single countries will cover the entire value chain [131,188]. European countries should leverage their comparative advantages for key equipment and upstream components, while MENA countries should prioritize supporting activities during the installation and operation phase, as well as reducing investment risks [40,141].

Creation of fair value for LH_2 exporting countries avoids the risk of neo-colonial dynamics and is critical for the long-term stability and acceptance [189–191]. Policymakers in Europe should support infrastructure projects in exporting countries in the Global South and establish socioeconomic sustainability criteria for imported LH_2. Policymakers in the MENA region should implement local content requirements and support capacity building at the local level.

Geopolitical resilience and technological sovereignty avoid dependencies. Policymakers in Europe should protect critical industries to prevent the relocation of key component manufacturing. At the same time, they should diversify LH_2 import options and promote innovation [145,192]. Policymakers in the MENA region should also diversify their key component suppliers and promote supporting sectors that contribute to employment and income.

Effective management of structural change requires reliable planning. The transition towards LH_2 networks creates opportunities and challenges for national economies due to demographic changes and labour market disruptions [186,193]. Policymakers in Europe should support qualification programs and address labour shortages induced by demographic change. It is also recommended that policymakers in the MENA region adopt this approach, alongside efforts to build capacity and implement programs that address regional disparities within the country.

Unlocking capital and mitigating financial risk reduces the costs of the LH_2 network, which represent a critical bottleneck [194,195]. To reduce these costs and unlock private capital, policymakers in Europe should implement stable, long-term incentive systems such as blended finance and purchase guarantees. Meanwhile, policymakers in the MENA region should increase political stability and provide clear legislation to reduce investment risks.

Sustainability management must consider more than just GHG emissions. Long-term acceptance hinges on land and water use, biodiversity protection, and social impacts in producing countries [189,196]. Policymakers in Europe must establish sustainability criteria for both domestic LH_2 production and imports. Policymakers in the MENA region must implement robust monitoring of ecological and social indicators and engage with local stakeholders.

SUMMARY AND CONCLUSION

9 Summary and conclusion

This report provides a comprehensive, multi-faceted analysis of the opportunities and challenges associated with establishing an LH_2 supply infrastructure for European aviation. The investigation, which integrated techno-economic, environmental, and macroeconomic perspectives, demonstrates that while significant hurdles remain, a transition to H_2-powered aviation is technically feasible and can generate substantial benefits across the value chain.

The analysis of LH_2 demand across the three distinct scenarios (Baseline, Ambitious policy, and Moonshot) shows that future infrastructure needs are highly dependent on the level of political ambition and the pace of technology adoption. In the Baseline scenario, with limited policy support, LH_2 demand remains comparably low corresponding to around 3% of all flights in the airport network. The Ambitious policy scenario, reaching about 1.8 $MtLH_2$ per year by 2050, represents a realistic and actionable pathway for coordinated infrastructure development. In this scenario, around 17% of the flights within the network are powered by H_2 in 2050, which corresponds to around 39% of all flights of the airport network. In the Moonshot scenario, the LH_2 demand rises sharply to around 13 $MtLH_2$ per year by 2050. This level of consumption would require a highly developed European LH_2 supply network. It implies massive investments in production, storage, and distribution capacities, as well as close coordination between the aviation sector, energy producers, and policymakers. The scenario demonstrates that achieving such a transformation is technically feasible but only under strong and long-term policy support combined with early infrastructure planning at the European level.

The techno-economic assessment of this network highlights several critical insights. First, the cost of LH_2 supply is heavily influenced by the availability of renewable energy sources and economies of scale. Locations with favourable conditions for wind and solar power exhibit significantly lower production costs. This finding suggests a network-centric approach is essential, where production hubs are located in cost-optimal regions and connected to airports via an efficient transport infrastructure. Second, the model demonstrates the crucial role of the European Hydrogen Backbone (EHB) in enabling cost-effective, large-scale H_2 distribution. Without this pipeline network, the reliance on truck and vessel transport would significantly increase supply costs and limit the geographic reach of H_2-powered aviation. The transition phase analysis for a case study of German airports confirms this, showing a shift from high-cost, small-scale initial investments to a more efficient, pipeline-driven network as demand grows. Also, the import via LH_2 vessel and trucks especially in the initial development phase leads to lower costs as low LH_2 demands at the airports would require a dedicated small-scale liquefaction plant for on-site H_2 production or GH_2 import.

The economic viability of H_2-powered flights remains a significant challenge. The flight network analysis shows that under current assumptions, H_2 is not yet cost-competitive with kerosene. A substantial price gap must be bridged through subsidies or other policy support instruments to drive widespread airline adoption. This finding reinforces the need for strong policy support, such as production tax credits or targeted subsidies with price thresholds, to de-risk investments and incentivize market uptake beyond industrial and technological bottlenecks.

Environmentally, the life cycle assessment confirms that while H_2-powered aviation eliminates direct CO_2 emissions, the overall climate impact is highly dependent on the energy mix and infrastructure. On-site production using renewable energy, particularly wind power, results in the lowest emissions. However, the study also identifies H_2 leakage as a critical issue that could significantly reduce the climate benefits of H_2 and potentially more than double the overall emissions. This highlights the need for a strong focus on advanced materials, engineering, and operation to minimize leakage across the entire supply chain.

The study on business models and policy instruments demonstrates that a one-size-fits-all approach will not be effective. Stakeholder constellations and their financial requirements have a decisive impact on the cost of H_2 supply. Policy instruments, therefore, must be tailored to these specific business models to effectively de-risk projects and lower the cost of capital. A synergistic combination of direct financial support (e.g., grants), market-based instruments (e.g., Contracts for Difference), and regulatory measures (e.g., blending mandates) will be essential to enable the transition from a vision to a large-scale, operational reality.

Finally, the macroeconomic analysis reveals that the benefits of developing H_2 infrastructure extend

beyond the aviation sector. The required investments in manufacturing, installation, and operations can generate substantial economic activity, creating jobs and stimulating growth across a wide range of industries. The analysis also highlights structural differences between countries, showing that while some, like Germany and Spain, are well-positioned for technological leadership in manufacturing, others, like Morocco, can derive significant benefits from their role in installation and operations. This suggests that international collaborations that leverage these comparative advantages could accelerate deployment while distributing economic gains more equitably.

In conclusion, the future of H_2-powered aviation depends on a coordinated, strategic approach that addresses the entire value chain. While the technological and logistical challenges are considerable, the analysis shows that they can be overcome. The path forward requires policy frameworks that reduce the risk of early-stage investment, a cohesive European infrastructure plan that builds on regional strengths, and technological innovation focused not only on cost reduction but also on minimizing environmental impact, particularly H_2 leakage. The decisions made by industry and policymakers in the coming years will determine whether H_2 becomes a niche solution or a cornerstone of sustainable, net-zero aviation.

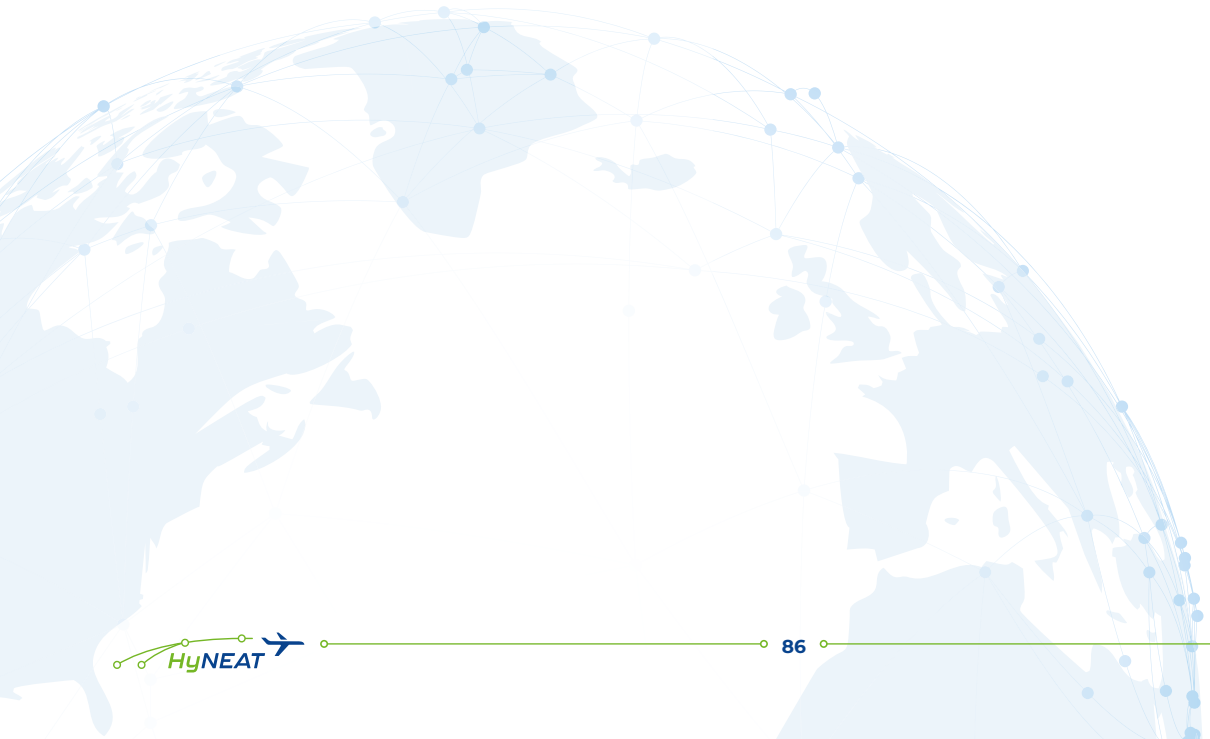

DEEP DIVE: HYDROGEN LIQUEFACTION AND LIQUID HYDROGEN AIRPORT INFRASTRUCTURE

A Deep dive: Hydrogen liquefaction in a liquid hydrogen supply network

Hydrogen (H_2) liquefaction plays a key role in the liquid hydrogen (LH_2) supply network, serving as a critical infrastructure component and one of the primary cost drivers. Despite the liquefiers' high energy requirements, they are often strategically located near end-use sites, such as airports, rather than in regions with lower energy costs. This is largely due to the logistical complexity associated with transporting and storing LH_2, which can outweigh the benefits of cheaper energy elsewhere. Thus, to enable optimal design of LH_2 supply networks, detailed knowledge of the techno-economics of H_2 liquefaction plants is essential. This deep dive will explore these aspects to provide a clearer understanding of cost structures and technological challenges.

A.1 Current status of hydrogen liquefaction plants

A H_2 liquefaction plant can be divided into several sections, as shown in Figure 55. Gaseous hydrogen (GH_2) is precooled to 80–130 K using liquid nitrogen (LN_2) or mixed refrigerants (MR). MR typically consist of nitrogen and hydrocarbons, such as methane, ethane, and butane. Afterwards, H_2 is purified in a cryogenic adsorption unit and enters the cryogenic refrigeration and liquefaction section. There, it is cooled and liquefied in plate-fin heat exchangers, using cryogenic refrigeration cycles, and via expansion in Joule-Thomson valves. For refrigeration, either a H_2 Claude cycle or a (reverse) helium Brayton cycle can be applied. In such cycles, the cooling power is generated by compression of the working fluid at ambient temperature, using cooling water for heat dissipation. Later in the cycle, the temperature is decreased by expansion in turbo expanders or Joule-Thomson valves. To minimize heat inleak, the cryogenic parts of the plant are placed within well-insulated coldboxes. Further, within the liquefaction plant, the exothermic conversion of ortho- to parahydrogen[1] takes place. This process is explained in more detail in Appendix C.

1 H_2 exists in its ortho and para forms, differing by nuclear spin. At room temperature, an equilibrium of 75% ortho and 25% para is observed, but cryogenic cooling shifts the equilibrium to parahydrogen, resulting in a conversion process facilitated within the liquefaction plant.

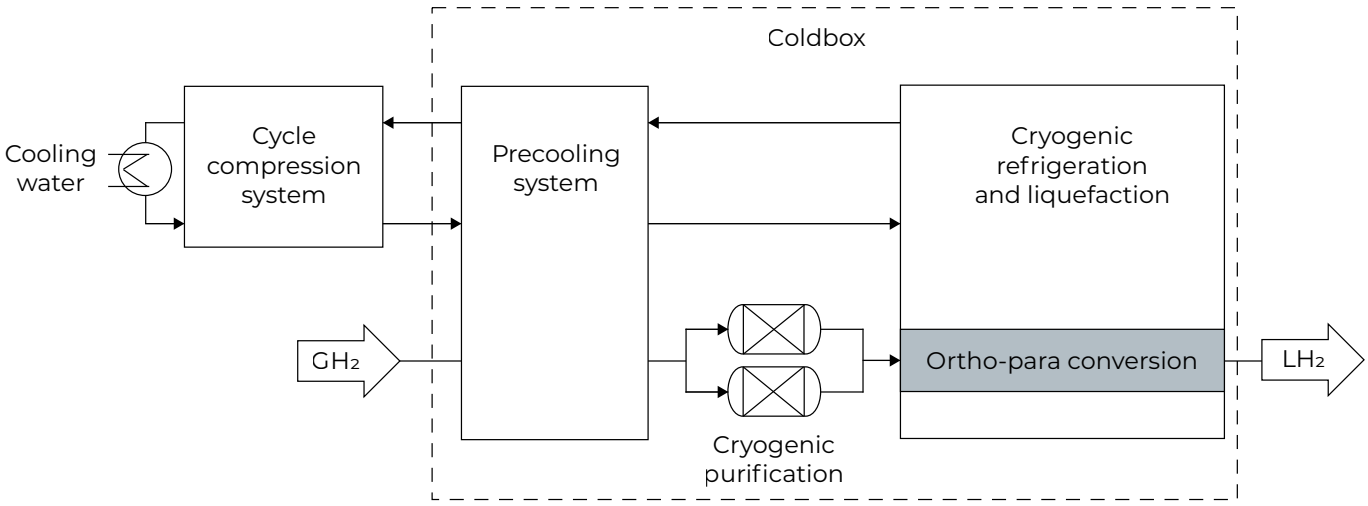

Figure 55: General setup of a H_2 liquefaction plant according to Cardella [197]

One of the key challenges for future LH_2 supply networks is the scale-up of H_2 liquefaction plants. While in 2021, the global H_2 liquefaction capacity was about 380 tons per day (tpd) [198], H_2 liquefaction is undergoing rapid development, with an increase in global capacity of more than 50% [199] between 2020 and 2024, and projects for large-scale plants of ≥ 100 tpd being announced [200]. Despite this momentum, the scale-up of H_2 liquefaction capacity is still in its early stages, and significant technological and economic challenges remain before it can meet future demands. As such, the scale-up might be limited as only a few companies have been building H_2 liquefaction plants so far, building periods may take up several years, and investment costs are high.

To investigate the main techno-economic challenges, the following section shows simulation results of H_2 liquefaction plants generated with the software Honeywell UniSim© Design. The results are evaluated techno-economically, based on a literature model by Turton 2018 [201] and several assumptions. The methodology and the assumptions are described in Appendix C.

A.2 Techno-economics of hydrogen liquefaction plants

To enable a comprehensive techno-economic evaluation of H_2 liquefaction plants across various scales, this study examines plants with capacities of 5, 50, 100, and 200 tpd, comparing them with data from existing literature.

The 5 tpd plant, representing a comparable small-scale plant considering the projected demands, is modelled after the Leuna plant from Linde [202]. It utilizes a H_2 Claude cycle for cryogenic cooling and an open nitrogen (N_2) cycle for precooling. Hence, LN_2 is provided to the plant (i.e., from an air separation plant), evaporated, heated, and released to the environment after precooling. Given that the largest operational H_2 liquefaction plants today have capacities around 30 tpd [198], designs for the 50, 100, and 200 tpd plants are only conceptual. The 50 tpd plant is based on the IDEALHY study [203], employing a closed MR cycle for precooling and a Brayton cycle using a helium-neon mixture as working fluid for cryogenic cooling. The 100 tpd plant follows the conceptual design by Cardella 2018 [197], featuring a H_2 Claude cycle similar to the 5 tpd plant, but with MR precooling. For the 200 tpd plant, the 100 tpd design was scaled up in this study. The performance of each plant is assessed with three metrics: the specific energy consumption (SEC), the specific capital expenditure (CAPEX), and the specific liquefaction cost (SLC). More details on the methodology are provided in Appendix C.

Figure 56 shows the SEC for the studied plants alongside literature data. Whereas the theoretical minimum of the SEC is about 2.88 kWh/kgLH_2 for the considered conditions [204], in real processes, significantly higher values are required. As such, the SEC values of the simulated plants range between 9.77 and 5.65 kWh/kgLH_2.

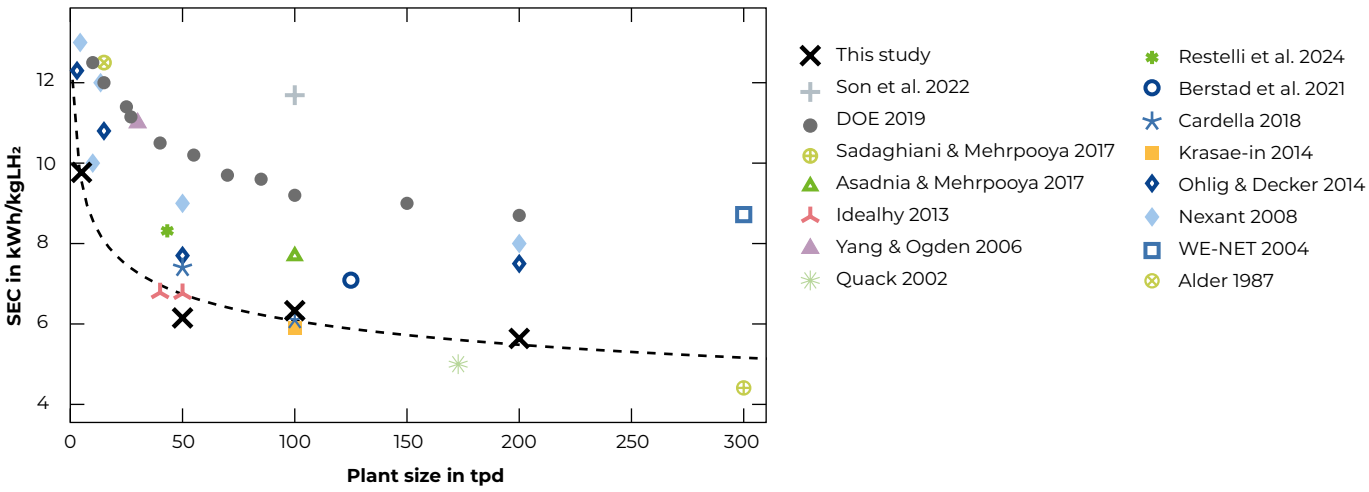

Figure 56: Specific energy consumption SEC of the considered plants based on [205], compared to literature data [197,202,204,206–216]

While the SEC drops notably with increasing plant size, the reduction plateaus beyond 50 tpd. This trend mainly results from more efficient precooling methods in larger plants. Generally, this study's results align with trends observed in the literature, though they report relatively low SEC values. This is likely due to assumptions of high component efficiencies and narrow temperature profiles within the heat exchangers, as discussed in Section C.1. This may not reflect current small-scale plant performance, but using energetically optimized designs will be essential for future large-scale LH_2 infrastructure.

Figure 57 illustrates the results for the specific CAPEX alongside literature data, showing values between 4.47 and 1.92 million USD2023/tpd and a similar trend to the SEC. Primarily driven by economies of scale, the specific CAPEX decreases as plant size increases. However, no substantial reduction is observed beyond a plant size of 50 tpd.

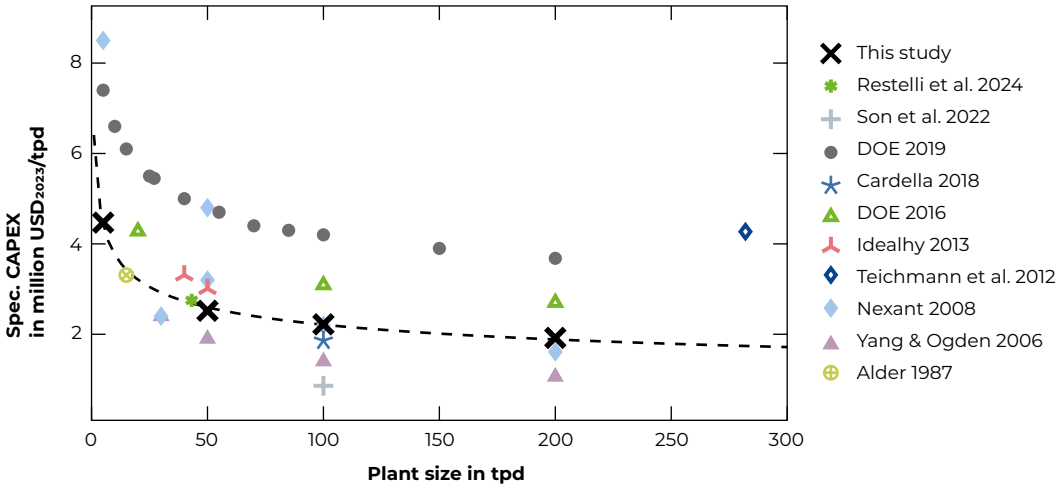

Figure 57: Specific CAPEX of the considered plants based on [205], compared to literature data [197,204,209,212,214–219]

Figure 58 breaks down the contributions of individual components to the CAPEX for each of the four plants considered. Regardless of plant size, precooling method, and applied refrigeration cycle, the compressors[2] and heat exchangers are the main cost drivers for the plant's CAPEX. All other components have only a minor influence.

2 including cooling water related costs

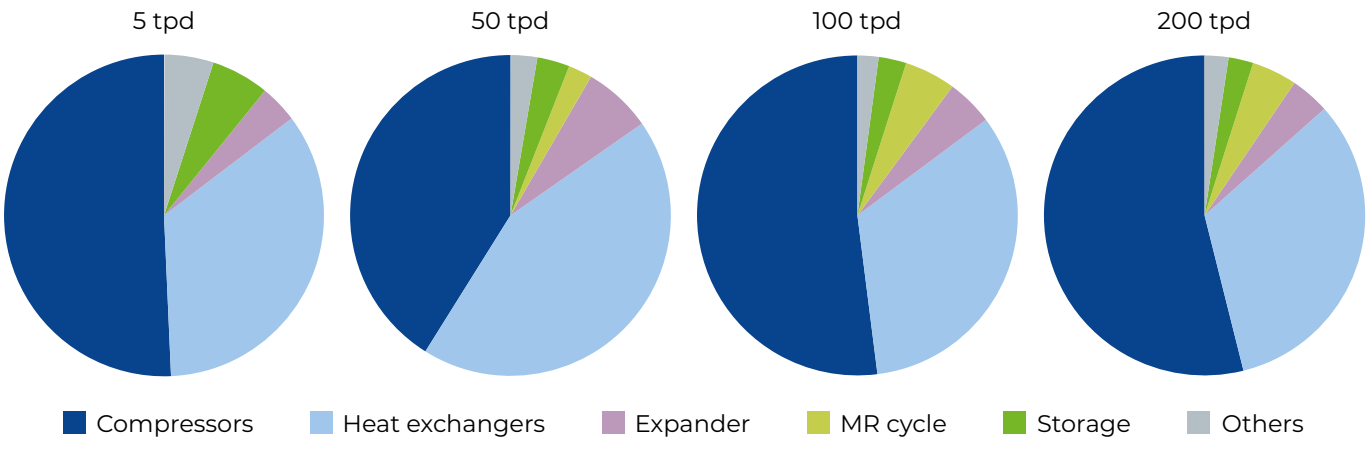

Figure 58: Contributions of individual plant components to the CAPEX

Finally, using an electricity price of 50 USD/MWh, an Operation and Maintenance (O&M) factor of 2%, and further assumptions outlined in section C.1.2, the SLC results in Figure 59 are obtained. They indicate that large-scale H_2 liquefaction plants achieve significantly lower SLC, approaching 1 USD/kgLH_2. While both CAPEX and OPEX contribute substantially to the overall costs, CAPEX tends to be the more influential. Nevertheless, these outcomes are highly sensitive to variations in electricity pricing and the chosen O&M factor.

One of the key factors influencing the plant's efficiency is the choice of precooling method. In this study, the 5 tpd uses an open N_2 cycle, while larger-scale plants apply closed MR cycles, where the MR are circulated within a dedicated refrigeration cycle. As a third option, N_2 could also be deployed in a closed cycle, where it is compressed, expanded, and recirculated rather than vented after precooling. To compare these three methods, each was applied to the 5 tpd plant and evaluated against the reference case with an open N_2 cycle. The closed N_2 cycle is based on the concept by Hu et al. [220], while the MR cycle is a scaled-down version of the concept by Cardella [197]. For the open N_2 cycle, it is assumed that supplying LN_2 requires a specific energy consumption of 0.5 kWh/kgLN_2.

Table 4 presents a comparison of the energy consumption in the precooling section, the overall SEC of the plant, and its CAPEX, where the open N_2 cycle serves as baseline. The results show that switching to a closed cycle can significantly reduce energy requirements for precooling. The MR cycle, in particular, decreases the energy consumption due to more effective compression and closer temperature profiles in the heat exchangers. However, MR components have higher melting points, limiting the precooling temperature to 100 K compared to 80 K for N_2. This leads to higher energy demand in the cryogenic section but still improves overall energy efficiency.

Table 4: Influence of the precooling method on techno-economic plant characteristics

Precooling method	Energy consumption of precooling	SEC (overall)	CAPEX (overall)
Open N_2 cycle	100%	100%	100%
Closed N_2 cycle	78%	90%	119%
Closed MR cycle	36%	79%	145%

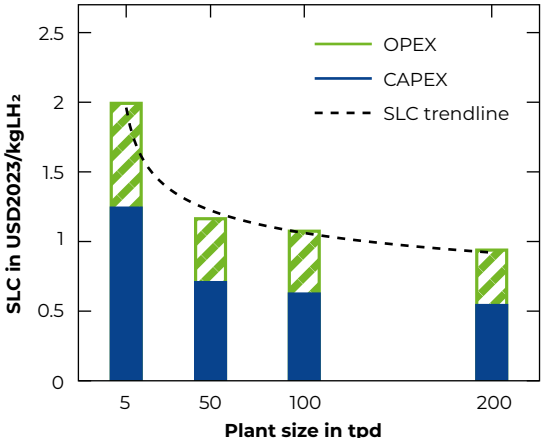

Figure 59: Specific liquefaction cost SLC of the considered plants with contributions of CAPEX and OPEX

Since precooling accounts for a notable share of the plant's total energy requirement, using a closed cycle can also substantially lower the overall SEC. However, the closed-cycle systems require additional equipment, such as more compressors and larger heat exchangers, and, thus, increase the CAPEX. While the closed MR cycle is most energy efficient, the additional equipment results in a significant increase in CAPEX, making it economically viable for larger-scale plants only. Using a closed N_2 cycle, instead, is a compromise regarding energy efficiency and investment costs. In contrast, the open N_2 cycle requires less equipment but depends on an external N_2 supply, making it suitable only when, e.g., an air separation unit, is available on-site.

Beyond precooling, a critical design decision is whether a Claude cycle, such as in the 5, 100, and 200 tpd plants, or a Brayton cycle, as in the 50 tpd plant, is applied. This study's results in Figure 56 to Figure 59 show similar results for SEC and specific CAPEX for all larger-scale plants, regardless of the refrigeration cycle. However, the 50 tpd plant using the Brayton cycle demonstrates a slightly lower SEC, primarily due to greater power recovery from turbo expanders. Additionally, helium is easier to handle, and by using a mixture of helium and neon, the effort for compression of the working fluid can be improved [221]. Despite these advantages, helium's limited availability and high cost pose challenges for large-scale applications [222].

While large-scale H_2 liquefaction plants are essential for reducing costs, the demand for LH_2 and, thus, the need for efficient large-scale systems is only now emerging. From a cost perspective, in this deep dive, CAPEX is found to contribute most to the overall liquefaction costs, with the compressors and heat exchangers as the main cost drivers.

The applied plate-fin heat exchangers are relatively mature, as they are commonly used in various cryogenic applications. In contrast, compressors remain a cost and efficiency bottleneck, as compressing H_2 is particularly challenging. While turbo compressors would offer high efficiency and low specific CAPEX at the required capacities, H_2 low molecular weight limits pressure ratios [200]. Consequently, most designs rely on reciprocating compressors. However, they face volume flow limitations, typically at around 20,000–30,000 m^3 [200].

As a result, scaling up liquefaction capacity might lead to doubling the number of compressors rather than increasing their size, as is the case in the scale-up from 100–200 tpd in this study. This also leads to significant space requirements; for example, a 40 tpd plant already demands about 2,700 m^2 for compressors alone [223]. The compressors' high capital and operational costs make them a key target for cost reduction efforts. Hence, the development of affordable and high-efficiency turbo compressors could significantly decrease the overall liquefaction costs in the long term [197,224].

Furthermore, the integration of renewable energy sources into H_2 supply chains introduces variability in energy availability, making the part-load behaviour of H_2 liquefaction plants increasingly relevant. The conceptual IDEALHY study [203] studied this aspect for a 40 tpd plant and found that operating at 50% resulted in a 43% reduction in energy consumption, while reducing the load to 25% led to a 63% decrease in energy use. Thereby, in the IDEALHY study, design decisions were specifically aimed at enabling part-load. In contrast, most currently operating H_2 liquefaction plants are not primarily designed for part-load flexibility. Components like compressors and expanders are typically optimized for full-load conditions and may not perform efficiently at off-design speeds. Moreover, no empirical data on part-load operations are available in the literature.

Despite this, part-load operation remains technically feasible. One practical approach would be to maintain the design speed and volume flow rate of compressors and expanders while reducing the working pressure within the refrigeration cycles. This method, however, is thermodynamically limited, as falling below the critical pressure could lead to unintended formation of liquid in components not designed for such conditions.

Thus, to enable energy-efficient part-load operation in future plants, the development of part-load-capable equipment and plant designs is required. Nevertheless, given that H_2 liquefaction remains one of the main cost drivers in the H_2 supply networks, the use of a buffer storage tank whenever feasible may offer a more cost-effective solution for enhancing system flexibility [225].

A.3 Hydrogen liquefaction plants as part of the liquid hydrogen supply chain

H_2 liquefaction plants are among the most cost- and energy-intensive components of the LH_2 supply network. Further, their strategic placement within the supply network significantly influences the design and efficiency of the remaining infrastructure. Since H_2 will typically be produced at locations with cheap renewable energy, which is often far from its point of use, the location of the liquefaction plant becomes a critical decision. If the plant is situated near the production site, transportation of LH_2 is required, which involves LH_2 storage tanks and distribution with trucks and ships. Conversely, if placing the liquefier closer to the end user, the network relies on transportation of GH_2, typically via pipelines, which require large compression units.

Such pipelines are expected to feature diameters of DN1000, operate at pressures of 85 bar, and support volume flows of 3.6 million m^3/h [226]. In Europe, the European Hydrogen Backbone will be a central component of the future pipeline network, with estimated costs as low as 0.16 €/1000 km [226]. To maintain continuous H_2 flow, compression units are projected to be required at least every 65–160 km [227]. Given current technological capabilities, reciprocating compressors are the most viable solution [228]. Furthermore, in the gaseous H_2 supply network, caverns are anticipated for large-scale H_2 storage. A typical cavern with a fill pressure of 175 bar could store around 100 million Nm^3 of H_2 [229]. The primary energy demand associated with cavern storage arises from the injection and pressurization of H_2, again using reciprocating compressors [229]. Additionally, post-purification processes, such as gas sweetening and dehydration, will be necessary due to contamination risks, including the formation of H_2 sulfide [230]. One major advantage of large GH_2 caverns is their ability to function as buffer storage to balance fluctuations in energy supply and H_2 production. This reduces the flexibility requirements for downstream components,

particularly H_2 liquefaction plants, which are generally more challenging to operate under variable loads.

Regarding LH_2 infrastructure components, LH_2 storage tanks are technologically mature, but must be scaled up to meet the demands outlined in this study. Currently, the largest operational tank has a volume of approximately 3,500 m^3 [231], though designs up to 40,000 m^3 are available [232]. For such large storage, spherical tanks are typically preferred. Given the extreme temperature difference between ambient conditions and LH_2, high-performance insulation is critical to minimize boil-off losses. Most tanks use perlite-filled vacuum jackets, though glass bubbles have recently demonstrated superior performance [231]. However, for tanks exceeding 50,000 m^3, maintaining vacuum-jacketed insulation may become a technical challenge [224].

For LH_2 transport and distribution, ships and trailer trucks are the preferred modes. Again, the predicted demands necessitate a substantial increase in both the number and capacity. Currently, only one LH_2 ship is in operation with a capacity of 1,250 m^3. Plans are underway to upscale such ships to capacities of up to 160,000 m^3 [233]. Technologically, the onboard storage tank can be considered similar to the stationary LH_2 tanks, but the extended storage duration at sea between loading and unloading introduces unavoidable boil-off losses. Hence, strategies to utilize the boil-off, e.g., for on-board power management, should be investigated.

For shorter-range distribution, trailer trucks are essential. These typically employ multi-layer insulation (MLI) to reduce thermal losses, and transport payloads of 566,000 L or about 3.6 tLH_2 (in the EU) [234]. However, this implies a huge number of trucks required to supply LH_2 to large-scale end-users such as airports. Key challenges include long loading and unloading times up to 6 h [235] and significant transfer losses, which will be discussed in Section B.1.4.

Currently, pumps for transferring LH_2 are not yet industrially mature. While high-pressure pumps (350–700 bar) are available in the automotive sector, pumps for pressurizing LH_2 for the transfer between different storage systems and pumps for transferring large LH_2 flows are still under development [235]. Nevertheless, as the first pumps are being commercially built and demonstrated [223,236], these developments can significantly improve the efficiency of LH_2 distribution and enable customized pressure levels for diverse applications.

A.4 Boil-off losses in liquid hydrogen supply networks

When considering LH_2 supply networks, H_2 losses due to boil-off must be carefully considered. H_2 losses emerge whenever H_2 is stored, either stationary in storage tanks or during transport on ships and trucks, and when it is transferred between such systems. A main reason for boil-off, especially relevant for stationary tanks and long-term storage onboard ships, is heat ingress into the tank.

To characterize this boil-off behaviour, this study utilizes the BoilFAST [237] software. For simplicity, only spherical tanks are considered, with insulation thickness assumed to be 5% of the tank's diameter. The ambient temperature is set to 25 °C, the initial fill level to 90%, and both the starting and venting pressures to 3 bar. BoilFAST simulates the thermodynamic states of the liquid and gas phases in the tank and the boil-off dynamics, beginning from thermal equilibrium [237]. Since the tank is assumed to be already at the venting pressure at the start of the simulation, venting starts immediately. However, due to the initial thermal equilibrium assumption, the boil-off behaviour evolves slightly over time. Thus, to estimate the daily boil-off relative to the H_2 stored, the average over the first three days is used.

Figure 60 presents the resulting boil-off rates for three different insulation qualities. For perlite-based insulation, a typical thermal conductivity is 1 mW/(mK) [231], while glass bubbles offer improved performance at 0.7 mW/(mK) [231]. A less effective insulation is modelled at 1.5 mW/(mK), which could, e.g., result from slightly worse vacuum quality. The results show a strong influence of storage size on the boil-off rate: a 20 m^3 tank exhibits a daily boil-off of ~1%, whereas a 3,500 m^3 tank (the largest currently in operation) has a boil-off rate below 0.05%. For even larger tanks, boil-off rates approach values below 0.01%. Further, Figure 61 illustrates totalled boil-off over a one-week period for three tank sizes. Initially, boil-off rates are higher, but then decrease over time, as thermal stratification develops in the tank and as the temperature difference between the ullage gas and the ambient decreases.

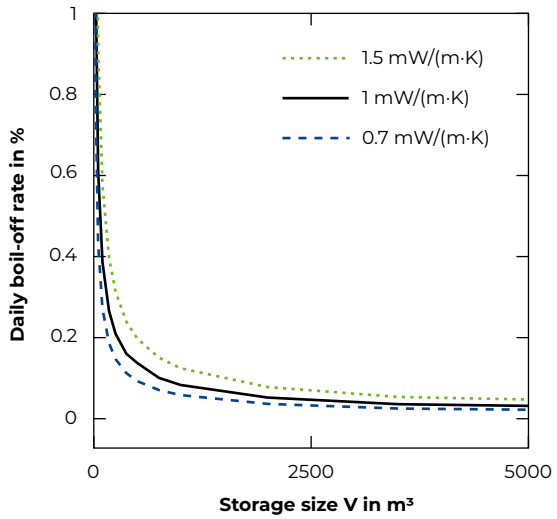

Figure 60: Daily boil-off rate of LH_2 tanks relative to stored mass depending on storage size for different effective thermal conductivities

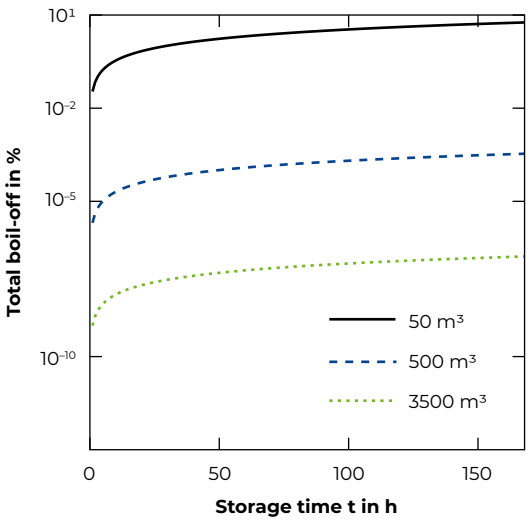

Figure 61: Total boil-off of LH_2 tanks relative to stored mass as a function of the storage time for different tank sizes

While minimizing boil-off is important for economic and ecologic [238] reasons, the losses of large-scale tanks are relatively low, and it is relatively easy to collect the emerging boil-off gas. Near H_2 liquefaction plants, recycling boil-off gas into the liquefier is already integrated to existing designs. Moreover, continuous H_2 withdrawal from the storage can reduce the temperature [205] and therefore further lower boil-off rates.

In contrast, transfer processes, such as filling a stationary LH_2 tank from a trailer, can result in significantly higher losses, as literature suggests losses of 3–13% [239,240]. A large contribution of these losses is due to the transfer method used in today's LH_2 trailers, which relies on pressure difference rather than pumps. Heat is deliberately introduced into the trailer to raise the pressure, allowing H_2 to flow into the receiving tank at lower pressure. This process leads to losses from various effects: replacement of cold gas in the receiving tank, evaporation due to the heat input, evaporation within the transfer system, and flash gas formation due to the depressurization in the receiving tank [235]. Therefore, to enable sustainable transfer processes, the application of suitable pumps is essential. Several LH_2 pumps are currently under development and are expected to reduce these losses significantly, as well as lower filling times [235]. Overall, finding economically viable methods for re-using or re-liquefying boil-off and flash gas losses will become more important as LH_2 networks are being scaled up.

A.5 Summary and recommendations

H_2 liquefaction has seen rapid growth in recent years, with the first large-scale plants now being planned. However, to ensure the broad availability of LH_2 by 2050, the pace of development must accelerate further.

A key limitation remains the high investment cost, especially given the uncertainty around future demand for LH_2. To support cost reduction and efficiency improvements, large-scale H_2 liquefiers, including efficient precooling and refrigeration cycles, need to be built. Thereby, technological advancements, particularly in H_2 turbo compressors, could significantly decrease the overall liquefaction costs, though such components are not available in the foreseeable future. Moreover, energy-optimized solutions, like recovery of power generated in the liquefiers' turbo expanders, are key. Additionally, the load flexibility of H_2 liquefaction plants will play a role in integrating renewable energy sources, especially if space for large buffer storage is limited.

As LH_2 supply networks expand, boil-off losses during storage, transport, and, most importantly, transfer processes will become increasingly relevant. Future systems should include concepts to recover or utilize boil-off H_2, for example, through re-liquefaction or integration with energy systems. Further, the development of H_2 transfer pumps is key to decreasing losses in LH_2 distribution.

In summary, the following recommendations can be drawn from this deep dive:

- The scale-up of H_2 liquefaction must be accelerated to meet 2050 availability targets. Therefore, clearer demand forecasts and supportive policy frameworks can lower the uncertainties regarding huge investments.
- To reduce liquefaction costs, energy- and cost-efficient large-scale H_2 liquefaction plants > 50 tpd, featuring highly integrated refrigeration and precooling cycles, as well as energetically optimized equipment, e.g., for recovering energy from expanders, should be built.
- The development of high-efficiency and load-flexible components, like H_2 turbo compressors and LH_2 pumps, should be advanced to lower energy consumption and H_2 losses.
- Boil-off recovery strategies should be developed to utilize unavoidable losses in large-scale LH_2 supply networks.

B Deep dive: Liquid hydrogen airport infrastructure

B.1 Use of liquid hydrogen at airports

ILK Dresden's work focusses on the technical and economic analysis of LH_2 refuelling processes at airports, including purification processes. Their requirements are challenging due to both, high costs of components and a large energy consumption for liquefaction. The availability of a sufficient amount of high-density H_2, preferably LH_2, is however a precondition of a H_2-powered aviation. In particular, the following aspects have been analysed:

- Technical analysis of the general design of an LH_2 refuelling system at airports, the necessary components, and possible implementation options (refuelling via trailer or ring pipeline, as well as combined use of both methods); detailed for a model case and generally with scaling effects
- Fundamental technical analysis of purification systems and conveyor systems for refuelling systems
- Comparison of the various refuelling options from a technical and economic perspective, depending on the size of the airport and the expected air traffic
- Technical, economic, and ecological analysis of the possibilities for recycling the H_2 flash gas generated during refuelling. Different scenarios (release to the atmosphere, use of H_2 at room temperature, for example, for electricity generation via fuel cells, various re-liquefaction and purification processes) will be compared under these aspects for all three implementation forms of LH_2 refuelling, depending on the size of the airport and the expected air traffic.
- Purification of LH_2 (cryogenic separation of contaminants in storage and circulation systems using cryogenic liquid pumps and cryocoolers).

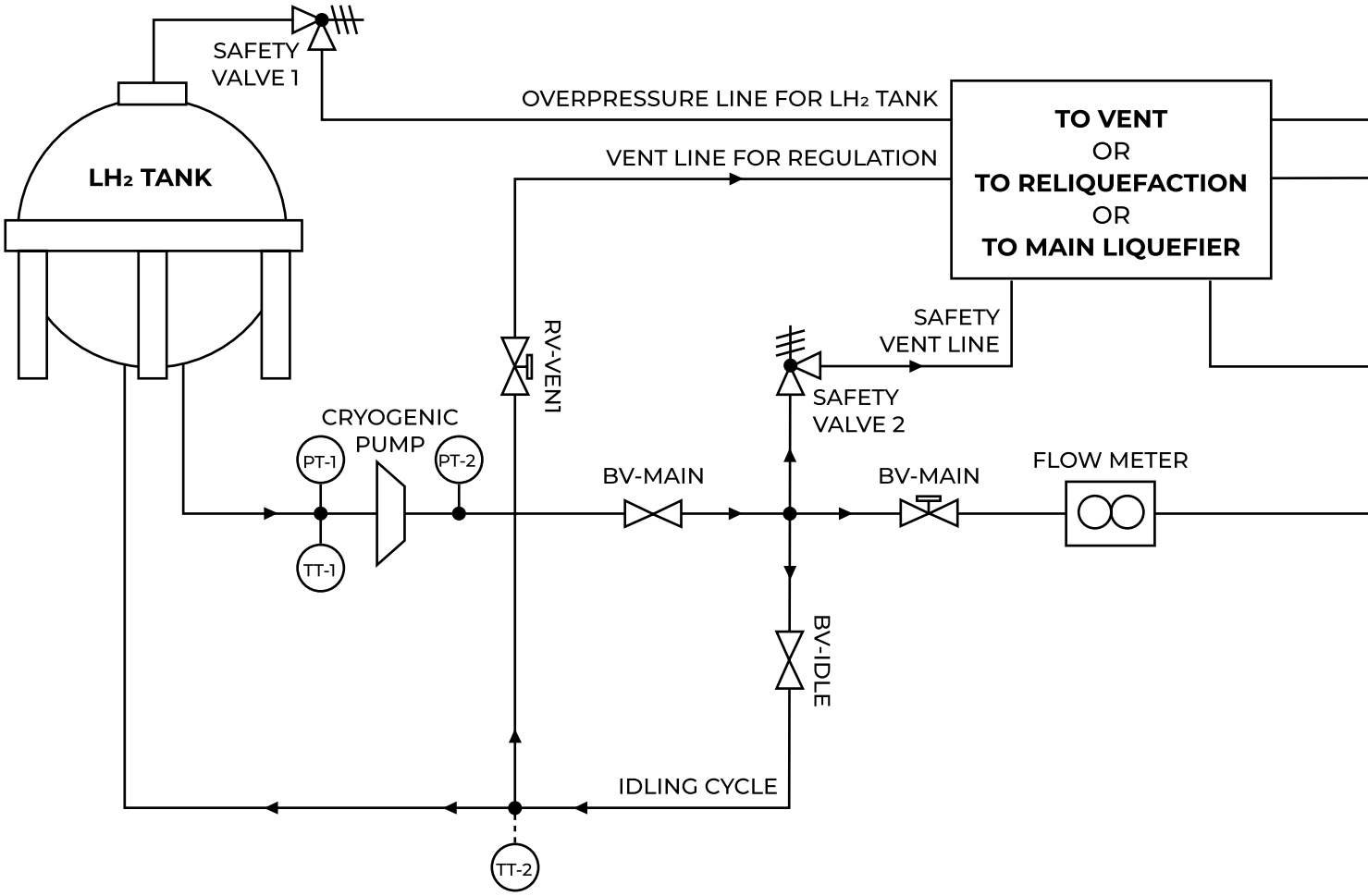

B.2 Basic infrastructure for LH_2 refueling at the airport

At first, the deep-dive analysis has focussed on larger airports such as Hamburg. Trailer-based logistics is not adequate to the requirements of this type of airports. An estimated need of more than 55 tons per day (projection for 2050) is confronted with a standard trailer capacity of approx. 1.5 tons. It is assumed, that between 10 and 30 trailers per day can be managed without disturbances. But 55 tons per day (equivalent to 20 kt p.a.) are equal to 37 trailers. Consequently, an LH_2 infrastructure at airports including a liquefier is strongly preferred for such or even larger capacities.

An LH_2 infrastructure is quite complex and includes customized components which partially are expensive and naturally require greater expenditure in terms of planning and space requirements.

The required components of an LH_2 infrastructure largely consist of the following components:

- LH_2 storage tank, assumed as a large cryogenic vessel (numerous smaller tanks are more flexible regarding varying H_2 needs but bear higher cost)
- Ring (circulation) pipeline – their dimensions depend sensitively on the topography of the analysed airport
- Cryocoolers for re-liquefaction due to heat loads and H_2 evaporation
- Filters
- Fuelling system (only prototypes available at current stage, no serial solution)
- Cleaning system against impurities in LH_2/H_2 components (this is relevant for safety since oxygen might freeze out and could be enriched what after its evaporation can result in dangerous mixtures of gases)
- Cryogenic valves (shut-off, regulating)
- Cryogenic liquid pumps for various purposes as tank filling and pipeline circulation (R&D is required for energy-efficient high mass-flow pumps)
- Instrumentation (e.g. pressure, mass flow, temperatures)

The whole infrastructure is sketched in Figure 62.

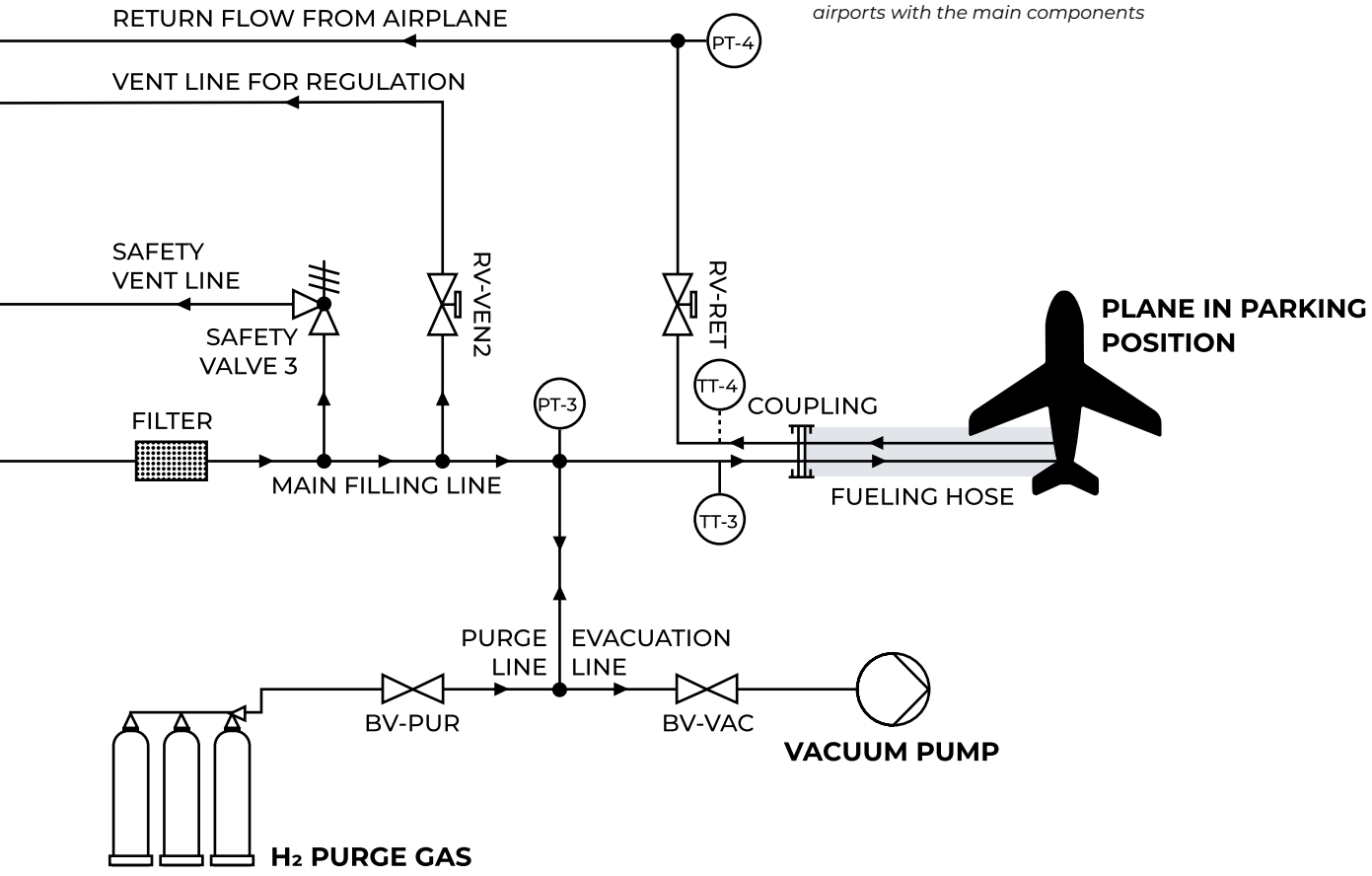

Figure 62: General scheme of a cryogenic H_2 infrastructure for airports with the main components

B.3 Cost of main components

For Hamburg, investment costs for the liquefaction of H_2 would be approximately € 240 million (55 tLH_2 per day). This value concerns the liquefier, only, and is the result of a future needs-based assessment. For comparison, a typical liquefier as that of Leuna in Germany, provides 5 tLH_2 per day. Its CAPEX is € 22 million (regarding the liquefier only, excluding buildings, storage dewars, and filling).

Further main costs originate from the vacuum-insulated circulation pipeline (assumed length: 1 800 m), € 3 million (without cryogenic cooler for re-liquefaction), an LH_2 storage tank of e.g. 255 m^3, € 1 million.

Noteworthy, an integrated design of the LH_2 infrastructure at an early stage can save costs significantly. For example, a separate H_2 purification unit may be dispensable if the liquefaction unit is designed appropriate to the requirements of the H_2/LH_2 circuits under operating conditions.

Based on the above considerations for both refuelling options (trailer vs. LH_2 infrastructure) the matrix results as shown in Table 5.

Table 5: Qualitative overview of LH_2 trailer refueling and LH_2 pipeline and hydrant system

	LH_2 trailer (without liquefaction)	LH_2 infrastructure with circulation
Production costs	low	high
Space requirements	low	medium
Operating costs	low	high
Independent power supply necessary	no	yes
Losses due to filling and transport	medium	low
Supply guarantee	medium	high

At this point, each airport must evaluate if a secure supply via trailers can be guaranteed. Such analysis should not only include required amounts of LH_2 but also issues of, e.g., transports distances and possible obstacles.

Moreover, instead of a stand-alone circulation pipeline, a combination of a liquefier with on-site trailers which distribute the LH_2 at the airport can be suited for certain sites, see Table 6.

Table 6: Qualitative overview of LH2 trailer refueling and LH_2 pipeline and hydrant system with on-site liquefaction

	Ring (circulation) pipeline	On-site trailers	Note
Production costs	high	low	
Heat load	compensable	boil-off	resulting effect
LH_2-transportation costs	medium[3]	high	
Handling	low	intensive	filling, fuelling
Usage	large airports	small/ mid-size airports	

3 Circulation pumps, cryocooler

B.4 Storage tanks for aircraft

A further part of the study has examined whether there are alternatives to a direct refuelling of aircrafts with LH_2 via pipeline. A promising version utilises integrated storage tanks. It is particularly interesting to note that swappable tanks could be mounted on top of an aircraft offering numerous advantages, see Figure 63.

The advantages are as follows:

- Both options ideally require an LH_2 liquefier at the airport
- Swappable tanks are conditioned and filled directly at the liquefier ▸ gas is reliquefied at an appropriate location
- Transport to the aircraft can be carried out using available infrastructure (manageable costs)
- Anchoring on the aircraft (seated on top of the aircraft)
- Minimal gas emissions from the aircraft
- Demand-based filling of the tanks (prevents boil-off during extended periods of non-use)
- From an energy perspective, the swappable tank option is preferable
- Pre-requisites:
- Uniform standard for these tanks/swap bodies
- Ideally, the same interfaces on all aircraft worldwide (standardisation)
- The geometry can be adapted, but must be suitable for the size of the aircraft
- Advantage: Existing aircraft could largely continue to be used and retain the number of passenger seats. No loss of space due to internal storage.
- Manageable effort for conversion from kerosine to LH_2 possible (general design of the aircraft can remain as it is)

B.5 Findings/Summary

There are currently no H_2 terminals for aviation, and the use of H_2 in flight operations is limited to a few demonstration projects. Consequently, the development of a refuelling infrastructure is highly urgent. For larger airports, refuelling via cryogenic ring pipelines will be necessary, as H_2-fuelled trailers transport too little H_2 to meet the airport's needs, and supply problems may arise. This is consistent with reference results [241]. Alternatively, swap tanks can be conditioned and filled at the airport's H_2 liquefier.

A parallel H_2 -integrated electrification (using boil-off gas) of further facilities of the airport infrastructure appears to be economically viable. Relevant components for H_2-fueled operations at airports have been identified and analysed

Figure 63: A 320 / 3900 km reach [Source of the 3D model of the A320: https://grabcad.com/library/a320-5 (29.09.2025)]

The swappable tank in Figure 63 contains the amount of LH_2 necessary to replace the conventionally carried kerosene.

APPENDIX

C Appendix

In the following, the techno-economic assumptions for the project analysis, additional details on the used methodology and data as well as additional project results are shown.

C.1 Common techno-economic assumptions

Table C.1 shows the techno-economic assumptions for the analysis of Chapter 4 and 5. For more detail on cost trends and economics of scale refer to the paper published as in the course of the project from Hoelzen et al. [36,130], Schenke et al. [39,63] and Lohr et al. [242].

Table C.1: Techno-economic assumptions for the project analysis. The values for the years not shown are interpolated linearly.

Component	Parameter	Unit	2020	2035	2050	Source
Wind onshore	Specific total CAPEX	USD_{2023}/kW	1,373.00	1,158.00	1,056.00	[243]
	Depreciation period	Years	30.00	30.00	30.00	[243]
	O&M factor	%	1.20	1.20	1.20	[243]
Wind offshore	Specific total CAPEX	USD_{2023}/kW	2,551.00	2,161.00	1,962.00	[243]
	Depreciation period	Years	30	30	30	[243]
	O&M factor	%	1.85	1.85	1.85	[243]
PV	Specific total CAPEX	USD_{2023}/kW	616.00	412.00	348.00	[243]
	Depreciation period	Years	40.00	40.00	40.00	[243]
	O&M factor	%	1.97	1.97	1.97	[243]
Electric energy storage system	Specific total CAPEX	USD_{2023}/kW	463.00	265.00	198.00	[130]
	Depreciation period	Years	15.00	15.00	15.00	[130]
	O&M factor	%	3.00	3.00	3.00	[130]
	Self-discharge	%/day	0.1	0.1	0.1	[130]
	Charging efficiency	%	95.00	95.00	95.00	[130]
	Discharging efficiency	%	95.00	95.00	95.00	[130]
Electrolysis system	Specific total CAPEX	USD_{2023}/kW	2,007.00	1200.00	750.00	[39]
	Depreciation period	Years	30.00	30.00	30.00	[130]
	Stack lifetime	Years	15.00	15.00	15.00	[130]
	Stack replacement	% of CAPEX	20.00	20.00	20.00	[130]
	O&M factor	%	3.00	3.00	3.00	[130]
	Specific energy demand	kWh/kgH_2	50.00	47.50	45.00	[130]
GH_2 compression	Specific total CAPEX[1]	USD_{2023}/kW	2165.00	1970.00	1645.00	[130]
	Depreciation period	Years	15.00	15.00	15.00	[130]
	O&M factor	%	2.00	2.00	2.00	[130]
	H_2 losses	% of H_2 feed	0.50	0.50	0.50	[130]
	Isentropic efficiency	%	85.00	85.00	85.00	[130]
	Electric efficiency	%	95.00	95.00	95.00	[130]
	Motor efficiency	%	91.00	91.00	91.00	[130]
	Specific energy demand GH_2 cavern	kWh/kgH_2	1.10	1.10	1.10	[130]
	Specific energy demand GH_2 tank	kWh/kgH_2	1.18	1.18	1.18	[130]

GH_2 cavern storage	Specific total CAPEX[1]	$USD_{2023}/kgGH_2$ stored	23.82	23.82	23.82	[130]
	Depreciation period	Years	30.00	30.00	30.00	[130]
	O&M factor	%	2.00	2.00	2.00	[130]
GH_2 above ground tank	Specific total CAPEX[1]	$USD_{2023}/kgGH_2$ stored	727.41	662.31	553.38	[130]
	Depreciation period	Years	20.00	20.00	20.00	[130]
	O&M factor	%	1.50	1.50	1.50	[130]
GH_2 pipeline	Specific total CAPEX[1] (new pipeline)	Mn USD_{2023}/km	-	4.56	3.65	[130]
	Depreciation period	Years	-	40.00	40.00	[130]
	O&M factor	%	-	1.00	1.00	[130]
EHB transport	Specific transport costs	USD_{2023}/kgH_2 per 1000 km	-	0.40	0.28	[244]
Liquefaction plant[2]	Specific total CAPEX[1]	Mn USD_{2023}/tpd	4.23	2.07	1.63	Own calculations see Chapter A
	Depreciation period	Years	20.00	30.00	30.00	
	O&M factor	%	5.00	5.00	5.00	
	H_2 losses	%	1.00	1.00	1.00	
	Specific energy demand under full load[1]	kWh/kgH_2	10.56	9.50	6.20	
LH_2 cryo-pump	Specific total CAPEX	USD_{2023}/(kg/h)	-	468.00	350.00	[130]
	Depreciation period	Years	-	10.00	10.00	[130]
	O&M factor	%	-	3.00	3.00	[130]
	Specific energy demand	kWh/kgH_2	-	0.10	0.10	[130]
LH_2 storage	Specific total CAPEX[1]	$USD_{2023}/kgLH_2$ stored	33.46	28.10	21.41	[130]
	Depreciation period	Years	20.00	20.00	20.00	[130]
	O&M factor	%	2.00	2.00	2.00	[130]
	Boil-off rates[1]	%/day	0.03	0.03	0.03	
LH_2 vessel[3]	Specific total CAPEX[1]	Mn USD_{2023} per vessel	-	452.50	362.53	[130]
	Depreciation period	Years	-	25.00	25.00	[130]
	O&M factor	%	-	4.00	4.00	[130]
	Variable OPEX (crew etc.)	Mn USD_{2023}/a	-	14.96	14.96	[130]
LH_2 truck (FC truck incl. LH_2 trailer)[3]	Specific total CAPEX	Mn USD_{2023} per truck	1.47	1.14	0.85	[39]
	Depreciation period	Years	12.00	12.00	12.00	[39]
	O&M factor	%	3.00	3.00	3.00	[39]
LH_2 refueling truck	Specific total CAPEX	USD_{2023} per truck incl. dispensing unit	-	3.69	2.81	[39]
	Depreciation period	Years	12.00	12.00	12.00	[39]
	O&M factor	%	3.00	3.00	3.00	[39]

[1]at largest available design size, [2]see Chapter A for more details, [3]For detailed assumptions and model equations on vessel and truck transport see [39]

C.2 Data basis for the System Dynamics Model

C.2.1 Airline data basis and assumptions

The different aircraft segments are defined based on flight distance. All values relevant to the airline are summarized in Table C.2. The regional-range covers distances up to 500 km, the short-range segment extends to 1,500 km, and the medium-range segment to 3,500 km. The airline's fleet size is modelled as a stock, which requires an initial value. This initial fleet is derived from the current European fleet and allocated across the three segments. Since H_2-powered aircraft will be introduced later, the initial number is set to zero.

Maintenance times differ between technologies. For kerosene-based aircraft, maintenance takes 2 days, while maintenance for H_2-powered aircraft is assumed to take 10 days due to the novelty and complexity of the technology. This duration decreases as more H_2-powered aircraft enter the fleet. For all segments and fuels, the interval between maintenance checks is set to 1.5 months. The average lifetime of a kerosene-based aircraft is assumed to be 20 years, whereas H_2-powered aircraft have a shorter lifetime of 10 years.

Seat capacities vary by segment: regional-range aircraft offer 60 seats, short-range aircraft 172 seats, and medium-range aircraft 263 seats [245]. Within the same distance segment, H_2-powered aircraft have 80% of the seat capacity of their kerosene-based equivalents [36]. Given varying flight distances and durations, the number of flights per segment is considered explicitly. Across all segments and fuels, an optimal seat occupancy of 80% is assumed [246].

Table C.2: Overview of the data basis for the airline

Airline fleet at time t_0	
Regional-range kerosene-based aircraft	844 aircraft
Regional-range H_2-powered aircraft	0 aircraft
Short-range kerosene-based aircraft	3,020 aircraft
Short-range H_2-powered aircraft	0 aircraft
Medium-range kerosene-based aircraft	738 aircraft
Medium-range H_2-powered aircraft	0 aircraft
Maintenance time	
H_2-powered aircraft	0.335 months
Kerosene-based aircraft	0.067 months
Average aircraft lifetime	
Kerosene-based aircraft	20 years
H_2-powered aircraft	10 years
Time until next maintenance event	
All segments and fuels	1.5 months
Segment definition	
Regional-range	500 km
Short-range	1,500 km
Medium-range	3,500 km
Available sets per segment and aircraft type	

Regional-range kerosene-based aircraft	60 seats
Regional-range H_2-powered aircraft	48 seats
Short-range kerosene-based aircraft	172 seats
Short-range H_2-powered aircraft	138 seats
Medium-range kerosene-based aircraft	263 seats
Medium-range H_2-powered aircraft	210 seats
Aircraft use per month	
Regional-range	242 flights
Short-range	183 flights
Medium-range	60 flights
Optimal aircraft seat occupancy	
All segments and fuels	80%

C.2.2 Aircraft manufacturer data basis and assumptions

The backlog is derived from Airbus's current order backlog [58]. All relevant values for the aircraft manufacturer are summarised in Table C.3. The number of H_2-powered aircraft is set to zero, as they enter the market at a later stage. Airbus's production capacities serve as the basis for the capacities assumed in the system. A delay of six months is assumed between the point at which a new aircraft is required and the placement of an order. Aircraft production itself also takes six months [58]. If the time between order and delivery exceeds five years, production capacity is assumed to increase by 20%.

Table C.3: Overview of the data basis for the aircraft manufacturer

Backlog	
Regional-range kerosene-based aircraft	377 aircraft
Regional-range H_2-powered aircraft	0 aircraft
Short-range kerosene-based aircraft	7655 aircraft
Short-range H_2-powered aircraft	0 aircraft
Medium-range kerosene-based aircraft	196 aircraft
Medium-range H_2-powered aircraft	0 aircraft
Aircraft production time	
All segments and fuels	6 months
Aircraft order time	
All segments and fuels	6 months
Aircraft production capacity	
Regional-range	5 aircraft
Short-range	51 aircraft
Medium-range	3 aircraft
Aircraft initial production capacity	
Regional-range kerosene-based aircraft	5 aircraft
Regional-range H_2-powered aircraft	0.5 aircraft

Short-range kerosene-based aircraft	51 aircraft
Short-range H_2-powered aircraft	5.1 aircraft
Medium-range kerosene-based aircraft	3 aircraft
Medium-range H_2-powered aircraft	0.3 aircraft
Desired time production aircraft	
All segments and fuels	5 years
Production capacity increase until 2050	
All segments and fuels	20%

C.2.3 Kerosene-based aircraft data basis and assumptions

All values for kerosene are summarised in Table C.4. The initial kerosene price is set at 1 USD/kg and is assumed to grow annually by 1%. In the Moonshot scenario, an additional kerosene tax is applied. All data for kerosene taxes is provided in the ***Taxes Kerosene.cin*** file. Kerosene consumption is determined based on the specific aircraft types within each segment. The number of flights reflects the average number of flights operated by an aircraft over its lifetime. Purchase prices vary across segments, with maintenance costs amounting to 50,000 USD [247,248].

Table C.4: Overview of the data basis for kerosene-based aircraft

Kerosene price	
All segments	1 USD/kg
Kerosene price growth	
All segments	1%
Kerosene tax (Moonshot scenario)	
2030–2040	5%
2041–2050	10%
Kerosene consumption	
Regional-range	1.22 kg/km
Short-range	2.75 kg/km
Medium-range	6 kg/km
Annual number of flights	
Regional-range	2,900 flights
Short-range	2,200 flights
Medium-range	730 flights
Purchase price kerosene-based aircraft	
Regional-range	32,000,000 USD
Short-range	101,000,000 USD
Medium-range	231,500,000 USD
Maintenance cost kerosene-based aircraft	
All segments	50,000 USD

H_2-based aircraft data basis and assumptions

All values for H_2-based aircraft are summarised in Table C.5. The initial LH_2 price is set at 13.16 USD/kgH_2 in 2030 and decreases to 5.92 USD/kgH_2 in 2036 and 3.57 USD/kgH_2 in 2041. In the Moonshot scenario, the hydrogen subsidy is assumed to be 20% in 2035, declining to 10% in 2046. In the Ambitious policy scenario, the LH_2 subsidy is set at 10% in 2040, decreasing to 5% in 2046 and 1% in 2051. All data for the subsidy of LH_2 is provided in the ***Subsidy Hydrogen.cin*** file. Purchase prices differ in each segment, with maintenance costs amounting to 57,000 SUD [36]. LH_2 consumption amounts to 0.4392 kg/km for regional-range aircraft, while short-range segment aircraft consume 1.1 kg/km, and medium-range aircraft 2.52 kg/km [245]. All LH_2 price data is provided in the ***Hydrogen price.cin*** file.

Table C.5: Overview of the data basis for H_2-based aircraft

LH_2 price	
2030–2035	13.16 USD/kgH_2
2036–2040	5.92 USD/kgH_2
2041–2050	3.57 USD/kgH_2
LH_2 subsidy (Moonshot)	
2035–2045	20%
2046–2050	10%
LH_2 subsidy (Ambitious policy)	
2040–2045	10%
2046–2050	5%
2051–2060	1%
LH_2 consumption	
Regional-range	0.4392 kg/km
Short-range	1.1 kg/km
Medium-range	2.52 kg/km
Purchase price H_2-powered aircraft	
Regional-range	35,200,000 USD
Short-range	111,100,000 USD
Medium-range	254,650,000 USD
Maintenance cost H_2-powered aircraft	
All segments	57,000 USD

C.2.4 EU ETS data basis and assumptions

All values for the EU ETS are summarised in Table C.6. The current market price for the EU ETS is 76.21 USD/tCO_2 [249]. For the conservative scenario (Baseline), an annual increase of 3% is assumed. The ambitious policy scenario considers an annual growth rate of 5%, reaching a value of 122 USD/tCO_2 by 2030 [250]. The Moonshot scenario projects a price of 149 USD/tCO_2 in 2030, corresponding to an annual growth rate of 6% [251]. All EU ETS data is provided in the ***EU ETS.cin*** file.

Table C.6: Overview of the data for EU ETS

Year	Baseline (3% p.a.) in %	Ambitious policy (+5% p.a.) in %	Moonshot (+6% p.a.) in %
2025	76.21	76.21	76.21
2026	78.50	83.73	87.15
2027	80.85	91.99	99.65
2028	83.28	101.07	113.95
2029	85.78	111.04	130.30
2030	88.35	122.00	149.00
2031	91.00	128.10	157.94
2032	93.74	134.51	167.41
2033	96.55	141.24	177.44
2034	99.45	148.30	188.09
2035	102.44	155.71	199.40
2036	105.51	163.49	211.36
2037	108.67	171.66	224.04
2038	111.93	180.24	237.48
2039	115.30	189.26	251.73
2040	118.76	198.72	266.84
2041	122.33	208.65	282.85
2042	125.99	219.08	299.82
2043	129.78	230.03	317.81
2044	133.67	241.53	336.89
2045	137.68	253.61	357.20
2046	141.77	266.31	378.51
2047	146.03	279.63	401.22
2048	150.41	293.61	425.30
2049	154.92	308.29	450.81
2050	159.57	323.70	477.86

C.2.5 Passenger demands

All passenger demand data is provided in the ***PKM.cin*** file. These demand values are calculated for each airport on a monthly basis.

C.3 Methodology H_2 supply network optimization model

C.3.1 Model details

For the "Target Picture 2050" mathematical model, please refer to the following publication [252]:

Ögrük, A., Marx, R., Thies, C., Stiller, S. (2025). Green Hydrogen Supply Chain Network Design for Aviation: Model Development and Case Study for German Airports in 2050. In: Voigt, G., Fliedner, M., Haase, K., Brüggemann, W., Hoberg, K., Meissner, J. (eds) Operations Research Proceedings 2023. OR 2023. Lecture Notes in Operations Research. Springer, Cham. https://doi.org/10.1007/978-3-031-58405-3_58

The "Transition Pathways" model builds upon the "Target Picture 2050" model. In this extended version, we introduce the following additional features:

- A multi-period framework capturing temporal evolution of the system, and
- Storage dynamics that are interdependent over time.

Details of the "Transition Pathways" model can be found in the following publication [253]:

Ögrük, A., Schenke, F., Hanke-Rauschenbach, R., Thies, C. (2025). Design of hydrogen supply networks for aviation: dynamic optimization model and transition pathways for German airports. Preprint. https://doi.org/10.15480/882.16268

C.3.2 Case study details

Table C.7 shows the considered H_2 production locations for the target picture 2050 and the transition pathway model. The available H_2 production volumes and costs are determined by the energy system analysis discussed in Chapter 5.

Table C.7: Potential H_2 production location list for the target picture 2050 model and the transition pathway model

Target picture 2050		**Transition pathway**	
Supplier	**NUTS1 Code/ Country Name**	**Supplier**	**NUTS1 Code/ Country Name**
Centro	ES4	Centro	ES4
Cesko	CZ0	Cesko	CZ0
Chile	Chile	Chile	Chile
Continente	PT1	Continente	PT1
Danmark	DK0	Danmark	DK0
Ireland	IE0	Ireland	IE0
Kentriki Ellada	EL6	Kentriki Ellada	EL6
Lietuva	LT0	Makroregion Polnocny	PL4
Macroregiunea Patru	RO4	Manner Suomi	FI1
Makroregion Polnocny	PL4	Morocco	Morocco
Manner Suomi	FI1	Niedersachsen	DE9
Morocco	Morocco	Northern Ireland	UKN
Niedersachsen	DE9	Norway	NO0
Norra Sverige	SE3	Sodra Sverige	SE2
Northern Ireland	UKN	Voreia Ellada	EL5

Norway	NO0
Ostra Sverige	SE1
Sodra Sverige	SE2
Voreia Ellada	EL5
Wschodni	PL3

C.3.3 Further results

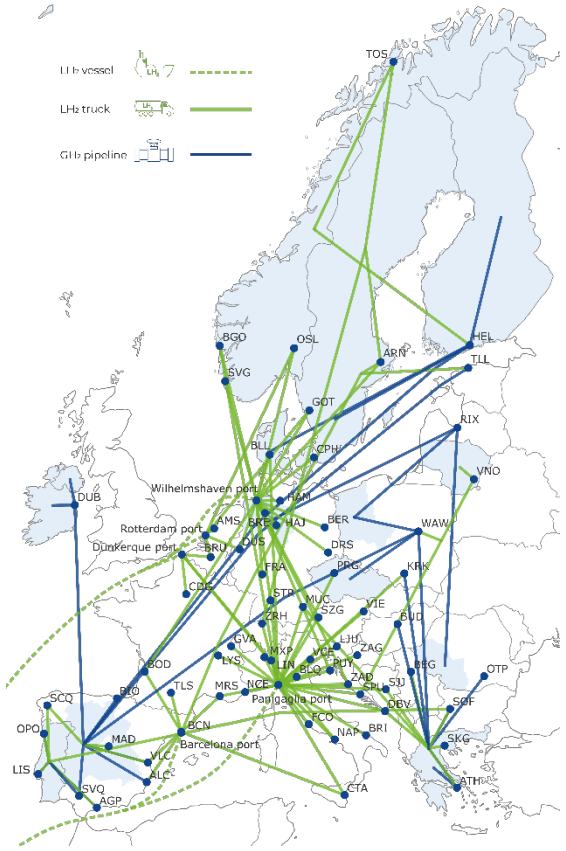

Figure C.1: Optimal network map for the target year 2050 for the moonshot scenario

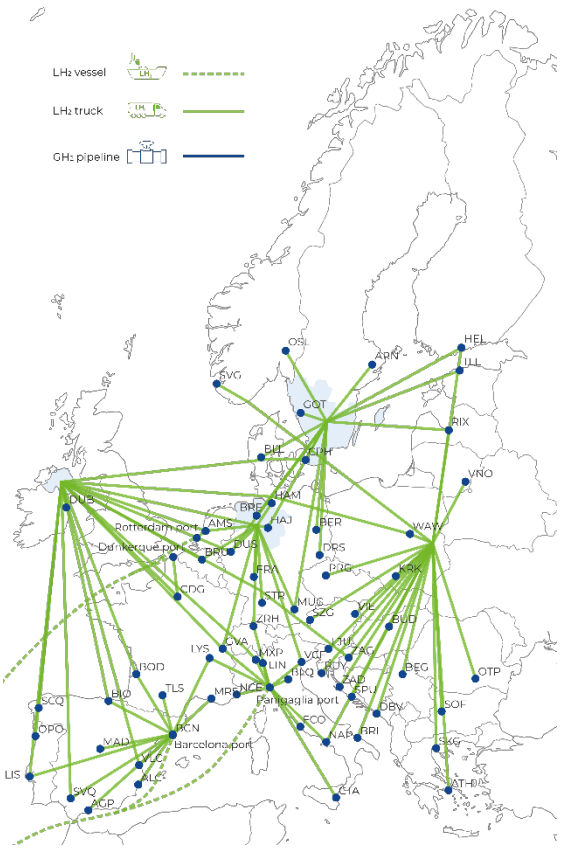

Figure C.2: Optimal network map for the target year 2050 for the baseline demand scenario

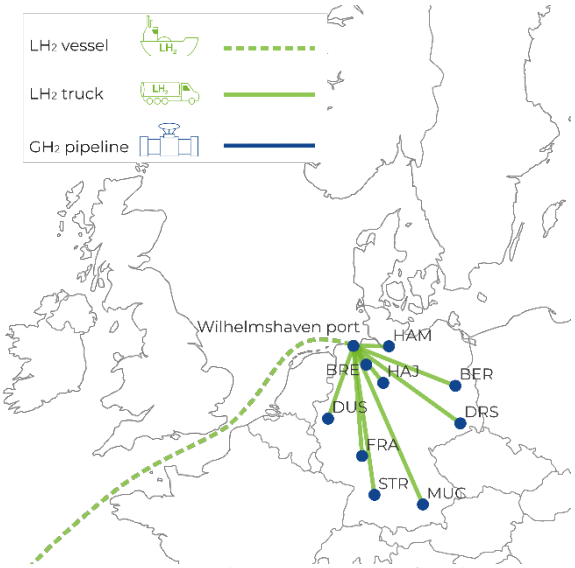

Figure C.3: Optimal network map for the ambitious policy scenario for the period 2041-2045

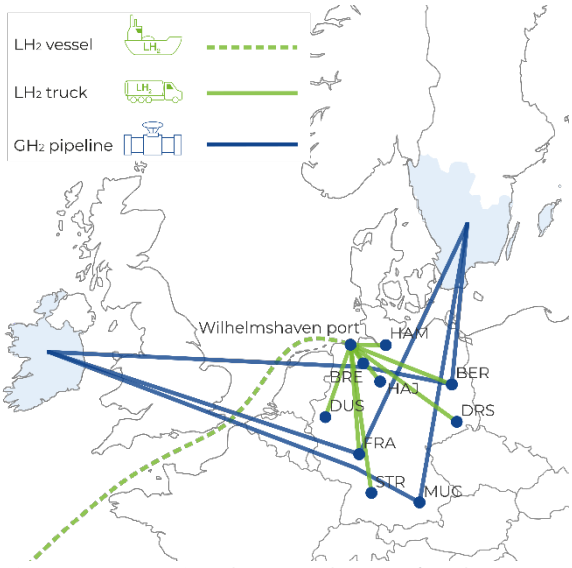

Figure C.4: Optimal network map for the ambitious policy scenario for the period 2046-2050

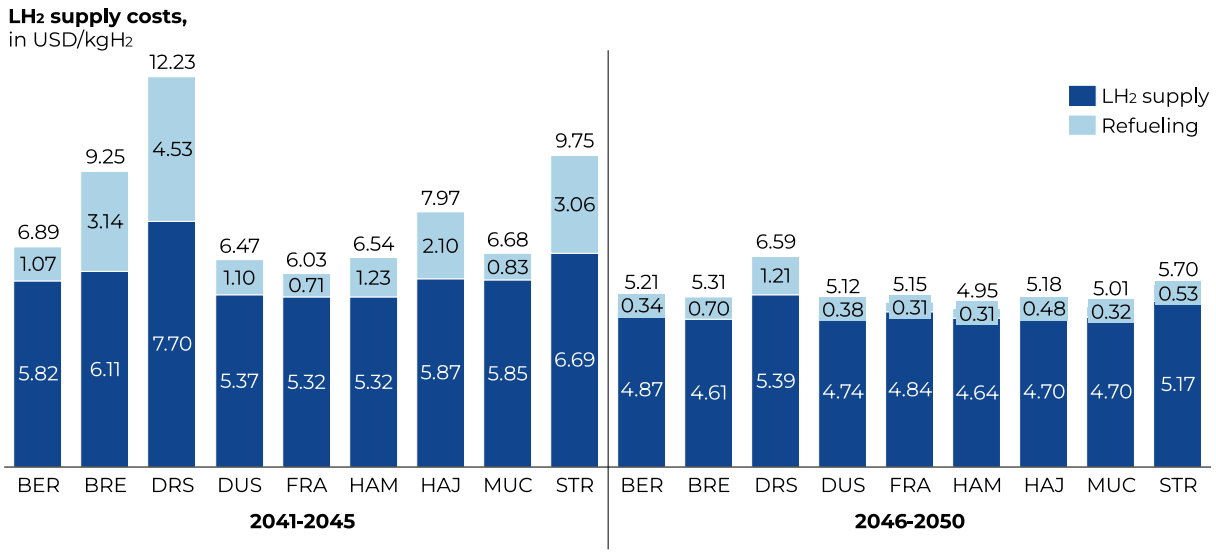

Figure C.5: Supply and refuelling costs at each airport for different periods for the Ambitious policy scenario

C.4 Methodology for the flight network model

To be able to introduce the H_2 Aviation Network Problem (HANP) it was necessary to adopt some assumptions given in the following:

Network Representation

The aviation network is modelled as a bidirectional graph $G = (V, A)$, where:

V = set of airports (vertices)

A = set of possible flight connections (arcs)

Each arc can be operated by H_2-powered and/or kerosene-powered aircraft.

Arc costs and feasibility depend only on propulsion type; no other operational constraints (e.g., weather, congestion) are included.

Kerosene Operations

Cost: Fixed per arc and per passenger; includes maintenance.

Availability: Unlimited fuel supply.

Price: Uniform across all airports; cost variation arises only from arc length.

Hydrogen Operations

Feasibility: Arc *a* is operable if distance between source and target airport is within the range of proposed H_2-operated aircraft (ca. 2000 NM)

Supply: Each airport *v* has a limited H_2 capacity

Price: H_2 cost c_v^h varies by airport.

Transport: H_2 can be carried across multiple legs via H_2 *excess paths*.

Refueling Restrictions:

No refueling between aircraft.

No empty flights carrying H_2.

Capacity Limits: H_2 carried per arc cannot exceed a specified tank size per passenger derived from the maximum range of a H_2-powered aircraft

Usage Constraint: H_2 load on an arc must meet the operational requirement r_a.

Passenger Demand and Flow

Demand: Fixed for each origin–destination (OD) pair; no elasticity modeled.

Flow Types: Separate flows for hydrogen (h) and kerosene (k).

Units: Flow represents passengers

Conservation: Passenger flow is preserved across the network.

Market Penetration: Share of H_2-powered demand limited proportional to an estimated market share of H_2-powered aircraft

Next, an overview of the parameters that are used to introduce the HANP is provided in Table C.8.

Table C.8: Overview of the parameters used to introduce the HANP

Parameter	Name	Source
Airports	V	(subset of) all European airports
Flight legs	A	all possible connections
Commodities	$(\{O_1, D_1\}, \dots, \{O_N, D_N\})$	from Eurostat [57]
Demand	$d_i, i \in [N]$	from Eurostat [57]
H_2-consumption per passenger/flight leg	r_a	[245]
H_2-capacity per airport	H_v	See Chapter 3
H_2-tank size per passenger	T	18 kg/passenger
Cost for H_2	c_v^h	See Chapter 4
Maintenance cost for H_2	c_a^m	[245]
Cost for kerosene	c_a^k	1 USD/kg
H_2-market penetration	Q	See Chapter 3

C.4.1 Definition of the Model

Determining where to integrate H_2-powered aircraft into the existing aviation system – and how to modify current flight path networks to accommodate their unique range and seating capacities – is a complex challenge. This section introduces a mixed-integer linear program (MILP) designed to identify a cost-optimal solution to these integration and routing decisions.

We model the aviation network as a bidirectional graph $G = (V, A)$, where V denotes the set of airports and A the set of possible flight connections. Each arc $a \in A$ can be operated using H_2- or kerosene-powered aircraft. Kerosene operation is characterized solely by a cost per arc and per passenger, and is assumed to be unconstrained in terms of fuel availability. In contrast, H_2-powered operation is subject to range and supply limitations.

Let $\{\{O_1, D_1\}, \dots, \{O_N, D_N\}\}$, with $N \in \mathbb{N}$, denote the set of origin–destination (OD) pairs representing multiple commodities, each corresponding to an estimated passenger demand in the considered aviation system. This demand can be served by H_2-powered aircraft or by aircraft fueled with kerosene. To model this, we introduce two separate flow types for each OD pair: one for H_2-powered transport and one for kerosene-fueled transport. Flow in this context can be interpreted either as the estimated number of aircraft operating on this flight path or as the estimated number of passengers who want to travel from the origin to the destination. In this work, we adopt the latter interpretation, considering flow as passenger demand.

For $n \in \mathbb{N}$, we define $[n] \coloneqq \{1,2, \dots, n\}$, and let $n \in [N]$ index the commodities. Let $\omega \in \{h, k\}$ denote the propulsion type, where h refers to H_2 and k to kerosene. We define a flow function $f_i^\omega \colon P(A) \to \mathbb{Z}_{\geq 0}$, which maps subsets of A to non-negative integers, representing the aggregated flow of commodity i using propulsion type ω over each arc. In other words, $f_i^\omega(a)$ denotes the total flow of commodity i using fuel type ω that passenger an arc set $A' \subseteq A$,

$$f_i^{\omega}(A') = \sum_{a \in A'} \varphi_i^{\omega}(a), \qquad \text{(C.1)}$$

where $\varphi_i^{\omega}(a)$ is the flow value on arc $a \in A$.

We now introduce the constraints governing passenger flow. To this end let $\delta^+: V \to P(A)$ and $\delta^-: V \to P(A)$ be the functions assigning its set of outgoing and ingoing arcs to each vertex, respectively. First, we define flow conservation constraints to ensure that the total number of passengers transported between each origin–destination pair matches the specified demand,

$$f_i^h(\delta^+(O_i)) + f_i^k(\delta^+(O_i)) = d_i + f_i^h(\delta^-(O_i)) + f_i^k(\delta^-(O_i)) \qquad \forall i \in [N] \qquad \text{(C.2)}$$

$$f_i^h(\delta^-(D_i)) + f_i^k(\delta^-(D_i)) = d_i + f_i^h(\delta^+(D_i)) + f_i^k(\delta^+(D_i)) \qquad \forall i \in [N]. \qquad \text{(C.3)}$$

Here, d_i denotes the estimated demand for commodity $i \in [N]$. Next, we impose flow conservation constraints on each intermediate vertex to ensure that passenger flow is preserved across the network, such that each passenger ultimately reaches their designated destination,

$$f_i^h(\delta^+(v)) + f_i^k(\delta^+(v)) = f_i^h(\delta^-(v)) + f_i^k(\delta^-(v)) \qquad \forall v \in V\{O_i, D_i\}, \forall i \in [N]. \qquad \text{(C.4)}$$

Since no H_2-powered commercial aircraft are currently in operation and their market introduction is expected to occur in the future [254], it is necessary to account for the limited availability of H_2-powered aircraft in the model,

$$f_i^h(\delta^+(O_i)) \leq Q d_i \qquad \forall i \in [N], \qquad \text{(C.5)}$$

such that the H_2-powered flow cannot exceed an explicit upper bound given by the market penetration Q. In this context, market penetration refers to the proportion of H_2-powered aircraft within the total operational fleet. Since our model does not explicitly represent individual aircraft, we approximate this value by applying the penetration rate to passenger flows instead.

A further critical aspect in addressing the above questions is the availability of H_2. Let T denote the transportable H_2 amount per passenger, obtained by dividing the estimated tank size of a H_2-powered aircraft by its seating capacity. For each arc a, we define r_a as the H_2 requirement per passenger for operating the arc with a H_2-powered aircraft. An arc is feasible for H_2-powered operation if $r_a \leq T$. In addition, each airport v provides only a limited H_2 supply, denoted by H_v, with H_2 costs assumed to be airport-specific.

Since H_2 production is highly energy-intensive and its sustainability depends on regional availability of renewable energy, both the quantity and cost of H_2 may differ between airports. This spatial heterogeneity can incentivize strategies such as refueling for multiple subsequent flights at airports with lower H_2 prices, thereby reducing operational costs and enabling H_2-powered operation on routes that would otherwise be infeasible. To capture this behaviour within the model, it is necessary to track the portion of H_2-powered demand on each arc that is supplied by H_2 not procured at the arc's source airport. To facilitate this, we introduce the concept of H_2 excess paths, which represent paths over which H_2 is carried from a source to a destination, where it can then be used on outgoing arcs.

Definition 3.1 (H_2 Excess Path). *Let $p = (a_1, \dots, a_M)$ be a path in G with $M \geq 1$. Let $T^p := T - \sum_{j=1}^{M} r_{aj}$ be a so-called transport capacity at the target of a_M. Then p is a H_2 excess path if and only if $T^p > 0$ holds. Let P^{ex} be the set of all H_2 excess paths in G.*

Outgoing arcs of the target of a_M are called outgoing arcs of p and for better readability let $\delta^+(p) := \delta^+(a_M)$.

For each H_2 excess path $p \in P^{ex}$ and arc $a \in \delta^+(p)$, let t_a^p be the amount of flow on arc a that is operated at least partially using H_2 originating from the transport capacity of path p. Capturing this requires not only the proportion of demand served by H_2-powered aviation but also the distribution of H_2 usage across arcs. To model this, we introduce two types of variables related to H_2 usage. The first, $h_a \in \mathbb{R}_{\leq 0}$ for all $a \in A$, denotes the amount of H_2 purchased at the source airport of arc a and directly used to operate a. The second type, $h_a^p \in \mathbb{R}_{\leq 0}$, is defined for all H_2 excess paths $p \in P^{ex}$ and arcs $a \in \delta^+(p)$. This variable represents the quantity of H_2 purchased at the source of path p that remains unused on all arcs on p and is therefore available for use on arc a.

To incorporate H_2-related constraints into the network model, we begin by introducing an inequality that limits the amount of H_2 that can be purchased at each airport v,

$$\sum_{a \in \delta^+(v)} h_a + \sum_{a \in \bigcup_{p \in P_v} \delta^+(p)} h_a^p \leq H_v \qquad \forall v \in V. \qquad \text{(C.6)}$$

Here $P_a \subseteq P^{ex}$ denotes the set of H_2 excess paths beginning with the vertex $v \in V$. There is also a limit on the amount of H_2 that can be carried on each flight,

$$h_a + \sum_{p: a \in \delta^+(p)} h_a^p + \sum_{a \in \bigcup_{p \in P_v} \delta^+(p)} h_e^p \leq T \sum_{i \in [N]} f_i^h(a) \qquad \forall a \in A, \qquad \text{(C.7)}$$

where $P_a \subseteq P^{ex}$ denotes the set of all H_2 excess paths that begin with arc $a \in A$. This constraint ensures that the total H_2 required to operate arc a, along with the H_2 carried for future use, does not exceed the amount of H_2 transportable per passenger, T. Specifically, the second term captures the H_2 used from a transport capacity at the source of a, while the third term accounts for H_2 purchased at the source of *an* intended for later use. It is then necessary to ensure that each flight is loaded with sufficient H_2, which leads to the following constraint:

$$h_a + \sum_{p: a \in \delta^+(p)} h_a^p \leq r_a \sum_{i \in [N]} f_i^h(a) \qquad \forall a \in A, \qquad \text{(C.8)}$$

where r_a denotes the amount of H_2 required per passenger to operate flight leg $a \in A$, and only the H_2 drawn from the transport capacity at the source of a needs to be accounted for.

Finally, our model should account for the possibility of refueling a H_2-powered aircraft for multiple subsequent flights. To this end, several characteristics of the refueling process must be incorporated. In particular, we exclude empty flights from the network. This means that the amount of H_2 flow on an arc that uses transport capacity cannot exceed the amount of H_2 flow on the respective H_2 excess path from this transport capacity, leading to

$$\sum_{a \in \delta^+(v)} t_a^p \leq \sum_{i \in [N]} f_i^h(a^*) \qquad \forall v \in V, \forall p \in P^v, \forall a^* \in p \qquad \text{(C.9)}$$

Where $P^v \subseteq P^{ex}$ denotes the set of all H_2 excess paths in G which are ending in $v \in V$. Furthermore, for each arc $a \in A$, we impose a constraint to ensure that the portion

of demand utilizing transport capacity does not exceed the actual H_2-powered demand on arc a,

$$\sum_{p:a\in\delta^+(p)} t_a^p \leq \sum_{i\in[N]} f_i^h(a) \qquad \forall a \in A, \qquad \text{(C.10)}$$

Lastly, refueling an aircraft from another aircraft must not be permitted. Since individual aircraft are not explicitly tracked in our model, we enforce this constraint at the passenger level. To that end, we first restrict t_a^p to integer values, ensuring that only whole passengers are considered. Additionally, we constrain the amount of H_2 using a specific transport capacity to be a multiple of this transport capacity,

$$h_a^p \leq T_p t_a^p \qquad \forall p \in P^{ex}, \forall a \in \delta^+(p). \qquad \text{(C.11)}$$

After introducing the necessary constraints, the final component of the model is the objective function. As outlined earlier, the objective is to minimize the total operating cost of all flights in the reconfigured flight network. To this end, let c_a^m denote the maintenance cost per arc $a \in A$ and per passenger for H_2-powered aircraft. Let c_v^h represent the cost of H_2 at airport $v \in V$ We assume that kerosene prices are uniform across all airports, so cost variations for kerosene operations arise solely from differences in arc lengths. Let c_a^k denote the total cost per arc and per passenger for kerosene-powered flights, including maintenance.

Combining these elements yields the MILP-formulation of the H_2 aviation network problem.

$$\min \sum_{\forall i\in[N]} \Big(\sum_{a\in A} c_a^m f_i^h(a) + \sum_{a\in A} c_a^k f_i^k(a) \Big) + \sum_{v\in V} c_v^h \sum_{a\in\delta^+(v)} h_a \qquad \text{(C.12)}$$

$$f_i^h(\delta^+(O_i)) + f_i^k(\delta^+(O_i)) = d_i + f_i^h(\delta^-(O_i)) + f_i^k(\delta^-(O_i)) \qquad \forall i \in [N] \qquad \text{(C.13)}$$

$$f_i^h(\delta^-(D_i)) + f_i^k(\delta^-(D_i)) = d_i + f_i^h(\delta^+(D_i)) + f_i^k(\delta^+(D_i)) \qquad \forall i \in [N] \qquad \text{(C.14)}$$

$$f_i^h(\delta^+(v)) + f_i^k(\delta^+(v)) = f_i^h(\delta^-(v)) + f_i^k(\delta^-(v)) \qquad \forall v \in V\{O_i, D_i\}, \forall i \in [N] \qquad \text{(C.15)}$$

$$f_i^h(\delta^+(O_i)) \leq Q d_i \qquad \forall i \in [N] \qquad \text{(C.16)}$$

$$\sum_{a\in\delta^+(v)} h_a + \sum_{a\in\bigcup_{p\in P_v}\delta^+(p)} h_a^p \leq H_v \qquad \forall v \in V \qquad \text{(C.17)}$$

$$h_a + \sum_{p:a\in\delta^+(p)} h_a^p + \sum_{a\in\bigcup_{p\in P_v}\delta^+(p)} h_e^p \leq T \sum_{i\in[N]} f_i^h(a) \qquad \forall a \in A \qquad \text{(C.18)}$$

$$h_a + \sum_{p:a\in\delta^+(p)} h_a^p \leq r_a \sum_{i\in[N]} f_i^h(a) \qquad \forall a \in A \qquad \text{(C.19)}$$

$$\sum_{a\in\delta^+(v)} t_a^p \leq \sum_{i\in[N]} f_i^h(a^*) \qquad \forall v \in V, \forall p \in P^v, \forall a^* \in p \qquad \text{(C.20)}$$

$$\sum_{p:a\in\delta^+(p)} t_a^p \leq \sum_{i\in[N]} f_i^h(a) \qquad \forall a \in A \qquad \text{(C.21)}$$

$$h_a^p \leq T_p t_a^p \qquad \forall p \in P^{ex}, \forall a \in \delta^+(p) \qquad \text{(C.22)}$$

$$f_i^\omega(A') \in \mathbb{Z}_{\leq 0} \qquad \forall i \in [N], \forall \omega \in \{h,k\}, \forall A' \in P(A) \qquad \text{(C.23)}$$

$$h_a^p \in \mathbb{R}_{\leq 0} \qquad \forall p \in P^{ex}, \forall a \in \delta^+(p) \qquad \text{(C.24)}$$

$$\mathbb{Z}_{\geq 0} t_a^p \in \mathbb{Z}_{\leq 0} \qquad \forall p \in P^{ex}, \forall a \in \delta^+(p) \qquad \text{(C.25)}$$

$$h_a \in \mathbb{R}_{\leq 0} \qquad \forall a \in A \qquad \text{(C.26)}$$

The main computational challenge of this model arises from the large number of variables, which severely affects tractability. In the literature, this issue is commonly addressed using a column generation framework, where the pricing problem is solved via a labeling algorithm. However, due to the complexity of our resource constraints, the pricing problem becomes particularly difficult to solve. For this reason, we adopt a labeling algorithm called Hydrogen Aviation Network Labeling Alorithm (HANLA) that directly solves the entire problem in a unified manner.

The HANLA solves the HANP by gradually building up feasible flight paths across the network, while carefully tracking H_2-related constraints. It starts by identifying how much H_2 can be transported between airports and then initializes with a basic but valid flight assignment that uses either H_2 or kerosene, depending on which is cheaper and available.

From this starting point, the algorithm iteratively explores better paths by "labeling" segments of the network—essentially marking potential route fragments with information such as cost, previous connections, power source (H_2 or kerosene), and H_2 availability. Each time a new route is evaluated, the algorithm checks whether it is cheaper and still feasible within the H_2 limits before accepting it. In the end, the algorithm delivers an optimized routing and fueling plan that minimizes cost while fully respecting H_2-specific operational constraints.

Table C.9: Flight network results based on the H_2 subsidy with a total of 3340 available OD-pairs

Subvention in USD/kgH2	Threshold	Number of (at least partly) H_2-operated OD-pairs	Number of H_2-operated flight connections	Number of passengers operated by H_2	Share of passengers operated by H_2	Total costs for subventions
0.6	-	7	7	2,966,210.00	0.47%	4,271,282.78
0.6	3.2	7	7	2,966,210.00	0.47%	4,234,397.23
0.6	3.1	7	7	2,966,210.00	0.47%	4,271,282.78
0.7	-	18	18	4,352,560.00	0.70%	7,102,877.76
0.7	3.2	18	18	4,352,560.00	0.70%	6,354,111.74
0.7	3.1	18	18	4,352,560.00	0.70%	7,065,992.21
0.8	-	18	18	4,352,560.00	0.70%	8,117,574.58
0.8	3.2	18	18	4,352,560.00	0.70%	6,555,535.03
0.8	3.1	18	18	4,352,560.00	0.70%	7,368,808.57
0.9	-	59	61	11,985,296.00	1.91%	48,467,896.69
0.9	3.2	32	33	9,201,036.00	1.47%	15,539,429.57
0.9	3.1	32	33	9,201,036.00	1.47%	16,554,126.40
1.0	-	94	100	26,238,326.00	4.19%	83,744,611.89
1.0	3.2	68	72	23,435,111.00	3.74%	46,578,111.57
1.0	3.1	68	72	23,431,166.00	3.74%	48,013,598.77
1.1	-	215	233	50,761,098.00	8.11%	240,418,454.59
1.1	3.2	130	141	38,702,988.00	6.18%	81,285,624.46
1.1	3.1	131	142	37,783,242.00	6.03%	85,158,128.85
1.2	-	325	426	71,657,250.00	11.44%	326,662,701.71
1.2	3.2	235	282	58,883,764.00	9.40%	138,697,720.62
1.2	3.1	239	285	58,732,947.00	9.38%	145,487,143.49
1.3	-	461	627	99,101,729.00	15.82%	657,461,224.11
1.3	3.2	323	414	75,559,730.00	12.07%	213,333,578.51
1.3	3.1	330	452	74,766,306.00	11.94%	199,128,274.15
1.4	-	628	909	129,349,755.00	20.65%	959,559,938.14
1.4	3.2	347	450	82,870,202.00	13.23%	274,941,560.14
1.4	3.1	347	464	80,824,484.00	12.91%	268,202,093.82
1.5	3.2	381	492	104,153,233.00	16.63%	388,019,591.50
1.5	3.1	384	527	99,538,602.00	15.89%	367,494,692.77
1.6	3.2	382	479	107,408,892.00	17.15%	429,800,886.48
1.6	3.1	384	548	102,031,041.00	16.29%	415,554,093.26
1.7	3.2	400	505	110,570,095.00	17.66%	450,013,862.32
1.7	3.1	399	520	107,736,443.00	17.20%	452,222,839.80
1.8	3.2	407	501	112,905,926.00	18.03%	473,457,705.42
1.8	3.1	406	529	109,045,666.00	17.41%	469,494,654.88
1.9	3.2	407	484	112,344,272.00	17.94%	476,637,413.30
1.9	3.1	408	520	111,127,230.00	17.74%	491,941,343.99
2.0	3.2	409	501	114,028,527.00	18.21%	487,467,576.64
2.0	3.1	409	518	111,862,646.00	17.86%	495,353,448.83

C.5 Methodology for the energy system transformation model

Limiting global warming to well-below 2°C by the end of the century requires a defossilization of the energy system. This means that the energy system must undergo a transition from using fossil fuels across all sectors to using electricity in most sectors. Energy system analysis aims at finding cost-optimal transition pathways that adhere to the remaining carbon budget according to the Paris Agreement. Transition pathways show how the current energy system can evolve from its current configuration towards highly renewable in feasible incremental steps.

ESTRAM is a framework for energy system analysis developed at the Leibniz University Hannover. It is a flexible framework written in the python programming language that allows for the optimization of overnight as well as transition pathway scenarios on a local but also on a European scale. To this end, the energy system is divided into multiple interconnected nodes. In a typical calculation, these nodes correspond to administrative regions according to the NUTS classification. The granularity of the calculations range between aggregated over multiple NUTS-0 nodes (countries) to NUTS-3 nodes (municipalities), depending on the research question. The temporal resolution can be adjusted as well with typical calculations performed using an hourly resolution. For computationally intensive calculations, the temporal resolution may be adjusted to a multi-hourly time step.

ESTRAM uses a linear programming approach (LP) to find a cost-optimal solution to both overnight and transition pathways calculations. Overnight scenarios are often referred to as 'greenfield scenarios' as they are not based on the current state of the energy system, but show a configuration optimal if the whole energy were to be built from scratch. On the other hand, transition pathway studies evolve from a given state of the energy system and show it changes in evolutionary steps. In both options, ESTRAM optimises both the dimensioning and dispatch of all system components while minimising the annualised total system costs. To this end, each component is associated with techno-economic assumptions. These assumption cover capital expenditures (CAPEX), operational and maintenance expenditures (OPEX), component lifetime and technical data such as energy conversion efficiency in case of converters or maximum energy-to-power ratio in case of battery storages. Capital expenditures are specific to the dimensioning of each component, that means they depend on the installed power and energy, respectively. Total system costs are annualised using weighted average cost of capital (WACC). To optimise the European energy system (Section 5.1), we use a WACC of 5.3%. For country-specific WACC values in the non-European island calculations (Section 5.2.), we use a database with global investment risk assessments by Damodaran [61] and a calculation methodology used in Terrapon-Pfaff et al. [59] and Horst et al. [60]. The results of this methodology are shown in Figure C.6. The values shown apply to less mature technologies such as electrolysers, H2 storage and liquefaction plants. For more mature technologies such as solar power plants or wind turbines we use a WACC value decreased by 1% abs. This distinction also applies to the WACC used for the European energy system model.

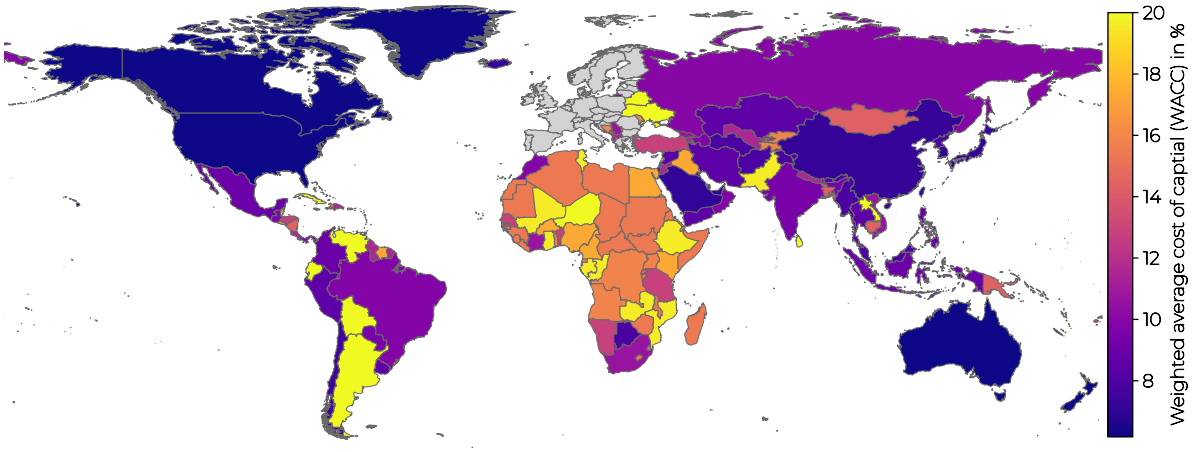

Figure C.6: Country-specific weighted average costs of capital used to annualise the total system costs.

For all ESTRAM scenarios, the LP is constrained by a set of rules that have to be fulfilled at all times. Most importantly, the power flows between components at each time step must be balanced for all carriers. There are numerous carriers modelled in ESTRAM, that are needed to describe a fully interconnected energy system. Further examples for carriers are heat, gas, biomass, H_2 and oil. An exemplary overview of a climate neutral energy system is shown in Figure C.7. As can be seen in Figure C.7, components are divided into sources, storages, converters and consumers. Sources contribute with a positive term to the balance equation for one carrier. One example for sources are renewable energy sources that provide electricity for the energy system. Another example are imports of carriers like H_2 and biomass from outside the scope of the energy system model. Converter as well as storages contribute both with a negative and a positive term to the balance equation. In the first case one carrier is converted into another carrier, typically applying conversion losses. In the latter case, excess energy for a specific carrier is stored for later use. Consumer contribute with a negative term to the balance equation. Consumer provide the useful energy for a specific application. Typically, this can be achieved in various ways, as the useful energy may be provided by different carriers. One example is the aviation sector, where the energy needed by the airplane can be supplied using either synthetic aviation fuels or H_2.

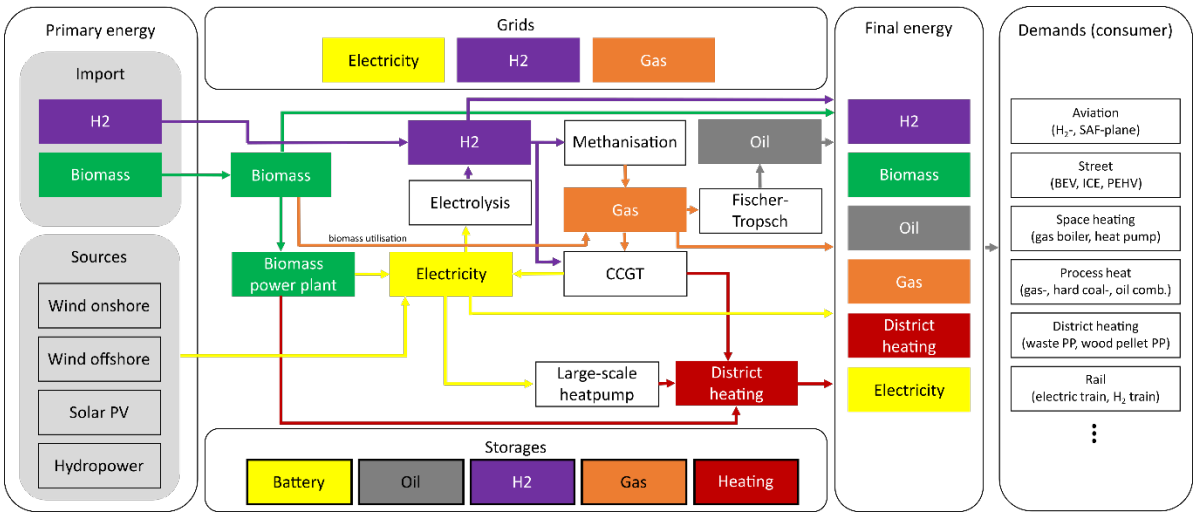

Figure C.7: Exemplary depiction of a climate neural energy system showing a single node in ESTRAM. Please note that this is a simplified illustration not showing all ESTRAM components and demands.

In particular for transition pathway studies, detailed knowledge on the current state of the energy system is essential. To this end, ESTRAM contains a database with current power plants, grid interconnections between nodes and demands. Based on various assumptions such as demographic evolution, renovation rates in the building stock and evolution of demands in sectors like aviation or information technology, the current demands are projected into the future. In the end, the power balance equation including the forecasted demands must hold for all timesteps within a year, for all steps of the transition pathway and all nodes. Figure C.8 shows the evolution of the total primary energy demand (TPED) aggregated over the entire European energy system. Please note that in the following, we show results from our reference scenario without an additional aviation demand (Section 5.1 and 5.3). The TPED is the result of our energy system optimisation, in which the present and forecasted demands must be met by the available energy carriers and technologies. As can be seen in Figure C.8, due to the CO_2 pathway, fossil fuels are gradually replaced by renewable energy sources. Please note that the share of nuclear power (uranium) is exogenously determined due to national decisions and thus not a result of our optimisation. Interestingly, the TPED decreases over the course of the energy transition. This is because of efficiency gains due to the electrification of most sectors in the energy system.

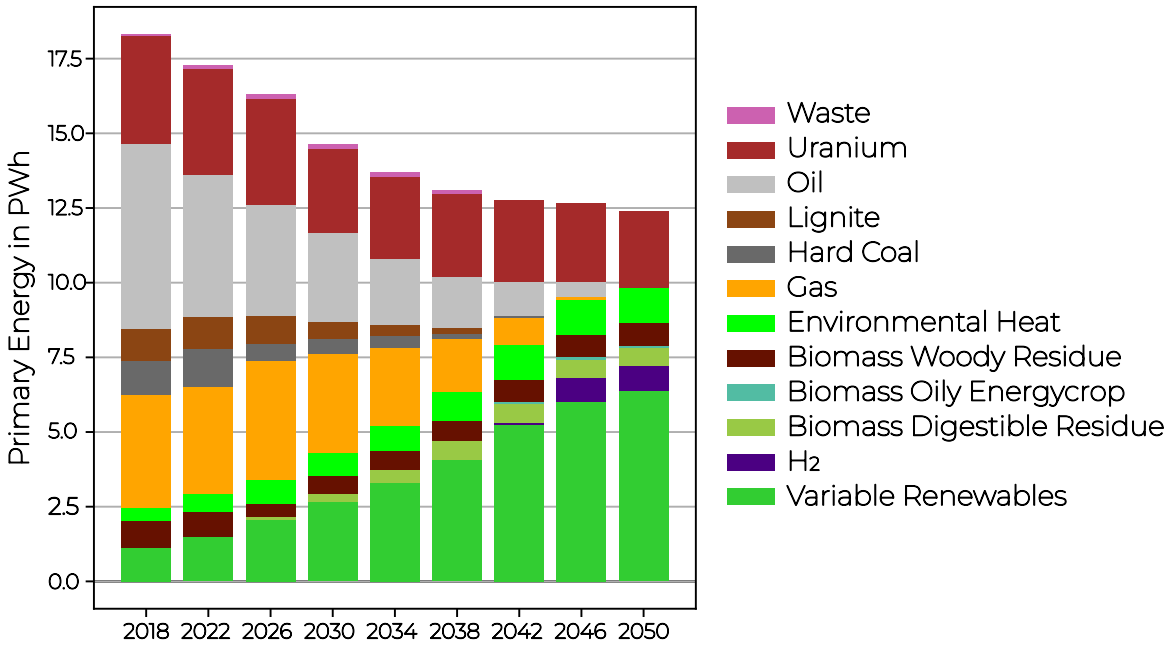

Figure C.8: Total primary energy demand (TPED) in Europe over the course of the energy system transition. The TPED decreases because of efficiency gains due to the electrification of most sectors in the energy system.

In addition to that, the database also contains information on weather data and potentials for renewable energy sources. The electricity generated by renewable energy sources depend on insolation in the case of solar PV and windspeed in the case of wind power. Thus, both sources are highly variable which poses challenges for their integration into the energy system. To account for this, ESTRAM uses a global weather database based on ERA5 reanalysis weather data provided by the Copernicus Climate Change Service. We calculate the spatially and temporally resolved capacity factor for both solar PV and wind power. Capacity factors are the ratio of generated electrical power to installed power at each time step. Therefore, capacity factors are useful for calculating the total electrical power of an installation

based on its installed power capacity. The installed power capacity is restricted by the available potentials. The expansion of renewable energy sources is often associated with land consumption and thus competes with other forms of land use. Therefore, we estimate the maximum installable power capacity for each technology based on a hybrid approach using geospatial analysis of land use data and applying expert opinions on actually usable fractions of the technical potential.

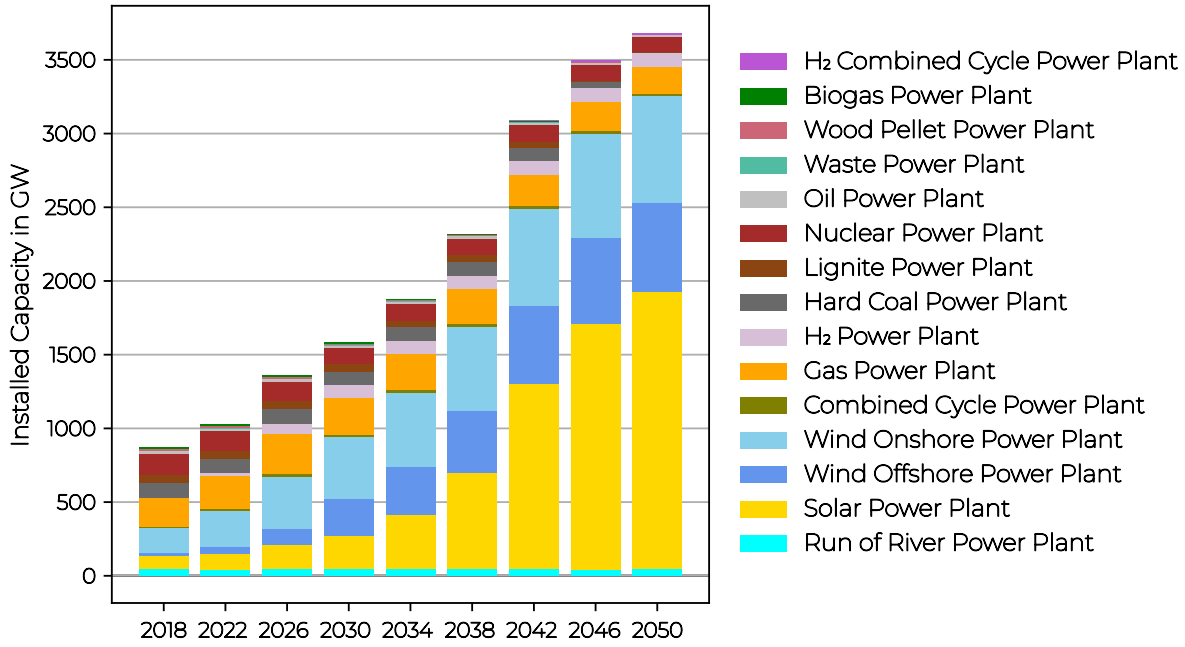

Figure C.9: Installed capacity of power plants in the European energy system according to our optimisation. By 2050, solar PV and wind power will account for 88% of total installed capacity.

Figure C.9 displays the evolution of installed power plant capacities across the European energy system. According to our calculation, the installed power plants in the future energy system will be mainly solar PV and wind power by 2050. Wind power comprises onshore and offshore installations. Interestingly, we find about 1,930 GW of installed solar PV capacity and 1,330 GW of wind power capacity by 2050 which requires a pronounced increase in the annual installation rates for both technologies. Please note that the values for the installed capacity are highly dependent on our cost assumptions for the import of green energy carriers from outside of Europe [125].

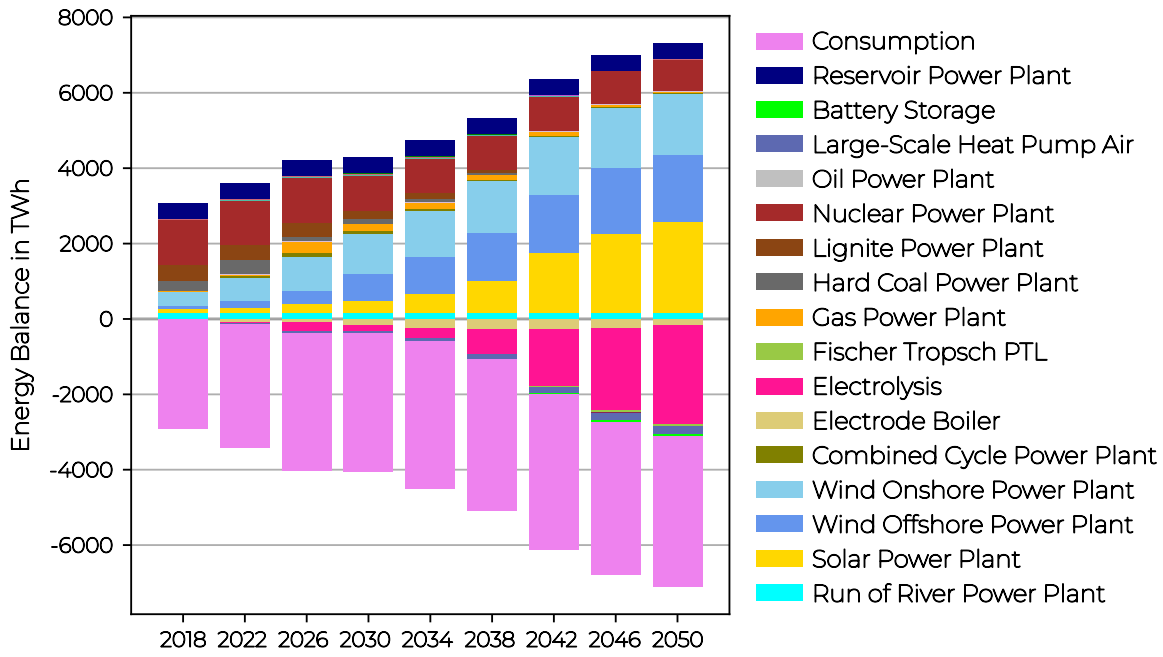

Figure C.10: Annual electricity balance of the European energy system.

Figure C.10 shows the annual electricity balance of the European energy system. The consumption bar contains all electricity demands by consumers, therefore demands for converters are shown separately. It can be clearly seen that there is a pronounced increase in electricity demand for electrolysis by 2050. In contrast, the electricity demand for consumers initially rises but then remains about the same towards the end of the transition path. A mathematical description of the ESTRAM framework can be found in the final report of the MET-project [242].

C.6 Methodology life cycle assessment

Energy data for electrolysis, liquefaction, and compression storage are sourced from project partners, ensuring accuracy and relevance. Transport methodologies involving pipelines, vessels, and trucks are meticulously designed based on extensive literature, providing a strong foundational understanding. Components are strategically assembled according to specific supply chain configurations to offer a tailored analysis of the environmental impacts, driving forward the pursuit of sustainable aviation fuels and reducing carbon footprints in global aviation.

The Life Cycle Assessment (LCA) was carried out in strict accordance with ISO 14040 and ISO 14044 standards to quantify the cradle-to-grave environmental impacts of H_2 production and distribution infrastructure. The study is structured around four sequential phases—goal and scope definition, life cycle inventory (LCI) compilation, life cycle impact assessment (LCIA), and interpretation—and adopts a functional unit of one kilogram of LH_2 ready for aircraft refueling. Although multiple impact categories exist within LCA methodology, this analysis concentrates exclusively on Global Warming Potential (GWP, expressed in $kgCO_2$-equivalents), since climate mitigation represents the primary decision-making criterion for aviation H_2 applications; other midpoint or endpoint indicators are omitted here.

To represent mid-century conditions, all foreground processes were parameterized for the year 2050 using the Shared Socioeconomic Pathway 2 (SSP2 "Middle of the Road," characterized by moderate mitigation and adaptation challenges). Background data were drawn from the Ecoinvent 3.9.1 database via the Activity Browser, and impacts were calculated with the ReCiPe 2016 (H) midpoint method v. 1.03. European-average projections from the Premise database under SSP2 ensure that energy mixes, material efficiencies, and technology maturities reflect a coherent mid-century scenario.

The modular LCA model architecture mirrors the HyNEAT project's baseline component designs, which were numbered up to represent commercially relevant scales.

Electrolyser systems were assessed at 5 MW and 100 MW capacities for both PEM and AWE technologies. For the evaluation conducted in this study, a 100 MW PEM electrolysis system was assumed as the reference scale for H_2 production. [255]

Liquefaction units were modelled at 5 tH_2/day and 100 tH_2/day throughputs. For the evaluation, a liquefaction facility with a capacity of 100 tons per day (100 tpd) was assumed for 2050 (see Chapter A).

It includes storage solutions involving GH_2 cavern storage and LH_2 storage. GH_2 storage utilizes underground caverns equipped with compressors to maintain appropriate pressure levels. Meanwhile, LH_2 storage features expansive 50,000m^3 tanks, allowing for large-scale storage of liquefied H_2.

The assessment of pipeline infrastructure encompasses both reused and newly constructed GH_2 pipelines. These pipelines are designed with strategically placed compressors every 125 km to maintain optimal pressure and flow efficiency. This approach not only extends the lifespan of existing infrastructure but also enhances the overall effectiveness of H_2 distribution. [256–258]

For H_2 transportation, the study includes the use of a 280,000 m^3 LH_2 vessel equipped with fuel cells, designed to navigate the logistical challenges of maritime transport. Additionally, it examines the use of 4.6-ton LH_2 trucks, which are integral to land-based H_2 distribution. These transport methods highlight the innovations

required for effective H_2 logistics, with information sourced from industry leaders such as Linde and detailed studies.

The refueling infrastructure consists of cryogenic pumps, which are essential for the efficient transfer of H_2 to aircraft. This infrastructure ensures the safe and effective delivery of H_2 fuel, supporting the broader goal of sustainable aviation.

Energy inputs for electrolysis, liquefaction, and compression were supplied by project partners; equipment lifetimes and operating hours were used to amortize construction burdens to the functional unit of 1 kgH_2.

Where LH_2 demand substantially exceeds current demonstration scales – such as at large airports – potential upscaling benefits (e.g. economies of scale in electrolyser and liquefier fabrication, longer-lived infrastructure, and optimized logistics) could yield additional GWP savings beyond those reported. These scaling effects are not explicitly modelled here.

Table C.10: Considered input data for the components in the target year 2050

Electricity	
Wind	ecoinvent: electricity production, wind, 1–3 MW turbine, offshore, DE
PV	ecoinvent: electricity production, photovoltaic, 570 kWp open ground installation, mulit-Si, ES
Hybrid	50% wind / 50% PV dataset
Electrolysis	
Construction	20 a, 100MW
Operation	45 kWh/kgH_2
GH_2 storage cavern	GH_2 compressor: 1.1 kWh/kgH_2
Liquefaction	
Construction	100 tpd, 20a, 8,000 h/a
Operation	6.1755 kWh/kgH_2
LH_2 storage tank	50,000 m^3
Refueling	0.04 $kWh/kgLH_2$
GH_2 pipeline	compressor a 125 km, new/old pipeline EHB
LH_2 vessel	280,000 m^3 (20,000 t) fuel cell
LH_2 truck	4.6 t (65 m^3) Linde truck, fuel cell

Table C.11: Considered H2 losses along the supply chain for the components

On site	
Electrolyser --> GH_2 storage	1%
GH_2 storage	0%
GH_2 --> liquefaction	0.25%
Liquefaction	0%
Liquefaction --> LH_2 storage airport	0.25%
LH_2 storage airport	0.048%
LH_2 storage airport --> refueling station	1%
Refueling station --> aircraft tank	1%
Total	3.548%
Off-site GH_2	
Electrolyser --> GH_2 storage	1%
GH_2 storage	0%
GH_2 storage --> pipeline	0.25%
Pipeline	0.25%
Pipeline --> liquefaction	0.25%
Liquefaction	0%
Liquefaction --> LH_2 storage airport	0.25%
LH_2 storage airport	0.048%
LH_2 storage airport --> refueling station	1%
Refueling station --> aircraft tank	1%
Total	4.048%

Table C.12: Considered leakages along the supply chain

Leakages		
LH_2 storage tank boil-off	0.00048	1/d
Liquefaction	0.005	1/kgLH_2
Pipeline	0.005	1/km
Fueling station	0.02	1/kgLH_2
GH_2 storage (GH_2 cavern)	0.01	1/kgH_2
LH_2 truck	0.005	1/d
Electrolyser	0.01	1/kgH_2

C.7 Financing strategies and model equations for the business model and policy support analysis

In this section, further results as well as the model equations and the optimisation problem of the analysis in Section 7 is provided. Figure C.11 shows the possible stakeholder constellations for LH_2 supply for airports. The numbers stand for the archetypical stakeholder constellations identified (1: Single-source supply chain, 2: Dyadic supply chain, 3: Supply chain network) and the different versions as for instance the water electrolysis could be owned and operated either by a H_2 actor or a renewable energy actor. In addition, the off-site case is shown where transport options are included which in this study is not directly included but seen as an external service.

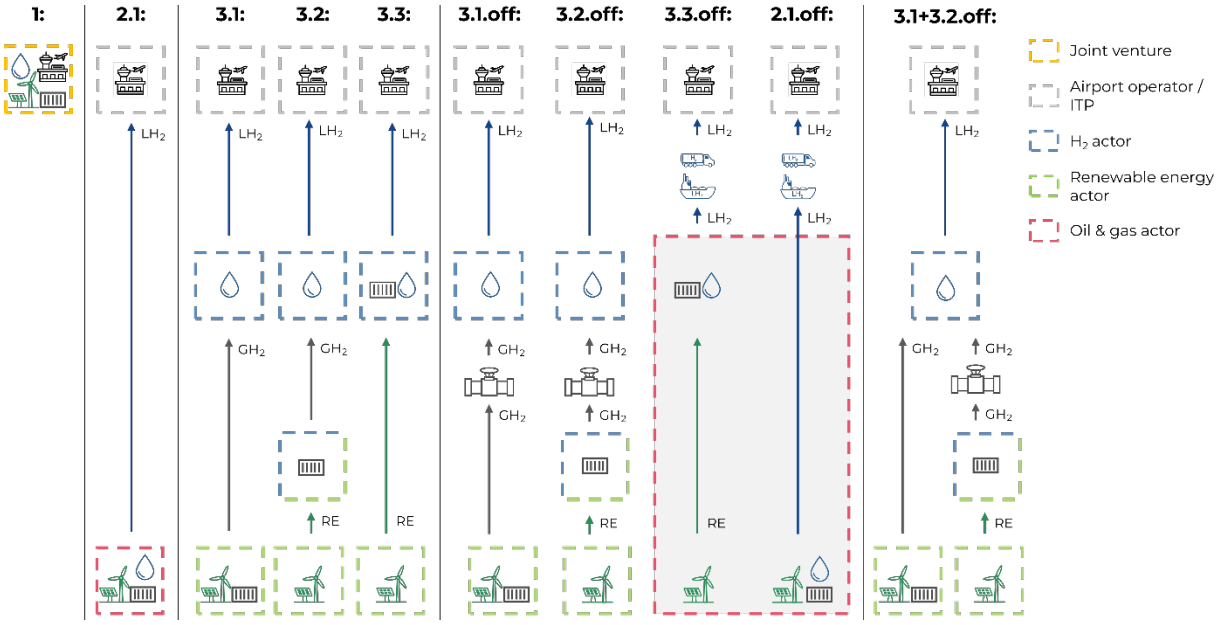

Figure C.11: Possible stakeholder constellations for the LH_2 supply for H_2-powered aviation

In the following, the financing options available for stakeholders included in the H_2 for aviation ecosystem are discussed. In Section C.7.2 further results of the study are shown, while Section C.7.3 presents the full model equations and the optimization problem. For more details refer to the full paper on this topic by Schenke et al. [259].

C.7.1 Financing strategies

The financial framework for LH_2 supply infrastructure is significantly shaped by the financing strategies available to different stakeholders, influencing the viability and structure of infrastructure projects. These financing options can be characterized by their features, typical areas of application, and the types of recipients they address. Based on insights from the financing of renewable energy and H_2 projects [16,67,260], multiple financing options are conceivable for LH_2 infrastructure.

Commercial loans provide debt financing from commercial banks, typically featuring fixed repayment terms and interest rates determined by credit risk assessments. These loans primarily finance capital expanses (CAPEX) for mature, low-risk infrastructure and are generally utilized by large energy companies, such as oil and gas suppliers, utilities, and infrastructure developers.

Government loans or grants represent another important financing opportunity. Loans under these schemes are repayable under favourable conditions, while grants constitute non-repayable public contributions. Such instruments are typically directed towards early-stage research and development, pilot projects, or infrastructure serving the public good, and are often accessed by research institutions, start-ups, small and medium-sized enterprises, and non-profit or community energy projects.

Conventional corporate bonds are debt securities issued by companies to raise capital, with repayments made over time and without a specific focus on sustainability criteria. They are commonly used to finance the large-scale deployment of commercially viable technologies, similar to commercial loans, and are typically issued by large corporations, including OEMs, energy firms, and multinational project developers engaged in major CAPEX programs.

Green bonds or loans specifically earmark funds for environmentally beneficial projects, requiring transparent reporting and clear use-of-proceeds documentation. These instruments support investments in infrastructure projects with clear climate benefits and are typically utilized by corporates with eligible green projects, municipalities, utilities, infrastructure operators, and financial special purpose vehicles established for managing green assets.

Private capital, in the form of equity or debt, is provided by private investors such as private equity firms and infrastructure funds seeking returns, often combined with active ownership approaches. This type of financing is frequently used for high-risk, high-return phases, including early-stage start-ups and innovative technology components, and typically involves venture capital for start-ups, private equity for growth-stage firms, and infrastructure funds for project financing.

Multilateral bank loans and grants (MDB), provided by institutions such as the European Investment Bank or the World Bank, offer financing under favourable terms and may include technical assistance or risk guarantees. These instruments often support large-scale, cross-border infrastructure projects or facilitate risk sharing in early-stage markets. They are typically accessed by national or regional governments, public-private consortia, utilities in emerging markets, and projects of strategic importance.

Public-private partnerships (PPPs) are also a viable financing mechanism, involving long-term contractual agreements between public authorities and private entities to finance, build, and operate infrastructure. Commonly applied in the transport and energy sectors, PPPs enable investment in end-to-end infrastructure, including operational expenditures, and can facilitate H_2 supply-as-a-service models. They are typically structured with infrastructure operators under concession or availability contracts and often involve private partners within joint public infrastructure delivery or utility-scale renewable energy consortia.

Table C.13 shows a semi-quantitative evaluation using an ordinal scale (1-5) based on literature-based criteria to investigate the risk for lenders and investors, the cost of capital and the stakeholder access.

Table C.13: Overview of the financing options for stakeholders of the H_2 aviation ecosystem and the involved risk for lenders or investors as well as the cost of capital and the accessibility of these financing options

Financing option	Risk for lenders / investors	Cost of capital[1]	Stakeholder access
Commercial loans	Moderate – depends on borrower's creditworthiness and project cash flow stability.	Moderate to high – interest rates reflect risk, market conditions, and collateral.	Accessible to: Large, financially strong entities such as airports, oil & gas companies, and major H_2/RES players. Limited for: Small service providers or new joint ventures.
Government loans or grants	Very low – repayment risk is minimal due to sovereign guarantee or grant nature.	Low to zero – grants are free capital; loans may have below-market rates.	Accessible to: Airports, RES developers, and H_2 players aligned with national strategies. Not accessible to: Purely private actors without policy relevance or strategic alignment.
Conventional corporate bonds	Moderate – unsecured; dependent on overall corporate solvency, not project-specific assets.	Moderate – typically lower than loans for investment-grade issuers, but higher if risk perceived.	Accessible to: Large corporations with strong credit ratings (e.g. oil & gas players, airport operators). Not accessible to: SMEs or project-specific entities without track record.
Green bonds or loans	Low to moderate – aligned with ESG criteria, but reliant on issuer creditworthiness.	Low – strong demand from ESG investors can reduce financing costs.	Accessible to: H_2 and RES companies with ESG-compliant structures and reporting capacity. Limited for: Traditional oil & gas firms or entities lacking green alignment.
Private capital	High – capital is fully at risk until project success; limited recourse and liquidity.	High – investors expect substantial returns, reflecting risk and opportunity cost.	Accessible to: Scalable, high-return projects (e.g. innovative H_2 providers, vertically integrated ventures). Not accessible to: Public entities or low-return infrastructure.
Multilateral bank loans and grants	Very low – MDB involvement typically includes guarantees or concessional lending structures, significantly reducing perceived credit risk.	Very low – subsidized interest rates or grants; MDBs also reduce project risk via guarantees.	Accessible to: Public stakeholders (e.g. airports), large PPPs, and infrastructure-focused consortia. Not accessible to: Small private firms or commercial-only entities.
Public-Private partnerships	Moderate – risk is shared and often mitigated by public guarantees, but still project-bound.	Moderate to high – depends on project structure; private capital is more expensive but partially de-risked by public involvement.	Accessible to: Airports, joint ventures, and service providers with the capacity to engage in long-term infrastructure contracts. Not accessible to: Isolated small actors.

[1] Cost of capital in this table is presented from the perspective of capital providers (lenders or investors), reflecting the risk-adjusted return they require. It may differ from the effective financing cost borne by stakeholders within the H_2 aviation ecosystem

C.7.2 Further results

Impact on LH_2 supply infrastructure

The different stakeholder constellations have varying financial criteria, influencing their WACC and, consequently, the design of the infrastructure ramp-up. Due to the mechanics of the discounted cash flow method, a lower WACC increases the relative weight of future cash flows, making earlier investments more economically favourable. Figure C.12 presents the component installations for the archetypal stakeholder constellations. For wind power, PV and electrolysis capacity, installations increase in line with growing demand, with only minor variations between stakeholder constellations (see Figure C.12a–c). In contrast, for storage systems and liquefaction plants, where economies of scale are relevant, the stakeholder constellations result in different installation patterns (see Figure C.12d-f). Here, a lower WACC combined with economies of scale encourages larger single-year investments in storages and LFP within the dyadic supply chain. Although these storages and LFP capacities are initially oversized for the following years, the cost savings achieved through economies of scale outweigh the disadvantages of temporary oversizing. For a detailed analysis of these effects, refer to Schenke et al. [39]. The business model therefore can influence the design of the infrastructure and subsequently the timing and scale of investments.

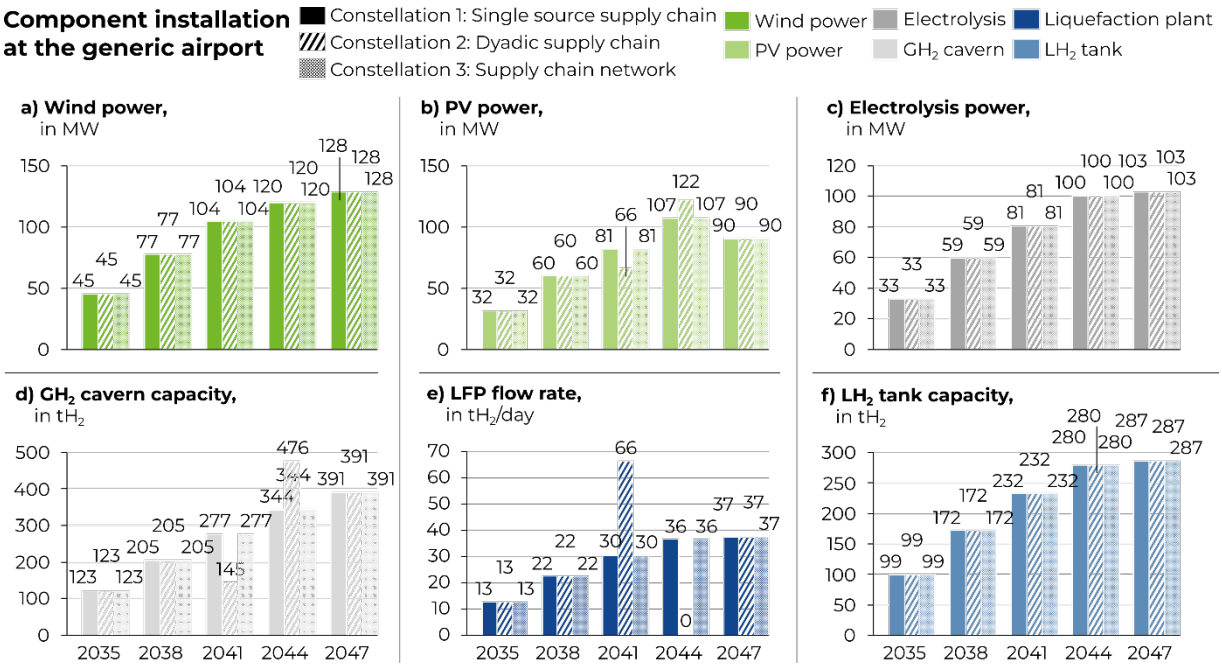

Figure C.12: Component installation for the single source supply chain (filled), dyadic supply chain (dashed) and supply chain network (points) for a) Wind power, b) PV power, c) Electrolysis power, d) GH_2 cavern capacity, e) Liquefaction plant, f) LH_2 tank capacity

C.7.3 Model equations and optimisation problem

In contrast to previous models used to evaluate LH_2 supply infrastructure for aviation, this study applies a cash flow-based method rather than the annuity approach. While the annuity approach is well suited for determining supply costs, it considers only constant repayments, which do not reflect the real dynamics of investment and capital recovery. Consequently, the resulting infrastructure

designs from both approaches are only partially comparable and do not add value for the objectives of this study.

The optimization model employed here builds on the bi-level optimization framework developed by Schenke et al. [39]. The objective function, shown in Equation 1, minimizes the net present value of the system costs over the analysis period. At the top level, the model optimizes the design of LH_2 supply components and therefore the capital expenditures $C_{\mathrm{CAPEX},t}$ in every year t, while at the bottom level, a linear dispatch optimization is conducted for each analyzed year to verify the feasibility of the transition pathway and to determine operational expenditures (OPEX) $C_{\mathrm{OPEX},t}$. In this model, two types of OPEX are considered, fixed OPEX, which represent the operation and maintenance costs as a share of the components CAPEX and variable OPEX like water or transport costs.

$$\min \sum_t^{\mathrm{T}} \frac{C_{\mathrm{CAPEX},t}+C_{\mathrm{OPEX},t}-C_{\mathrm{SALVAGE},t=\mathrm{T}}}{(1+i)^t} \qquad \forall\, t \in T \quad \text{(C.27)}$$

where the salvage value $C_{\mathrm{SALVAGE},t=T}$ at the end of the period T is calculated with the lifetime L_n of a component n as:

$$C_{\mathrm{SALVAGE},t=T} = \sum_n C_{\mathrm{CAPEX},n,t=t_{inv}} \cdot \frac{L_n-(T-t_{inv})}{L_n} \qquad \text{(C.28)}$$

Given the three-year step size applied in this study, five investment periods are considered. This selection is discussed in detail in our previous study [39]. The result of the model is the cost-optimal infrastructure design across five investment years, which are subsequently analysed as individual project segments to determine the resulting LH_2 price. The study assumes staggered investments with payback periods that vary according to the stakeholder involved. As highlighted in previous studies, off-take agreements can serve as effective mechanisms to mitigate high initial costs and ensure supply security [39], therefore, a constant LH_2 price is assumed for each investment period within this analysis.

As shown in Equation (C.29, the objective of the subsequent step is to minimize the resulting LH_2 price p_{H2} for each investment period i:

$$\min p_{\mathrm{H2},i} \qquad \forall\, i \in I \quad \text{(C.29)}$$

To ensure financial viability, each investment must be recovered within the defined payback period while achieving the required share for economic profit f_{EP}, enforced through the constraint expressed in Equation (C.30:

$$\sum_{t=t_i}^{T_i=t_i+15} \frac{m_{\mathrm{H2demand},i,t} \cdot p_{\mathrm{H2},i}-C_{\mathrm{OPEX},t}-C_{\mathrm{CAPEX},i}}{(1+i)^t} \geq C_{\mathrm{CAPEX},i} \cdot f_{\mathrm{EP}} \qquad \forall\, i \in I, t \in t_i \quad \text{(C.30)}$$

Due to differing investment and payback periods across stakeholder types, there are periods in which certain assets have already been depreciated and the required economic profit has been achieved. To reflect the pricing of these fully amortised components, this study employs the opportunity cost of capital, as shown in Equations (C.31 and (C.32. The opportunity cost of capital represents the foregone return from using a fully depreciated asset for LH_2 supply instead of deploying it in an alternative investment and are calculated with the residual value W_{residual} of an asset and the opportunity factor r_{opp}, for which in this study the WACC are assumed.

$$\sum_{t=T_{\mathrm{ROIC}}+1}^{T_i} \frac{m_{\mathrm{H2demand},i,t} \cdot p_{\mathrm{H2},i} - C_{\mathrm{OPEX},t} - W_{\mathrm{residual},t} \cdot r_{\mathrm{opp}}}{(1+i)^t} \geq 0 \quad \text{(C.31)}$$

where the residual value of the asset is calculated as:

$$W_{\mathrm{residual},t} = \sum_n C_{\mathrm{CAPEX},n,t=t_{inv}} \cdot \frac{L_n - (t - t_{inv})}{L_n} \quad \text{(C.32)}$$

All cost assumptions utilised in the model are based on Schenke et al. [39], ensuring consistency with prior infrastructure cost evaluations.

Economic equations:

$$C_{\mathrm{CAPEX},t} = \sum_n C_{\mathrm{CAPEX,direct},n,t}(x_{n,t}) \cdot f_{\mathrm{inst},n,t} \cdot f_{\mathrm{ind,n},t} \cdot \frac{1}{f_{\mathrm{avail},n,t}} \quad \forall\, n,t \quad \text{(C.33)}$$

$$C_{\mathrm{OPEX},t} = \sum_n C_{\mathrm{CAPEX,direct},n,t}(x_{n,t}) \cdot c_{\mathrm{OM},n,t} + C_{\mathrm{H2O},n,t} + C_{\mathrm{refri},n,t} + C_{\mathrm{transport},n,t} \quad \forall\, n,t \quad \text{(C.34)}$$

Balancing equations:

$$P_{\mathrm{WON},t,k,g} + P_{\mathrm{PV},t,k,g} = P_{\mathrm{GH2Stor,COMP},t,k,g} + P_{\mathrm{ELY},t,k,g} + P_{\mathrm{LFP},t,k,g} + P_{\mathrm{cryopump},t,k,g} \quad \forall\, t,k,g \quad \text{(C.35)}$$

$$\dot{m}_{\mathrm{LFP,in},t,k,g} = \dot{m}_{\mathrm{ELY},t,k,g} - \dot{m}_{\mathrm{GH2Stor,char},t,k,g} + \dot{m}_{\mathrm{GH2Stor,dis},t,k,g} \quad \forall\, t,k,g \quad \text{(C.36)}$$

$$\dot{m}_{\mathrm{LH2demand},t,k,g} = \dot{m}_{\mathrm{LFP,out},t,k,g} - \dot{m}_{\mathrm{LH2T,char},t,k,g} + \dot{m}_{\mathrm{LH2T,dis},t,k,g} \quad \forall\, t,k,g \quad \text{(C.37)}$$

Renewable energy constraints:

$$P_{\mathrm{WON},k,g} \leq P_{\mathrm{WIND,max}} \cdot f_{\mathrm{WON,cap},k,g} \quad \forall\, k,g \quad \text{(C.38)}$$

$$P_{\mathrm{PV},k,g} \leq P_{\mathrm{PV,max}} \cdot f_{\mathrm{PV,cap},k,g} \quad \forall\, k,g \quad \text{(C.39)}$$

Electrolysis constraints:

$$P_{\mathrm{ELY},k,g} \leq \dot{m}_{\mathrm{ELY,out},k,g} \cdot e_{\mathrm{ELY,max}} \quad \forall\, k,g \quad \text{(C.40)}$$

$$P_{\mathrm{ELY},k,g} \leq P_{\mathrm{ELY,max}} \quad \forall\, k,g \quad \text{(C.41)}$$

$$\dot{m}_{\mathrm{ELY},k,g} \leq a_{\mathrm{lin},j} \cdot P_{\mathrm{ELY},k,g} - b_{\mathrm{lin},j} \quad \forall\, k,g,j \quad \text{(C.42)}$$

$$a_{\mathrm{lin},j} = \frac{j+1}{\epsilon_{ELY,j+1}} - \frac{j}{\epsilon_{ELY,j}} \quad \forall\, j \quad \text{(C.43)}$$

$$b_{\mathrm{lin},j} = \frac{\frac{j}{J-1} \cdot P_{\mathrm{ELY,max}}}{\epsilon_{ELY,j}} - a_{\mathrm{lin},j} \cdot \frac{j}{J-1} \cdot P_{\mathrm{ELY,max}} \quad \forall\, j \quad \text{(C.44)}$$

GH_2 compressor constraints:

$$P_{\mathrm{GH2Stor,COMP},k,g} = \frac{1}{\eta_{\mathrm{isen}} \cdot \eta_{\mathrm{el}} \cdot \eta_{\mathrm{mech}}} \cdot e_{\mathrm{COMP}} \cdot \dot{m}_{\mathrm{GH2Stor,COMP,in},k,g} \quad \forall\, k,g \quad \text{(C.45)}$$

$$P_{\mathrm{GH2Stor,COMP},k,g} \leq P_{\mathrm{GH2Stor,COMP,max}} \quad \forall\, k,g \quad \text{(C.46)}$$

$$D_{\mathrm{pipe}} = 2 \cdot \sqrt{\frac{\dot{m}_{\mathrm{GH2P,max}}}{\pi \cdot \rho_{\mathrm{m}} \cdot \dot{v}_{\mathrm{pipe,m}}}} \quad \text{(C.47)}$$

$$\rho_{\mathrm{m}}(p_m) = -5 \cdot 10^{-5} \cdot p_{\mathrm{m}}^2 + 0.0841 \cdot p_{\mathrm{m}} + 0.0007 \quad \text{(C.48)}$$

$$p_m = \frac{2}{3} \cdot \frac{p_{\mathrm{pipe},1}^3 - p_{\mathrm{pipe},2}^3}{p_{\mathrm{pipe},1}^2 - p_{\mathrm{pipe},2}^2} \quad \text{(C.49)}$$

Storage constraints (for GH_2 cavern and LH_2 tank):

$$m^{\text{inter}}_{\text{stor},k=1} = 0.5 \cdot m_{\text{stor,max}} \quad \text{(C.50)}$$

$$m^{\text{inter}}_{\text{stor},k=1} = m^{\text{inter}}_{\text{stor},t_{\text{ges}}} \quad \text{(C.51)}$$

$$m^{\text{intra}}_{\text{stor},k,g=1} = 0 \qquad \forall\, k \quad \text{(C.52)}$$

$$m^{\text{inter}}_{\text{stor},k} \leq m_{\text{stor,max}} \qquad \forall\, k \quad \text{(C.53)}$$

$$m^{\text{intra}}_{\text{stor},t} \leq m_{\text{stor,max}} \qquad \forall\, t \quad \text{(C.54)}$$

$$\dot{m}_{\text{stor,char},t} \leq \dot{m}_{\text{stor,max}} \qquad \forall\, t \quad \text{(C.55)}$$

$$\dot{m}_{\text{stor,dis},t} \leq \dot{m}_{\text{stor,max}} \qquad \forall\, t \quad \text{(C.56)}$$

$$m^{\text{intra}}_{\text{stor},k,g+1} = m^{\text{intra}}_{\text{stor},k,g} \cdot \left(1 - f_{\text{stor,loss}} \cdot \Delta t\right) + \Delta t \cdot (\dot{m}_{\text{stor,char},k,g} - \dot{m}_{\text{stor,dis},k,g}) \qquad \forall\, k,g \quad \text{(C.57)}$$

$$m^{\text{inter}}_{\text{stor},i+1} = m^{\text{inter}}_{\text{stor},i} + m^{\text{intra}}_{\text{stor},k=f(i),N_g+1} \qquad \forall\, i \quad \text{(C.58)}$$

$$m^{\text{intra}}_{\text{stor},k=f(i)} + m^{\text{inter}}_{\text{stor},i} \leq m_{\text{stor,max}} \qquad \forall\, i,g \quad \text{(C.59)}$$

Liquefaction plant constraints:

$$P_{\text{LFP},k,g} = e_{\text{LFP}} \cdot \dot{m}_{\text{LFP,in},k,g} \qquad \forall\, k,g \quad \text{(C.60)}$$

$$P_{\text{LFP},k,g} \leq P_{\text{LFP,max}} \qquad \forall\, k,g \quad \text{(C.61)}$$

Cryo-pump constraints:

$$P_{\text{LH2T,Cryopump},k,g} = e_{\text{Cryopump}} \cdot \dot{m}_{\text{cryopump,in},k,g} \qquad \forall\, k,g \quad \text{(C.62)}$$

Table C.14 shows the equation variables and their definition. For more detailed description of the dispatch model refer to Schenke et al. [63]. The non-linear electrolysis is linearized with the Equations (C.42–(C.44 a detailed description can be found in Brandt et al. [261].

Table C.14: Dispatch optimization variables and corresponding definition

Variable	Definition
$C_{\text{CAPEX,direct}}$	Direct CAPEX
f_{inst}	Installation factor
f_{ind}	Indirect cost factor
f_{avail}	Availability factor
c_{OM}	Operation and maintenance factor
C_{H2O}	Water costs
C_{refri}	Refrigerant costs
$C_{\text{transport}}$	Transport costs
P_{WON}	On-shore wind power

$f_{\mathrm{WON,cap}}$	On-shore wind capacity factor
P_{PV}	PV power
$f_{\mathrm{PV,cap}}$	PV capacity factor
P_{ELY}	Electrolysis power
$\dot{m}_{\mathrm{ELY,out}}$	Electrolysis mass flow
e_{ELY}	Electrolysis specific energy demand
$P_{\mathrm{GH2Stor,COMP}}$	Compressor electric power
η_{isen}	Compressor isentropic efficiency
η_{el}	Compressor electric efficiency
η_{mech}	Compressor motor efficiency
e_{COMP}	Compressor specific energy demand
$\dot{m}_{\mathrm{GH2Stor,COMP,in}}$	Compressor mass flow
$\dot{m}_{\mathrm{GH2P}}$	GH_2 pipeline mass flow
D_{pipe}	GH_2 pipeline diameter
ρ_{m}	Mean density of H_2
$\dot{v}_{\mathrm{pipe,m}}$	Mean flow speed
p_{m}	Mean pressure
p_{pipe}	GH_2 pipeline pressure
m_{stor}	Storage capacity
$m_{\mathrm{stor}}^{\mathrm{inter}}$	Storage capacity within a typical day
$m_{\mathrm{stor}}^{\mathrm{intra}}$	Storage capacity between typical days
$\dot{m}_{\mathrm{stor,char}}$	Storage charging mass flow
$\dot{m}_{\mathrm{stor,dis}}$	Storage discharging mass flow
$f_{\mathrm{stor,loss}}$	Storage self-discharge losses (boil-off for LH_2 tanks)
P_{LFP}	Liquefaction plant power
$\dot{m}_{\mathrm{LFP,in}}$	Liquefaction plant mass flow
e_{LFP}	Liquefaction plant specific energy demand
P_{Cryopump}	Cryo-pump power
$\dot{m}_{\mathrm{cryopump,in}}$	Cryo-pump mass flow
e_{Cryopump}	Cryo-pump specific energy demand

Table C.15 shows the stakeholders financial criteria assumed in this this study.

Table C.15: Stakeholders financial criteria assumed for the analysis of stakeholder constellations

Stakeholder	**WACC[1]**	**ROIC**	**Payback period**
Constellation 1: Single source supply chain			
Joint venture	10%	11%	15 years
Constellation 2: Dyadic source supply chain			
Into plane service provider	10%	14%	5 years
Oil & Gas actor	7%	13%	15 years
Constellation 2: Supply chain network			
Into plane service provider	10%	14%	5 years
H_2 actor	9%	10%	15 years
Renewable energy actor	6%	7%	10 years

[1] To reflect the larger risk in H_2 business plans the WACC is increased by 2% for all stakeholders except the renewable energy actors [33]

C.8 Methodology of the macroeconomic impact analysis

In this section, the methodology for the macroeconomic analysis presented in Chapter 8 is discussed.

C.8.1 System of National Accounts and Social Accounting Matrix

The System of National Accounts (SNA) is a sequence of statistical tables that represent the circular monetary flow of a national economy. The classification of industries, goods and services, institutional sectors, and capital and financial accounts follows an internationally agreed standard [262]. Countries have committed to making the processed data available to the United Nations Statistics Division. Generally, data relate to the economy over the course of a single year. Industries are defined in the same way as in the International Standard Industrial Classification (ISIC) [53], products are classified according to the Central Product Classification (CPC) [263]. The institutional sectors typically include non-financial corporations, financial corporations, government, private households, non-profit organizations, and the rest of the world. Depending on the focus of the analysis, institutional sectors can be further disaggregated, and products and industries can be represented at various aggregation levels.

From the sequence of SNA tables, meaningful macroeconomic indicators can be derived, starting with the domestic product, and followed by the balance of primary income (national income), disposable income, savings, change in net worth, and net lending/borrowing. Whether the balancing figures are net or gross depends on how the consumption of fixed capital is recorded. Trade with the rest of the world generates a sequence of external balances, namely the balance of goods and services, the primary and secondary income balance summing up to the current accounting balance, the capital balance, and finally the financial balance, which corresponds to the national indicator with an opposite sign.

The Social Accounting Matrix (SAM) is the representation of SNA statistics in a matrix based on the principle of double-entry bookkeeping. Figure C.13 shows a consolidated SAM with subsequent macroeconomic indicators as balancing items. The columns of the matrix show the expenditures (use of resources) and the rows show the revenues (generation of resources) of specific sectors. Expenditures must equal revenues, so that the sum of a column in the matrix is equal to the sum of the corresponding row. In its consolidated format, the standard SAM includes accounts for goods & services, production, income generation, primary and secondary distribution of income, use of income, saving, investment, and the exchange with the rest of the world. The diagonal sub-matrices show the redistribution of income and capital among the national institutional sectors.

The matrix provides an initial overview of a country's economic situation: Disposable income, for example, indicates the extent to which the income of institutional sectors is used for final consumption and savings, while the capital account provides information on the financing of investments by national institutional sectors and the extent to which a country is dependent on foreign capital markets as a net lender or net borrower of capital. The matrix format is flexible and allows for cross-classification of sub-matrices. The cross-classification of industries and value-added categories, for example, shows how different industries contribute to the compensation of employees, payment of production tax, and the distribution of operating surplus to different institutional sectors. This cross-classification facilitates the elaboration of the linkages between supply and use tables and institutional sector accounts [262].

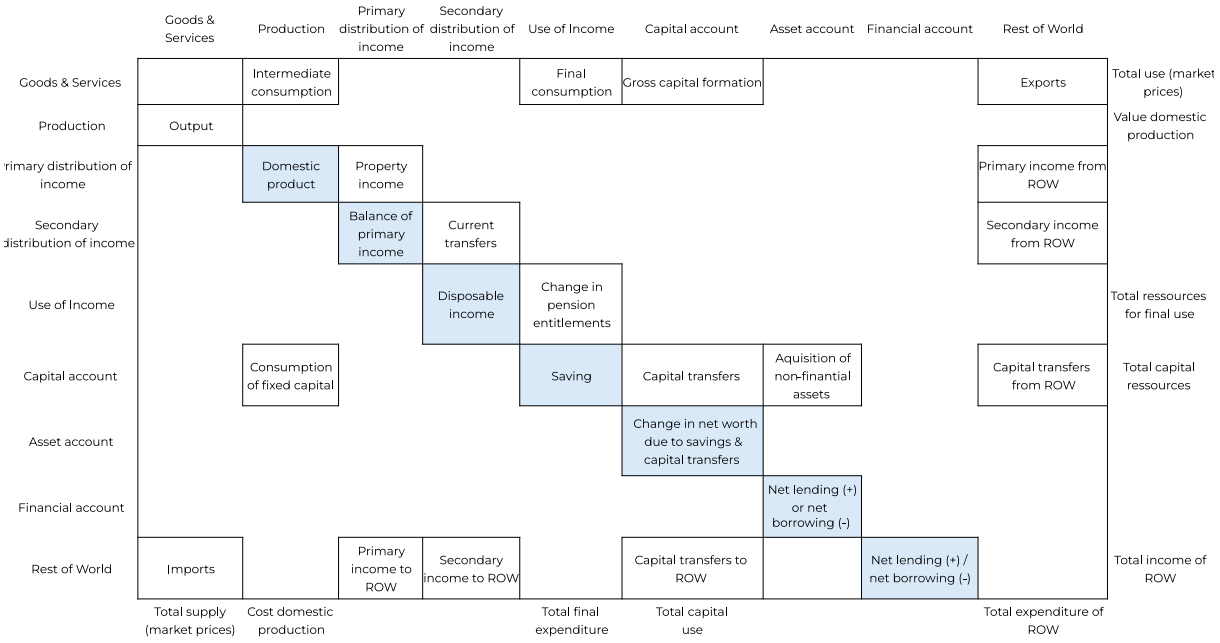

Figure C.13: Schematic and consolidated social accounting matrix. The blue cells show macroeconomic indicators that can be retrieved from the matrix.

The monetary SAM can be extended by physical data, which allows for the allocation of emissions and the use of natural resources and energy to individual industries and institutional sectors [264]. The SNA's satellite systems focus on various topics that are not covered by the standard system, such as water, biodiversity, energy, material flows, and land, and they highlight the connections between these topics and the economic system [265].

Due to the flexible matrix configuration of the SNA data, the SAM serves as a data framework for linear and non-linear models. In this study, a linear SAM-based multiplier model is applied that analyses the effects of exogenous shocks on the economy, as described in the subsequent sections.

C.8.2 Multiplier and linkage analysis

The origin of the multiplier model lies in the traditional input-output (IO) analysis [266]. In this approach, the economy is depicted as a linear system of equations with interdependencies among different suppliers and demanders:

$$\begin{pmatrix} x_{11} + & \cdots & +x_{1n} + Y_1 = X_1 \\ \vdots & \ddots & \vdots \\ x_{n1} + & \cdots & +x_{nn} + Y_n = X_n \end{pmatrix} \tag{C.63}$$

The rows indicate that the total sectoral output X_i of each industry i must equal the sum of intermediate demand from other sectors j and the aggregated final demand Y_i. Analogously, the columns imply the intermediate inputs needed to produce each industry's output. This relationship can be rewritten as:

$$x_i = \sum_j^n a_{i,j} * x_j + y_i \tag{C.64}$$

describing the intermediate demand from other industries j by their respective output level x_j and the technical input coefficient $a_{i,j}$. Using the technical

coefficient matrix A and the identity matrix I, the impact on industrial output Δx as a result of final demand change Δy can be derived as

$$\Delta x = (I - A)^{-1} \Delta y \tag{C.65}$$

The direct multipliers contain the initial demand stimulus ($I * \Delta Y$) and the first-round effects ($A * \Delta Y$). Indirect effects reflect the inter-industrial dependencies as further-round production effects [$(A^2 + A^3 + \cdots + A^n) * \Delta Y$] [267].

As the traditional IO model is limited to inter-industrial dependencies, it neglects the consumption-induced effects resulting from income generation. Next to intermediate inputs, primary production factors, including labour, capital, and taxes, contribute to the total production output. These factors generate income for households which is partially used for consumption and thus, triggers further economic activities [46]. Considering these effects leads to an extension of the technical coefficient matrix A to a general coefficient matrix Z with additional feedback loops:

$$Z = \begin{pmatrix} a_{11} + b_1 * c_1 & \cdots & a_{1n} + b_1 * c_n \\ \vdots & \ddots & \vdots \\ a_{n1} + b_n * c_1 & \cdots & a_{nn} + b_n * c_n \end{pmatrix} \tag{C.66}$$

Within this adjusted system, the technical coefficients $a_{i,j}$ are complemented by household income shares from primary production factors b_i and marginal consumption propensities c_j that represent the consumption preferences of households. The adjusted multiplier effect can be derived as

$$\Delta X = (I - Z)^{-1} \Delta Y \tag{C.67}$$

The flows of income, including generation, distribution and use, are displayed within the SAM and thus, the SAM-based multiplier model can account for these consumption-induced effects [268,269]. Typically, households are endogenous in SAM-based multiplier models, while remaining final demand groups (governmental expenditures, investments, exports) appear exogenous. To reflect the income distribution process more precisely, enterprises and tax accounts are part of the endogenous matrix in this study.

The SAM displays only monetary transactions. However, the multiplier model also allows for quantifying the impact of exogenous stimuli on physical indicators [46,47]. This study evaluates the impact on employment as physical indicator. For this purpose, employment coefficients γ are calculated as a ratio of employment demand q per monetary production output x:

$$\gamma_i = \frac{q_i}{x_i} \tag{C.68}$$

Based on these coefficients, the resulting total impact on employment can be calculated as

$$\Delta q = diag(\gamma_j)(I - Z)^{-1} \Delta y \tag{C.69}$$

In addition to deriving multiplier effects, the macroeconomic assessment uses a linkage analysis to compare the macroeconomic relevance of aviation-related industries and other potential H2-demanding sectors in the EU28. Linkages build on the initial IO approach and characterize the interconnectedness of an industry within the domestic economic system [153]. Backward linkages reflect the integration of a sector on the upstream side, while forward linkages represent the

downstream perspective, indicating how important an industry is as a supplier for other sectors. Normalized backward linkages can be obtained from the entries $l_{i,j}$, derived from the Leontief inverse $(I - A)^{-1}$ for IO-based linkages or from $(I - Z)^{-1}$ for SAM-based linkages:

$$BL_j = \frac{\frac{1}{n}\sum_i l_{i,j}}{\frac{1}{n^2}\sum_{i,j} l_{i,j}} \tag{C.70}$$

Because forward linkages reflect how a sector's output supports other industries, they are subject to theoretical controversies in the context of the demand-driven Leontief model. It is often argued that forward linkages are better captured by the Ghosh model [153]. In contrast to the approach described above, the Ghosh model is supply-driven, meaning that it looks at how changes in the supply or primary inputs of one sector spread forward through the economy to affect the outputs of other sectors [270]. Therefore, we calculate the normalized forward linkages by using the entries of the Ghosh inverse $g_{i,j}$ as follows:

$$FL_i = \frac{\frac{1}{n}\sum_j g_{i,j}}{\frac{1}{n^2}\sum_{i,j} g_{i,j}} \tag{C.71}$$

Based on the normalized linkages, industries can be classified according to their dependence on the remaining economy, which represents their importance vice versa. The categorization of industries is oriented to four quadrants, which are shown in Figure C.14.

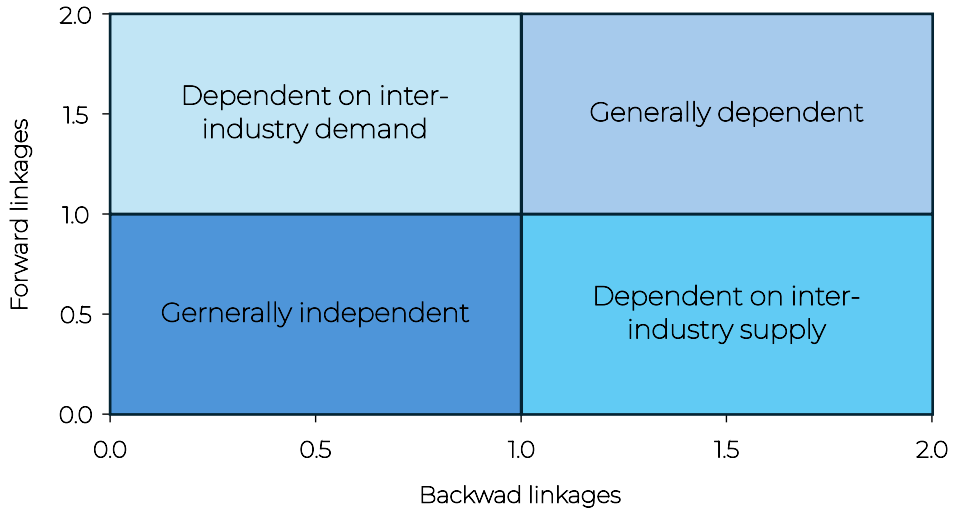

Figure C.14: Classification of industries based on the linkage analysis [12].

These theoretical relationships serve as methodological foundation for the assessment conducted in this study. The exogenous stimulus simulated is the introduction of novel LH_2 industries which trigger a cascade of feedback loops within the economy. Subsequent analyses examine the scale-up of an aggregated LH_2 infrastructure in detail by integrating the novel activities into the SAM framework. This procedure is further described in the following section.

C.8.3 Integration of novel liquid hydrogen industries

Based on the method described before, it is possible to investigate the impact of investments or production increases in specific sectors on the broader economy. This requires, however, that the respective sector is empirically covered within the SAM. Novel industries do often not exist as part of the SAM and have to be treated in an alternative way [43,44,271]. For the integration of LH_2 into the SAM, we apply a comprehensive approach, consisting of five main steps, as displayed in Figure C.15.

Supply chain analysis

In a first step, the supply chain of LH_2 infrastructure is investigated [50,130]. All technologies required for the LH_2 supply network are identified, covering RES, conversion, storage, transport, and refuelling technologies. The technologies are presented in Section C.8.5. Based on the techno-economic modelling, the cost contribution of each technology to the total network costs is examined. Every technology is further analysed in the subsequent steps.

Phase-differentiated cost transformation

In the second step, each technology is considered separately. To capture the temporal dynamics of LH_2 network deployment, the techno-economic cost data are converted into three phases of economic activity: (i) key component manufacturing, (ii) installation & balance-of-plant (BoP) supply, and (iii) operation. The corresponding cost shares are determined for each technology and phase, based on the techno-economic categories CAPEX and OPEX. In addition, financing costs are extracted from the CAPEX as they do not translate into economic activity but reflect net operating surplus that the industry needs to generate. This step translates techno-economic cost data into a format suitable for SAM integration [41,272,273].

Component-level cost breakdown and mapping to SAM activities

The third step comprises the component-level cost breakdown of every phase in each LH_2 technology. Based on a comprehensive review of techno-economic literature, the activity phases are broken into cost components as detailed as possible. Further information is provided in Section C.8.5. Subsequently, the cost parts are allocated to existing SAM activities [50,52,272,274]. For this mapping process, ISIC is used [53]. The cost share of each component determines its mapped activity's weight in the synthetic industry composition, which is described in the next step.

Construction of aggregated synthetic industries

Based on the mapped cost structures of each technologies' activity phases and the cost contribution of each technology in the overall LH_2 supply costs, synthetic LH_2 industries are constructed as composition of industries existent within the SAM [51,52,275]. Thus, three distinct LH_2 sectors are compiled from the prior analysis.

Integration into the SAM

In the final step, the synthetic LH_2 industries are integrated into the SAM. This is executed by multiplying the synthetic industry composition with the production input coefficients of the respective industries from the SAM. This ensures that the LH_2 industries are characterized by a SAM-consistent production input structure, consisting of intermediate commodity inputs and primary production factors. Let Z' be the $n \times m$ sub-matrix of the $m \times m$ SAM, representing the input columns of n industries. For each LH_2 activity k, a cost-share vector $s^k = (s_1^k, s_2^k, \dots, s_n^k,)$ is defined, representing the relative contribution of each existing industry i to the LH_2 activity, such that

$$\sum_i^n s_i^k = 1 \text{ and } s_i^k \geq 0. \quad \text{(C.72)}$$

The corresponding input coefficients of the synthetic LH_2 industry are then obtained as a cost-weighted combination of the existing sectoral input structures, in matrix notation:

$$z^k = Z' s^k \quad \text{(C.73)}$$

In addition, an aggregated LH_2 industry is added to the SAM, representing the entire network, once it is set up and supplying LH_2. This industry has three inputs: (i) LH_2 operation to cover the OPEX; (ii) LH_2 assets to reflect the depreciation of CAPEX; and (iii) LH_2 net operating surplus to cover the financing costs of the network. The latter two are implemented as additional primary production factors to accurately capture the gross value added during the operation of the LH_2 supply network. Next to these LH_2 gross value-added components, commodity counterparts for the four LH_2 industries are integrated into the SAM. This allows for variations in the import dependencies at different stages of the LH_2 supply chain as part of the economic scenarios, which are described in Section C.8.6.

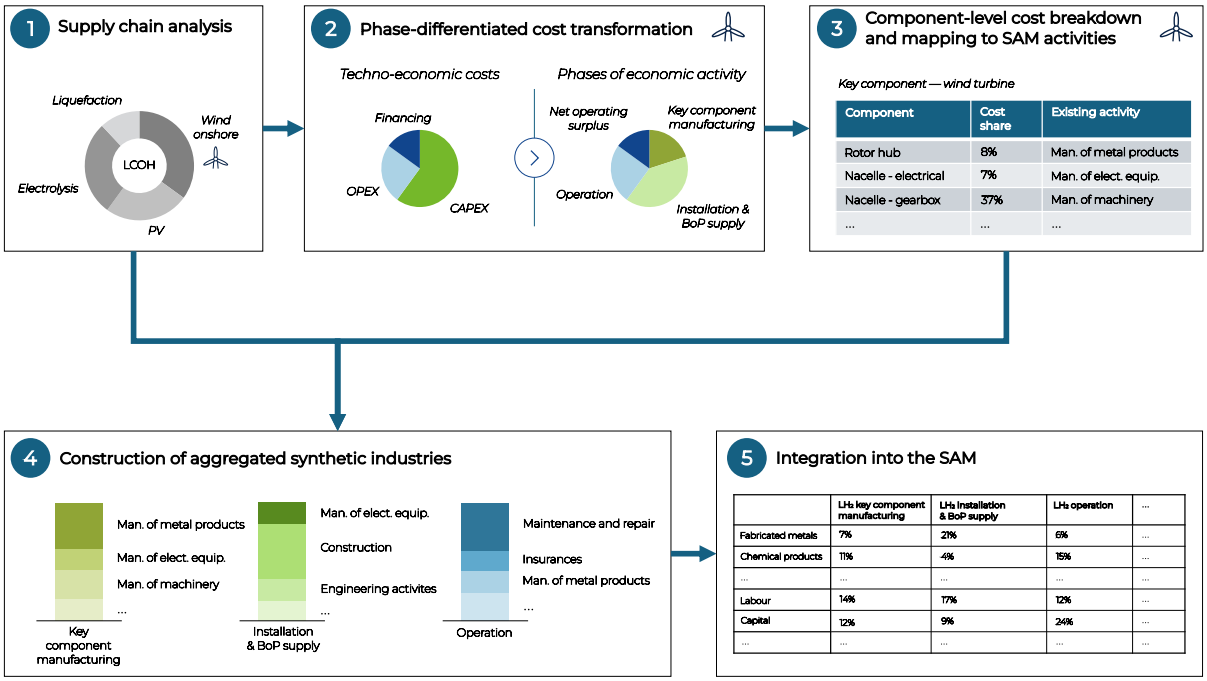

Figure C.15: Methodological procedure for LH_2 integration into the SAM framework

C.8.4 Country selection for the study

The macroeconomic analysis is conducted for a selected set of countries, focusing on Europe and the Middle East and Northern Africa (MENA). Due to the effort required for data collection and the construction of the SAMs, the analysis is limited to five countries plus the European Union (EU) which is included to represent the broader and trans-national European context. The selection is based on several criteria, including the size of the aviation market, the level of ambition in sustainable energy transition, political and economic stability, investment environment, and overall economic conditions. These criteria capture both the demand- and supply-side relevance of countries within a future LH_2 network. The following indicators are used to characterize and compare the selected countries:

Aircraft passengers (PAX):
The number of air passengers carried by domestic airlines serves as a proxy for the scale and relevance of national aviation markets. It reflects the potential future demand for sustainable aviation fuels and H_2 infrastructure. Data is obtained from the World Bank for 2019 as it is the most recent year unaffected by the COVID-19 pandemic [101].

Gross domestic product (GDP):
The GDP represents the overall economic size and capacity to invest in new technologies and infrastructure. Data is obtained from the World Bank for 2024 [100].

Weighted average cost of capital (WACC):
The WACC reflects the country-specific investment risk and cost of financing. Lower WACC values typically indicate favourable conditions and reduced perceived risk for investors. Data is obtained from project-internal estimations for LH_2 infrastructure projects.

Foreign Direct Investment inflows (FDI):
FDI inflows serve as an indicator of international investor confidence and openness to foreign participation in infrastructure projects, which is critical for capital-intensive LH_2 investments. Data is obtained from the most recent United Nations World Investment Report for 2023 [102].

Economic Complexity Index (ECI):
The ECI is an indicator constructed by the Harvard Growth Lab and captures the diversification and technological sophistication of a country's economy. It indicates its ability to develop and produce complex products, which also play a key role for LH_2 infrastructure. Data is taken for 2023 [276].

Fragile States Index (FSI):
This index measures political and institutional stability. Lower fragility scores suggest a stable environment for long-term investments and cross-border energy cooperation. Data is taken for 2024 [103].

Renewable energy share in electricity generation (RES):
This indicator shows the current integration of renewables in the national electricity mix which is a key requirement for green H_2 production. Data is obtained from the Ember Energy Research Institute for 2023 [277].

Green Future Index (GFI):
The GFI is constructed by MIT Technology Review and reflects national progress and commitment towards low-carbon technologies and green innovation, offering a broader view of environmental ambition. Data is taken for 2023 [278].

Energy Transition Index (ETI):
This indicator, constructed by the World Economic Forum, evaluates how effectively countries pursue the energy transition. It considers the current performance regarding sustainable energy as well as the readiness for transitioning towards a sustainable energy system, including economic, political and institutional factors. The most recent scores for 2025 are obtained [279].

Yet, the relevance of the individual criteria differs between Europe and MENA. For the European perspective, countries are expected to represent mature aviation markets with potentially high LH_2 demand in a future network. Therefore, the pre-selection starts with the ten largest aviation markets in Europe, based on the pre-pandemic (2019) domestic and international aircraft passengers of air carriers registered in the country. Beyond market size, structural diversity and different roles in a transnational LH_2 network are considered. The final selection aims to capture countries with distinct economic profiles and LH_2 production prerequisites. The comparison of the pre-selected countries for Europe is presented in Table C.16.

Table C.16: Comparison of European countries regarding relevant indicators, sorted by passengers (PAX).

	PAX [101]	**GDP (USD)** [100]	**WACC**	**FDI (USD)** [102]	**ECI** [276]	**FSI** [103]	**RES** [277]	**GFI** [278]	**ETI** [279]
European Union (EU28)	895 m	23,067 bn	6.5%	199.7 bn	-	-	45%	-	-
Ireland	170 m	577 bn	6.5%	-2.7 bn	1.72	18.6	45%	5.69	61.1
United Kingdom	142 m	3,644 bn	5.9%	52.2 bn	1.81	40.8	47%	6.12	66.8
Turkey	111 m	1,323 bn	10.8%	10.5 bn	0.46	84.0	42%	3.83	57.9
Germany	110 m	4,660 bn	4.9%	52.0 bn	2.01	24.0	53%	5.92	68.8
Russia	109 m	2,174 bn	8.8%	9.0 bn	-0.66	81.6	18%	3.57	-
Spain	88 m	1,723 bn	7.1%	46.7 bn	0.61	44.0	51%	5.92	66.6
France	71 m	3,162 bn	5.9%	42.3 bn	1.26	28.3	27%	5.99	67.1
Sweden	51 m	610 bn	5.3%	25.0 bn	1.64	20.6	69%	6.34	77.5
Austria	46 m	522 bn	5.7%	6.8 bn	1.67	23.1	85%	5.37	70.6
Netherlands	46 m	1,228 bn	5.1%	-184.4 bn	1.29	19.5	47%	6.22	69.2

Germany, Spain, and the UK are among the six largest national aviation markets in Europe. In addition, they have large economies with varying profiles. Germany represents a highly industrialized country with strong technological capacity. Despite being a frontrunner of the energy transition, Germany is likely to depend on green H_2 imports due to the limited RES capacity [123–125]. Spain, in contrast, has high renewable potential [118–120] and a moderate share of value creation in

manufacturing industries [280]. The UK complements the selection as a major aviation hub in Europe with a differing economic structure, which has undergone a transition from an industrialized to a service- and finance-oriented economy [167–169,281]. Moreover, all three countries are ambitious with regards to green H_2 and engage in projects and partnerships [127,282–284].

In contrast, for the MENA region, the focus lies on countries with high RES potential and the capability to export green H_2. Given the region's heterogeneity, political stability and investment environment are particularly relevant to assess the feasibility of large-scale infrastructure projects. The definition of MENA countries is obtained from UNICEF [285]. Of the 20 countries included in this definition, the ten largest economies are pre-selected and compared in Table C.17.

Table C.17: Comparison of MENA countries regarding relevant indicators, sorted by GDP.

	PAX [101]	**GDP (USD)** [100]	**WACC**	**FDI (USD)** [102]	**ECI** [276]	**FSI** [103]	**RES** [277]	**GFI** [278]	**ETI** [279]
Saudi Arabia	46 m	1,238 bn	6.1%	22.8 bn	0.07	63.2	1%	4.11	55.0
United Arab Emirates	93 m	537 bn	5.8%	30.7 bn	0.61	34.7	8%	4.78	58.4
Iran	22 m	437 bn	7.4%	-	-0.29	82.9	6%	2.57	47.6
Egypt	13 m	389 bn	14.8%	9.8 bn	-0.24	82.8	11%	3.99	53.1
Iraq	5 m	280 bn	15.6%	-5.4 bn	-0.91	88.6	1%	-	-
Algeria	7 m	264 bn	12.7%	1.2 bn	-0.65	68.6	0.9%	3.09	50.7
Qatar	33 m	218 bn	6.4%	-0.5 bn	-0.35	39.8	0.3%	3.43	53.0
Kuwait	7 m	160 bn	6.5%	2.1 bn	-0.13	49.3	2%	4.05	48.6
Morocco	9 m	154 bn	7.8%	1.1 bn	-0.50	68.8	22%	4.73	53.7
Oman	11 m	107 bn	8.9%	4.7 bn	-0.15	47.4	4%	-	52.2

Qatar, the United Arab Emirates and Kuwait are excluded due to their small size which makes the implementation of large-scale LH_2 infrastructure highly questionable [286,287]. In addition, Iraq and Iran are not further considered due to their political situation and the unpredictable risk, which is reflected in the high FSI and WACC.

Based on the comparison of the remaining countries, Saudi Arabia and Morocco are selected as case studies for the MENA region. Both countries are already engaged in H_2 partnerships with the EU or European countries [40,109–117] and have considerable RES capacities [104,107,105,106,108]. Saudi Arabia combines substantial financial resources, economic power and relatively low investment risks. In addition, Saudi Arabia aims to foster the transition from an oil-exporting country to a more diversified economy with a focus on sustainable energy [288]. Despite its controversial position concerning democracy and human rights, it is chosen for the analysis due to its relevant economic position in the region. Morocco, in contrast reflects the case of a smaller but highly ambitious economy with improving

institutional stability and expanding renewable energy generation [289,290]. Although Morocco does not have the lowest WACC or the best FSI score, it aims to become a considerable player in the future H_2 economy [291].

As noted, and as a large focus of the project is on Europe, the EU is added to the macroeconomic analysis to capture the broader European context of a transnational LH_2 network on the continent. The analysis refers to the EU28, including the current member states as well as the UK. The reason for that is the base year of the SAMs used in this study. The goal is to use the most recent and validated macroeconomic data and to have a consistent base year for all countries. This criterion excludes the years 2024 and 2023 as the required data is not yet available for all countries under consideration. However, it is also important to use a base year with a representative snapshot of the economy, meaning that it should not be distorted by exceptional events. Therefore, the years 2020–2022 are also rejected as they are heavily influenced by the COVID-19 pandemic (2020–2021) and the Russian invasion of Ukraine (2022) which had a major impact of European energy markets [129]. Consequently, 2019 is the most recent and representative year and thus serves as the base year for all SAMs.

One main advantage of a SAM is its flexibility in terms of aggregation, which allows sector-specific analyses. For this study, the SAM is structured into a format suitable for multiplier analyses with details on industrial interdependencies. The SAM format used for the analyses is shown in Table C.18, exemplary for the EU28 data.

Table C.18: Structure of the aggregated SAM, filled exemplary with data for the EU28 (given in EUR_{2019} bn). G&S = Goods and services; Marg. = Margins for trade and transport; Prod. = Production activities; CTax = Taxes minus subsidies on commodities; PTax = Taxes minus subsidies on production; Lab. = Labor; Sur. = Gross operating surplus; FE = Financial enterprises; NFE = Non-financial enterprises; HH = Households; Gov. = Government; S-I = Savings and investments; RoW = Rest of the world.

	G&S	Marg.	Prod.	CTax	PTax	Lab.	Sur.	FE	NFE	HH	Gov.	S-I	RoW	**Total**
G&S			15,358							9,123	3,390	3,644	3,121	**34,635**
Marg.														**0**
Prod.	30,034													**30,034**
CTax	1,754													**1,754**
PTax			208											**208**
Lab.			7,884											**7,884**
Sur.			6,584											**6,584**
FE							295		100		375		110	**880**
NFE							3,435	14			6			**3,455**
HH						7,884	2,428	358	812		263		34	**11,779**
Gov.				1,754	208		427	81	450	1,724			19	**4,662**
S-I								324	2,051	914		500	2	**3,791**
RoW	2,847							103	42	19	127	148		**3,286**
Total	**34,635**	**0**	**30,034**	**1,754**	**208**	**7,884**	**6,584**	**880**	**3,455**	**11,779**	**4,662**	**3,791**	**3,286**	

As this study aims to provide an in-depth analysis, the SAMs are constructed with a large level of disaggregation. However, some activities are found to be more relevant (see Section 8.2.2) for the LH_2 infrastructure and thus, not each industry/commodity is presented separately. Moreover, to provide comparability among countries, the SAMs are constructed as consistent as possible. The macroeconomic data, used for constructing the SAMs, vary in terms of consistency and degree of detail. For instance, the number of industries and commodities available in national supply and use tables, differs among the countries. While the SAMs for the European countries have the same format due to unified European standards, the SAMs for Morocco and Saudi Arabia have a different level of aggregation. In particular, Saudi Arabia has a low level of detail regarding commodities and industries. An overview of the aggregation levels in the SAM, along with macroeconomic indicators obtained from the SAM and the data sources used for construction, is presented in Table C.19. The data sources used also contain the data used for deriving employment coefficients.

Table C.19: Overview of the aggregation level of the SAMs, along with macroeconomic indicators obtained from the SAM and the data sources used for construction. COM = Commodities; ACT = Activities; GDP = Gross domestic product. Import share refers to the total commodity supply, while export share refers to the total commodity use, both at market prices. Domestic production and GDP are given in USD_{2023}. The data for Morocco has been provided by the statistical office on request. The data source used here for Morocco refers to the general publications on national accounts in Morocco.

	Number of COM	Number of ACT	Domestic production (USD)	GDP (USD)	Import share	Export share	Data sources used
Germany	63	63	8,537 bn	4,631 bn	15.8%	18.5%	[292,293]
Spain	63	63	2,988 bn	1,660 bn	12.8%	12.8%	[294–296]
United Kingdom	63	63	5,817 bn	3,404 bn	14.3%	13.7%	[297–300]
EU28	63	63	40,033 bn	21,900 bn	8.2%	9.0%	[301–306]
Morocco	54	54	254 bn	153 bn	17.3%	11.8%	[307]
Saudi Arabia	20	20	1,610 bn	997 bn	12.6%	16.4%	[308–310]

C.8.5 Design of the supply chain analysis

As described in Section C.8.3, the macroeconomic analysis of LH_2 infrastructure is not straight-forward due to the current lack of relevant production volumes and empirical data. Therefore, an alternative approach of integrating LH_2 industries into the SAM framework is used, based on supply chain analysis, detailed cost breakdown and synthetic industry construction. The starting point of this procedure is the supply chain analysis, which aims to identify and structure all technologies relevant to build-up and operate LH_2 supply networks. This analysis is closely aligned with the remaining work packages of the project, particularly with the techno-economic assessments. Table C.20 provides an overview of all

categories and the associated technologies, including the respective energy carrier outputs and key components. In addition, the references used for the component-level cost breakdown are given in the last column.

Table C.20: Overview of supply chain categories, technologies, energy carriers, key components, and references used for the component-level cost breakdown.

Category	Technology	Energy carrier (output)	Key component(s)	References for component-level cost breakdown
Renewable energy sources	PV power plant	Electricity	PV module	[311,312]
	Onshore wind power plant	Electricity	Wind turbine	[313,314]
	Offshore wind power plant	Electricity	Wind turbine	[313,315]
Conversion systems	PEM electrolysis plant	GH_2	PEM electrolyser stack	[316–318]
	H_2 liquefaction plant	LH_2	Claude-cycle liquefier	[319,320]
Storage systems	Battery storage	Electricity	Li-Ion battery module	[311]
	GH_2 storage (above ground)	GH_2	H2 compressor	[321–324]
	GH_2 storage (cavern / underground)	GH_2	H2 compressor	[321,325]
	LH_2 storage	LH_2	Cryopump	[321,323,326]
Transport systems	Power grid	Electricity	-	[327]
	GH_2 pipeline	GH_2	H2 compressor	[328]
	LH_2 vessel	LH_2	Cryopump	[329–332]
	LH_2 truck	LH_2	Cryopump Fuel cell	[321,329,332–335]
Refuelling systems	Refuelling truck	LH_2	Cryopump Fuel cell	[36,321,328,329,332–335]
	Refuelling pipeline + hydrant	LH_2	Cryopump Fuel cell	[36,328,332–335]

The key components comprise PV modules, wind turbines, PEM electrolyser stacks, Claude-cycle liquefiers, Li-Ion battery modules, H_2 compressors, cryopumps, and fuel cells. They are identified in accordance with technical experts and represent equipment that is inevitable for the implementation of LH_2 supply networks. In addition, most of these components constitute a high degree of complexity with regard to their production process or the required know-how [131,132]. The manufacturing of the key components is mostly located in clusters with few firms or regions that dominate the world market [133,134]. Therefore, it is unlikely that manufacturing of these key components will take place in every country. To reflect these country-specific discrepancies, key component manufacturing is separated

from the installation and supply of BoP equipment. Further details are provided in the following section.

C.8.6 Design of economic scenarios

The macroeconomic analysis includes scenario-specific assessments. The scenarios are designed along three dimensions to reflect different pathways, based on structural conditions and recent trends.

The first dimension concerns the **degree of self-supply for key components**. As described in Section C.8.5, key components comprise technologically complex and critical equipment, requiring specific industrial conditions and capabilities. As such conditions do not equally exist in every country [135], the scenarios contain country-specific shares of self-supply for key components. The second dimension addresses the **domestic share in the installation and operation phase**. These phases are characterized by less specialized activities with a lower degree of complexity and preconditions. The variation of domestic contribution in these phases accounts for local content policies, which are particularly discussed in the Global South [136,137]. Their goal is to enable economic participation for host countries and to avoid extractive and neocolonial patterns, which are criticized in the context of green H_2 [189–192]. The third dimension reflects the **origin of investments**. The large financial resources pose a challenge for a green H_2 economy and lead to large implementation gap for projects [138,139,150]. In particular, emerging countries often depend on capital from industrialized countries [140,141]. In these cases, revenues generated in the project are likely to flow out of the country, thus reducing the potential to create income-induced feedback effects within the respective economy.

The scenarios are tailored to country-specific conditions and current trends. For the EU28 and the European countries, scenarios focus on key component manufacturing and the origin of investments. Particularly the self-supply for key components reflects current discussions in Europe [142–144].

Figure C.16 shows the trade balance of LH_2 key components in the EU28 between 2013 and 2021, based on data from the Comtrade database. The key components are assigned to respective HS codes [336]. While the EU28 has a trade surplus for most components, there is a large dependency on importing PV modules and batteries. This dependency has intensified during the last decade, which has enhanced the controversial about geopolitical resilience and energy independence in Europe [145]. As a consequence, the EU plans to protect its key industries, particularly those being relevant for the energy transition [146]. Thus, the scenarios for the EU28, Germany, Spain and the UK vary the self-supply for key components. In addition, the share of foreign investments is differentiated. In contrast, the MENA countries are already dependent on the imports of key components, and it is not realistic that this will change in the near term [131,132]. Instead, the focus for Morocco and Saudi Arabia lies on local content policies and thus, the domestic contribution in the installation and operation phase are varied.

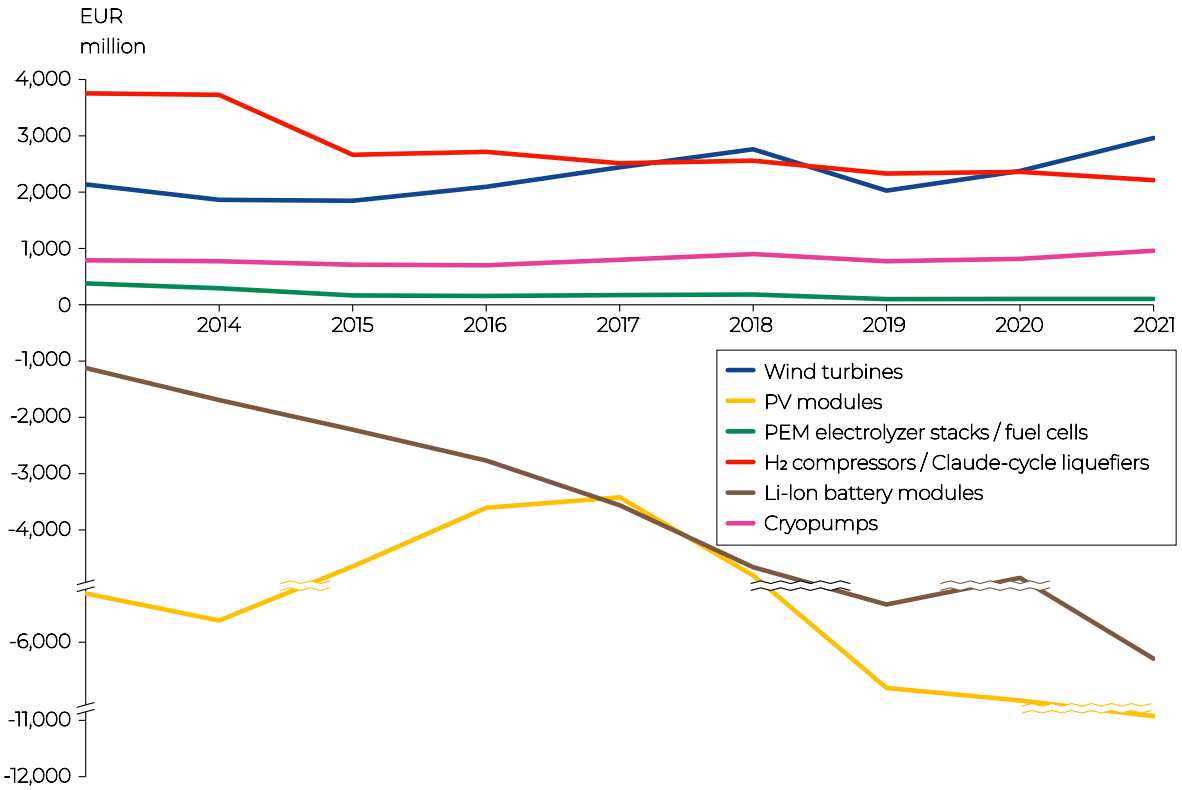

Figure C.16: Trade balance of LH_2 key components in the EU28 between 2013 and 2021. The data are obtained from the Comtrade database, using corresponding HS codes for product allocation [149].

For each country, three scenarios are considered. The **base** scenarios reflect a projection based on the status-quo in each country. The degree of self-supply for key components is derived from the countries' trade activities for the respective products, using the Comtrade database and corresponding HS codes [149]. Concretely, the 2019 data are used to ensure consistency with the SAM base year. Figure C.17 shows the trade balances for the key components for 2019 in the selected countries.

For the share of self-supply in key component manufacturing in the base scenarios, the export share of the total trade volume is used. For the domestic share in the subsequent phases, the relevant LH_2 enabler industries are considered, using their contribution to the corresponding commodity supply within the SAM. Finally, the origin of investment in the base scenarios builds on FDI data. Concretely, the FDI stock as a share of the country's GDP is used as the base share of foreign investments. For European countries and the EU28, this benchmark share is limited to non-service industries as these are more comparable to LH_2 infrastructure projects and since a large FDI stock in the financial and information technology sector would distort the benchmarks. For MENA countries, such refinement is not possible due to a lack of disaggregated data. However, for these countries, the distorting influence of FDI stock in financial and information technology sectors is less relevant. For consistency purposes, the FDI data are also obtained for 2019, except for the UK where 2017 is the most recent year with detailed data. For the same reason, the EU base value refers to the EU27. An overview of the base scenarios is shown in Table C.21. The respective data sources are also provided.

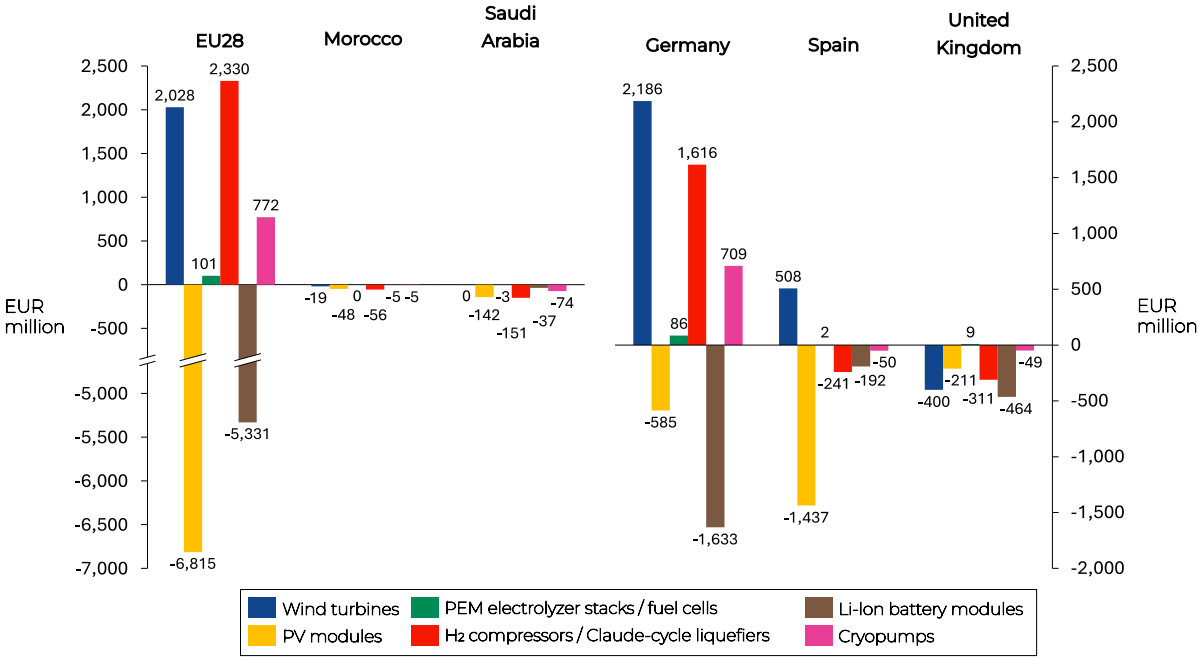

Figure C.17: Trade balance of LH_2 key components in 2019 in the selected countries. The data are obtained from the Comtrade database, using corresponding HS codes for product allocation [149].

Table C.21: Overview of values used in the base scenarios. The countries are abbreviated by the ISO 3155 ALPHA-3 codes. The foreign investment share is taken for the EU27. Foreign investment share for UK is based on data for 2017. The remaining figures are based on 2019 data.

	EU28	MAR	SAU	DEU	ESP	GBR
Self-supply for key components *[149]*						
Wind turbines	89.4%	0.9%	0.0%	96.0%	85.0%	0.3%
PV modules	16.9%	12.7%	0.1%	44.7%	4.0%	31.0%
PEM electrolyser stacks / fuel cells	71.6%	0.5%	0.0%	81.6%	54.4%	72.4%
H_2 compressors / Claude-cycle liquefiers	69.5%	1.8%	5.9%	66.8%	20.5%	40.2%
Li-Ion battery modules	17.5%	10.8%	0.7%	35.5%	15.7%	24.6%
Cryopumps	75.3%	0.7%	0.1%	75.7%	22.0%	40.7%
Average domestic share of activities during the installation & BoP supply and operation phase	87.2%	74.9%	90.4%	81.7%	84.1%	79.9%
Foreign investment share *[100,102,337,338]*	39.7%	51.6%	16.8%	5.4%	33.3%	73.6%

In addition, a set of **domestic boost** scenarios is constructed to consider a more optimistic pathway regarding local value chains and industrial development. As noted before, the scenario variation considers country-specific details and thus, the scenarios have different focuses. The domestic boost scenario for the EU28 reflects the objectives set out with regard to technological sovereignty and supply chain

resilience for critical components. Thus, key component manufacturing is prioritized, and a minimum of 50% domestic key component manufacturing is assumed. If the share is higher in the base scenario, it grows by 10% due to favourable policies. In addition, no foreign investment is assumed for the EU28. For the MENA countries, the self-supply of key components is set at 10% or the base share, if that already exceeds 10%. Yet, the focus is on local content policies, which are already discussed in Morocco [339]. Thus, a minimum of 50% domestic contribution for installation and operation activities is assumed. In terms of foreign capital, Morocco is likely to depend more on external investors and thus, the share is not reduced. Saudi Arabia, in contrast, is assumed to mobilize the investments from its domestic financial resources, such as the public investment fund [180]. Similarly to the EU28's scenario, the domestic boost scenarios for Germany, Spain and the UK focus on key components. For wind turbines, PV modules and batteries, the domestic share increases by 10%, while 20% increase is assumed for compressors/liquefiers, cryopumps and electrolysers/fuel cells. The differentiation is due to China's dominance in the established markets of wind turbines, PV modules and batteries. For the less mature technologies, European market leadership seems more realistic. Regarding capital resources, the foreign investment share for Spain and the UK is reduced by using the FDI flow shares relatively to the gross fixed capital formation for 2019. These values are significantly lower than the FDI's stock. For Germany, however, the foreign investment share is taken from the base scenario as it is already very low. An overview of the domestic boost scenarios is provided in Table C.22.

Table C.22: Overview of values used in the domestic boost scenarios. The countries are abbreviated by the ISO 3155 ALPHA-3 codes.

	EU28	MAR	SAU	DEU	ESP	GBR
Self-supply for key components *[149]*						
Wind turbines	98.4%	10.0%	10.0%	100.0%	93.5%	0.4%
PV modules	50.0%	12.7%	10.0%	49.2%	4.4%	34.1%
PEM electrolyser stacks / fuel cells	78.7%	10.0%	10.0%	98.0%	65.3%	86.9%
H_2 compressors / Claude-cycle liquefiers	76.5%	10.0%	10.0%	80.1%	24.6%	48.2%
Li-Ion battery modules	50.0%	10.8%	10.0%	39.0%	17.3%	27.1%
Cryopumps	82.9%	10.0%	10.0%	90.8%	26.4%	48.8%
Average domestic share of activities during the installation & BoP supply and operation phase	87.2%	78.4%	90.4%	81.7%	84.1%	79.9%
Foreign investment share *[100,102,337,338]*	0.0%	51.6%	0.0%	5.4%	12.4%	0.3%

Finally, the **foreign dependency** scenarios represent a more pessimistic counterpart. For the EU28, PV modules and batteries are fully imported in that case, reflecting the development shown in Figure C.16. Self-sufficiency of wind turbines decreases by 50%. For the remaining key components, 10% decline in domestic manufacturing is assumed. The foreign investment share is now obtained as the FDI stock relatively to the GDP in all industries, leading to a much higher share of foreign capital. For Morocco, the foreign dependency scenario assumes full dependency on key component imports and external investors, while the share of

domestic contribution in installation and operation is taken from the base case. Saudi Arabia is also fully dependent on key component imports in this scenario. However, due to the demographic and structural change in Saudi Arabia's economy, it is assumed that a stronger dependence exists in supporting activities, leading to a 50% share of imports in the installation and operation phase. For capital provision, the average FDI stock as a share of the GDP is taken from the period between 2020 and 2024, resulting in 43.5% foreign investment. The foreign dependency scenarios for the European countries assume the same share of local content during installation and operation as in the base case. In contrast, the domestic share of wind turbines is reduced by 50%, while PV modules and batteries are fully imported, accounting for a growing dominance of Chinese firms in these technologies. For the remaining key components, it is assumed that European suppliers remain in a better position and thus, there is only 10% decrease. The foreign investment share is also derived as the average FDI stock between 2020 and 2024, relatively to the national GDP. An overview of the foreign dependency scenarios is provided in Table C.23.

Table C.23: Overview of values used in the foreign dependency scenarios. The countries are abbreviated by the ISO 3155 ALPHA-3 codes.

	EU28	MAR	SAU	DEU	ESP	GBR
Self-supply for key components *[149]*						
Wind turbines	44.7%	0.0%	0.0%	48.0%	42.5%	0.2%
PV modules	0.0%	0.0%	0.0%	0.0%	0.0%	0.0%
PEM electrolyser stacks / fuel cells	64.4%	0.0%	0.0%	73.5%	49.0%	65.2%
H_2 compressors / Claude-cycle liquefiers	62.6%	0.0%	0.0%	60.1%	18.5%	36.2%
Li-Ion battery modules	0.0%	0.0%	0.0%	0.0%	0.0%	0.0%
Cryopumps	67.8%	0.0%	0.0%	68.1%	19.8%	36.6%
Average domestic share of activities during the installation & BoP supply and operation phase	87.2%	74.9%	50.0%	81.7%	84.1%	79.9%
Foreign investment share *[100,102,337,338]*	78.3%	100%	43.5%	26.7%	53.4%	89.3%

C.9 Methodology on hydrogen liquefaction deep dive

This section gives a more detailed overview of the methodology used for the results on H_2 liquefaction plants shown in Chapter A.

C.9.1 Process Simulation

For this study, four different H_2 liquefaction plants were simulated and techno-economically assessed. For all plants, a comprehensive process simulation was conducted in Honeywell UniSim© Design. Thereby, special focus was on the ortho-para conversion. Finally, all plants were assessed by calculating the plant's economic characteristics according to the model by Turton 2018 [201] and several assumptions.

Selected Flowsheets and Technical Assumptions

The selected plants for this study range from medium to large-scale and have liquefaction capacities of 5, 50, 100, and 200 tpd. In all selected plants, REFPROP [340] is used to provide property data, employing the equation of state by Leachman et al. 2009 [341] for ortho and parahydrogen. Only for mixed refrigerant (MR) properties, the Peng-Robinson equation of state is used. To ensure comparability across all plants, identical feed and product conditions are used, as listed in Table C.24. Since the H_2 working pressure varies among the liquefiers, feed compression from 20 bar to the respective pressure is included in both the simulation and the techno-economic evaluation. Additional pre-compression to 20 bar or pre-purification are neglected.

The smallest selected plant is based on the 5 tpd plant by Linde [202] in Leuna. While it is the smallest plant considered in this study, it is one of the four industrial-scale H_2 liquefaction plants currently operated in Europe [342]. The 5 tpd plant uses a H_2 Claude cycle with maximum pressures of 20 bar for cryogenic cooling, an open nitrogen (N_2) cycle for precooling to 80 K, and continuous ortho-para conversion in the heat exchangers.

For the 50 tpd plant, the concept from the IDEALHY study [215] was chosen. For precooling, a closed cycle of MR, consisting of nitrogen, methane, ethane, propane, and n-butane, is applied. With MR, a narrower temperature profile in the heat exchangers can be achieved due to the different dew points of the components in the MR. Additionally, as MR consists mainly of hydrocarbons, standard equipment from natural gas plants can be applied. However, the precooling temperature of the 50 tpd plant is only 130 K, thus, more of the cooling demand is shifted to the cryogenic section. Further, the 50 tpd plant is the only selected plant featuring a Brayton cycle instead of a Claude cycle for cryogenic cooling. The main difference is that Brayton cycles only apply expanders for pressure and temperature decrease, while Claude cycles also deploy Joule-Thomson valves. The working fluid is a mixture of helium and neon (3:1) to achieve the required cryogenic temperatures, but also allow for easier compression to pressures above 60 bar. In addition to continuous ortho-para conversion in the heat exchangers, the plant also uses adiabatic conversion reactors down to temperatures of 85 K. Further, in contrast to the other considered plants, the H_2 feed is compressed to a significantly higher pressure. While the 5, 100, and 200 tpd plants work with 24 and 25 bar of feed pressure, in the 50 tpd the H_2 is compressed up to 82 bar.

The 100 tpd plant is modelled according to the concept by Cardella 2018 [197], which is oriented on the 5 tpd plant. It also applies a H_2 Claude cycle with working pressures up to 50 bar. Like the 50 tpd plant, it applies MR precooling, using a

mixture of nitrogen, methane, ethane, and i-butane, to cool down H_2 to approximately 100 K. While in the cryogenic section, the ortho-para conversion takes place continuously in the heat exchangers, the plant also deploys a conversion reactor after precooling. For simplicity, the 200 tpd in this study is a scaled-up version of the 100 tpd plant. However, due to size limitations, the number of H_2 compressors had to be doubled instead of using larger equipment.

Further, intermediate temperature levels are selected to achieve minimum temperature differences of 1–4 K within the heat exchangers. This approach ensures narrow temperature profiles, which are desirable for minimizing exergetic losses. The heat exchangers, which are among the main cost drivers in H_2 liquefaction plants, are modelled as aluminium plate-fin heat exchangers. Required heat exchange areas are calculated using heat transfer coefficients of 200 W/(m²·K) in the precooling section and 100 W/(m²·K) in the cryogenic section [197]. Additionally, a specific surface area of 600 m²/m³ [197] is assumed for typical plate-fin heat exchangers.

The plants' expanders are modelled as turbo expanders with an isentropic efficiency of 85% [197], except for the expanders with liquid at the outlet only deployed in the final expansion of the 50 tpd plant, which operate at a higher efficiency of 90% [343]. Additionally, it is assumed that the energy generated by the turbo expanders can be recovered with an efficiency of 80% [197]. While this is not yet standard in industrial applications, it is key for energy-efficient systems, particularly in large-scale plants.

All H_2 and helium compressors are modelled as reciprocating compressors, whereas turbo compressors are assumed to be available for MR cycles. Compressor isentropic efficiencies are generally assumed to be 80% [197], with the exception of one cold compressor in the 50 tpd plant, which has an efficiency of 70% [343]. Each plant includes a cooling water infrastructure to cool the compressors. To estimate the required cooling water flow, a temperature increase of 10 K [343] and a heat transfer coefficient of 200 W/(m²·K) is assumed.

For simplification, the adsorption units are only modelled by means of a pressure drop of 0.1 bar and a temperature increase of 0.2 K. In the heat exchangers, pressure drops of 0.2 bar are assumed for catalyst-filled channels and 0.025–0.05 bar for the remaining channels, depending on the stream's pressure level.

Table C.24: Simulation boundary conditions and main assumptions

Feed temperature	293 K
Feed pressure	20 bar
Feed parahydrogen fraction	25%
Product pressure	2 bar
Product parahydrogen fraction	> 97%
Compressor isentropic efficiency	80 %
Expander isentrobic efficiency	85 %
Minimal temperature difference in HEX	1 – 4 K

Ortho-Para Conversion

H_2 exists as a mixture of its two spin isomers: orthohydrogen and parahydrogen. Its equilibrium composition depends on the temperature and is shown in Figure C.18.

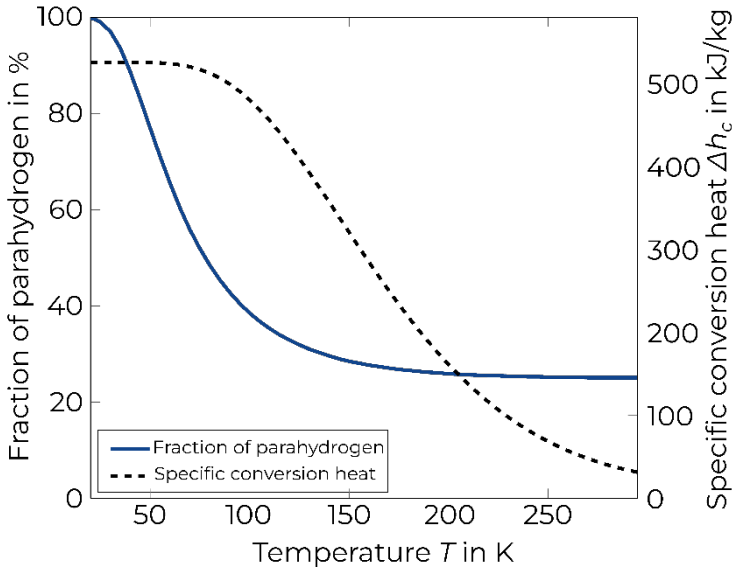

Figure C.18: Parahydrogen fraction at equilibrium and specific conversion heat of the ortho-para conversion as a function of the temperature

At ambient temperature, the equilibrium is at a mixture of 75% orthohydrogen and 25% parahydrogen. As the temperature drops, the equilibrium shifts toward parahydrogen, and at LH_2 temperatures, nearly all is parahydrogen. Consequently, the liquefaction process inherently drives the conversion from ortho- to parahydrogen. While this process would naturally occur over several days or weeks [224], it releases temperature-dependent conversion heat, also shown in Figure C.*18*. Thus, the conversion could risk unwanted boil-off if it happens inside LH_2 storage tanks. To prevent this, the ortho-para conversion is facilitated within the liquefaction plant using catalyst-packed heat exchangers that promote continuous conversion during the cryogenic cooling process. REFPROP [340], used for property data in this study, does not support equilibrium H_2. Still, considering the ortho-para conversion is substantial for reliable results, as ortho- and parahydrogen differ in property data, and as the conversion heat adds noticeably to the overall cooling duty of the plant. Hence, the method proposed by Kanz et al. 2025 [344] based on the van't Hoff equation is implemented to accurately model the conversion and its associated heat. As presented in [345], it is assumed that the H_2 composition is always lagging 2 K behind the equilibrium composition.

C.9.2 Techno-Economic Evaluation

To evaluate the process from a techno-economic perspective, the UniSim© results serve as the foundation for estimating capital expenditures (CAPEX) and operational expenditures (OPEX), based on the methodology in [345]. All cost figures are expressed in 2023 USD, adjusted using the Chemical Engineering Plant Cost Index (CEPCI) [346]. The CAPEX is calculated using the factor-based method proposed by Turton 2018 [201], which scales equipment costs based on parameters such as size and type. For elevated pressure and specific materials, cost factors are applied. This approach incorporates historical cost data from the chemical industry, while also accounting for installation, indirect costs, contingencies, engineering fees, and auxiliary systems. When equipment dimensions exceed the applicability range of Turton's model, cost extrapolation is performed using the scaling function introduced by Couper 2003 [347]. It is assumed that all components handling H_2 are made of stainless steel, while other materials are made of cheaper carbon steel. The main cost components for CAPEX are compressors, heat exchangers,

expanders, storage, vessels, pumps, coldboxes, and cooling water infrastructure. Thereby, the latter one is assumed to rely on tube bundle heat exchangers.

To estimate the required storage tank size, for the 5 tpd plant, a storage period of 5 days, and for the larger plants, a storage period of 2 days is assumed. Due to a lack of economic data on insulation material for the storage and coldboxes, it is assumed that insulation adds 20% to the vessel costs. The adsorption units are modelled by means of a vessel filled with molecular sieves, assuming costs of 2 USD/kg. Finally, for the ortho-para catalyst, costs of 100 USD_{2012}/kg, as mentioned in Essler et al. 2012 [348], are assumed. The mass of catalyst is estimated based on the H_2 volume flow rate and the catalyst's space velocity provided in the Ionex® catalyst datasheet [349].

OPEX estimation is primarily driven by the process's power consumption, as determined by the simulation. An electricity price of 50 USD/MWh is assumed. No costs for the H_2 feed are required, since this study only aims to calculate the cost of liquefaction, not the cost of LH_2. In the 5 tpd plant, where LN_2 is supplied externally for precooling, no LN_2 price but a specific energy consumption of 0.5/kg_{LN2} [197] is applied for OPEX estimation. It is assumed that supplying LN_2 for precooling is only viable if a reliable LN_2 source is on-site, e.g., an air separation unit. While a 1% H_2 loss due to compression is considered in the techno-economic evaluation, losses of any refrigerants are neglected. In addition to the direct power requirement, auxiliary power demands are considered as 3% of the total power [197].

Additionally, operation and maintenance (O&M) costs are included in the OPEX, estimated as a fixed annual rate of 2% of the CAPEX. This value is on the lower side of industry standards for chemical processing facilities [350] and follows from parameter studies of previous work [345]. The low O&M value for H_2 liquefaction plants is further justified, as there are no moving parts involved besides compressors and expanders, and as there are no corrosive materials or chemical reactions involved. An overview of the main techno-economic assumptions is provided in Table C.25.

The techno-economic results are evaluated based on three parameters: the specific CAPEX, the specific energy consumption (SEC), and the specific liquefaction costs (SLC). The specific CAPEX is the CAPEX of the plant relative to the mass flow rate of liquefied H_2, typically expressed in million USD/tpd. The SEC quantifies the net electrical power demand per mass flow rate of LH_2. It is calculated as the difference between the power required, primarily for compression and precooling, and the power recovered through turbo expanders, assuming an energy recovery efficiency of 80%. Finally, the SLC represents the cost of liquefaction per mass flow rate of LH_2 and is derived from the sum of annual OPEX and the annualized share of capital costs ($CAPEX_a$), related to the annual output of LH_2.

$$\text{Spec. CAPEX} = \frac{\text{CAPEX}}{\dot{M}_{\text{LH}_2}} \tag{C.74}$$

$$\text{SEC} = \frac{P_{\text{required}} - P_{\text{recovered}}}{\dot{M}_{\text{LH}_2}} \tag{C.75}$$

$$\text{SLC} = \frac{\text{CAPEX}_a + \text{OPEX}}{\dot{M}_{\text{LH}_2}} \tag{C.76}$$

Table C.25: Main techno-economic assumptions regarding H_2 liquefaction plants

Operation and maintenance (O&M) factor	2% of CAPEX
Electricity price	50 USD/MWh
Specific energy consumption for supplying LN_2	0.5 kWh/kg_{LN2} [197]
Depreciation period	20 years
Plant availability	95%
Interest rate	7%
H_2 loss	1%
Turbine energy recovery efficiency	80%
Auxiliary power demand	3% of total power [197]
Storage capacity	5 days for 5 tpd, 2 days for ≥ 50 tpd
Insulation	20% of vessel cost
Ortho-para catalyst cost	100 USD_{2012}/kg [348]
Pipes, valves, etc.	Neglected for economics

Glossary

AEL	Alkaline Electrolysis
BL	Backward Linkage
BoP	Balance of Plant
CAPEX	Capital Expenditures
CEEAG	EU State Aid Guidelines
CEPCI	Chemical Engineering Plant Cost Index
CfD	Contracts for Difference
EHB	European Hydrogen Backbone
EIB	European Investment Bank
EIS	Entry-Into-Service
ESG	Environmental Sustainability Goals
ESTRAM	Energy System Transformation Model
ETS	Emissions Trading System
EU	European Union
FDI	Foreign Direct Investment
FL	forward linkage
FSI	Fragile States Index
GDP	Gross Domestic Product
GH_2	Gaseous Hydrogen
GWP	Global Warming Potential
H_2	Hydrogen
HANLA	Hydrogen Aviation Network Labeling Algorithm
HANP	Hydrogen Aviation Network Problem
HEFA	Hydrotreated Esters and Fatty Acids
HSCN	Hydrogen Supply Chain Networks
ICAO	International Civil Aviation Organization
IO	Input-Output
IATA	International Air Transport Association
IRA	US Inflation Reduction Act
ISIC	Internationally Standardized Classification of Economic Activities
ITP	Into plane service provider
KfW	German Credit Institute for Reconstruction
LCA	Life Cycle Assessment
LFP	Liquefaction Plant
LH_2	Liquid Hydrogen
LN_2	Liquid Nitrogen
LP	Linear Programming
MENA	Middle East and Northern Africa
MILP	Mixed-Integer Linear Programming
MLI	Multi-Layer Insulation
MR	Mixed Refrigerants
N_2	Nitrogen
NOx	Nitrogen Oxides
NUTS	European Union Nomenclature of territorial units for statistics
OEM	Original Equipment Manufacturer
OPEX	Operational Expenditures
PAX	Passengers
PEMEL	Proton Exchange Membrane Electrolysis
PtL	Power-to-Liquid
PV	Photovoltaic
RED III	Renewable Energy Directive
RES	Renewable energy sources
ROIC	Return of Invested Capital
SAF	Sustainable Aviation Fuel
SAM	Social Accounting Matrix
SEC	Specific Energy Consumption
SLC	Specific Liquefaction Cost
SOEL	Solid Oxide Electrolysis
TCO	Total Cost of Ownership
tpd	Tons per Day
WACC	Weighted Average Cost of Capital

Bibliography

[1] ICAO, Trends in Emissions that affect Climate Change, (n.d.). https://www.icao.int/environmental-protection/trends-emissions-affect-climate-change (accessed August 28, 2025).
[2] Clean Air Task Force, Decarbonizing Aviation: Enabling Technologies for a Net-Zero Future, 2024. https://cdn.catf.us/wp-content/uploads/2024/04/03083920/decarbonizing-aviation-technologies-net-zero-future.pdf?_gl=1*1gl84sw*_ga*R0ExLjEuMTcyNTgxNDE4MS4xNzU2Mzg4NTE2*_ga_88025VJ2M0*czE3NTYzODg1MTUkbzEkZzEkdDE3NTYzODg1MTgkajU4JGwwJGg3MjA1OTA4Ng.. (accessed August 28, 2025).
[3] Aviation Impact Accelerator, Five years to chart a new future for aviation, 2024.
[4] D.S. Lee, D.W. Fahey, A. Skowron, M.R. Allen, U. Burkhardt, Q. Chen, S.J. Doherty, S. Freeman, P.M. Forster, J. Fuglestvedt, A. Gettelman, R.R. De León, L.L. Lim, M.T. Lund, R.J. Millar, B. Owen, J.E. Penner, G. Pitari, M.J. Prather, R. Sausen, L.J. Wilcox, The contribution of global aviation to anthropogenic climate forcing for 2000 to 2018, Atmospheric Environment 244 (2021) 117834. https://doi.org/10.1016/j.atmosenv.2020.117834.
[5] T&E, The aviation industry and the stall in aircraft innovation, 2025. https://www.transportenvironment.org/uploads/files/The-aviation-industry-and-the-stall-in-aircraft-innovation_Aircraft-tech-briefing.pdf (accessed August 28, 2025).
[6] nlr, seo, DESTINATION 2050 - ROADMAP, 2025. https://umbraco.asd-europe.org/media/ndmp5o0b/destination-2050-roadmap-2025.pdf?rmode=pad&v=1db76cc3369a890 (accessed February 4, 2025).
[7] FlyZero, ATI, SUSTAINABILITY REPORT The Lifecycle Impact of Hydrogen-Powered Aircraft, 2022. https://www.ati.org.uk/wp-content/uploads/2022/03/FZO-STY-REP-0005-FlyZero-Sustainability-Report.pdf#page=13.48 (accessed September 3, 2025).
[8] Airbus, Airbus showcases hydrogen aircraft technologies during its 2025 Airbus Summit | Airbus, (2025). https://www.airbus.com/en/newsroom/press-releases/2025-03-airbus-showcases-hydrogen-aircraft-technologies-during-its-2025 (accessed August 25, 2025).
[9] ZeroAvia, Powertrains, ZeroAvia (n.d.). https://zeroavia.com/powertrains/ (accessed August 25, 2025).
[10] Clean Sky 2 JU, Fuel Cells and Hydrogen 2 JU, Hydrogen-powered aviation A fact-based study of hydrogen technology, economics, and climate impact by 2050, 2020. https://cleansky.paddlecms.net/sites/default/files/2021-10/20200507_Hydrogen-Powered-Aviation-report.pdf.
[11] IATA, Aviation contrails and their climate effect, (2024).
[12] BDLI, DLR, Zero Emission Aviation German Aviation Research White Paper, 2020. https://www.dlr.de/en/media/publications/brochures/2020/white-paper-dlr-bdli-zero-2020-en.
[13] World Economic Forum, Unlocking Sustainable Battery and Hydrogen-Powered Flight, 2022.
[14] Clean Skies for Tomorrow, World Economic Forum, WEF Clean Skies for Tomorrow Power to Liquid Deep Dive 2022, 2022.
[15] Energy Transistion Commission, Carbon Capture, Utilisation & Storage in the Energy Transition: Vital but Limited, 2022.
[16] World Economic Forum, Financing The Airports Of Tomorrow: A Green Transition Toolkit, 2023. https://www3.weforum.org/docs/WEF_Financing_The_Airports_Of_Tomorrow_2023.pdf (accessed November 21, 2023).
[17] IATA, Aviation Value Chain, (2023).
[18] IATA, Profitability and the air transport value chain, 2013. https://www.icafrica.org/fileadmin/documents/Knowledge/Transport/IATA-profitability-and-the-air-transport-value_chain.pdf (accessed January 13, 2025).
[19] IATA, Understanding the pandemic's impact on the aviation value chain, 2022. https://www.iata.org/en/iata-repository/publications/economic-reports/understanding-the-pandemics-impact-on-the-aviation-value-chain (accessed January 13, 2025).
[20] Linde, Annual Report 2024, 2025. https://assets.linde.com/-/media/global/corporate/corporate/documents/investors/full-year-financial-reports/2024-annual-report-to-shareholders.pdf (accessed June 24, 2025).
[21] Air Products, 2024 Annual Report, 2025.
[22] Air Liquide, Integrated Annual Report 2024, 2025.
[23] IEA, Clean Energy Market Monitor – November 2024, (2024).
[24] eurostat, Oil and petroleum products - a statistical overview, (2025). https://ec.europa.eu/eurostat/statistics-explained/index.php?title=Oil_and_petroleum_products_-_a_statistical_overview (accessed May 23, 2025).
[25] M.Z. Hussain, B.A. Hamilton, Investment in Air Transport Infrastructure, (2010). https://ppp.worldbank.org/public-private-partnership/sites/default/files/2022-06/Investment_Air_Transport_MZHussain.pdf (accessed June 24, 2025).
[26] Air Liquide, Groupe ADP, JOINT PRESS RELEASE, (2022).
[27] B. Kumar, J. Kumar, A.Q. Amjad, L. Kumar, C. Sassanelli, Sustainable aviation finance: Integration of environmental impact mitigation and green investment strategies, Research in Transportation Business & Management 61 (2025) 101410. https://doi.org/10.1016/j.rtbm.2025.101410.
[28] Clean Hydrogen Alliance, LEARNBOOK: FINANCING OF HYDROGEN INFRASTRUCTURE, 2024. https://www.entsog.eu/sites/default/files/2024-09/European%20Clean%20Hydrogen%20Alliance%20T%26D%20RT_Learnbook%20on%20Financing%20of%20Hydrogen%20Infrastructure.pdf (accessed May 26, 2025).
[29] J. Hölzen, Hydrogen-powered aviation – techno-economics of flying with green liquid hydrogen, Gottfried Wilhelm Leibniz Universität Hannover, 2024. https://www.repo.uni-hannover.de/bitstream/handle/123456789/16518/240225_Hoelzen_Techno%20economics%20of%20H2%20aviation_vpublished.pdf?sequence=1&isAllowed=y (accessed March 1, 2024).
[30] European Commission, Commission Delegated Regulation (EU) 2023/1184 of 10 February 2023 supplementing Directive (EU) 2018/2001 of the European Parliament and of the Council by establishing a Union methodology setting out detailed rules for the production of renewable liquid and gaseous transport fuels of non-biological origin, 2023. http://data.europa.eu/eli/reg_del/2023/1184/oj (accessed September 6, 2024).
[31] T. Smolinka, N. Wiebe, P. Sterchele, A. Palzer, F. Lehner, M. Jansen, S. Kiemel, R. Miehe, S. Wahren, F. Zimmermann, Studie: IndWEDe Industrialisierung der Wasserelektrolyse in Deutschland: Chancen und Herausforderungen für nachhaltigen Wasserstoff für Verkehr, Strom und Wärme, (2018) 201.
[32] U. Bünger, J. Michalski, F. Crotogino, O. Kruck, 7 - Large-scale underground storage of hydrogen for the grid integration of renewable energy and other applications, in: M. Ball, A. Basile, T.N. Veziroğlu (Eds.), Compendium of Hydrogen Energy, Woodhead Publishing, Oxford, 2016: pp. 133–163. https://doi.org/10.1016/B978-1-78242-364-5.00007-5.
[33] J. Hoelzen, L. Koenemann, L. Kistner, F. Schenke, A. Bensmann, R. Hanke-Rauschenbach, H2-powered aviation – Design and economics of green LH2 supply for airports, Energy Conversion and Management: X 20 (2023) 100442. https://doi.org/10.1016/j.ecmx.2023.100442.
[34] M. Reuß, T. Grube, M. Robinius, D. Stolten, A hydrogen supply chain with spatial resolution: Comparative analysis of infrastructure technologies in Germany, Applied Energy 247 (2019) 438–453. https://doi.org/10.1016/j.apenergy.2019.04.064.
[35] EHB, Guidehouse, European Hydrogen Backbone, 2022. https://ehb.eu/files/downloads/ehb-report-220428-17h00-interactive-1.pdf (accessed March 27, 2023).
[36] J. Hoelzen, M. Flohr, D. Silberhorn, J. Mangold, A. Bensmann, R. Hanke-Rauschenbach, H2-powered aviation at airports – Design and economics of LH2 refueling systems, Energy Conversion and Management: X 14 (2022) 100206. https://doi.org/10.1016/j.ecmx.2022.100206.
[37] J. Hoelzen, D. Silberhorn, F. Schenke, E. Stabenow, T. Zill, A. Bensmann, R. Hanke-Rauschenbach, H2-powered aviation – Optimized aircraft and green LH2 supply in air transport networks, Applied Energy 380 (2025) 124999. https://doi.org/10.1016/j.apenergy.2024.124999.
[38] Chemical Engineering, The Chemical Engineering Plant Cost Index, Chemical Engineering (2024). https://www.chemengonline.com/pci-home/ (accessed January 17, 2024).

[39] F. Schenke, L. Koenemann, J. Hoelzen, T. Schelm, A. Bensmann, R. Hanke-Rauschen, Planning LH2 infrastructure for H2-powered aviation: From the initial development to market penetration, Applied Energy 401 (2025) 126663. https://doi.org/10.1016/j.apenergy.2025.126663.
[40] V.P. Müller, M. Besler, D. van Vuuren, W. Eichhammer, Can green hydrogen drive economic transformation in Saudi Arabia? – An input–output analysis of different Power-to-X configurations, Energy Conversion and Management: X 24 (2024) 100798. https://doi.org/10.1016/j.ecmx.2024.100798.
[41] R. Gupta, T.M.M. Guibentif, M. Friedl, D. Parra, M.K. Patel, Macroeconomic analysis of a new green hydrogen industry using Input-Output analysis: The case of Switzerland, Energy Policy 183 (2023) 113768. https://doi.org/10.1016/j.enpol.2023.113768.
[42] D. Chun, C. Woo, H. Seo, Y. Chung, S. Hong, J. Kim, The role of hydrogen energy development in the Korean economy: An input–output analysis, International Journal of Hydrogen Energy 39 (2014) 7627–7633. https://doi.org/10.1016/j.ijhydene.2014.03.058.
[43] G.J. Allan, The Regional Economic Impacts of Biofuels: A Review of Multisectoral Modelling Techniques and Evaluation of Applications, Regional Studies 49 (2015) 615–643. https://doi.org/10.1080/00343404.2013.799761.
[44] T. Mueller, S. Gronau, Fostering Macroeconomic Research on Hydrogen-Powered Aviation: A Systematic Literature Review on General Equilibrium Models, Energies 16 (2023) 1439. https://doi.org/10.3390/en16031439.
[45] T. Mueller, E. Winter, U. Grote, Decarbonizing the aviation sector: Multiplier effects of power-to-liquid fuel production on the German economy, Sustainable Energy Technologies and Assessments 82 (2025) 104478. https://doi.org/10.1016/j.seta.2025.104478.
[46] C. Mardones, C. Brevis, Constructing a SAMEA to analyze energy and environmental policies in Chile, Economic Systems Research 33 (2021) 576–602. https://doi.org/10.1080/09535314.2020.1839386.
[47] V. Ferreira, L. Pié, A. Terceño, Economic impact of the bioeconomy in Spain: Multiplier effects with a bio social accounting matrix, Journal of Cleaner Production 298 (2021) 126752. https://doi.org/10.1016/j.jclepro.2021.126752.
[48] United Nations, System of national accounts 2008, United Nations, New York, 2009.
[49] G. Pyatt, J.I. Round, SOCIAL ACCOUNTING MATRICES FOR DEVELOPMENT PLANNING 1, 1977. https://doi.org/10.1111/j.1475-4991.1977.tb00022.x.
[50] S. Gronau, J. Hoelzen, T. Mueller, R. Hanke-Rauschenbach, Hydrogen-powered aviation in Germany: A macroeconomic perspective and methodological approach of fuel supply chain integration into an economy-wide dataset, International Journal of Hydrogen Energy (2022) S0360319922048972. https://doi.org/10.1016/j.ijhydene.2022.10.168.
[51] H. Garrett-Peltier, Green versus brown: Comparing the employment impacts of energy efficiency, renewable energy, and fossil fuels using an input-output model, Economic Modelling 61 (2017) 439–447. https://doi.org/10.1016/j.econmod.2016.11.012.
[52] T. Mueller, E. Winter, U. Grote, Economic impacts of power-to-liquid fuels in aviation: A general equilibrium analysis of production and utilization in Germany, Energy Conversion and Management: X 23 (2024) 100632. https://doi.org/10.1016/j.ecmx.2024.100632.
[53] United Nations, International Standard Industrial Classification of All Economic Activities, (2008). https://unstats.un.org/unsd/publication/seriesm/seriesm_4rev4e.pdf.
[54] J.J. Häußermann, M.J. Maier, T.C. Kirsch, S. Kaiser, M. Schraudner, Social acceptance of green hydrogen in Germany: building trust through responsible innovation, Energ Sustain Soc 13 (2023). https://doi.org/10.1186/s13705-023-00394-4.
[55] S. Farokhi, Future Propulsion Systems and Energy Sources in Sustainable Aviation, Wiley (2019). https://doi.org/10.1002/9781119415077.
[56] EUROCONTROL, EUROCONTROL Aviation Long-Term Outlook Flights and CO_2 emissions forecast 2024 – 2050, 2024.
[57] Eurostat, [avia_par_] Air passenger transport routes between partner airports and main airports., (2025). https://doi.org/10.2908/AVIA_PAR.
[58] Airbus, Orders and deliveries - past years, (2023). https://www.airbus.com/en/products-services/commercial-aircraft/orders-and-deliveries (accessed September 8, 2025).
[59] J. Terrapon-Pfaff, M. Prantner, S.R. Ersoy, Risikobewertung und Risikokostenanalyse der MENA-Region, 2022.
[60] J. Horst, U. Klann, MENA-Fuels Analyse eines globalen Marktes für Wasserstoff und synthetische Energieträger hinsichtlich künftiger Handelsbeziehungen, izes gGmbH - Institut für ZukunftsEnergie- und Stoffstromsysteme (IZES), 2022.
[61] A. Damodaran, Country Default Spreads and Risk Premiums, (2025). https://pages.stern.nyu.edu/~adamodar/New_Home_Page/datafile/ctryprem.html (accessed November 3, 2025).
[62] Hersbach, H., Cobb, A., Kaandrop, M., P. Poli, Bell, B., Berrisford, P., Biavati, G., Horányi, A., Muñoz Sabater, J., Nicolas, J., Peubey, C., Radu, R., Rozum, I., Schepers, D., Simmons, A., Soci, C., Dee, D., Thépaut, J-N., ERA5 hourly time-series data on single levels from 1940 to present, (2025). https://cds.climate.copernicus.eu/datasets/reanalysis-era5-single-levels-timeseries?tab=documentation.
[63] F. Schenke, J. Hoelzen, D. Bredemeier, L. Schomburg, A. Bensmann, R. Hanke-Rauschenbach, LH2 supply for the initial development phase of H2-powered aviation, Energy Conversion and Management: X 24 (2024) 100797. https://doi.org/10.1016/j.ecmx.2024.100797.
[64] F. Schenke, L. Koenemann, J. Hoelzen, T. Schelm, A. Bensmann, R. Hanke-Rauschenbach, LH2 supply infrastructure for H2-powered aviation: Business models, financing strategies and policy instruments, (2025).
[65] World Economic Forum, Financing Sustainable Aviation Fuels: Case Studies and Implications for Investment, 2025. https://reports.weforum.org/docs/WEF_Financing_Sustainable_Aviation_Fuels_2025.pdf (accessed February 27, 2025).
[66] IATA, Finance - Net Zero CO2 Emissions Roadmap, 2024. https://www.iata.org/contentassets/8d19e716636a47c184e7221c77563c93/finance-net-zero-roadmap.pdf (accessed November 25, 2024).
[67] Oxford Institute for Energy Studies, Financing a world scale hydrogen export project, (2023).
[68] ESMAP, OECD, Global Infrastructure Facility, Hydrogen Council, Scaling Hydrogen Financing for Development, 2023. https://documents1.worldbank.org/curated/en/099022024121527489/pdf/P1809201780da10e518c061a2e73041a6fc.pdf (accessed December 12, 2024).
[69] Hydrogen Council, Hydrogen-Council-–-Closing-the-cost-gap, 2025. https://hydrogencouncil.com/wp-content/uploads/2025/03/Hydrogen-Council-%E2%80%93-Closing-the-cost-gap.pdf#page=4.56 (accessed March 18, 2025).
[70] L. Pickert, H2 Förderkompass - Kriterien und Instrumente zur Förderung von Wasserstoffanwendungen für den Markthochlauf, (2022).
[71] P. Mastropietro, P. Rodilla, A taxonomy of support mechanisms for the low-carbon hydrogen supply chain, International Journal of Hydrogen Energy 105 (2025) 169–178. https://doi.org/10.1016/j.ijhydene.2025.01.275.
[72] M. Zardoshti Zadeh Yazdi, G. Walther, Analyzing policy measures for renewable fuel supply chain design in transport sectors, Transportation Research Part D: Transport and Environment 144 (2025) 104789. https://doi.org/10.1016/j.trd.2025.104789.
[73] Airlines for Europe, The Cost and Profitability of European Airports How Effective is Regulation under the Airport Charges Directive?, 2017. https://a4e.eu/wp-content/uploads/a4e-study-york-aviation-the-cost-and-profitability-of-european-airports-2017-08-04.pdf (accessed January 13, 2025).
[74] IATA, Value Chain Profitability, (2006).
[75] KPMG, Cost of Capital Study 2023, 2023.
[76] IEA, World Energy Investment 2024, (2024).
[77] OECD, Bridging the clean energy investment gap: Cost of capital in the transition to net-zero emissions, 2024. https://one.oecd.org/document/ENV/WKP(2024)15/REV1/en/pdf (accessed January 13, 2025).
[78] Fraunhofer ISE, Stromgestehungskosten Erneuerbare Energien, (2024).
[79] bp, bp Annual Report and Form 20-F 2023, 2024. https://www.bp.com/content/dam/bp/business-sites/en/global/corporate/pdfs/investors/bp-annual-report-and-form-20f-financial-statements-2023.pdf (accessed August 13, 2025).
[80] Shell, Shell Annual Report and Accounts 2014 - Financial Statements and Supplements, 2025. https://www.shell.com/investors/results-and-reporting/annual-report/_jcr_content/root/main/section_2113846431/link_list/links/item3.stream/1742873107360/49960c3d82d1be73613bc3aa9e62863ae5eb3dc2/consolidated-financial-statements-ar24.pdf (accessed August 13, 2025).

[81] D. Riedl, The magnitude of energy transition risk embedded in fossil fuel company valuations, Heliyon 7 (2021) e08400. https://doi.org/10.1016/j.heliyon.2021.e08400.
[82] European Commission, Commission approves up to €6.9 billion of State aid by seven Member States for the third Important Project of Common European Interest in the hydrogen value chain, 2024.
[83] European Commission, Commission approves €3 billion German State aid scheme to support the development of Hydrogen Core Network, (2024). https://ec.europa.eu/commission/presscorner/api/files/document/print/en/ip_24_3405/IP_24_3405_EN.pdf (accessed June 26, 2025).
[84] OECD, Financing solutions to foster industrial decarbonisation in emerging and developing economies, Organisation for Economic Co-Operation and Development (OECD), 2023. https://doi.org/10.1787/24a155ab-en.
[85] EUROPEAN PARLIAMENT, EU Investment Protection Law: Article-by-Article Commentary, 2023. https://doi.org/10.5040/9781509968374.
[86] KFW, "Green Bonds – Made by KfW" Framework 2024, 2024. https://www.kfw.de/PDF/Investor-Relations/PDF-Dokumente-Green-Bonds/20231206-KfW-Green-Bond-Framework.pdf#page=8.24 (accessed June 26, 2025).
[87] DOE, DOE Announces $1.66 Billion Loan Guarantee to Plug Power to Produce and Liquify Clean Hydrogen Fuel, Energy.Gov (2025). https://www.energy.gov/lpo/articles/doe-announces-166-billion-loan-guarantee-plug-power-produce-and-liquify-clean-hydrogen (accessed June 26, 2025).
[88] Hydrogen Europe, The European Hydrogen Bank Kickstarting the European hydrogen market, 2023. https://hydrogeneurope.eu/wp-content/uploads/2023/03/2023.03_Hydrogen-Bank_H2Europe_paper.pdf (accessed January 14, 2025).
[89] H2Global Foundation, H2Global – Idea, Instrument and Intentions, (2023).
[90] European Commission, The EU Emissions Trading System (EU ETS), 2016. https://climate.ec.europa.eu/document/download/5dee0b48-a38f-4d10-bf1a-14d0c1d6febd_en?filename=factsheet_ets_en.pdf (accessed June 26, 2025).
[91] ICCT, Final regulations for the Inflation Reduction Act's Section 45V Clean Hydrogen Production Tax Credit, (2025).
[92] FfE, Superabschreibungen, (2022). https://www.ffe.de/wp-content/uploads/2022/06/Infografik-Was-sind-Superabschreibungen.pdf (accessed June 26, 2025).
[93] NOW, Renewable Energy Directive III (RED III), 2024. https://www.now-gmbh.de/wp-content/uploads/2024/01/Factsheet_REDIII.pdf (accessed June 26, 2025).
[94] European Commission, Regulation (EU) 2023/2405 of the European Parliament and of the Council of 18 October 2023 on ensuring a level playing field for sustainable air transport (ReFuelEU Aviation), 2024.
[95] Le Ministère de l'Économie, Investing in low-carbon energy and deep decarbonisation in France, 2023. https://www.economie.gouv.fr/files/files/2023/DP_Paris_deep_decarbonisation_EN.pdf (accessed June 26, 2025).
[96] European Commission, IPCEI: EU-Kommission gibt grünes Licht zur Förderung von Wasserstofftechnologie – auch in Deutschland - Europäische Kommission, (2022). https://germany.representation.ec.europa.eu/news/ipcei-eu-kommission-gibt-grunes-licht-zur-forderung-von-wasserstofftechnologie-auch-deutschland-2022-07-15_de (accessed March 18, 2025).
[97] European Hydrogen Observatory, The European hydrogen market landscape, 2024.
[98] S.-L. Penttinen, Navigating the hydrogen landscape: An analysis of hydrogen support mechanisms in the US and the EU, Review of European, Comparative & International Environmental Law 33 (2024) 397–411. https://doi.org/10.1111/reel.12575.
[99] European Commission, Guidelines on State aid for climate, environmental protection and energy 2022, 2021. https://eur-lex.europa.eu/resource.html?uri=cellar:65072bf9-627f-11ec-a033-01aa75ed71a1.0001.02/DOC_2&format=PDF (accessed July 16, 2025).
[100] World Bank, GDP (current US$), (2025). https://api.worldbank.org/v2/en/indicator/NY.GDP.MKTP.CD?downloadformat=excel (accessed October 7, 2025).
[101] World Bank, Air transport, passengers carried, (2025). https://api.worldbank.org/v2/en/indicator/IS.AIR.PSGR?downloadformat=excel (accessed October 7, 2025).
[102] United Nations Conference on Trade and Development, World Investment Report 2025, (n.d.). https://unctad.org/system/files/official-document/wir2025_en.pdf.
[103] FFP, Fragile States Index 2024, (2025). https://fragilestatesindex.org/global-data/.
[104] P. Benalcazar, A. Komorowska, Techno-economic analysis and uncertainty assessment of green hydrogen production in future exporting countries, Renewable and Sustainable Energy Reviews 199 (2024) 114512. https://doi.org/10.1016/j.rser.2024.114512.
[105] D. Franzmann, H. Heinrichs, F. Lippkau, T. Addanki, C. Winkler, P. Buchenberg, T. Hamacher, M. Blesl, J. Linßen, D. Stolten, Green hydrogen cost-potentials for global trade, International Journal of Hydrogen Energy 48 (2023) 33062–33076. https://doi.org/10.1016/j.ijhydene.2023.05.012.
[106] M.G. Gado, H. Hassan, Potential of prospective plans in MENA countries for green hydrogen generation driven by solar and wind power sources, Solar Energy 263 (2023) 111942. https://doi.org/10.1016/j.solener.2023.111942.
[107] M.G. Gado, Techno-economic-environmental assessment of green hydrogen production for selected countries in the Middle East, International Journal of Hydrogen Energy 92 (2024) 984–999. https://doi.org/10.1016/j.ijhydene.2024.10.272.
[108] M. Nasser, H. Hassan, Feasibility analysis and Atlas for green hydrogen project in MENA region: Production, cost, and environmental maps, Solar Energy 268 (2024) 112326. https://doi.org/10.1016/j.solener.2024.112326.
[109] F. Plank, B. Daum, J. Muntschick, M. Knodt, C. Hasse, I. Ott, A. Niemann, Hydrogen: Fueling EU-Morocco Energy Cooperation?, Middle East Policy 30 (2023) 37–52. https://doi.org/10.1111/mepo.12699.
[110] A. Caillard, R. Yeganyan, C. Cannone, F. Plazas-Niño, M. Howells, A Critical Analysis of Morocco's Green Hydrogen Roadmap: A Modelling Approach to Assess Country Readiness from the Energy Trilemma Perspective, Climate 12 (2024) 61. https://doi.org/10.3390/cli12050061.
[111] Deutsche Gesellschaft für Internationale Zusammenarbeit (GIZ) GmbH, German-Moroccan Energy Partnership, (2024). https://www.giz.de/en/worldwide/152595.html.
[112] Federal Ministry for Economic Cooperation and Development, Providing climate-friendly energy, Core Area "Climate and Energy, Just Transition" (2023). https://www.bmz.de/en/countries/morocco/core-area-climate-and-energy-just-transition-169858#:~:text=The%20expected%20rise%20in%20global,future%20back%20in%20June%202020.
[113] KfW Development Bank, Energy of the future, Sustainable Production of Hydrogen (2024). https://www.kfw-entwicklungsbank.de/Global/North-Africa-and-Middle-East/Project-information_Morocco_Hydrogen_2024/.
[114] SEFE Securing Energy for Europe GmbH, SEFE and Saudi ACWA Power partner to deliver 200,000 tonnes of green hydrogen annually to Germany and Europe, (n.d.). https://www.sefe.eu/en/media/files/press-releases/2025/250203_en_pressrelease_sefe_and_saudi_acwa_power_green_hydrogen.pdf.
[115] Federal Ministry for Economic Affairs and Climate Action, Hydrogen cooperation potential between Saudi Arabia and Germany, (2022). https://www.bundeswirtschaftsministerium.de/Redaktion/EN/Downloads/J/joint-study-saudi-german-energy-dialogue.pdf?__blob=publicationFile&v=1.
[116] M. Michailidis, E. Zafeiriou, A. Kantartzis, S. Galatsidas, G. Arabatzis, Governance, Energy Policy, and Sustainable Development: Renewable Energy Infrastructure Transition in Developing MENA Countries, Energies 18 (2025) 2759. https://doi.org/10.3390/en18112759.
[117] J.F. Braun, F. Frischmuth, N. Gerhardt, M. Pfennig, R. Schmitz, M. Wietschel, B. Carlier, A. Réveillère, G. Warluzel, D. Wesoly, Clean Hydrogen Deployment in the Europe-MENA Region from 2030 to 2050. A Technical and Socio-Economic Assessment, (2020) 49.
[118] G. Kakoulaki, I. Kougias, N. Taylor, F. Dolci, J. Moya, A. Jäger-Waldau, Green hydrogen in Europe – A regional assessment: Substituting existing production with electrolysis powered by renewables, Energy Conversion and Management 228 (2021) 113649. https://doi.org/10.1016/j.enconman.2020.113649.

[119] N. Wolf, M.A. Tanneberger, M. Höck, Levelized cost of hydrogen production in Northern Africa and Europe in 2050: A Monte Carlo simulation for Germany, Norway, Spain, Algeria, Morocco, and Egypt, International Journal of Hydrogen Energy 69 (2024) 184–194. https://doi.org/10.1016/j.ijhydene.2024.04.319.
[120] C. Back, L. González-Morán, A. Iranzo, Green hydrogen from renewable surplus: Production and storage potential in Spain's 2040 energy horizon, International Journal of Hydrogen Energy 140 (2025) 2–10. https://doi.org/10.1016/j.ijhydene.2025.05.221.
[121] X.L. Fernández, P. Coto-Millán, B. Díaz-Medina, The impact of tourism on airport efficiency: The Spanish case, Utilities Policy 55 (2018) 52–58. https://doi.org/10.1016/j.jup.2018.09.002.
[122] D. Balsalobre-Lorente, O.M. Driha, F.V. Bekun, F.F. Adedoyin, The asymmetric impact of air transport on economic growth in Spain: fresh evidence from the tourism-led growth hypothesis, Current Issues in Tourism 24 (2021) 503–519. https://doi.org/10.1080/13683500.2020.1720624.
[123] N. Wolf, L. Kühn, M. Höck, International supply chains for a hydrogen ramp-up: Techno-economic assessment of hydrogen transport routes to Germany, Energy Conversion and Management: X 23 (2024) 100682. https://doi.org/10.1016/j.ecmx.2024.100682.
[124] R. Quitzow, A. Nunez, A. Marian, Positioning Germany in an international hydrogen economy: A policy review, Energy Strategy Reviews 53 (2024) 101361. https://doi.org/10.1016/j.esr.2024.101361.
[125] F. Peterssen, M. Schlemminger, C. Lohr, R. Niepelt, A. Bensmann, R. Hanke-Rauschenbach, R. Brendel, Hydrogen supply scenarios for a climate neutral energy system in Germany, International Journal of Hydrogen Energy 47 (2022) 13515–13523. https://doi.org/10.1016/j.ijhydene.2022.02.098.
[126] P. Suau-Sanchez, A. Voltes-Dorta, H. Rodríguez-Déniz, The role of London airports in providing connectivity for the UK: regional dependence on foreign hubs, Journal of Transport Geography 50 (2016) 94–104. https://doi.org/10.1016/j.jtrangeo.2014.11.008.
[127] K. Kendall, Green Hydrogen in the UK: Progress and Prospects, Clean Technol. 4 (2022) 345–355. https://doi.org/10.3390/cleantechnol4020020.
[128] A. Giampieri, J. Ling-Chin, A.P. Roskilly, Techno-economic assessment of offshore wind-to-hydrogen scenarios: A UK case study, International Journal of Hydrogen Energy 52 (2024) 589–617. https://doi.org/10.1016/j.ijhydene.2023.01.346.
[129] A.M. Habib, U.N. Kayani, Price reaction of global economic indicators: evidence from the COVID-19 pandemic and the Russia–Ukraine conflict, SN Bus Econ 4 (2024). https://doi.org/10.1007/s43546-023-00619-w.
[130] J. Hoelzen, L. Koenemann, L. Kistner, F. Schenke, A. Bensmann, R. Hanke-Rauschenbach, H2-powered aviation – Design and economics of green LH2 supply for airports, Energy Conversion and Management: X 20 (2023) 100442. https://doi.org/10.1016/j.ecmx.2023.100442.
[131] V.P. Müller, W. Eichhammer, Economic complexity of green hydrogen production technologies - a trade data-based analysis of country-specific industrial preconditions, Renewable and Sustainable Energy Reviews 182 (2023) 113304. https://doi.org/10.1016/j.rser.2023.113304.
[132] S.R. Ersoy, J. Terrapon-Pfaff, T. Pregger, J. Braun, E.M. Jamea, A. Al-Salaymeh, P. Braunschweig, Z. Bereschi, O.T. Ciobotaru, P. Viebahn, Industrial and infrastructural conditions for production and export of green hydrogen and synthetic fuels in the MENA region: insights from Jordan, Morocco, and Oman, Sustain Sci 19 (2024) 207–222. https://doi.org/10.1007/s11625-023-01382-5.
[133] M. Wappler, D. Unguder, X. Lu, H. Ohlmeyer, H. Teschke, W. Lueke, Building the green hydrogen market – Current state and outlook on green hydrogen demand and electrolyzer manufacturing, International Journal of Hydrogen Energy 47 (2022) 33551–33570. https://doi.org/10.1016/j.ijhydene.2022.07.253.
[134] M. Leseure, C.E. Onyeocha, D. Robins, Stimulating investments in manufacturing: can policy create supply chains from a void?, JMTM 35 (2024) 1397–1415. https://doi.org/10.1108/JMTM-10-2023-0479.
[135] F. Scheifele, M. Bräuning, B. Probst, The impact of local content requirements on the development of export competitiveness in solar and wind technologies, Renewable and Sustainable Energy Reviews 168 (2022) 112831. https://doi.org/10.1016/j.rser.2022.112831.
[136] S. Semelane, N. Nwulu, N. Kambule, H. Tazvinga, Evaluating economic impacts of utility scale solar photovoltaic localisation in South Africa, Energy Sources, Part B: Economics, Planning, and Policy 16 (2021) 324–344. https://doi.org/10.1080/15567249.2021.1894513.
[137] T. Wuttke, Global Value Chains and Local Inter-Industry Linkages: South Africa's Participation in the Automotive GVC, The Journal of Development Studies 59 (2023) 153–169. https://doi.org/10.1080/00220388.2022.2110491.
[138] M. Lee, D. Saygin, Financing cost impacts on cost competitiveness of green hydrogen in emerging and developing economies, OECD Environment Working Papers 227 (2023). https://doi.org/10.1787/15b16fc3-en.
[139] F. Taghizadeh-Hesary, Y. Li, E. Rasoulinezhad, A. Mortha, Y. Long, Y. Lan, Z. Zhang, N. Li, X. Zhao, Y. Wang, Green finance and the economic feasibility of hydrogen projects, International Journal of Hydrogen Energy 47 (2022) 24511–24522. https://doi.org/10.1016/j.ijhydene.2022.01.111.
[140] K. Imasiku, A. Ballo, K.V. Koffi, F. Farirai, S.N. Agbo, J. Olwoch, B. Korgo, K.O. Ogunjobi, D. Koné, M. Savadogo, T. Budzanani, Potential Financing Mechanisms for Green Hydrogen Development in Sub-Saharan Africa, Hydrogen 6 (2025) 59. https://doi.org/10.3390/hydrogen6030059.
[141] D. Gabor, N.S. Sylla, Derisking Developmentalism: A Tale of Green Hydrogen, Development and Change 54 (2023) 1169–1196. https://doi.org/10.1111/dech.12779.
[142] M. Lambert, A. Barnes, A. Marcu, O. Imbault, A. Bhashyam, M. Tengler, C. Cavallera, G. Romeo, 2024 State of the European Hydrogen Market Report, (2024) 34.
[143] A. Herranz-Surralles, The EU Energy Transition in a Geopoliticizing World, Geopolitics 29 (2024) 1882–1912. https://doi.org/10.1080/14650045.2023.2283489.
[144] G. Allan, D. Comerford, K. Connolly, P. McGregor, A.G. Ross, The economic and environmental impacts of UK offshore wind development: The importance of local content, Energy 199 (2020) 117436. https://doi.org/10.1016/j.energy.2020.117436.
[145] A. Nuñez-Jimenez, N. Blasio, Competitive and secure renewable hydrogen markets: Three strategic scenarios for the European Union, International Journal of Hydrogen Energy 47 (2022) 35553–35570. https://doi.org/10.1016/j.ijhydene.2022.08.170.
[146] European Parliament, Critical technologies: how the EU supports key industries, (2023). https://www.europarl.europa.eu/topics/en/article/20231012STO07016/critical-technologies-how-the-eu-supports-key-industries#why-does-the-eu-need-to-invest-in-technologies--5 (accessed September 18, 2025).
[147] U.F. Saeed, A.K. Twum, G.E. Klugah, Navigating Carbon Peaking and Neutrality in MENA: The Impact of Foreign Direct Investment and Trade Openness Using Panel PCSE and FGLS Techniques, Environmental Quality Mgmt 34 (2024). https://doi.org/10.1002/tqem.22352.
[148] H. Hamdi, A. Hakimi, Trade Openness, Foreign Direct Investment, and Human Development: A Panel Cointegration Analysis for MENA Countries, The International Trade Journal 36 (2022) 219–238. https://doi.org/10.1080/08853908.2021.1905115.
[149] United Nations, UN Comtrade Database, (2025). https://comtradeplus.un.org/.
[150] A. Odenweller, F. Ueckerdt, The green hydrogen ambition and implementation gap, Nat Energy 10 (2025) 110–123. https://doi.org/10.1038/s41560-024-01684-7.
[151] A. Odenweller, F. Ueckerdt, G.F. Nemet, M. Jensterle, G. Luderer, Probabilistic feasibility space of scaling up green hydrogen supply, Nat Energy 7 (2022) 854–865. https://doi.org/10.1038/s41560-022-01097-4.
[152] A.H. Azadnia, C. McDaid, A.M. Andwari, S.E. Hosseini, Green hydrogen supply chain risk analysis: A european hard-to-abate sectors perspective, Renewable and Sustainable Energy Reviews 182 (2023) 113371. https://doi.org/10.1016/j.rser.2023.113371.
[153] R.E. Miller, P.D. Blair, Input-Output Analysis, Cambridge University Press, 2012. https://doi.org/10.1017/CBO9780511626982.
[154] L. Zeng, H. Chen, M. Chen, X. Zhao, Resilience assessment of the aircraft manufacturing core products supply chain: the international trade network perspective, Ann Oper Res (2024). https://doi.org/10.1007/s10479-024-06359-w.
[155] B. Sarh, J. Buttrick, C. Munk, R. Bossi, eds., Aircraft Manufacturing and Assembly, n.d. https://doi.org/10.1007/978-3-540-78831-7_51.

[156] J. Pauwels, S. Buyle, W. Dewulf, B. Jourquin, Reconsidering airport economic impact assessments: A bottom-up comparative analysis of Belgian airports, Journal of Air Transport Management 128 (2025) 102854. https://doi.org/10.1016/j.jairtraman.2025.102854.
[157] J. Hakfoort, T. Poot, P. Rietveld, The Regional Economic Impact of an Airport: The Case of Amsterdam Schiphol Airport, Regional Studies 35 (2001) 595–604. https://doi.org/10.1080/00343400120075867.
[158] M.G. Alatriste-Contreras, The relationship between the key sectors in the european union economy and the intra-European Union trade, Economic Structures 4 (2015). https://doi.org/10.1186/s40008-015-0024-5.
[159] J. Wensveen, Air Transportation, Routledge, London, 2023. https://doi.org/10.4324/9780429346156.
[160] F. Zhang, D.J. Graham, Air transport and economic growth: a review of the impact mechanism and causal relationships, Transport Reviews 40 (2020) 506–528. https://doi.org/10.1080/01441647.2020.1738587.
[161] P. Ulrich, M. Distelkamp, U. Lehr, Employment Effects of Renewable Energy Expansion on a Regional Level—First Results of a Model-Based Approach for Germany, Sustainability 4 (2012) 227–243. https://doi.org/10.3390/su4020227.
[162] T. Ejdemo, P. Söderholm, Wind power, regional development and benefit-sharing: The case of Northern Sweden, Renewable and Sustainable Energy Reviews 47 (2015) 476–485. https://doi.org/10.1016/j.rser.2015.03.082.
[163] World Population Review, Median Income by Country, (n.d.). https://worldpopulationreview.com/country-rankings/median-income-by-country.
[164] ILOSTAT, Statistics on labour productivity, (2024). https://ilostat.ilo.org/topics/labour-productivity/.
[165] Eurostat, Households - statistics on income, saving and investment, (2024). https://ec.europa.eu/eurostat/statistics-explained/index.php?title=Households_-_statistics_on_income,_saving_and_investment.
[166] OECD, Taxing Wages 2025, (2025). https://doi.org/10.1787/b3a95829-en.
[167] B. Christophers, The rentierization of the United Kingdom economy, Environ Plan A 55 (2023) 1438–1470. https://doi.org/10.1177/0308518X19873007.
[168] S. High, "The Wounds of Class": A Historiographical Reflection on the Study of Deindustrialization, 1973–2013, History Compass 11 (2013) 994–1007. https://doi.org/10.1111/hic3.12099.
[169] N. Elhefnawy, Comparative Deindustrialization: A Note on American and British Manufacturing Since the 1970s, SSRN Journal (2021). https://doi.org/10.2139/ssrn.3873241.
[170] M. Javid, F.J. Hasanov, Determinants of remittance outflows: The case of Saudi Arabia, OPEC Energy Review 47 (2023) 320–335. https://doi.org/10.1111/opec.12291.
[171] S. Hathroubi, C. Aloui, On interactions between remittance outflows and Saudi Arabian macroeconomy: New evidence from wavelets, Economic Modelling 59 (2016) 32–45. https://doi.org/10.1016/j.econmod.2016.06.018.
[172] K.A. Alkhathlan, The nexus between remittance outflows and growth: A study of Saudi Arabia, Economic Modelling 33 (2013) 695–700. https://doi.org/10.1016/j.econmod.2013.05.010.
[173] United Nations, World Income Inequality Database (WIID), (2023). https://doi.org/10.35188/UNU-WIDER/WIID-281123.
[174] V. Chang, Y. Chen, Z. Zhang, Q.A. Xu, P. Baudier, B.S.C. Liu, The market challenge of wind turbine industry-renewable energy in PR China and Germany, Technological Forecasting and Social Change 166 (2021) 120631. https://doi.org/10.1016/j.techfore.2021.120631.
[175] A. Ibourk, Z. Elouaourti, Structural transformation in Morocco: an early tertiarization, IJDI 24 (2025) 207–225. https://doi.org/10.1108/IJDI-04-2024-0119.
[176] C.-E. Moussir, A. Chatri, Structural change and labour productivity growth in Morocco, Structural Change and Economic Dynamics 53 (2020) 353–358. https://doi.org/10.1016/j.strueco.2019.06.005.
[177] T. Němečková, Morocco as emerging regional economic power?, The Journal of North African Studies 26 (2021) 51–72. https://doi.org/10.1080/13629387.2019.1657843.
[178] R.B. Ayed Mouelhi, M. Ghazali, Structural transformation in Egypt, Morocco and Tunisia: Patterns, drivers and constraints, Econ of Transit and Inst Chang 29 (2021) 35–61. https://doi.org/10.1111/ecot.12258.
[179] O. McPherson-Smith, Diversification, Khashoggi, and Saudi Arabia's Public Investment Fund, Global Policy 12 (2021) 190–203. https://doi.org/10.1111/1758-5899.12917.
[180] A. Montambault Trudelle, The Public Investment Fund and Salman's state: the political drivers of sovereign wealth management in Saudi Arabia, Review of International Political Economy 30 (2023) 747–771. https://doi.org/10.1080/09692290.2022.2069143.
[181] S.M. Al Naimi, Economic Diversification Trends in the Gulf: the Case of Saudi Arabia, Circular Economy and Sustainability 2 (2022) 221–230. https://doi.org/10.1007/s43615-021-00106-0.
[182] B.A. Albassam, Economic diversification in Saudi Arabia: Myth or reality?, Resources Policy 44 (2015) 112–117. https://doi.org/10.1016/j.resourpol.2015.02.005.
[183] Eurostat, Labour market statistics at regional level, (2025). https://ec.europa.eu/eurostat/statistics-explained/index.php?title=Labour_market_statistics_at_regional_level.
[184] A. Mason, R. Lee, Six Ways Population Change Will Affect the Global Economy, Population & Development Rev 48 (2022) 51–73. https://doi.org/10.1111/padr.12469.
[185] M. Cristea, G.G. Noja, P. Stefea, A.L. Sala, The Impact of Population Aging and Public Health Support on EU Labor Markets, International Journal of Environmental Research and Public Health 17 (2020). https://doi.org/10.3390/ijerph17041439.
[186] G. Bonoli, P. Emmenegger, A. Felder-Stindt, Re-Skilling in the Age of Skill Shortage: Adult Education Rather Than Active Labor Market Policy, Regulation & Governance (2025). https://doi.org/10.1111/rego.70065.
[187] B. Brucker Juricic, M. Galic, S. Marenjak, Review of the Construction Labour Demand and Shortages in the EU, Buildings 11 (2021) 17. https://doi.org/10.3390/buildings11010017.
[188] L. Eicke, N. Blasio, Green hydrogen value chains in the industrial sector—Geopolitical and market implications, Energy Research & Social Science 93 (2022) 102847. https://doi.org/10.1016/j.erss.2022.102847.
[189] J. Tunn, F. Müller, J. Hennig, J. Simon, T. Kalt, The German scramble for green hydrogen in Namibia: Colonial legacies revisited?, Political Geography 118 (2025) 103293. https://doi.org/10.1016/j.polgeo.2025.103293.
[190] J. Tunn, T. Kalt, F. Müller, J. Simon, J. Hennig, I. Ituen, N. Glatzer, Green hydrogen transitions deepen socioecological risks and extractivist patterns: evidence from 28 prospective exporting countries in the Global South, Energy Research & Social Science 117 (2024) 103731. https://doi.org/10.1016/j.erss.2024.103731.
[191] A.G. Dagnachew, S.G. Yalew, M. Tesfamichael, C. Okereke, E. Abraham, A green hydrogen revolution in Africa remains elusive under current geopolitical realities, Climate Policy 25 (2025) 291–302. https://doi.org/10.1080/14693062.2024.2376740.
[192] T. van de Graaf, I. Overland, D. Scholten, K. Westphal, The new oil? The geopolitics and international governance of hydrogen, Energy Research & Social Science 70 (2020) 101667. https://doi.org/10.1016/j.erss.2020.101667.
[193] K. Beasy, S. Emery, K. Pryor, T.A. Vo, Skilling the green hydrogen economy: A case study from Australia, International Journal of Hydrogen Energy 48 (2023) 19811–19820. https://doi.org/10.1016/j.ijhydene.2023.02.061.
[194] F. Egli, F. Schneider, A. Leonard, C. Halloran, N. Salmon, T. Schmidt, S. Hirmer, Mapping the cost competitiveness of African green hydrogen imports to Europe, Nat Energy (2025). https://doi.org/10.1038/s41560-025-01768-y.
[195] S. Scholvin, A. Black, G. Robbins, De-risking green hydrogen? Insights from Chile and South Africa, Energy Policy 198 (2025) 114485. https://doi.org/10.1016/j.enpol.2024.114485.

[196] M. Blohm, F. Dettner, Green hydrogen production: Integrating environmental and social criteria to ensure sustainability, Smart Energy 11 (2023) 100112. https://doi.org/10.1016/j.segy.2023.100112.
[197] U.F. Cardella, Large-scale hydrogen liquefaction under the aspect of economic viability, Dissertation, Technical University of Munich, 2018.
[198] T. Zhang, J. Uratani, Y. Huang, L. Xu, S. Griffiths, Hydrogen liquefaction and storage: Recent progress and perspectives, Renew. Sustain. Energy Rev. 176 (2023) 113204. https://doi.org/10.1016/j.rser.2023.113204.
[199] C. Wolf, F. Primke, A. Alekseev, S. Rehfeldt, H. Klein, Validation of a Thermodynamic Model for the Liquid Hydrogen Distribution Utilizing Novel Data from an Operational Trailer, Available at SSRN: https://ssrn.com/abstract=5388184 (2025).
[200] Air Liquide, Hydrogen Liquefaction, (n.d.). https://engineering.airliquide.com/technologies/hydrogen-liquefaction.
[201] R. Turton, Analysis, synthesis, and design of chemical processes, 5th edition, Prentice Hall, Boston, 2018.
[202] K. Ohlig, L. Decker, The latest developments and outlook for hydrogen liquefaction technology, in: AIP Conf. Proc., 2014: pp. 1311–1317. https://doi.org/10.1063/1.4860858.
[203] K. Stolzenburg, R. Mubbala, Integrated Design for Demonstration of Efficient Liquefaction of Hydrogen (IDEALHY), (2013).
[204] E. Conelly, M. Penev, A. Elgowainy, C. Hunter, DOE Hydrogen and Fuel Cells Program Record: Current Status of Hydrogen Liquefaction Costs, (2019).
[205] L. Stops, D. Siebe, A. Stary, J. Hamacher, V. Sidarava, S. Rehfeldt, H. Klein, Generalized thermodynamic modeling of hydrogen storage tanks for truck application, Cryogenics 139 (2024) 103826. https://doi.org/10.1016/j.cryogenics.2024.103826.
[206] M. Asadnia, M. Mehrpooya, A novel hydrogen liquefaction process configuration with combined mixed refrigerant systems, Int. J. Hydrog. Energy 42 (2017) 15564–15585. https://doi.org/10.1016/j.ijhydene.2017.04.260.
[207] D. Berstad, G. Skaugen, Ø. Wilhelmsen, Dissecting the exergy balance of a hydrogen liquefier: Analysis of a scaled-up claude hydrogen liquefier with mixed refrigerant pre-cooling, International Journal of Hydrogen Energy 46 (2021) 8014–8029.
[208] S. Krasae-in, Optimal operation of a large-scale liquid hydrogen plant utilizing mixed fluid refrigeration system, Int. J. Hydrog. Energy 39 (2014) 7015–7029. https://doi.org/10.1016/j.ijhydene.2014.02.046.
[209] Nexant Inc., Air Liquide, Argonne National Laboratory, Chevron Technology Venture, Gas Technology Institute, National Renewable Energy Laboratory, Pacific Northwest National Laboratory, TIAX LLC, 2H2A Hydrogen Delivery Infrastructure Analysis Models and Conventional Pathway Options Analysis Results: Interim Report, (2008).
[210] K. Ohira, A Summary of Liquid Hydrogen and Cryogenic Technologies in Japan's WE-NET Project, in: AIP Conf. Proc., 2004: pp. 27–34. https://doi.org/10.1063/1.1774663.
[211] H. Quack, Conceptual design of a high efficiency large capacity hydrogen liquefier, in: AIP Conf. Proc., 2002: pp. 255–263. https://doi.org/10.1063/1.1472029.
[212] F. Restelli, E. Spatolisano, L.A. Pellegrini, S. Cattaneo, A.R. de Angelis, A. Lainati, E. Roccaro, Liquefied hydrogen value chain: A detailed techno-economic evaluation for its application in the industrial and mobility sectors, Int. J. Hydrog. Energy 52 (2024) 454–466. https://doi.org/10.1016/j.ijhydene.2023.10.107.
[213] M.S. Sadaghiani, M. Mehrpooya, Introducing and energy analysis of a novel cryogenic hydrogen liquefaction process configuration, Int. J. Hydrog. Energy 42 (2017) 6033–6050. https://doi.org/10.1016/j.ijhydene.2017.01.136.
[214] H. Son, T. Yu, J. Hwang, Y. Lim, Simulation methodology for hydrogen liquefaction process design considering hydrogen characteristics, Int. J. Hydrog. Energy 47 (2022) 25662–25678. https://doi.org/10.1016/j.ijhydene.2022.05.293.
[215] K. Stolzenburg, R. Mubbala, Integrated Design for Demonstration of Efficient Liquefaction of Hydrogen (IDEALHY): Hydrogen Liquefaction Report, (2013).
[216] C. Yang, J. Ogden, Determining the lowest-cost hydrogen delivery mode, Int. J. Hydrog. Energy 32 (2007) 268–286. https://doi.org/10.1016/j.ijhydene.2006.05.009.
[217] K. Reddi, A. Elgowainy, D. Brown, DOE Hydrogen Fuel Cells Program Annual Merit Review: Hydrogen Delivery Infrastructure Analysis, (2016). https://doi.org/10.13140/RG.2.1.5159.8964.
[218] Swiss Group, Hydrogen in air transportation. Feasibility study for Zurich airport, Switzerland, Int. J. Hydrog. Energy 12 (1987) 571–585.
[219] D. Teichmann, W. Arlt, P. Wasserscheid, Liquid Organic Hydrogen Carriers as an efficient vector for the transport and storage of renewable energy, International Journal of Hydrogen Energy 37 (2012) 18118–18132. https://doi.org/10.1016/j.ijhydene.2012.08.066.
[220] Q. Hu, W. Shan, W. Zhang, Y. Li, W. Wang, J. Zhu, Y. Liu, B. Xie, X. Yu, Optimization and experiment on the dual nitrogen expansion liquefaction process with pre-cooling, Cryogenics 114 (2021) 103243. https://doi.org/10.1016/j.cryogenics.2020.103243.
[221] I. Seemann, C. Haberstroh, H. Quack, Efficient Large Scale Hydrogen Liquefaction, (2013).
[222] S. Wilkinson, F. Gerth, A Review of the Sustainability of Helium: An Assessment of Its Past, Present and a Zero-Carbon Future, Regional Science and Environmental Economics 1 (2025) 78–103. https://doi.org/10.3390/rsee1010006.
[223] European Comission, Airport-Level DemonstRatIon of Ground refuelling of Liquid Hydrogen for AviaTion (ALRIGH2T), (2024). https://cordis.europa.eu/project/id/101138105.
[224] Al Ghafri et al., Hydrogen liquefaction: a review of the fundamental physics, engineering practice and future opportunities, Energy Environ. Sci. 15 (2022) 2690–2731. https://doi.org/10.1039/D2EE00099G.
[225] Y. Liu, T. Guo, J. Shen, X. Kong, Q. Jiang, X. Tong, Optimization and Control Strategy of Hydrogen Liquefaction Process on Offshore Platform, in: 2024 9th International Conference on Clean Energy and Power Generation Technology (CEPGT), IEEE, 2024: pp. 5–9. https://doi.org/10.1109/CEPGT64143.2024.11064777.
[226] J. Göbelbecker, Wie sieht das neue Wasserstoff-Netz für Deutschland aus?, (2021). https://www.chemietechnik.de/energie-utilities/wasserstoff/plaene-fuer-ein-nationales-wasserstoff-netz-in-deutschland-341.html.
[227] J.L. Gillette, R.L. Kolpa, Overview of Interstate Hydrogen Pipeline Systems, (2007). https://www.corridoreis.anl.gov/documents/docs/technical/APT_61012_EVS_TM_08_2.pdf.
[228] P. Adam, R. Bode, M. Groissboeck, Readying pipeline compressor stations for 100% hydrogen, Turbomachinery Magazine (2020). https://www.turbomachinerymag.com/view/readying-pipeline-compressor-stations-for-100-hydrogen.
[229] J. Wulff, Wasserstoffspeicherung in Salzkavernen, (n.d.). https://www.neuman-esser.com/aktuelles-medien/magazin/wasserstoffspeicherung-in-salzkavernen/.
[230] M.P. Laban, Hydrogen storage in salt caverns: Chemical modelling and analysis of large-scale hydrogen storage in underground salt caverns, Master's Thesis, TU Delft, 2020.
[231] J.E. Fesmire, A.M. Swanger, A. Jacobson, B. Notardonato, Energy efficient large-scale storage of liquid hydrogen, in: Cryogenic Engineering Conference, 2021.
[232] CBI, Liquid hydrogen storage solutions, (2022). https://www.cbi.com/wp-content/uploads/2024/05/cbi-liquid-hydrogen-brochure-2022-digital.pdf.
[233] Kawasaki, Building a global shipping network for hydrogen, (n.d.). https://www.nature.com/articles/d42473-025-00001-4.
[234] Cryolor, Storage and transport of liquid hydrogen: Unique and innovative cryogenic equipment, (2023). https://www.cryolor.com/cryogenic-transport/liquid-hydrogen-transport.
[235] A. Alekseev, M.J. Wolf, T. Arndt, T. Jordan, A. Pundt, K.-P. Weiss, C. Schulz, C. Haberstroh, C. Wu, C. Wolf, P. Saß, D. Lindackers, J.S. Palacios Vera, Wasserstoff-Verflüssigung, Speicherung, Transport und Anwendung von flüssigem Wasserstoff, (n.d.). https://doi.org/10.5445/IR/1000155199.

[236] Cryostar, Liquid Hydrogen Transfer Pumps, (n.d.). https://cryostar-hydrogen-solutions.com/liquid-hydrogen-transfer-pumps/.
[237] V. Jusko, S.Z.S. Al Ghafri, E.F. May, BoilFAST: Cryogenic Boil-off Simulator, (2021).
[238] M. Sand, R.B. Skeie, M. Sandstad, S. Krishnan, G. Myhre, H. Bryant, R. Derwent, D. Hauglustaine, F. Paulot, M. Prather, D. Stevenson, A multi-model assessment of the Global Warming Potential of hydrogen, Commun Earth Environ 4 (2023) 203. https://doi.org/10.1038/s43247-023-00857-8.
[239] R.K. Ahluwalia, H.S. Roh, J.-K. Peng, D. Papadias, On-board liquid hydrogen storage for long haul trucks, (2022). https://www.energy.gov/sites/default/files/2022-03/Liquid%20H2%20Workshop-ANL2.pdf.
[240] G. Petitpas, Boil-off losses along LH2 pathway, 2018. https://doi.org/10.2172/1466121.
[241] Institut für Luft- und Kältetechnik gemeinnützige Gesellschaft mbH, Studie Wasserstoff-Technologie, 2025. https://fkt.com/forschungsberichte/bericht/?no_cache=1&tx_fktdocumentmanagment_fktdocmanager%5Bdocument%5D=212&tx_fktdocumentmanagment_fktdocmanager%5Baction%5D=detail&tx_fktdocumentmanagment_fktdocmanager%5Bcontroller%5D=Document (accessed October 20, 2025).
[242] C. Lohr, M. Schlemminger, F. Peterssen, D. Bredemeier, A. Mahner, L. Schomburg, R. Niepelt, A. Bensmann, M.H. Breitner, R. Hanke-Rauschenbach, R. Brendel, ESTRAM - ein Framework für die Erstellung und Optimierung von Energiesystemmodellen, (2025). https://doi.org/10.15488/18471.
[243] ENTSOG, ENTSO-E, TYNDP 2022 Scenario Building Guidelines | Version. April 2022, (2022).
[244] Guidehouse, EHB Implementation Roadmap: Public support as catalyst for hydrogen infrastructure, 2024. https://ehb.eu/files/downloads/EHB-2024-Implementation-Roadmap-Part-2.pdf (accessed November 26, 2024).
[245] J. Hoelzen, D. Silberhorn, T. Zill, B. Bensmann, R. Hanke-Rauschenbach, Hydrogen-powered aviation and its reliance on green hydrogen infrastructure – Review and research gaps, International Journal of Hydrogen Energy 47 (2022) 3108–3130. https://doi.org/10.1016/j.ijhydene.2021.10.239.
[246] IATA, Global Air Passenger Demand Reaches Record High in 2024, (2025). https://www.iata.org/en/pressroom/2025-releases/2025-01-30-01/ (accessed November 20, 2025).
[247] Airbus, Airbus Aircraft 2018 Average List Prices, (2018). https://web.archive.org/web/20180624175349/http://www.airbus.com/content/dam/corporate-topics/publications/backgrounders/Airbus-Commercial-Aircraft-list-prices-2018.pdf.
[248] N. Kylie, What Are The Operating Costs Of An Airbus A350?, Simple Flying (2025). https://simpleflying.com/operating-costs-airbus-a350/ (accessed November 20, 2025).
[249] Traiding economics, EU Carbon Permits, (2025). https://tradingeconomics.com/commodity/carbon (accessed November 20, 2025).
[250] S. Twidale, Analysts forecast EU carbon price rise, but say supply could swell, Reuters (2024). https://www.reuters.com/markets/commodities/analysts-forecast-eu-carbon-price-rise-say-supply-could-swell-2024-07-23/ (accessed November 20, 2025).
[251] Bloomberg NEF, EU ETS II Pricing Scenarios, (2025). https://assets.bbhub.io/promo/sites/16/EU_ETS_II_Pricing_Scenarios_Balancing_Cuts_and_Costs.pdf (accessed November 20, 2025).
[252] A. Ögrük, R. Marx, C. Thies, S. Stiller, Green Hydrogen Supply Chain Network Design for Aviation: Model Development and Case Study for German Airports in 2050, Operations Research Proceedings (2023).
[253] A. Öğrük, F. Schenke, H.-R. Richard, C. Thies, Design of hydrogen supply networks for aviation: dynamic optimization model and transition pathways for German airports, (2025). https://doi.org/10.15480/882.16268.
[254] Airbus, ZEROe Towards the world's first zero-emission commercial aircraft, (2022). https://www.airbus.com/en/innovation/zero-emission/hydrogen/zeroe (accessed March 17, 2022).
[255] J. Gerhardt-Mörsdorf, F. Peterssen, P. Burfeind, M. Benecke, B. Bensmann, R. Hanke-Rauschenbach, C. Minke, Life Cycle Assessment of a 5 MW Polymer Exchange Membrane Water Electrolysis Plant, Adv Energy and Sustain Res 5 (2024) 2300135. https://doi.org/10.1002/aesr.202300135.
[256] C. Tsiklios, M. Hermesmann, T.E. Müller, Hydrogen transport in large-scale transmission pipeline networks: Thermodynamic and environmental assessment of repurposed and new pipeline configurations, Applied Energy 327 (2022) 120097. https://doi.org/10.1016/j.apenergy.2022.120097.
[257] A. Arrigoni, F. Dolci, C.R. Ortiz, E. Weidner, T. D'agostini, U. Eynard, V. Santucci, F. Mathieux, Environmental life cycle assessment (LCA) comparison of hydrogen delivery options within Europe, JRC Publications Repository (2024). https://doi.org/10.2760/5459.
[258] H. Inframap, H2 Infrastructure Map Europe, (2022). https://www.h2inframap.eu/ (accessed April 29, 2025).
[259] F. Schenke, L. Koenemann, J. Hoelzen, T. Schelm, A. Bensmann, R. Hanke-Rauschenbach, LH2 supply infrastructure for H2-powered aviation: Business models, financing strategies and policy instruments, (2025). https://doi.org/10.2139/ssrn.5742382.
[260] OECD, The World Bank, United Nations Environment Programme, Financing Climate Futures: Rethinking Infrastructure, OECD, 2018. https://doi.org/10.1787/9789264308114-en.
[261] J. Brandt, T. Iversen, C. Eckert, F. Peterssen, B. Bensmann, A. Bensmann, M. Beer, H. Weyer, R. Hanke-Rauschenbach, Cost and competitiveness of green hydrogen and the effects of the European Union regulatory framework, Nat Energy (2024) 1–11. https://doi.org/10.1038/s41560-024-01511-z.
[262] European Communities, International Monetary Fund, Organisation for Economic Co-operation and Development, United Nations, World Bank, System of National Accounts 2008, (2009). https://unstats.un.org/unsd/nationalaccount/docs/sna2008.pdf.
[263] United Nations, Central Product Classification (CPC), Statistical Papers Series M No. 77, Ver.2.1 (2015). https://unstats.un.org/unsd/classifications/unsdclassifications/cpcv21.pdf.
[264] United Nations, European Union, Food and Agriculture Organization of the United Nations, International Monetary Fund, Organisation for Economic Co-operation and Development, World Bank, System of Environmental-Economic Accounting 2012 - Central Framework, (2014). https://seea.un.org/sites/seea.un.org/files/seea_cf_final_en.pdf.
[265] United Nations, System of Environmental-Economic Accounting for Energy, (2019). https://seea.un.org/sites/seea.un.org/files/documents/seea-energy_final_web.pdf.
[266] W.W. Leontief, Input-Output Economics, Scientific American 185 (1951) 15–21.
[267] J. Kowalewski, Methodology of the input-output analysis, HWWI Research Paper No. 1-25 (2009).
[268] M. Llop, A. Manresa, Income distribution in a regional economy: a SAM model, Journal of Policy Modeling 26 (2004) 689–702. https://doi.org/10.1016/j.jpolmod.2004.04.012.
[269] C. Breisinger, M. Thomas, J. Thurlow, Social accounting matrices and multiplier analysis An Introduction with Exercises, International Food Policy Research Institute, 2009. https://doi.org/10.2499/9780896297838fsp5.
[270] A. Ghosh, Input-Output Approach in an Allocation System, Economica 25 (1958) 58. https://doi.org/10.2307/2550694.
[271] B. Kretschmer, S. Peterson, Integrating bioenergy into computable general equilibrium models — A survey, Energy Economics 32 (2010) 673–686. https://doi.org/10.1016/j.eneco.2009.09.011.
[272] T. Mueller, E. Winter, U. Grote, Decarbonizing the aviation sector: Multiplier effects of power-to-liquid fuel production on the German economy, Sustainable Energy Technologies and Assessments 82 (2025) 104478. https://doi.org/10.1016/j.seta.2025.104478.
[273] K. Connolly, The regional economic impacts of offshore wind energy developments in Scotland, Renewable Energy 160 (2020) 148–159. https://doi.org/10.1016/j.renene.2020.06.065.
[274] D.-H. Lee, Development and environmental impact of hydrogen supply chain in Japan: Assessment by the CGE-LCA method in Japan with a discussion of the importance of biohydrogen, International Journal of Hydrogen Energy 39 (2014) 19294–19310. https://doi.org/10.1016/j.ijhydene.2014.05.142.

[275] D. Stamopoulos, P. Dimas, I. Sebos, A. Tsakanikas, Does Investing in Renewable Energy Sources Contribute to Growth? A Preliminary Study on Greece's National Energy and Climate Plan, Energies 14 (2021) 8537. https://doi.org/10.3390/en14248537.
[276] Harvard Growth Lab, The Atlas of Economic Complexity, Country & Product Complexity Rankings (n.d.). https://atlas.hks.harvard.edu/.
[277] Ember Energy Research, Yearly Electricity Data, (n.d.). https://storage.googleapis.com/emb-prod-bkt-publicdata/public-downloads/yearly_full_release_long_format.csv.
[278] MIT Technology Review, The Green Future Index 2023, (2023). https://www.technologyreview.com/2023/04/05/1070581/the-green-future-index-2023/.
[279] World Economic Forum, Fostering Effective Energy Transition 2025, (2025). https://reports.weforum.org/docs/WEF_Fostering_Effective_Energy_Transition_2025.pdf.
[280] H. Aray, L. Pedauga, A. Velázquez, Characterization of the Spanish Economy based on Sector linkages: IO, SAM and FSAM Multipliers, (2018). https://www.iioa.org/conferences/26th/papers/files/3303_20180515071_Brasil_IIOA_2018_MCSF_FF-AV.pdf.
[281] L. Shaw-Taylor, The growth of the service sector, (2025). https://www.campop.geog.cam.ac.uk/blog/2025/01/16/service-sector/.
[282] MARCO ESTRATÉGICO DE ENERGÍA Y CLIMA, HOJA DE RUTA DEL HIDRÓGENO: UNA APUESTA POR EL HIDRÓGENO RENOVABLE, (2020). https://www.miteco.gob.es/content/dam/miteco/es/ministerio/planes-estrategias/hidrogeno/hojarutahidrogenorenovable_tcm30-525000.PDF.
[283] Bundesministerium für Wirtschaft und Klimaschutz, Fortschreibung der Nationalen Wasserstoffstrategie, (2023). https://www.bmftr.bund.de/SharedDocs/Downloads/DE/20/230726-fortschreibung-nws.pdf?__blob=publicationFile&v=4.
[284] Secretary of State for Business, Energy and Industrial Strategy, Energy White Paper, (2020) 170.
[285] United Nations Children's Fund, Seizing the Opportunity: Ending AIDS in the Middle East and North Africa, (2019). https://www.unicef.org/mena/media/5531/file/HIV%20MENA%2029%20Sep%202019%20FINAL%5B2%5D.pdf%20.pdf.
[286] K. Gandhi, H. Apostoleris, S. Sgouridis, Catching the hydrogen train: economics-driven green hydrogen adoption potential in the United Arab Emirates, International Journal of Hydrogen Energy 47 (2022) 22285–22301. https://doi.org/10.1016/j.ijhydene.2022.05.055.
[287] D. Hjeij, Y. Biçer, M. Koç, Hydrogen strategy as an energy transition and economic transformation avenue for natural gas exporting countries: Qatar as a case study, International Journal of Hydrogen Energy 47 (2022) 4977–5009. https://doi.org/10.1016/j.ijhydene.2021.11.151.
[288] M.T. Islam, A. Ali, Sustainable green energy transition in Saudi Arabia: Characterizing policy framework, interrelations and future research directions, Next Energy 5 (2024) 100161. https://doi.org/10.1016/j.nxener.2024.100161.
[289] K. Choukri, A. Naddami, S. Hayani, Renewable energy in emergent countries: lessons from energy transition in Morocco, Energ Sustain Soc 7 (2017). https://doi.org/10.1186/s13705-017-0131-2.
[290] M.I. Sabry, The green transition in Morocco: Extractivity, inclusivity, and the stability of the social contract, The Extractive Industries and Society 22 (2025) 101614. https://doi.org/10.1016/j.exis.2025.101614.
[291] Royaume du Maroc, Feuille de Route de l'Hydrogène Vert, (2021) 32.
[292] Destatis, Input-Output-Rechnung, 2019 (Revision 2019, Stand: August 2023). (2024). https://www.statistischebibliothek.de/mir/receive/DEHeft_mods_00157241.
[293] Destatis, Volkswirtschaftliche Gesamtrechnungen / Sektorkonten / Jahresergebnisse ab 1991, 1991/2022 - 2023,08. Stand: August 2023 (2023). https://www.statistischebibliothek.de/mir/receive/DEHeft_mods_00151383.
[294] Banco de España, Series: Statistical Bulletin., (2023). https://www.bde.es/wbe/en/publicaciones/informacion-estadistica/boletin-estadistico/junio-2023.html.
[295] Instituto Nacional de Estadística, Annual Non-Financial Accounts by Institutional Sectors, 1995.2024 Series (2025). https://www.ine.es/dyngs/INEbase/en/operacion.htm?c=Estadistica_C&cid=1254736177054&menu=resultados&idp=1254735576581#_tabs-1254736195672.
[296] Instituto Nacional de Estadística, Annual Spanish National Accounts: Supply and Use Tables, (2025). https://www.ine.es/dyngs/INEbase/en/operacion.htm?c=Estadistica_C&cid=1254736177059&idp=1254735576581.
[297] Office for National Statistics, Industry (two, three and five-digit Standard Industrial Classification) – Business Register and Employment Survey (BRES): Table 2, 2019 (Revised) Edition of This Dataset (2025). https://www.ons.gov.uk/employmentandlabourmarket/peopleinwork/employmentandemployeetypes/datasets/industry235digitsicbusinessregisterandemploymentsurveybrestable2.
[298] Office for National Statistics, Broad Industry Group (Standard Industrial Classification) – Business Register and Employment Survey (BRES): Table 1, 2019 (Revised) Edition of This Dataset (2025). https://www.ons.gov.uk/employmentandlabourmarket/peopleinwork/employmentandemployeetypes/datasets/broadindustrygroupsicbusinessregisterandemploymentsurveybrestable1.
[299] Office for National Statistics, UK National Accounts, The Blue Book: 2023, (2023). https://www.ons.gov.uk/releases/uknationalaccountsthebluebook2023.
[300] Office for National Statistics, Input-output supply and use tables, (2025). https://www.ons.gov.uk/economy/nationalaccounts/supplyandusetables/datasets/inputoutputsupplyandusetables.
[301] Eurostat, Non-financial transactions - annual data, (2025). https://ec.europa.eu/eurostat/databrowser/view/nasa_10_nf_tr__custom_11888239/default/table.
[302] Eurostat, Employed persons by detailed economic activity (NACE Rev. 2 two-digit level) (2008-2026), (2025). https://ec.europa.eu/eurostat/databrowser/view/lfsa_egan22d__custom_13426957/default/table.
[303] Eurostat, Use table at basic prices, (2025). https://ec.europa.eu/eurostat/databrowser/view/naio_10_cp1610__custom_18820367/default/table.
[304] Eurostat, Supply table at basic prices incl. transformation into purchasers' prices, (2025). https://ec.europa.eu/eurostat/databrowser/view/naio_10_cp15__custom_18820309/default/table?page=time:2019.
[305] Eurostat, Table of trade and transport margins, (2025). https://ec.europa.eu/eurostat/databrowser/view/naio_10_cp1620__custom_18820466/default/table.
[306] Eurostat, Table of taxes less subsidies on product, (2025). https://ec.europa.eu/eurostat/databrowser/view/naio_10_cp1630__custom_18820507/default/table.
[307] Haut-Commissariat au Plan du Maroc, Economie, Publications Comptes Nationaux (n.d.). https://www.hcp.ma/Publications-Comptes-nationaux_r340.html.
[308] General Authority for Statistics, Supply and Use Tables and Input - Output Tables, Supply and Use Tables and Input-Output Tables by Sections (2018-2023) (2025). https://www.stats.gov.sa/en/statistics-tabs?tab=436312&category=419265.
[309] General Authority for Statistics, Gross Domestic Product Statistics, Annual National Accounts Publication 2024 (2025). https://www.stats.gov.sa/en/statistics-tabs?tab=436312&category=120038.
[310] General Authority for Statistics, Labor Force, Labour Market First Quarter 2019 (n.d.). https://www.stats.gov.sa/en/statistics-tabs?tab=436312&category=1333429&delta=20&start=2.
[311] V. Ramasamy, J. Zuboy, E. O'Shaughnessy, D. Feldman, J. Desai, M. Woodhouse, P. Basore, R. Margolis, U.S. Solar Photovoltaic System and Energy Storage Cost Benchmarks, With Minimum Sustainable Price Analysis: Q1 2022, (2022) 77.
[312] M. Woodhouse, D. Feldman, V. Ramasamy, B. Smith, T. Silverman, T. Barnes, J. Zuboy, R. Margolis, Research and Development Priorities to Advance Solar Photovoltaic Lifecycle Costs and Performance, (2021). https://docs.nrel.gov/docs/fy22osti/80505.pdf.
[313] T. Stehly, P. Duffy, D. Mulas Hernando, 2022 Cost of Wind Energy Review, (2023) 71.
[314] J. Bröcker, J. Burmeister, J.H. Preißler-Jebe, F. Alberty, Wertschöpfungs- und Beschäftigungseffekte als Folge des Ausbaus Erneuerbarer Energien in Schleswig-Holstein, Beiträge Aus Dem Institut Für Regionalforschung Der Universität Kiel (2014). https://www.re2.uni-kiel.de/de/archiv/forschung/IFR_EKSH_wertschoepfungEE.pdf.

[315] BVG Associates, Value breakdown for the offshore wind sector, A Report Commissioned by the Renewables Advisory Board (2010). https://assets.publishing.service.gov.uk/government/uploads/system/uploads/attachment_data/file/48171/2806-value-breakdown-offshore-wind-sector.pdf.
[316] B. Lee, H. Chae, N.H. Choi, C. Moon, S. Moon, H. Lim, Economic evaluation with sensitivity and profitability analysis for hydrogen production from water electrolysis in Korea, International Journal of Hydrogen Energy 42 (2017) 6462–6471. https://doi.org/10.1016/j.ijhydene.2016.12.153.
[317] A. Mayyas, M. Ruth, B. Pivovar, G. Bender, K. Wipke, Manufacturing Cost Analysis for Proton Exchange Membrane Water Electrolyzers, (2019) 65.
[318] M.P. Novoa, C. Rengifo, M. Cobo, M. Figueredo, Techno-economic assessment of the Synthetic Natural Gas production using different electrolysis technologies and product applications, International Journal of Hydrogen Energy 78 (2024) 889–900. https://doi.org/10.1016/j.ijhydene.2024.06.354.
[319] C. Yilmaz, Optimum energy evaluation and life cycle cost assessment of a hydrogen liquefaction system assisted by geothermal energy, International Journal of Hydrogen Energy 45 (2020) 3558–3568. https://doi.org/10.1016/j.ijhydene.2019.03.105.
[320] P.B. Tamarona, R. Pecnik, M. Ramdin, Viability assessment of large-scale Claude cycle hydrogen liquefaction: A study on technical and economic perspective, International Journal of Hydrogen Energy 77 (2024) 383–396. https://doi.org/10.1016/j.ijhydene.2024.06.021.
[321] Z. Abdin, K. Khalilpour, K. Catchpole, Projecting the levelized cost of large scale hydrogen storage for stationary applications, Energy Conversion and Management 270 (2022) 116241. https://doi.org/10.1016/j.enconman.2022.116241.
[322] B.D. James, C. Houchins, J.M. Huya-Kouadio, D.A. DeSantis, Final Report: Hydrogen Storage System Cost Analysis, (2016) 54.
[323] M. Raab, S. Maier, R.-U. Dietrich, Comparative techno-economic assessment of a large-scale hydrogen transport via liquid transport media, International Journal of Hydrogen Energy 46 (2021) 11956–11968. https://doi.org/10.1016/j.ijhydene.2020.12.213.
[324] X. Xu, B. Xu, J. Dong, X. Liu, Near-term analysis of a roll-out strategy to introduce fuel cell vehicles and hydrogen stations in Shenzhen China, Applied Energy 196 (2017) 229–237. https://doi.org/10.1016/j.apenergy.2016.11.048.
[325] A.S. Lord, P.H. Kobos, D.J. Borns, Geologic storage of hydrogen: Scaling up to meet city transportation demands, International Journal of Hydrogen Energy 39 (2014) 15570–15582. https://doi.org/10.1016/j.ijhydene.2014.07.121.
[326] M. Riemer, F. Schreiner, J. Wachsmuth, Conversion of LNG terminals for liquid hydrogen or ammonia, (2022). https://doi.org/10.24406/publica-464.
[327] L. Schreiner, R. Madlener, A pathway to green growth? Macroeconomic impacts of power grid infrastructure investments in Germany, Energy Policy 156 (2021) 112289. https://doi.org/10.1016/j.enpol.2021.112289.
[328] M.A. Khan, C. Young, C. Mackinnon, D.B. Layzell, The Techno-Economics of Hydrogen Compression, Transition Accelerator Technical Briefs 1 (2021). https://transitionaccelerator.ca/wp-content/uploads/2023/04/TA-Technical-Brief-1.1_TEEA-Hydrogen-Compression_PUBLISHED.pdf (accessed January 1, 2021).
[329] R.K. Ahluwalia, H.-S. Roh, J.-K. Peng, D. Papadias, A.R. Baird, E.S. Hecht, B.D. Ehrhart, A. Muna, J.A. Ronevich, C. Houchins, N.J. Killingsworth, S.M. Aceves, Liquid hydrogen storage system for heavy duty trucks: Configuration, performance, cost, and safety, International Journal of Hydrogen Energy 48 (2023) 13308–13323. https://doi.org/10.1016/j.ijhydene.2022.12.152.
[330] A.NFNR. Alkhaledi, S. Sampath, P. Pilidis, Economic analysis of a zero-carbon liquefied hydrogen tanker ship, International Journal of Hydrogen Energy 47 (2022) 28213–28223. https://doi.org/10.1016/j.ijhydene.2022.06.168.
[331] O.V. Tarovik, O.M. Mudrova, ESTIMATED TRANSPORTATION COST OF LOW-TONNAGE LNG, Mir Transp. 17 (2020) 130–163. https://doi.org/10.30932/1992-3252-2019-17-5-130-163.
[332] K. Koosup Yum, Energy Demand and Cost Analysis for a Hydrogen Fueled RoPax Ferry Using Design Lab Framework, (2023). https://www.nordicenergy.org/wordpress/wp-content/uploads/2023/05/The-Hope-project-Deep-dives.pdf.
[333] R. Lago Sari, A. Fogue Robles, J. Monsalve Serrano, D. Cleary, Techno-economic assessment of hydrogen as a fuel for internal combustion engines and proton exchange membrane fuel cells on long haul applications, Energy Conversion and Management 311 (2024) 118522. https://doi.org/10.1016/j.enconman.2024.118522.
[334] X. Hong, V.B. Thaore, I.A. Karimi, S. Farooq, X. Wang, A.K. Usadi, B.R. Chapman, R.A. Johnson, Techno-enviro-economic analyses of hydrogen supply chains with an ASEAN case study, International Journal of Hydrogen Energy 46 (2021) 32914–32928. https://doi.org/10.1016/j.ijhydene.2021.07.138.
[335] G. Kleen, W. Gibbons, J. Fornaciari, Heavy-Duty Fuel Cell System Cost – 2022, DOE Hydrogen Program Record (n.d.). https://www.hydrogen.energy.gov/docs/hydrogenprogramlibraries/pdfs/23002-hd-fuel-cell-system-cost-2022.pdf.
[336] United Nations, UN Comtrade Database, (2025). https://comtradeplus.un.org/.
[337] Eurostat, EU direct investment positions by country, ultimate and immediate counterpart and economic activity (BPM6), (2025). https://ec.europa.eu/eurostat/databrowser/view/bop_fdi6_pos__custom_17989185/default/table.
[338] Eurostat, Gross value added and income by main industry (NACE Rev.2), (2025). https://ec.europa.eu/eurostat/databrowser/view/nama_10_a10__custom_17989247/default/table.
[339] World Bank, The Disruptive Energy Transition and Opportunities for Job Creation in the Middle East and North Africa: Case Study—Morocco, (2024). https://documents1.worldbank.org/curated/en/099012324071522189/pdf/P1705461161e5d8813e9114dbf1b92a137252142a242.pdf.
[340] E.W. Lemmon, I.H. Bell, M.L. Huber, M.O. McLinden, NIST Reference Fluid Thermodynamic and Transport Properties Database (REFPROP) Version 10 - SRD 23, (2018). https://doi.org/10.18434/T4/1502528.
[341] J.W. Leachman, R.T. Jacobsen, S.G. Penoncello, E.W. Lemmon, Fundamental Equations of State for Parahydrogen, Normal Hydrogen, and Orthohydrogen, J. Phys. Chem. Ref. Data 38 (2009) 721–748. https://doi.org/10.1063/1.3160306.
[342] C. Haberstroh, Wasserstoff: Ortho/Para–Umwandlung und Verflüssigung, Chemie Ingenieur Technik 96 (2024) 43–54. https://doi.org/10.1002/cite.202300128.
[343] I. Seemann, J. Essler, C. Haberstroh, H. Quack, H.T. Walnum, D. Berstad, P. Nekså, J. Stang, M. Börsch, F. Holdener, L. Decker, P. Treite, Integrated design for demonstration of efficient liquefaction of hydrogen (IDEALHY): Report on the Analysis and Results of Boundary Condition and Duty Specification Worked Out in Task 1.2, (2012).
[344] B. Kanz, A. Tafone, L. Stops, T. Massier, H. Klein, A novel approach to simulate ortho-para conversion in hydrogen liquefaction based on the van't Hoff equation, Int. J. Hydrog. Energy (2025). https://doi.org/10.1016/j.ijhydene.2025.02.304.
[345] L. Stops, B. Kanz, K. Do, S. Rehfeldt, H. Klein, Process Simulation and Techno-Economic Assessment of Hydrogen Liquefaction Plants with Integrated Ortho-Para Conversion, in: Cryogenic Engineering Conference, 2025.
[346] Chemical Engineering, The Chemical Engineering Plant Cost Index, (2025). https://www.chemengonline.com/pci-home.
[347] J.R. Couper, Process engineering economics, Dekker, New York, NY, 2003.
[348] J. Essler, C. Haberstroh, H. Quack, H.T. Walnum, D. Berstad, P. Nekså, J. Stang, M. Börsch, F. Holdener, L. Decker, P. Treite, Integrated design for demonstration of efficient liquefaction of hydrogen (IDEALHY): Report on Technology Overview and Barriers to Energy- and Cost-Efficient Large Scale Hydrogen Liquefacti, (2012).
[349] Molecular Products Inc., Ionex\circledR – Type O-P Catalyst, (n.d.).
[350] M.S. Peters, K.D. Timmerhaus, R.E. West, Plant design and economics for chemical engineers, 5. ed., McGraw-Hill, Boston, 2003.

Contact

Finn Schenke
Institute of Electric Power Systems
schenke@ifes.uni-hannover.de

Leibniz University Hannover
Institute of Electric Power Systems
Department of Electric Energy Storage Systems
Appelstr. 9A
30167 Hannover
Germany

https://www.ifes.uni-hannover.de/de/ees


H2
H2
H2